

International Doctorate Program in Molecular Oncology and Endocrinology Doctorate School in Molecular Medicine

XIX cycle - 2003–2007
Coordinator: Prof. Giancarlo Vecchio

Molecular basis of thyroid cancer: role of inflammatory cells and molecules

Valentina Guarino

University of Naples Federico II
Dipartimento di Biologia e Patologia Cellulare e Molecolare
“L. Califano”

Administrative Location

Dipartimento di Biologia e Patologia Cellulare e Molecolare “L. Califano”
Università degli Studi di Napoli Federico II

Partner Institutions

Italian Institutions

Università degli Studi di Napoli “Federico II”, Naples, Italy
Istituto di Endocrinologia ed Oncologia Sperimentale “G. Salvatore”, CNR, Naples, Italy
Seconda Università di Napoli, Naples, Italy
Università del Sannio, Benevento, Italy
Università di Genova, Genoa, Italy
Università di Padova, Padua, Italy

Foreign Institutions

Johns Hopkins School of Medicine, Baltimore, MD, USA
Johns Hopkins Krieger School of Arts and Sciences, Baltimore, MD, USA
National Institutes of Health, Bethesda, MD, USA
Ohio State University, Columbus, OH, USA
Université Paris Sud XI, Paris, France
Universidad Autonoma de Madrid, Spain
Centro de Investigaciones Oncologicas (CNIO), Spain
Universidade Federal de Sao Paulo, Brazil
Albert Einstein College of Medicine of Yeshiwa University, USA

Supporting Institutions

Università degli Studi di Napoli “Federico II”, Naples, Italy
Ministero dell’Università e della Ricerca
Istituto Superiore di Oncologia (ISO)
Terry Fox Foundation, Canada
Istituto di Endocrinologia ed Oncologia Sperimentale “G. Salvatore”, CNR, Naples, Italy
Centro Regionale di Competenza in Genomica (GEAR)
Università Italo-Francese

Faculty

Italian Faculty

Giancarlo Vecchio, MD, Co-ordinator
Francesco Beguinot, MD
Angelo Raffaele Bianco, MD
Francesca Carlomagno, MD
Gabriella Castoria, MD
Angela Celetti, MD
Vincenzo Ciminale, MD
Annamaria Cirafici, PhD
Annamaria Colao, MD
Alma Contegiacomo, MD
Sabino De Placido, MD
Monica Fedele, PhD
Pietro Formisano, MD
Alfredo Fusco, MD
Massimo Imbriaco, MD
Paolo Laccetti, MD
Antonio Leonardi, MD
Barbara Majello, PhD
Rosa Marina Melillo, MD
Claudia Miele, PhD
Francesco Oriente, MD
Roberto Pacelli, MD
Giuseppe Palumbo, PhD
Silvio Parodi, MD
Giuseppe Portella, MD
Giorgio Punzo, MD
Antonio Rosato, MD
Massimo Santoro, MD
Giampaolo Tortora, MD
Donatella Tramontano, PhD
Giancarlo Troncone, MD
Bianca Maria Veneziani, MD

Foreign Faculty

National Institutes of Health (USA)

Michael M. Gottesman, MD
Silvio Gutkind, PhD
Stephen Marx, MD
Ira Pastan, MD
Phill Gorden, MD

Johns Hopkins School of Medicine (USA)

Vincenzo Casolaro, MD
Pierre Coulombe, PhD
James G. Herman MD
Robert Schleimer, PhD

Johns Hopkins Krieger School of Arts and Sciences (USA)

Eaton E. Lattman, MD

Ohio State University, Columbus (USA)

Carlo M. Croce, MD

Albert Einstein College of Medicine of Yeshiva University (USA)

Luciano D'Adamio, MD
Nancy Carrasco, MD

Université Paris Sud XI (France)

Martin Schlumberger, MD
Jean Michel Bidart, MD

Universidad Autonoma de Madrid (Spain)

Juan Bernal, MD, PhD
Pilar Santisteban

Centro de Investigaciones Oncologicas (Spain)

Mariano Barbacid, MD

Universidade Federal de Sao Paulo (Brazil)

Janete Maria Cerutti
Rui Maciel

Valentina Guarino

**Molecular basis of thyroid cancer: role
of inflammatory cells and molecules**

Doctoral Dissertation

<u>LIST OF PUBLICATIONS.....</u>	<u>8</u>
<u>ABSTRACT</u>	<u>10</u>
<u>1 INTRODUCTION.....</u>	<u>11</u>
1.1 THYROID CANCER	11
1.1.1 CLASSIFICATION	12
1.1.2 ETIOPATHOGENESIS, CLINICAL FEATURES AND MOLECULAR GENETICS OF THE THYROID TUMORS	13
1.1.3 HISTOTIPES OF THYROID CANCER	13
1.1.3.1 Papillary thyroid carcinoma	13
1.1.3.2 Follicular thyroid carcinomas	16
1.1.3.3 Anaplastic thyroid carcinomas	16
1.1.3.4 Medullary thyroid carcinomas	17
1.2 IMMUNE SYSTEM AND CANCEROGENESIS	17
1.2.1 Chronic inflammation and cancer	18
1.2.2 Inflammation and tumoral neoangiogenesis	21
1.4 MAST CELLS.....	21
1.5 THYROID CANCER AND INFLAMMATION	24
<u>2 AIMS OF THE STUDY.....</u>	<u>26</u>
<u>3 MATERIALS AND METHODS</u>	<u>27</u>
3.1 PLASMIDS	27
3.2 CELL CULTURES AND TRANSFECTIONS.....	27
3.3 RNA SILENCING.....	28
3.4 TISSUES SAMPLES	28
3.5 RNA EXTRACTION AND REVERSE TRANSCRIPTION POLIMERASE CHAIN REACTION	28
3.6 OLIGONUCLEOTIDE DNA MICROARRAY	29
3.7 PROTEIN STUDIES	29
3.8 ELISA ASSAY	
3.9 MATRIGEL INAVSION	
3.10 CHEMOTAXIS	
3.11 S-PHASE ENTRY	
3.12 XENOGRAFTS IN NU DE MICE	
3.13 STATISTICAL ANALYSIS	

4	<u>RESULTS</u>	<u>35</u>
4.1	THE RET/PTC-RAS-BRAF INDUCED CYTOKINES SUSTAIN THE MITOGENIC AND INVASIVE PHENOTYPE OF THYROID CANCER CELLS.....	35
4.1.1	A biochemical cascade linking RET/PTC to the activation of RAS, BRAF and ERK	35
4.1.2	Generation of the cellular model system	36
4.1.3	A gene expression signature of the RET/PTC3-RAS-BRAF axis in thyroid cells	37
4.1.4	Autocrine loops that sustain mitogenesis and motility of thyroid cancer cells	39
4.2	ROLE OF OSTEOPONTIN IN HUMAN PAPILLARY THYROID CARCINOMAS ..	43
4.2.1	OPN expression in PTC	43
4.2.2	OPN activates intracellular signaling and invasiveness of PTC cells	45
4.3	ROLE OF CXCR4 IN HUMAN ANAPLASTIC THYROID CARCINOMAS.....	48
4.3.1	CXCR4 expression in ATC.	48
4.3.2	CXCR4 is a functional receptor in human ATC cells	49
4.3.3	Biological activity of CXCR4 in ATC cells	50
4.3.4	AMD3100 inhibits ATC tumor formation in nude mice	51
4.4	ROLE OF MAST CELL INFILTRATE IN PTC	53
4.4.1	PRESENCE OF MAST CELLS IN PAPILLARY THYROID TUMORS	53
4.4.2	PTC CELLS ACTION ON THE MAST CELLS	55
4.4.3	MAST CELLS ACTION ON PTC CELL LINES.....	57
	4.4.3.1 Mast cells conditioned culture medium triggers chemotaxis and enhances the invasive behavior of PTC cells	58
	4.4.3.2 Identification of mediators of mast cells biological activities	58
5	<u>DISCUSSION</u>	<u>62</u>
6	<u>CONCLUSIONS</u>	<u>67</u>
7	<u>REFERENCES.....</u>	<u>68</u>

LIST OF PUBLICATION

- 1:** De Falco V, **Guarino V**, Avilla E, Castellone MD, Salerno P, Salvatore G, Faviana P, Basolo F, Santoro M, and Melillo RM
Biological Role and Potential Therapeutic Targeting of the Chemokine Receptor CXCR4 in Undifferentiated Thyroid Cancer
Cancer Res. In press
- 2:** Staibano S, Merolla F, Testa D, Iovine R, Mascolo M, **Guarino V**, Castellone MD, Di Benedetto M, Galli V, Motta S, Melillo RM, De Rosa G, Santoro M, Celetti A.
OPN/CD44v6 overexpression in laryngeal dysplasia and correlation with clinical outcome.
Br J Cancer. 2007 Nov 6
- 3:** Celetti A, Testa D, Staibano S, Merolla F, **Guarino V**, Castellone MD, Iovine R, Mansueto G, Somma P, De Rosa G, Galli V, Melillo RM, Santoro M.
Overexpression of the cytokine osteopontin identifies aggressive laryngeal squamous cell carcinomas and enhances carcinoma cell proliferation and invasiveness.
Clin Cancer Res. 2005 Nov 15;11(22):8019-27.
- 4:** **Guarino V**, Faviana P, Salvatore G, Castellone MD, Cirafici AM, De Falco V, Celetti A, Giannini R, Basolo F, Melillo RM, Santoro M.
Osteopontin is overexpressed in human papillary thyroid carcinomas and enhances thyroid carcinoma cell invasiveness.
J Clin Endocrinol Metab. 2005 Sep;90(9):5270-8. Epub 2005 Jul 5.
- 5:** De Falco V*, **Guarino V***, Malorni L, Cirafici AM, Troglio F, Erreni M, Pelicci G, Santoro M, Melillo RM.
*These authors contributed equally to this study
RAI(ShcC/N-Shc)-dependent recruitment of GAB 1 to RET oncoproteins potentiates PI 3-K signalling in thyroid tumors.
Oncogene. 2005 Sep 15;24(41):6303-13.
- 6:** Melillo RM, Castellone MD, **Guarino V**, De Falco V, Cirafici AM, Salvatore G, Caiazzo F, Basolo F, Giannini R, Kruhoffer M, Orntoft T, Fusco A, Santoro M.
The RET/PTC-RAS-BRAF linear signaling cascade mediates the motile and mitogenic phenotype of thyroid cancer cells.
J Clin Invest. 2005 Apr;115(4):1068-81. Epub 2005 Mar 10.
- 7:** Castellone MD, **Guarino V**, De Falco V, Carlomagno F, Basolo F, Faviana P, Kruhoffer M, Orntoft T, Russell JP, Rothstein JL, Fusco A, Santoro M, Melillo RM.
Functional expression of the CXCR4 chemokine receptor is induced by RET/PTC oncogenes and is a common event in human papillary thyroid carcinomas.
Oncogene. 2004 Aug 5;23(35):5958-67.

8: Castellone MD, Celetti A, **Guarino V**, Cirafici AM, Basolo F, Giannini R, Medico E, Kruhoffer M, Orntoft TF, Curcio F, Fusco A, Melillo RM, Santoro M.

Autocrine stimulation by osteopontin plays a pivotal role in the expression of the mitogenic and invasive phenotype of RET/PTC-transformed thyroid cells. *Oncogene*. 2004 Mar 18;23(12):2188-96.

ABSTRACT

Thyroid cancer is the most common endocrine malignancy, and its incidence is increasing worldwide. In the attempt to better understand thyroid cancerogenesis at the molecular level, we searched for transcriptional changes induced by oncogene-driven transformation in a model system of rat thyroid cells. By using global gene profiling through DNA microarrays, we identified a group of genes whose expression level increased as a consequence of ectopic expression of either RET/PTC, RAS or BRAF oncogene. These genes are typically involved in human papillary thyroid cancer (PTC). A subset of genes identified through this screening are related to inflammation and immunity, and include chemokines, cytokines, and their receptors. In particular, we found that the chemokine receptor CXCR2 and its ligand CXCL1, CXCR3 and its ligand CXCL10, CD44 and its ligand OPN, are expressed by transformed, but not by parental untransformed thyroid cells; we also found that CXCR4, another chemokine receptor, is expressed only by transformed cells, while its ligand, SDF-1 is not. In this thesis project, we focused on the role of these receptor-ligand couples, and on the role of the CXCR4 receptor by evaluating the biological activities of these molecules and by dissecting the molecular mechanisms underlying their biological action in human thyroid carcinogenesis. Here, we also evaluated the potential therapeutic targeting of CXCR4 in anaplastic thyroid carcinoma models. Finally, we investigate how molecules secreted by thyroid cancer cells can influence tumor microenvironment in these neoplasias.

INTRODUCTION

Cancer is a severe and progressive disease caused by the uncontrolled proliferation of a cellular clone, defined as neoplastic. The eminent oncologist Richard Willis has probably provided one of the most clarifying definitions of neoplastic disease: “it is an abnormal tissue whose excessive growth is not synchronous with that of the normal surrounding tissue. Moreover, the cancer cells proliferate even after the stimuli that have induced their growth are terminated” (Willis, 1952). Remarkably, cancer cells compete with the normal ones for nutrition and energy, thus causing disease into the host.

It is well known that the uncontrolled proliferation of neoplastic cells is caused by gene mutations, leading to activation of oncogenes (i.e., “gain-of-function” mutations) and/or inactivation of tumor suppressors (i.e., “loss-of-function” mutations). Moreover, the mutation in only one gene is not sufficient to produce cancer: many other genetic as well as epigenetic alterations are necessary to neoplastically transform cells.

Weinberg has proposed a model (known as the “six hallmarks of cancer”) according to which a normal cell has to acquire six unphysiological hallmarks to become a transformed one (Weinberg et al., 2000). These hallmarks are:

1. Self sufficient growth. Cancer cells synthesize the factors necessary for their growth or constitutively activate the receptors for these growth factors, thus sustaining their expansion in the absence of proliferation signals.
2. Loss of the ability to respond to growth-inhibiting signals from the surrounding tissues.
3. Resistance to terminal differentiation, senescence and apoptosis
4. Unrestrained proliferation
5. Self autonomous and unrestrained angiogenesis
6. Ability to move through basal membranes and vessels and, in turn, to invade distal tissues, a process known as metastatization.

Remarkably, however, some of the cancer cell characteristics are also influenced by signals coming from the surrounding microenvironment, including fibroblasts, endothelial cells and cells of the immune system.

Thyroid cancer

Thyroid cancer is the most frequent endocrine malignancy with an incidence of about 9-100000 cases/year; moreover, the incidence increases with the age, reaching a plateau at 50 years.

Although a minor cause of cancer mortality, thyroid tumors represent a simple and powerful experimental model for studying the cell and molecular biology of tumorigenesis in human epithelial cells.

The thyroid gland develops in the embryo as a tubular evagination of the pharyngeal endoderm at the bases of the tongue. It is located in the neck,

beside the trachea. The functional thyroid unit consists of the follicle, a hollow spheroid lined by a single layer of columnar epithelial (follicular) cells, filled with colloid containing thyreoglobulin secreted by these cells. A small minority of follicles include a second epithelial cell type, the C or parafollicular cell, which arises from a quite different embryological origin – the neuroectoderm of the neural crest.

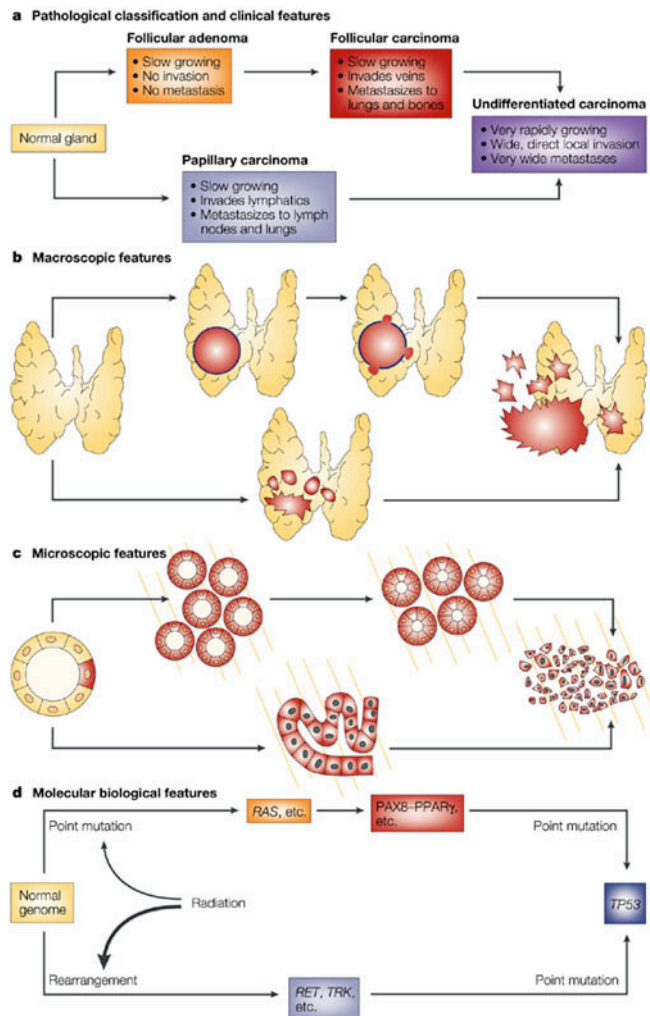


Figure 1: Features of thyroid tumors (Modified from Williams 2002).

Classification

Malignant thyroid tumors can derive from any of the gland cellular populations, being the cancers deriving from the epithelial cells the most frequent ones. The thyroid medullary carcinomas (MTC) derive from the calcitonin-secreting parafollicular C cells. From follicular cells derive: (1) the differentiated carcinomas, including the papillary carcinoma (PTC), the follicular-papillary carcinoma and the follicular carcinoma (FTC); (2) the recently identified poorly differentiated carcinomas, (PDC), histologically in

between the un- and the differentiated tumors; (3) the undifferentiated or anaplastic carcinomas (ATC) (Rosai 2004).

Etiopathogenesis, clinical features and molecular genetics of the thyroid tumors

The etiopathogenesis of thyroid tumors is still largely unknown; however, some risk factors have been identified. A well-established cause of thyroid carcinogenesis in humans is the exposure to ionizing radiation, especially in the neck region, predisposing to chromosomal breaks and, in turn, to chromosomal rearrangements and activation of oncogenes or loss of tumor suppressor genes. In fact, about 2-4% of the patients irradiated to treat diseases such as acne or enlarged thymus, develop a differentiated thyroid carcinoma after about 20-30 years. Accordingly, the frequency of papillary thyroid carcinomas is dramatically increased in the children exposed to the massive release of radionuclides that followed the explosion of the nuclear reactor in Chernobyl in 1986. In contrast, however, the therapy with I_{131} does not increase the risk of developing a thyroid tumor. On the contrary, the role of the iodine deficiency in thyroid carcinogenesis is not well established, being the epidemiological data collected in goitrogenic areas quite contradictory. Among the habitants of these areas the frequency of the thyroid adenocarcinomas, in particular of the more aggressive follicular histotypes, seems to be elevated. Thus, it has been hypothesized that TSH chronic stimulation has a pathogenetic role; this hypothesis has also been supported by the evidence that both the thyroid tumors and the metastasis do express TSH receptors. Accordingly, it has been demonstrated that suppressing the TSH synthesis with high doses of L-thyroxin reduces the risk of tumor recurrence and metastasis (Williams 2002).

The majority of patients presents with a nodule in their thyroid, which typically does not cause symptoms. Occasionally, in the more aggressive cases, symptoms caused by compression or infiltration, such as dysphonia, dysphagia or dyspnea, do occur. Malignant thyroid nodules, differently from the cystic benign ones, are generally single and their consistency is harder than that of the surrounding parenchyma. They are usually mobile; however, later on, the tumor can progress infiltrating other neck tissues and becoming fixed. Sometimes the first sign of disease is a laterocervical lymphadenopathy that can be caused by metastasis.

Histotypes of thyroid cancer

Papillary thyroid carcinomas

Papillary thyroid carcinomas (PTC) account for 75 to 80% of all thyroid cancers, showing an incidence peak at 40–50 years; They usually

metastasize to the cervical lymphonodes; distant metastasis are uncommon, but lung and bone are the most frequent sites.

Several studies on thyroid tumors have allowed the identification of many genetic alterations. In particular, in about 40-50% of papillary thyroid carcinomas the kinase domain of the tyrosine kinase receptor for the GDNF, c-Ret (REarranged during Transfection), is fused with the N-terminal region of constitutively expressed, heterologous genes, such as H4 (in RET/PTC1) or RFG (in RET/PTC3). In RET/PTC rearrangements, fusion with protein partners, possessing protein-protein interaction domains, provides RET/PTC proteins with coiled-coil domains, thereby resulting in ligand-independent activation of c-Ret tyrosine kinase activity (Santoro et al. 1995). Similar rearrangements of the high affinity receptor for NGF (Nerve Growth Factor), TRKA, can be also found, at a low prevalence (in about 10% of the tumors), in human PTC. RET activates many intracellular signaling pathways. Upon binding to ligand, it dimerizes and autophosphorylates various cytoplasmic tyrosines. The phosphorylated tyrosines thus become binding sites for intracellular molecules containing phosphotyrosine-binding motifs, thereby initiating a diverse array of signaling pathways (Santoro et al. 2004). In RET/PTC rearrangements, fusion with protein partners possessing coiled-coil domains provides RET/PTC kinases with dimerizing interfaces, thereby resulting in ligand-independent autophosphorylation. The RET intracellular domain contains at least 12 autophosphorylation sites, 11 of which are maintained in RET/PTC proteins (Kawamoto et al. 2004). Tyr 905 is located in the activation loop and its phosphorylation stabilizes the enzyme in an active conformation. Moreover, when phosphorylated, Tyr 905 binds some SH2-containing proteins, such as Grb7 and Grb10 (Pandey et al. 1996). Phosphorylated Tyr 1015 and Tyr 1096 are responsible for binding of PLC γ and GRB2, respectively (Jhiang S.M. 2000; Hansford et al. 2000; Airaksinen M.S. et al. 1999; van Weering et al. 1998). Several protein adaptors (Fig. 2), Shc, FRS2, IRS1/2, DOK1/4/5, RAI/NShc and Enigma recognize phosphorylated Tyr 1062 (Jhiang S.M. 2000; Hansford et al. 2000; Airaksinen M.S. et al. 1999; van Weering et al. 1998; Lorenzo et al. 1997, Pelicci et al. 2002, Melillo et al. 2001). The multi-docking site Tyr1062, upon phosphorylation, is responsible for the activation of the phosphatidylinositol 3-kinase (PI3K)/AKT and the mitogen-activated protein kinase (MAPK) pathways, the latter involving the extracellular-regulated kinase (ERK_s), c-Jun amino-terminal protein kinase (JNK_s) and the p38 MAPK (Jhiang S.M. 2000; Hansford et al. 2000; van Weering et al. 1998).

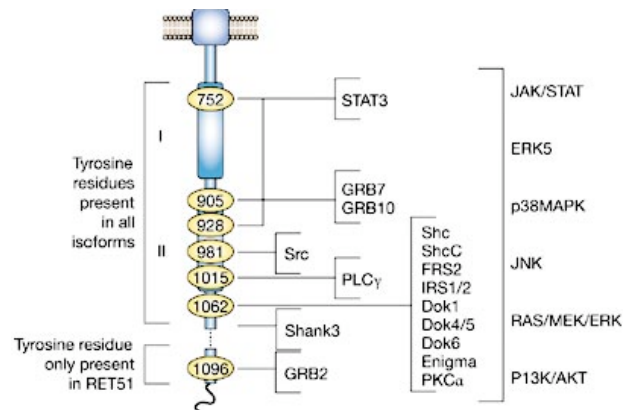


Figure 2: Signaling pathways activated by RET (modified from Drosten 2006)

Activating point mutations in RAS small GTPase are found roughly in 10% of PTC, mainly in those belonging to the follicular variant (PTC-FV) (Zhu et al. 2003). Point mutations in BRAF are the most common genetic lesion found in PTC (up to 50% of the cases) (Kimura et al. 2003; Xu et al. 2003; Soares et al. 2003). BRAF is a member of the RAF family of serine/threonine kinases and it is a component of the RAF-MEK-ERK signaling module. Activation of the RAF proteins is mediated through binding of RAS in its GTP-bound state. Once activated, RAF kinases phosphorylate MEK which in turn phosphorylates and activates ERK (Malumbres et al. 2003). A Glutamine for Valine substitution at residue 600 (V600E) in the activation segment accounts for more than 90% mutations of BRAF in PTC (Kimura et al. 2003; Cohen et al. 2003; Soares et al. 2003). This mutation enhances BRAF activity through disruption of the autoinhibited state of the kinase (Fig. 3).

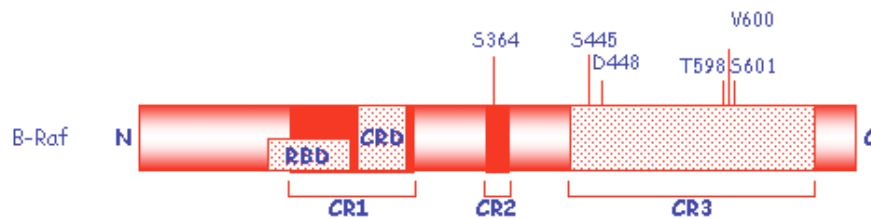


Figure 3: Structure of the BRAF gene. CR: conserved regions; triangles denote the common oncogenic mutations (modified form).

In human PTCs the genetic alterations of RET/PTC, RAS and BRAF are mutually exclusive, suggesting the existence of a common signaling cascade; moreover, mutations at more than one of these sites are unlikely to provide an additional biological advantage (Kimura et al. 2003, Cohen et al. 2003, Soares et al. 2003)

Follicular thyroid carcinomas

Follicular carcinoma is also a well-differentiated cancer developing from thyroid cells. About 10 to 30% of thyroid cancers are follicular cancers. Follicular carcinoma is particularly linked to dietary iodine deficiency (Williams et al. 1977) and both iodine deficiency and genetic influences could account for its link with a history of nodular goiter (Ron E et al. 1987).

In Follicular thyroid carcinoma (FTC) the presence of K-, H-, and N-RAS mutations is quite common. More recently, it has been shown that a quite high proportion of FTC carry the PAX8/PPAR γ rearrangement (Nikiforova MN et al. 2003). PAX8 encodes a thyroid-specific transcription factor, while PPAR γ is a nuclear receptor involved in lipid metabolism and tumorigenesis. The resulting fusion protein has dominant negative activity on wild type PPAR γ (Kroll et al. 2000).

Anaplastic thyroid carcinomas

Anaplastic thyroid carcinoma (ATC) is the most aggressive type of thyroid cancer. ATC cancer cells are extremely undifferentiated and spread rapidly to other parts of the body. ATCs make up only about 1% of all thyroid cancers, but they are highly malignant tumours that histologically appear wholly or partially composed of undifferentiated cells that exhibit immunohistochemical or ultrastructural features indicative of epithelial differentiation. Undifferentiated carcinomas typically spread beyond the thyroid by direct local extension. Metastases to regional nodes are also common but their presence is often overshadowed by the presence of extensive soft tissue invasion. Distant metastases may be present in any site. No effective therapy is known for ATC and prognosis is quite negative with a mean survival of less than one year.

Point mutations in the RAS oncogene and in the tumor suppressor p53 have been described in anaplastic carcinomas (Garcia-Rostan et al. 2003, Donghi et al. 1993, Fagin 1993). It is well known that p53 safeguards the cell cycle, the DNA repair and the apoptotic processes; thus, mutations in its sequence can account for the progression from a more differentiated to an anaplastic carcinoma, according to a model already described for the colon carcinoma by Vogelstein (Vogelstein et al., 1988). Garcia-Rostan and colleagues found somatic mutations within the PI3K catalytic subunit in 23% of analysed ATC (Garcia-Rostan et al. 2005) Mutations of BRAF gene have been detected in anaplastic carcinoma with well-differentiated components, presumably arising from preexisting papillary tumours (Nikiforova MN et al. 2003).

These tumors, because undifferentiated, do not significantly incorporate radioiodide; however, it can be utilized in the treatment protocols if a residual ability to incorporate it can be ascertained. Only very few responses have been reported with combined anthracyclines-paclitaxel regimens. If the

tumor is sensible, the radiation therapy of the neck can be exploited for a palliative cure.

Medullary thyroid carcinomas

The cells involved in medullary cancers are the neuroendocrine C cells of the thyroid that produce calcitonin. About 5 to 7% of all thyroid cancers are medullary cancers. Of the four types of thyroid cancer, only medullary cancer has a clear genetic predisposition that can be passed on in families.

Germline point mutations in RET cause the dominantly inherited cancer syndromes: multiple endocrine neoplasia (MEN) 2A and 2B, familial medullary thyroid carcinoma (FMTC). MEN2 patients are invariably affected by Medullary Thyroid Carcinoma (MTC), a malignant tumour arising from calcitonin-secreting C cells of the thyroid. Additional features can be present in MEN2A (pheochromocytoma and parathyroid adenoma) and MEN2B (pheochromocytoma, mucosal neuroma and ganglioneuroma of the intestine) (Brandi et al. 2001). Most MEN2B patients carry the M918T substitution in the P + 1 loop in the kinase domain. In MEN2A and most FMTC patients mutations affects one cysteine of the extracellular cysteine-rich domain of RET (609, 611, 618, 620, 630, 634) that can change to different residues. A good genotype-phenotype correlation is observed. In particular, about 90% of MEN2A patients have Cys634 mutation, and this mutation is highly predictive of the presence of pheochromocytoma and parathyroid hyperplasia. (Santoro et al. 1995; Carlomagno et al. 1997). RET activation by mutations targeting the intracellular domain is less understood (Santoro et al. 1995, Iwashita et al. 1999) but it can be envisaged that a modification of the structure of the kinase may switch on its enzymatic function.

Immune system and cancerogenesis

The first reports describing the presence of immune system cells in the neoplastic tissues were published at the end of the XIX century. Paul Ehrlich hypothesized that the immune system had a relevant role in blocking cancer cells spreading (Ehrlich, 1909). Burnet e Thomas further developed this hypothesis. In details, Burnet proposed that new, tumor-specific antigens could provoke an efficient immunological response, thus eliminating cancer cells (Burnet 1957, 1964, 1971). Thomas reasoned that complex and long-surviving organisms had to have biological mechanisms able to protect them from cancer cells proliferation (Thomas, 1959). However, in 1982, Thomas bitterly admitted, “the greatest trouble with the idea of immunosurveillance is that it cannot be shown to exist in experimental animals” (Thomas, 1982). Only later, thanks to the development of useful animal models, it has been possible to show that an immunosurveillance mechanism does exist and that it is indeed able to recognize and eliminate cancer cells.

Recently, Schreiber and colleagues have proposed a “seventh hallmark of cancer”, the ability to escape immunosurveillance (Dunn et al., 2004). The immunosurveillance mechanism has been proved in mice deficient for genes

(such as RAG, IFN- α , IFN- α R) necessary for the induction of an efficient immune response. These mice develop tumors either spontaneously or after treatment with carcinogenic agents. Moreover, the tumors are frequently very aggressive and develop even after treatment with very low doses of carcinogens (Dunn et al., 2004).

These, as well as other reports, have lead to the conclusion that both the innate and the adaptive immune systems recognize and attack cancer cells. Immunosurveillance is part of a more vast process defined by Schreiber as “immunoediting”. This process consist of three phases (Fig. 4):

1. An acute inflammatory response phase successfully induced and terminated by the immune system;
2. A steady-state phase, while cancer and immune system fight against each other, causing a chronic inflammatory response;
3. A third phase, when cancer prevail the immune system in two different ways: i) “immunoselection”, i.e., the selection of non-immunogenic clones; ii) “immunosubversion”. In this latter case, cancer cells actively escape the immune system, producing immunosuppressive cytokines or recruiting IDO⁺ dendritic cells, unable to present the antigen, or Treg CD4⁺CD25⁺, able to suppress immune response (Zitvogel et al. 2006).

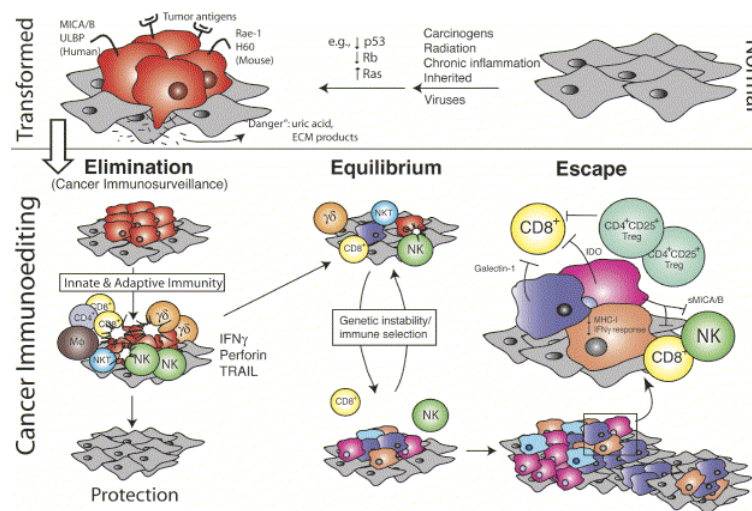


Figure 4: The Three Phases of the Cancer Immunoediting (modified from Dunn 2004)

Thus, an efficient immune response can eliminate cancer cells; however, the chronic activation of inflammatory cells present within or, more frequently, surrounding the neoplasia can sustain cancer cell proliferation.

Chronic inflammation and cancer

A functional relationship between chronic inflammation and cancer has been envisaged long ago and has been later demonstrated by several clinical and epidemiological evidences. Among the more compelling ones there are the association between: a) intestinal chronic inflammatory diseases (Chron’s disease and ulcerative rettocolitis) and the adenocarcinoma of the colon; b) chronic HCV hepatitis and liver carcinoma; c) Helicobacter pylori-induced

chronic gastritis and gastric carcinoma; d) asbestosis and mesothelioma; e) BPCO and lung cancer; f) chronic esophagitis and carcinoma of the esophagus (Coussens et al., 2002). Moreover, a 40-50% reduction in the incidence of colorectal cancer is associated with the regular use of non-steroidal anti-inflammatory drugs (NSAIDs), inhibiting the COX enzyme that catalyzes the synthesis of pro-inflammatory mediators, such as prostaglandins (Baron e Sadler, 2000; Williams et al., 1999). For most of the above-mentioned tumors, the etiopathogenic factors causing the chronic inflammatory response are well recognized, including a viral or a bacterial infection or a prolonged exposure to environmental chemicals. However, the molecular mechanisms causing the transition from a physiological response, such as inflammation, to neoplastic transformation are still largely unknown.

Inflammation is a physiological, protective response organized by the organism in response to tissue damages. Several chemical signals initiate and sustain the inflammatory response whose aim is repairing the damage. Several cells migrate in the sites of tissue damage, thanks to the action of chemotactic and adhesion proteins, including the integrin and selectin family members (Coussens et al., 2002). The first migrating cells are neutrophils, macrophages and mast cells, secreting ROS, vasoactive proteins, such as histamine and leukotrienes, and several other factors, such as cytokines, chemokines and proteases that remodel the extracellular matrix (de Visser et al., 2006).

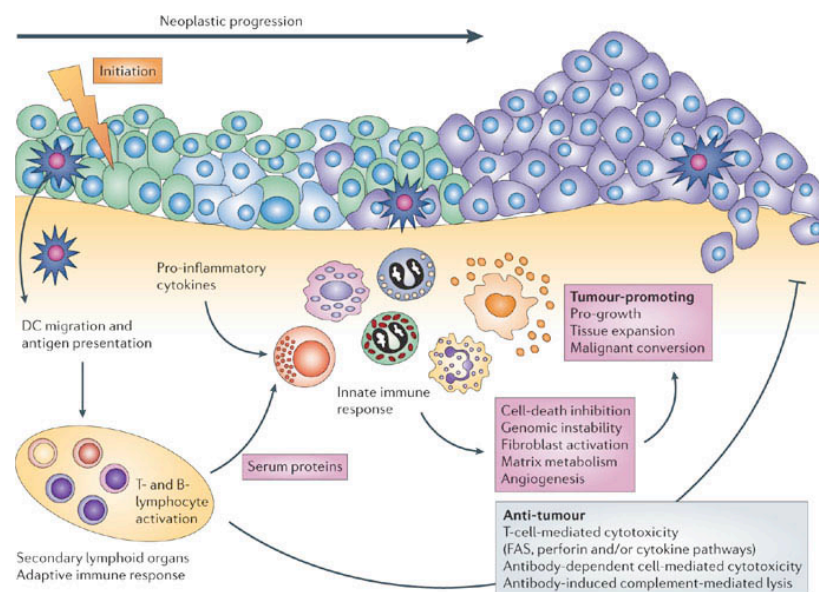


Figure 5: A model of innate and adaptive immune-cell function during inflammation-associated cancer development (modified from De Visser 2006).

Inflammation is an auto-limiting process; however, the abnormal persistence of the stimuli that first induced the inflammatory response or the failure of the mechanisms determining its termination cause chronic inflammation (Coussens et al., 2002).

Cancer cells secrete several cytokines and chemokines, thus recruiting leukocytes into tumor site. Leukocytes physiologically secrete ROS and RNS, to eliminate the pathogens. However, these highly reactive metabolites induce the production of peroxynitrite and other mutagenic agents; therefore, they can induce “DNA damage”, i.e. mutations in proliferating cells (Coussens et al., 2002). Thus, in the case of a persistent tissue damage the O₂ and N highly reactive metabolites secreted by the inflammatory cells induce point mutations, rearrangements and double strand breaks in the DNA of proliferating cells DNA. This results in a higher probability of oncogenes activation or of tumor suppressors loss of function. For example, Pollard and colleagues have shown that transgenic mice prone to breast cancer develop less proliferating and invasive tumors when crossed with mice deficient for CSF-1, a macrophage chemotactic factor (Lin et al. 2001).

Inflammation and tumoral neoangiogenesis

In adults angiogenesis is a process induced by tissue remodeling (Folkman, 1997). Thus, neoangiogenesis physiologically occurs in the endometrial regeneration during the menstrual cycle, in the wound healing processes and during the mammary gland evolution and involution of the mammary gland (Coussens et al., 1999). On the contrary, it pathologically ensues in inflammation and during tumoral growth (Ferrara, 1995; Hanahan and Folkman, 1996; Klein, 1999). In both cases, it induces activation, proliferation and migration of endothelial cell precursors. Moreover, endothelial cell proliferation and migration is facilitated by the proteolytic digestion of the extracellular matrix. In the case of a physiological neoangiogenetic response, such as the one occurring in the wound healing processes, the lesions induce the secretion of proangiogenic factor by inflammatory cells.

Neoplastic growth is influenced not only by proliferation but also by other phenomena, the most important one being the activation of angiogenic programs. In fact, the diameter of a tumor cannot overcome 1-2 mm, if it is not efficiently vascularized, because this is probably the maximal distance the oxygen and the nutritive factors can reach once left the vessels. Thus, if not vascularized, the tumor cannot get growing because hypoxia induces apoptosis. Neoangiogenesis has two effects on tumoral growth: i) it supplies oxygen and nutrition factors; ii) the newly formed endothelial cells induce cancer cells proliferation, by producing several growth factors, such as IGF, PDGF, GM-CSF and IL-1. Angiogenesis and lymphangiogenesis are essential characteristics not only for tumor growth but also for metastasization. Thus, a clear correlation exists among angiogenesis, cancer progression and the ability of the malignant cells to metastasize.

Both the cancer cells and the inflammatory cells infiltrating the tumor secrete several angiogenic factors, the most important being VEGF (Vascular Endothelial Growth Factor) and bFGF (Basic Fibroblast Growth Factor). These two growth factors are secreted by many different cancer cells, being their

blood levels higher in a significant percentage of neoplastic patients. Remarkably, however, cancer cells may also secrete anti-angiogenic proteins, such as angiostatin, endostatin and tumstatin (Ruegg, 2006). Thus, tumoral growth is the result of a fine balance between pro- and anti-angiogenic factors, this balance being extremely precarious during tumor progression. Thus, neoangiogenesis is a physiological phenomenon during, for example, wound healing: however, it becomes a pathological one when it sustains tumoral growth. In the first case the signals limiting angiogenesis do prevail; tumor progression is instead characterized by a shift in the balance between pro- and anti-angiogenic factors (Fig. 6).

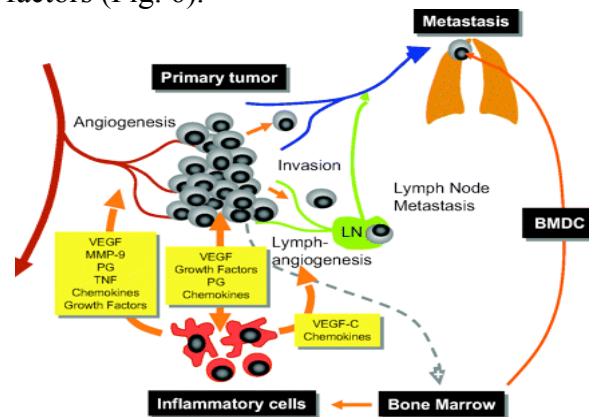


Figure 6: Leukocytes and bone marrow-derived inflammatory cells (BMDc) often infiltrate tumors, that “educate” these cells to produce tumor-promoting factors, which stimulate angiogenesis, lymphangiogenesis, and tumor cell invasion. (modified from Ruegg 2006)

Mast cells

Mast cells have been first identified in 1877 by a medical student, Paul Ehrlich (Beaven, 1976). They derive from bone marrow precursors and are present in all human tissues. Mast cells immunological activation results in the secretion of several pro-inflammatory factors, cytokines and chemokines. Moreover, mast cells have a relevant role in the pathogenesis of allergic diseases, being stimulated by the IgE-induced FcεRI receptor activation (Marone et al., 2005). Mast cells are histologically discriminated because metachromatic, this characteristic being a consequence of the interaction between dyes, such as toluidin blu, and the acidic proteoglycans in their cytoplasm. Moreover, mast cells can be also identified by immunohistochemistry, using antibodies direct against tryptase or the membrane c-kit receptor. Finally, they can be distinguished by basophils in electronic microscopy because they are characterized by a villic plasma membrane, by a monolobulate nucleus, often eccentric, and by a cytoplasm rich of eterogeneous granules and lipidic bodies.

In mammals and in the other vertebrates, there is a large number of mast cells in all the vascularized tissues, near vessels, nerves, muscle cells and mucosal glands. In details, mast cells are in all the tissues exposed to the external environment, such as the skin, the gastro-intestinal and the respiratory apparatus, being potential entry routes for pathogens and allergens. Thus,

together with dendritic cells, mast cells are among the first immune cell populations to interact with environmental antigens, allergens, bacteria, viruses and parasites (Galli et al., 2005). The c-kit receptor ligand, the Stem Cell Factor (SCF), is the most relevant factor for human mast cell maturation and differentiation (Galli et al., 2005). Several immunological and non-immunological stimuli can activate mast cells and stimulate the secretion of different proteins. Mast cells can be, in fact, activated by the canonical IgE-mediated response, by several immunological stimuli (such as C3a, C5a, the NGF-activated TRKA receptor, the IgG-activated Fc α RI, etc.), as well as by many non-immunological stimuli (such as P substance, VIP, somatostatin, morphin, etc.). Among the proteins secreted by activated mast cells there are preformed factors, lipidic mediators, cytokines and chemokines. The preformed factors are stored in secretory granules and are extracellularly released within few minutes. The secretory granules mainly contain: histamine, Tryptase, chymase, carboxypeptidase A e proteoglycans (heparin e chondroitin sulfate E). Histamine is one of the more important biogenic amine and exerts its biological effects by activating four different transmembrane receptors. Tryptase is a 110-130 kDa MW tetramer. This enzyme cleaves in vitro C3 to C3a; however, its function is still largely unknown (Hallgren and Pejler 2006).

Among the lipidic mediators there are the cyclo-oxygenases (PGD₂ e PGE₂) and the lipo-oxygenases (LTC₄, LTD₄, LTE₄) metabolites. The latter ones induce airways contractions and increase vascular permeability; on the other hand, PGD₂ exert a potent chemotactic activity. Human mast cells secrete several cytokines. Mast cell-produced TNF- α regulates adhesion proteins expression in epithelial and endothelial cells and increase bronchial reactivity. Among the other secreted cytokines there are IL-13, regulating TH2 cell differentiation and IgE synthesis; IL-3, GM-CSF and IL-5, critical for eosinophiles maturation and survival; and IL-6 (Prussin and Metcalfe, 2006). Finally, human mast cells secrete several chemokines: IL-8, CCL3/MIP-1 α , CXCL1/GRO- α e CXCL10/IP-10. Relevantly, mast cells secretory responses can be influenced by both genetic and environmental factors.

Mast cells are the primary cellular component in the immediate, Ig-E mediated, type I hypersensitive reactions. They also have a role in the innate immune responses as they can be activated via TLRs, phagocytosing microorganisms. Mast cells, as macrophages, are long surviving cells; moreover, the mast cells number in a specific site can increase as more precursors cells are recruited and/or induced to mature. Mast cells number increases in case of immediate hypersensitive reactions (rhinitis, eczema, asthma), of infections caused by intestinal worms, of chronic inflammation and/or tissue remodeling (rheumatoid arthritis, for example). During the last years it has been shown that mast cells also play an important role in case of neoplastic disease.

In 1891, Westphal first described the presence of a mast cell infiltrate in cancer tissues. This finding has been later on confirmed by studies describing

the presence of mast cells in tumors experimentally induced in mice as well as in several human cancers (Norrby e Wooley 1993; Meininger, 1995), including gastric adenocarcinomas, endometrial carcinomas (Ribatti et al., 2006), melanomas, squamo- and basocellular carcinomas of the skin (Coussens et al., 1999; Smirnova et al., 2005), prostate adenocarcinomas (Deng et al., 2004), cutaneous hemangiomas (Qu et al., 1995), lymphomas (Crocker, 1984), and myelomas (Ribatti et al., 1999; Vacca et al., 2001). Remarkably, the intense inflammatory reactions, induced in the host by three of the most aggressive human cancers, i.e. melanomas, breast carcinomas and colon carcinomas, involve several inflammatory cells populations, including mast cells, mainly localized at the tumor edge (Norrby e Wooley, 1993). However, mast cell function in tumor progression remains largely unknown.

Several evidences have shown that mast cell infiltration is elevated in different tumors (Coussens et al., 1999; Smirnova et al., 2005; Ribatti et al., 1999; Vacca et al., 2001; Qu et al., 1995; Crocker, 1984). Coussens and colleagues have developed an efficient transgenic mouse model of squamocellular carcinoma, induced by the HPV16 early region expression in the basal keratinocytes. In this tumor model, the authors have observed an intense inflammatory response, characterized by a rich mast cell infiltration and angiogenesis. Mast cells co-localized with subepithelial and subendothelial basal membranes that are active sites of extracellular matrix remodeling. Moreover, the authors identified two mast cells mediators, the Tryptase mMCP-6 and the chymase mMCP-4, stimulating fibroblast proliferation and progelatinase B (MMP-9) activation, respectively. Finally, these results have been further validated by the evidence that cancer progression is greatly impaired in mast cell deficient mice (Coussens et al., 1999). Thus, the authors have hypothesized that, during the first phases of tumors development (hyperplasia and dysplasia), the tumor infiltrating mast cells induce angiogenesis both directly and indirectly, activating proGelatinase B (MMP-9) and secreting proangiogenic factors captured by the extracellular matrix. Later during tumor progression, the transcription of proangiogenic factors is upregulated in cancer cells.

Multiple myeloma is characterized by a rich mast cell infiltration and by neoangiogenesis (Vacca et al., 2001). Tosato and coworkers have demonstrated that mast cells, recruited in situ by the VEGF-A secreted by multiple myeloma cells, induce tumor growth by producing angiopoietin-1 (Ang1) that, in turn, activates the endothelial specific tyrosine kinase receptor Tie2. Ang1-activated Tie2 induces endothelial cell proliferation and neo-vessels sprouting. Moreover, it stimulates the migration of stem cells that can differentiate in endothelial cells. Mast cell-secreted Ang1 and plasma cell-produced VEGF-A have, therefore, a synergistic effect (Tosato et al.2004). In conclusion, therefore, the above-described studies highlight how cancer cells take advantage of mast cells-secreted factors. In particular, mast cells have a relevant role in inducing tumoral neoangiogenesis by secreting several

proangiogenic factors, such as different VEGF isoforms, angiopoietin-1, heparin, histamine, metallo- and serine-proteases.

Thyroid cancer and inflammation

An association between Hashimoto's thyroiditis and thyroid cancer has been reported in about the 30% of the cases (Di Pasquale, 2001; Wirtschafter et al., 1997; Mechler et al., 2001; Segal et al., 1985; Eisemberg et al., 1989; Ott et al., 1987; Sclafani et al., 1993; Pisanu et al., 2003), the increased incidence of carcinomas in patients with thyroiditis suggesting they might be a precancerous condition. The vast majority of thyroiditis-associated carcinomas are papillary; however, also follicular, anaplastic, medullary and squamous carcinomas have been reported. Hashimoto thyroiditis is an autoimmune disorder in which the immune system reacts against a variety of thyroid antigens. The overriding feature of Hashimoto thyroiditis is the progressive depletion of thyroid epithelial cells (thyrocytes), which are gradually replaced by mononuclear cell infiltration and fibrosis. Multiple immunologic mechanisms may contribute to the death of thyrocytes. Sensitization of autoreactive CD4+ T-helper cells to thyroid antigens appears to be the initiating event. Hashimoto's thyroiditis is characterized by proliferating nodules as well as cytological alterations and nuclear modifications similar to those of the papillary carcinomas. The thyroid follicular cells may have chromosomal defects, such as the rare trisomy of chromosome 10 or the rearrangement RET/PTC1, the hallmark of many papillary thyroid carcinomas. Several other evidences suggest a role for RET/PTC in the association between thyroiditis and cancer. In fact, patients exposed to radiation from the Chernobyl nuclear power plant disaster often develop not only RET/PTC-induced papillary tumors but also an associated autoimmune thyroiditis (Williams et al 2002). Accordingly, transgenic mice engineered to express RET/PTC develop papillary carcinomas and chronic thyroiditis (Powell et al. 1998). Finally, Wirtschafter and colleagues have detected RET/PTC expression in about the 90% of the Hashimoto's thyroiditis they have analyzed (Wirtschafter et al., 1997). These data are, however, partially in contrast with the report by Rhoden and colleagues. These authors have found only few follicular cells expressing very low levels of the rearranged protein in Hashimoto's thyroiditis, thus suggesting that RET/PTC expression does not necessarily predict the development of a papillary carcinoma in patients with thyroiditis (Rhoden et al., 2006).

Two models have been hypothesized to explain the association between Hashimoto's thyroiditis and RET/PTC. The first one suggests that inflammation might facilitate the rearrangement. According to this hypothesis, free radicals production, cytokine secretion, cellular proliferation as well as other phenomena correlated with inflammation might predispose to the rearrangement in follicular cells. Another hypothesis suggests that it is the rearrangement that influences the thyroid inflammation. Accordingly, RET/PTC induces a severe inflammatory response in animal models (Powell et

al., 2003; Melillo et al., 2005; Puxeddu et al., 2003) and the synthesis of many inflammatory proteins in epithelial thyroid cells.

AIMS OF THE STUDY

Since the biochemical cascade RET/PTC3-RAS-BRAF is frequently activated in PTCs, and the mutations in these three genes are mutually exclusive, we sought to analyze the transcriptional program induced by these oncogenes in rat thyroid epithelial cells. The gene expression signature common to the three oncogenes revealed the induction of genes related to inflammation and immunity. These genes have been functionally characterized and their specific role in thyroid carcinogenesis has been investigated.

The specific aims were as follows:

- Development of an in vitro model of thyroid cells expressing RET/PTC3-HRAS-BRAF oncogenes
- Identification of gene expression profiles of rat thyroid cells expressing RET/PTC3-HRAS-BRAF
- Functional characterization of selected induced genes and of the biological effects exerted on thyroid cancer cells:
 - CXCL1/Gro α
 - CXCL10/IP10
 - Osteopontin (OPN)
 - CXCR4
- Characterization of the role(s) of mast cells infiltrate and in the development of human thyroid cancer.

MATERIALS AND METHODS

Plasmids

All the molecular constructs used in this study were cloned in pCDNA3(Myc-His) (Invitrogen, Groningen, The Netherlands). The RET/PTC constructs encode the short (RET-9) RET spliced form and are described elsewhere (Melillo et al 2001). For simplicity, we numbered the residues of RET/PTC proteins according to the corresponding residues in unrearranged RET. **RET/PTC1** and RET/PTC3 constructs encode the H4-RET and RFG-RET chimeric oncogenes, respectively. RET/PTC3(K-) is a kinase-dead mutant, carrying the substitution of the catalytic lysine (residue 758 in full-length RET) with a methionine. RET/PTC3(Y1062F) and RET/PTC3(Y1015F) carry substitutions of the indicated tyrosines with phenylalanine residues. BRAF and the kinase dead BRAF (K-) were kindly donated by C.J. Marshall (Davies et al 2002). BRAF(V600E) was obtained by site-directed mutagenesis using the QuickChange mutagenesis kit (Stratagene, La Jolla, CA). The mutation was confirmed by DNA sequencing. HRAS(V12) and HRAS(N17) plasmids are described elsewhere (Castellone et al 2003).

Cell cultures and transfections

PC Cl 3 (hereafter "PC") is a differentiated thyroid follicular cell line derived from 18-month-old Fischer rats. PC cells were cultured in Coon's modified Ham F12 medium supplemented with 5% calf serum and a mixture of 6 hormones (6H), including thyrotropin (TSH, 10 mU/ml), hydrocortisone (10 nM), insulin (10 µg/ml), apo-transferrin (5 µg/ml), somatostatin (10 ng/ml) and glycyl-histidyl-lysine (10 ng/ml) (Sigma Chemical Co., St. Louis, MO) (Fusco et al 1987). For stable transfections, 5×10^5 PC cells were plated 48 h before transfection in 60-mm tissue culture dishes. The medium was changed to Dulbecco's modified Eagle's medium (DMEM) (Invitrogen) containing 5% calf serum and 6H. Three hours later, calcium phosphate DNA precipitates were incubated with the cells for 1 h. DNA precipitates were removed, and cells were washed with serum-free DMEM and incubated with 15% glycerol in HEPES (N-2-hydroxyethylpiperazine-N'-2-ethanesulfonic acid)-buffered saline for 2 min. Finally, cells were washed with DMEM and incubated in Coon's modified F12 medium supplemented with 5% calf serum and 6H. Two days later, G418 (neomycin) was added at a concentration of 400 µg/ml. Mass populations (pool#3) of several hundred cell clones were pooled and expanded; two independent cell clones (Cl#1 and 2) for each transfection were also isolated. For the colony formation assay, two dishes of PC were transfected with each plasmid. Two days later, G418 was added to one dish, whereas the other dish was kept in medium containing 5% calf serum without 6H. After 15 days, cells colonies were fixed in 11 % glutaraldehyde in PBS, rinsed in distilled water, stained with 0.1% crystal violet in 20% methanol for 15 min

and counted. The percentage of hormone-independent colonies with respect to the total number of G418-resistant colonies was calculated as the average of three independent determinations \pm SD. HEK293 cells were from American Type Culture Collection (ATCC) and were grown in DMEM supplemented with 10% fetal calf serum. Transient transfections were carried out with 5 μ g of total DNA in the lipofectamine reagent according to the manufacturer's instructions (Invitrogen). TPC1, FB2, BCPAP, BHP2-7, and BHP5-16 human PTC cell lines were grown in DMEM supplemented with 10% fetal calf serum. The P5 primary culture of normal human thyroid follicular cells was kindly donated by F. Curcio and was grown as described (Curcio et al 1994). HMC-1 (Human Mast Cell Line) were kindly donated by JH Butterfield and grown in Iscove's (Life Technologies) supplemented with 10% fetal calf serum without α -thiglycerol (Butterfield et al. 1988). LAD-2 cells (kindly donated by AS Kirshenbaum) were grown in StemPro-34 (Life Technologies) supplemented with human recombinant Stem Cell Factor (100 ng/ml) (Peprotech, Rocky Hill, NY) (Kirstmbaum et al. 2003).

RNA silencing

Small inhibitor duplex RNAs targeting human BRAF have been previously described (Hingorani et al 2003). Duplex oligonucleotides targeting rat BRAF and CXCR4 were designed with a siRNA selection program available online at <http://jura.wi.mit.edu/siRNAext/>, and were chemically synthesized by PROLIGO, Boulder, CO. Sense strands for siRNA targeting were the following:

Rat BRAF: 5'-AAAGCCACAGCUGGCUAUUGUUA-3'

Human BRAF: 5'-AGAAUUGGAUCUGGAUCAUdTdT-3'

Human CXCR4: 5'-GAGGGGAUCAGCAGUAUAUAC -3'

Scrambled: 5'-rArCrCrgUrCrgrAUUUrCrArCrCrCrgTT-3'

For siRNA transfection, PC RET/PTC3, BHT101 and TPC1 cells were grown under standard conditions. The day before transfection, cells were plated in 6-well dishes at 50-60% confluency. Transfection was performed using 5-15 μ g of duplex RNA and 6 μ l of Oligofectamine reagent (Invitrogen), as previously described (Hingorani et al 2003). Cells were harvested at different time points post-transfection and analyzed. For growth curves, PC RET/PTC3 cells were transfected; 12 h after transfection, 1×10^5 cells were plated and counted at the indicated time points.

Tissue samples

Retrospectively-collected archival frozen thyroid tissue samples from 18 patients affected by papillary thyroid carcinomas (PTC) were retrieved from the files of the Pathology Department of the University of Pisa upon informed consent. Special care was taken to select cases whose corresponding histological samples were available for matched analysis. Sections (4- μ M

thick) of paraffin-embedded samples were stained with hematoxylin and eosin for histological examination to ensure that the samples fulfilled the diagnostic criteria required for the identification of PTC (enlarged nuclei with fine dusty chromatin, nuclear grooves, single or multiple micro/macro nucleoli and intranuclear inclusions). Normal thyroid tissue samples were also retrieved from the files of the Pathology Department of the University of Pisa.

RNA extraction and reverse transcription polymerase chain reaction

Total RNA was isolated by the RNeasy Kit (Qiagen, Crawley, West Sussex, UK) and subjected to on-column DNase digestion with the RNase-free DNase set (Qiagen) according to the manufacturer's instructions. Where indicated, cells were transfected with BRAF siRNA or treated with U0126 (20 μ M) and harvested 72h after treatment. The quality of RNA was verified by electrophoresis through 1% agarose gel and visualized with ethidium bromide. Random-primed first strand cDNA was synthesized in a 50 μ l reaction volume starting from 2 μ g RNA by using the GeneAmp RNA PCR Core Kit (Applied Biosystems, Warrington, UK). Primers were designed by using software available at <http://www-genome.wi.mit.edu/cgi-bin/primer/primer3> www.cgi and synthesized by the MWG Biotech (Ebersberg, Germany). To exclude DNA contamination, each PCR reaction was also performed on untranscribed RNA. Quantitative (real-time) reverse transcription polymerase chain reactions (Q-RT-PCR) were performed by using the SYBR Green PCR Master mix (Applied Biosystems) in the iCycler apparatus (Bio-Rad, Munich, Germany). Amplification reactions (25 μ l final reaction volume) contained 200 nM of each primer, 3 mM MgCl₂, 300 μ M dNTPs, 1x SYBR Green PCR buffer, 0.1U/ μ l AmpliTaq Gold DNA Polymerase, 0.01U/ μ l Amp Erase, RNase-free water, and 2 μ l cDNA samples. Thermal cycling conditions were optimized for each primer pair and are available upon request. To verify the absence of non-specific products, 80 cycles of melting curve (55°C for 10 sec) were performed. In all cases, the melting curve confirmed that a single product was generated. Amplification was monitored by measuring the increase in fluorescence caused by the SYBR-Green binding to double-stranded DNA. Fluorescent threshold values were measured in triplicate and fold changes were calculated by the formula: $2^{-(\text{sample 1 } \Delta Ct - \text{sample 2 } \Delta Ct)}$, where ΔCt is the difference between the amplification fluorescent thresholds of the mRNA of interest and the β actin mRNA.

Oligonucleotide DNA microarray

The detailed protocol for the microarray hybridizations, sample preparation, and the Rat Genome U34 Set is available from Affymetrix (Santa Clara, CA). Briefly, 10 μ g purified total RNA was transcribed into a first cDNA using Superscript RT (Invitrogen), in the presence of T7-oligo(dT)₂₄ primer, deoxyribonucleoside triphosphates (dNTPs), and T7 RNA polymerase

promoter (Invitrogen). The double-stranded (ds)-cDNA was cleaned and an *in vitro* transcription reaction was then performed to generate biotinylated cRNA which, after fragmentation, was used in a hybridization assay on RG-U34A and RG-U34B GeneChip microarrays. The A array contains probes representing full-length or annotated genes as well as EST clusters. The B array contains only EST clusters. Before hybridization, the efficiency of cDNA synthesis was estimated on a test chip by calculating the ratios for 5' and middle intensities relative to 3' for the control genes actin and glyceraldehyde-3-phosphate dehydrogenase (GAPDH). Biotinylated RNA used as a target in the microarray hybridization was stained with a streptavidin-phycoerythrin conjugation including an amplification step with a secondary antibody and scanned in a confocal laser-scanning microscope (Hewlett Packard GeneArray Scanner G2500A). Normalization was performed by global scaling, with the arrays scaled to an average intensity of 150. Analysis of differential expression was performed by Microarray Suite software 5.0 (Affymetrix). The final results were imported into Microsoft Excel (Microsoft).

Protein studies

Protein extractions and immunoblotting experiments were performed according to standard procedures. Briefly, cells were harvested in lysis buffer (50 mM HEPES, pH7.5, 150 mM NaCl, 10% glycerol, 1% Triton X-100, 1 mM EGTA, 1.5 mM MgCl₂, 10 mM NaF, 10 mM sodium pyrophosphate, 1 mM Na₃VO₄, 10 µg of aprotinin/ml, 10 µg of leupeptin/ml) and clarified by centrifugation at 10,000 x g. Protein concentration was estimated with a modified Bradford assay (Bio-Rad, Munich, Germany). Immune complexes were detected with the enhanced chemiluminescence kit (ECL, Amersham). Signal intensity was analyzed at the Phosphorimager (Typhoon 8600, Amersham Pharmacia Biotech) interfaced with the ImageQuant software. Anti-RET is an affinity-purified polyclonal antibody raised against the tyrosine kinase protein fragment of human RET. Anti-ERK (#9101) and anti-phospho-ERK (#9102) were from Cell Signaling (Beverly, MA). Anti-myc antibody and antibodies to D1 cyclin, BRAF and c-RAF were from Santa Cruz Biotechnology (Santa Cruz, CA, USA). Anti-RAS and anti-phosphotyrosine antibodies were from Upstate Biotechnology Inc., (Lake Placid, NY, USA). Anti-AKT and anti-phosphoAKT, specific for the active AKT phosphorylated at serine 473, were from Cell Signaling (Beverly, MA). Monoclonal anti- α tubulin was from Sigma Chemical Co. Anti-OPN goat polyclonal antibody (K20) and rabbit polyclonal anti-CD44 (H300) were obtained from Santa Cruz Biotechnology, Inc. (Santa Cruz, CA). Anti-CXCR4 antibodies were from Abcam Ltd. (Cambridge, UK). Histamine receptors antibody were from Chemicon International (U.S.A.) Secondary antibodies coupled to horseradish peroxidase were from Amersham Pharmacia Biotech. For the BRAF kinase assay, cells were cultured for 12h in serum-deprived medium and harvested. BRAF kinase was immunoprecipitated with the anti-myc epitope antibody and resuspended in a kinase buffer

containing 25mM sodium pyrophosphate, 10 μCi ^{32}P ATP and 1 μg of recombinant GST MEK (Upstate Biotechnology Inc.). After 30 min incubation at 4°C, reactions were stopped by adding 2X Laemmli buffer. Proteins were then subjected to 12% SDS gel electrophoresis. The radioactive signal was analyzed at the Phosphorimager.

ELISA assay

Thyroid cells plated in 6-well dishes were allowed to grow to 70% confluency and then serum-deprived for 24 h. Culture media were cleared by centrifugation at 2,000 RPM at 4°C to remove detached cells and debris. CXCL1, CXCL10, OPN and SDF-1 α levels in culture supernatants were measured using a quantitative immunoassay ELISA kit (QuantiKine colorimetric Sandwich assay ELISA, R&D Systems, UK), following the manufacturer's instructions. For chemokine detection in TPC1 BRAF-depleted cells, supernatants were harvested 96 h after siRNA transfection. Cells were serum starved for 4 h before harvesting. Triplicated samples were analyzed at 490 nm with an ELISA reader (Model 550 microplate reader, Bio-Rad).

Flow cytometric analysis

Subconfluent TPC1 cells were detached from culture dishes with a solution of 0.5 mM EDTA, and then washed three times in PBS buffer. After saturation with 1 $\mu\text{g}/10^5$ cells, cells were incubated for 20 min on ice with fluorescein- or phycoerythrin-labeled antibodies specific for human CXCR2, CXCR3, CD44v6 and CXCR4 (R&D Systems (Minneapolis, MN) or isotype control antibody. After incubation, unreacted antibody was removed by washing cells twice in PBS buffer. Cells resuspended in PBS were analyzed on a FACSCalibur cytofluorimeter using the CellQuest software (Becton Dickinson, San Jose, CA). Analyses were performed in triplicate. In each analysis, a total of 10^4 events were calculated.

Matrigel invasion

In vitro invasiveness through Matrigel was assayed using transwell cell culture chambers according to described procedures. Briefly, confluent cell monolayers were harvested with trypsin/EDTA and centrifuged at 800Xg for 10 min. The cell suspension (1×10^5 cells/well) was added to the upper chamber of a pre-hydrated polycarbonate membrane filter of 8 μm pore size (Costar, Cambridge, MA, USA) coated with 35 μg Matrigel (Collaborative Biomedical Products Inc., Bedford, MA, USA). The lower chamber was filled with complete medium and, when required, recombinant SDF-1, CXCL1 or 10 (Peprotech, Princeton Business Park, Rocky Hill, NJ), at the concentration of 100 ng/ml, were added to the lower chamber. When required, the cells were

pretreated for 12h with U0126 (20 μ M) or for 20 min with CXCL1, CXCL10, CXCR2 and CXCR3 blocking antibodies (1 μ g/ml, R&D), pertussis toxin (0.1 μ g/ml, Calbiochem, San Diego, CA) or the blocking compounds SB225002 (10 nM, Calbiochem) and TAK-779 (100 nM). The latter reagent was obtained through the NIH AIDS Research and Reference Reagent Program, Division of AIDS, NIAID, NIH (Rockville, MD). Where indicated, PC RET/PTC3 and TPC1 cells were transfected with BRAF siRNA, harvested, respectively, 48 and 72h after transfection, and plated on Matrigel. Cells were then incubated at 37°C in a humidified incubator in 5% CO₂ and 95% air for 24 h. Non-migrating cells on the upper side of the filter and Matrigel were wiped off and migrating cells on the reverse side of the filter were stained with 0.1% crystal violet in 20% methanol for 15 min, and photographed. The stained cells were lysed in 10% acetic acid. Triplicated samples were analyzed at 570 nm with an ELISA reader (Model 550 microplate reader, Bio-Rad). The results were expressed as percentage of migrating cells with respect to the PC RET/PTC3 or the chemokine-stimulated TPC1 cells.

Chemotaxis

In vitro chemotaxis through Fibronectin was assayed using transwell cell culture chambers according to described procedures. The cell suspension (1X10⁵ cells/well) was added to the upper chamber of a pre-hydrated polycarbonate membrane filter of 8 μ M pore size (Costar, Cambridge, MA, USA) coated with 50 μ l of 10% fibronectin in PBS (Sigma Chemical Co., St. Louis, MO). The lower chamber was filled with PTCs cells conditioned culture medium and, when required, purified blocking antibodies against VEGF-A (Santa Cruz Biotechnology, CA USA) were added to the lower chamber. Cells were then incubated at 37°C in a humidified incubator in 5% CO₂ and 95% air for 2 h. Non-migrating cells on the upper side of the filter and fibronectin were wiped off and migrating cells on the reverse side of the filter were stained with 0.1% crystal violet in 20% methanol for 15 min, and photographed. The stained cells were lysed in 10% acetic acid. Triplicated samples were analyzed at 570 nm with an ELISA reader (Model 550 microplate reader, Bio-Rad). The results were expressed as percentage of migrating cells with respect to the PC RET/PTC3 or the chemokine-stimulated TPC1 cells.

S-phase entry

S-phase entry was evaluated by BrdU incorporation and indirect immunofluorescence. Cells were grown on coverslips, and serum deprived for 30 h. When indicated, cells were treated with recombinant human CXCL1, CXCL10, SDF-1 α (Peprotech, Princeton Business Park, Rocky Hill, NJ) or OPN (R&D Systems, UK), at the concentration of 100 ng/ml, for 30 h. When required, the cells were treated for 24 h with CXCL1, CXCL10, CXCR2, CXCR3, CXCR4, CD44v6 blocking antibodies (1 μ g/ml, R&D), pertussis toxin

(0.1 µg/ml, Calbiochem, San Diego, CA) or the blocking compounds SB225002 (10 nM, Calbiochem), TAK-779 (100 nM), AMD3100 (Sigma Chemical Co., St. Louis, MO). BrdU was added at a concentration of 10 µM for the last 2 h. Subsequently, cells were fixed in 3% paraformaldehyde and permeabilized with 0.2% Triton X-100. BrdU-positive cells were revealed with Texas-Red-conjugated secondary antibodies, respectively (Jackson Immuno Research Laboratories, Inc. Philadelphia, PA). Cell nuclei were identified by Hoechst staining. Fluorescence was visualized with a Zeiss 140 epifluorescent microscope.

Xenografts in nude mice

Mice were housed in barrier facilities and 12-hour light-dark cycles and received food and water ad libitum at the Dipartimento di Biologia e Patologia Cellulare e Molecolare (University of Naples “Federico II”, Naples, Italy). This study was conducted in accordance with Italian regulations for experimentation on animals. All manipulations were performed while mice were under isoflurane gas anesthesia. No mouse showed signs of wasting or other signs of toxicity. BHT101, ARO, KAT4, Npa cells (5×10^6 /mouse) or HMC-1 (1×10^6 /mouse) were inoculated subcutaneously into the right dorsal portion of 4-week-old male BALB/c nu/nu mice (Jackson Laboratories, Bar Harbor, ME). For AMD3100 treatments started when tumors measured 40 mm³; mice were randomized to receive AMD3100 (n=10, 1.25 mg/kg/twice a day) or vehicle alone (n=10, PBS) by intraperitoneal injection for 5 consecutive days/week for 3-4 weeks. Tumor diameters were measured at regular intervals with calipers. Tumor volumes (V) were calculated with the formula: $V = A \times B^2/2$ (A=axial diameter; B= rotational diameter). Tumors were excised and fixed overnight in neutral buffered formalin and processed by routine methods.

Histamine release

Mast cells (6×10^4 cells/tube) were resuspended in PCG, and 0.3 ml of the cell suspension was placed in 12 x 75-mm polyethylene tubes (Sarsted-Princeton, NJ) and warmed to 37°C; 0.1 ml of each prewarmed releasing stimulus was added, and incubation was continued at 37°C (de Paulis et al 1996). The reactions were stopped by centrifugation (1000 x g, 22°C, 2 min), and the cell-free supernatants were assayed for histamine content with an automated fluorometric technique (Siranganian 1974). Total histamine content was assessed by lysis induced by incubating the cells with 2% HClO₄ before centrifugation. To calculate histamine release as a percentage of total cellular histamine, the spontaneous release of histamine from basophils (2–12% of the total cellular histamine) was subtracted from both the numerator and denominator (de Paulis et al 2006). All values are based on the means of duplicate determinations. Replicates differed in histamine content by <10%.

Statistical analysis

Significance was determined by the Mann-Whitney U Test (STATSOFT 6.0, Tulsa OK). A *P* value < 0.05 was considered statistically significant.

RESULTS

The RET/PTC-RAS-BRAF-induced cytokines sustains the mitogenic and invasive phenotype of thyroid cancer cells

A biochemical cascade linking RET/PTC to the activation of RAS, BRAF and ERK

We first wanted to investigate whether RET/PTC3, HRAS and BRAF belong to the same linear signaling pathway. To this aim we transiently co-transfected HEK293 cells with myc-tagged BRAF and with the RET/PTC3, HRAS, RET/PTC3 (Y1062F) and RET/PTC3 (Y1015F) constructs depicted in figure 7.

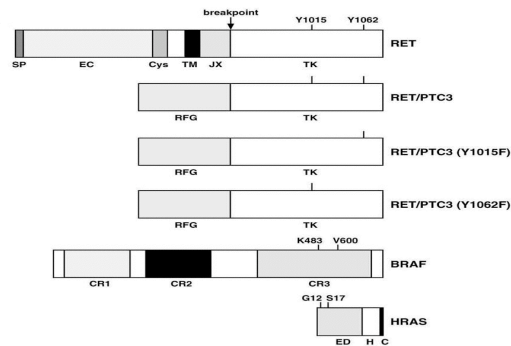


Figure 7: Schematic representation of the constructs used in this study. SP: RET signal peptide; EC: extracellular domain; Cys: cysteine-rich; TM: transmembrane; JX: juxtamembrane; TK: tyrosine kinase; CR: conserved BRAF regions; ED: RAS effector domain; H: heterogeneous region; C: CAAX tail

We examined BRAF activity in an immunocomplex kinase assay, with the oncogenic BRAF(V600E) and the kinase-dead BRAF(K-) mutants as positive and negative controls, respectively. BRAF activation was induced by co-transfection of the RET/PTC3 and HRAS(V12) oncogenes. BRAF activation (figure 8) depends on RET/PTC3 kinase activity, on the integrity of tyrosine 1062, crucial for RET activation of ERK1/2 pathway, and requires RAS. In fact RET/PTC3-mediated BRAF activation, is blocked by the expression of the dominant-interfering HRAS(N17) mutant.

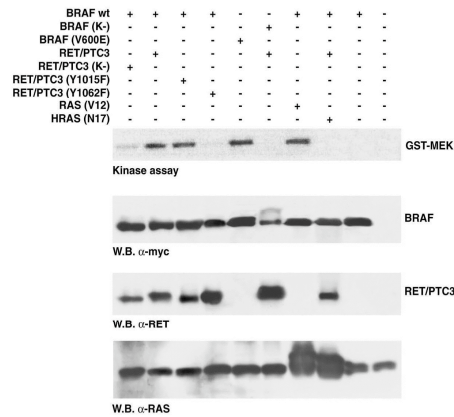


Figure 8: Protein lysates extracted from HEK293 cells transfected with the indicated plasmids underwent immunoprecipitation with anti-tag (myc) antibody. Kinase assay was performed with GST-MEK as a substrate. BRAF and RET/PTC3 were detected by western blot.

We tested the ERK1/2 stimulation downstream RET/PTC3(Y1062)-RAS-BRAF cascade. The immunoblot with phospho-specific antibody, shown in Figure 9, shows that RET/PTC3-stimulated ERK in a Y1062-, RAS- and BRAF- dependent fashion, being obstructed by the expression of HRAS(N17) and BRAF(K-) dominant negative mutants. Taken together, these findings demonstrate that the phosphorylation of RET/PTC tyrosine 1062 triggers RAS-dependent stimulation of BRAF signaling.

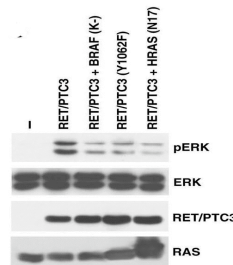


Figure 9: HEK293 cells transfected with the indicated plasmids were harvested, and protein extracts were subjected to immunoblotting with antiphospho-p44/p42 MAP kinase antibodies. The blot was re-probed with anti-p44/p42 antibodies for normalization. RET/PTC3 and RAS were detected by western blotting with specific antibodies.

Generation of the cellular model system

PC is a continuous line of follicular thyroid cells, derived from Fischer rats, that constitutes a model system to study differentiation and growth regulation in an epithelial thyroid cell setting. We generated marker-selected clones and mass-populations of PC cells stably transfected with RET/PTC3, HRAS(V12) or BRAF(V600E). The oncogene-transfected cell populations showed a similar, but not identical, transformed phenotype (figure 10). RET/PTC3, HRAS(V12) and BRAF(V600E) oncogenes abolished the dependency of PC cell proliferation from TSH, the major growth regulator for thyrocytes (not shown). Consistently, transformed cells maintained increased levels of G1 cyclin D1 under conditions of TSH-deprivation. Moreover, PC

cells transformed by the three oncogenes exerted an in vitro invasive phenotype through Matrigel and loss the differentiated phenotype, as shown by TG, TTF-1 and PAX-8, thyroid differentiation markers expression (not shown). In the case of RET/PTC3, all the transformation features depended on tyrosine 1062.

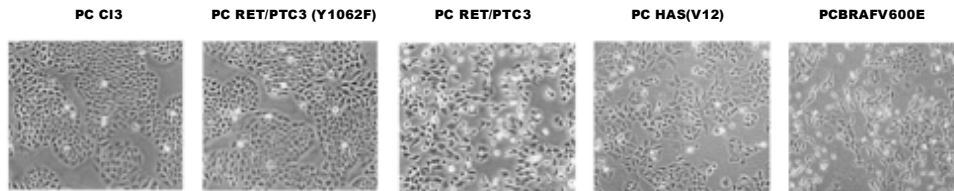


Figure 10: Mass populations of PC cells transfected with the indicated plasmids were photographed by using a phase-contrast light microscope (magnification X150). RET/PTC3, RET/PTC3(Y1015F), BRAF(V600E) and HRAS(V12) expressing cells displayed a transformed morphology, whereas RET/PTC3(Y1062F) cells were virtually indistinguishable from parental cells.

A gene expression signature of the RET/PTC3-RAS-BRAF axis in thyroid cells

We then explored gene expression changes after PC thyroid cell transformation mediated by RET/PTC3, HRAS(V12) or BRAF(V600E). As a control, we used cells expressing the RET/PTC3(Y1062F) mutant. To obtain the expression profiles of these cells, we used rat oligonucleotide-based DNA microarrays (Affymetrix, GeneChip) containing >16,000 known genes and EST clusters. RNA was extracted from mass populations of cells, converted into fluorescently labeled cRNA, and hybridized to arrays. Each chip was analyzed with the Affymetrix Microarray Suite 5.0 Software to generate raw expression data. Fold change (signal log ratio: SLR) was calculated by pair wise comparison of probe pairs from the experiment (cells expressing the different oncogenes) versus baseline (untransfected parental cells). Genes with changes in mRNA abundance in response to the different oncogenes were sorted by defining a filter query that "passed" only data sets that were denoted "increased" or "decreased" by the software.

By examining the expression profiles, we observed that some genes were regulated by only one or two oncoproteins. However, cross-comparison of the results revealed a group of sequences that were regulated in a similar fashion in RET/PTC3, HRAS(V12) and BRAF(V600E) cells. Whereas the former probably reflect the specific biological activity of each oncoprotein, the common targets represent a transcriptional signature of the expression of the three oncogenes in thyrocytes. As shown in figure 11, where genes with a fold change of 4 or more are depicted, many of the genes induced by RET/PTC3 were also induced by HRAS(V12) (54%) and BRAF(V600E) (48%). Overall, 60 (41%) of the oligonucleotide probe pairs induced in RET/PTC3 cells were induced in both HRAS(V12) and BRAF(V600E) cells, and as many as 87% were Y1062-dependent. Similarly, sorting of HRAS(V12)- and BRAF(V600E)-induced sequences showed that RET/PTC3 cells up-regulated a large set of them in a Y1062-dependent fashion. Of the 2,517 oligonucleotide

probes pairs whose expression was decreased in RET/PTC3 cells, 338 were down-regulated by 4-fold or more. Again, a large fraction of these sequences was also down-regulated in HRAS(V12) (44%) and in BRAF(V600E) (36%) cells. Overall, 104 (31%) genes were down-regulated by all the three oncogenes, with 66 of them (64%) being dependent on the integrity of Y1062.

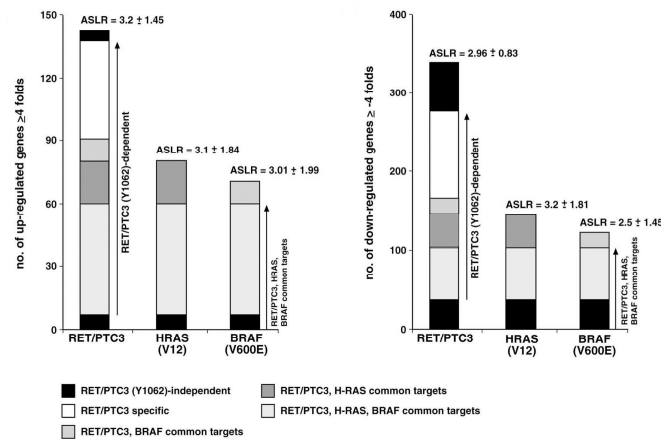


Figure 11: Graphic representation of the gene expression changes (fold-change ≥ 4) in RET/PTC3, BRAF(V600E) and HRAS(V12) cells versus baseline (PC): panel left: up-regulated genes and panel right: down-regulated genes. The number of up-regulated and down-regulated genes is represented on the y-axis. Arrows indicate the Y1062-dependent genes or the RET/PTC3, BRAF(V600E) and HRAS(V12) common targets. The different groups of genes are highlighted. Average signal log ratio (ASLR) is reported.

To assess the accuracy of the microarray results, we analyzed by reverse transcription polymerase chain reaction (RT-PCR) the expression of a subset of genes that had a fold change >4 in cells transformed by the three oncogenes. To exclude that gene expression changes may be due to a clonal effect during selection, we analyzed gene expression levels on the mass population (pool#3) and on two individual clones (Cl#1 and 2) for each cell line; thus, statistical analysis of expression changes induced by each oncogene was performed. To verify whether the activation of the RAS-BRAF-ERK pathway was required for gene expression regulation induced by RET/PTC3, the expression levels of the genes were measured by Q-RT-PCR in RET/PTC3 cells in which the pathway was transiently obstructed, either by BRAF siRNA or by treatment with the MEK inhibitor U0126. Expression changes of 60% of the genes were affected by both BRAF silencing and U0126 treatment and there was a complete concordance between U0126 and siRNA treatment. Scrambled siRNA, used as a negative control, did not affect expression levels (not shown).

Interestingly, a large set of genes associated with inflammation and immune response (cytokines, chemokines and their receptors) were up-regulated more than 4 fold in cells expressing RET/PTC3, HRAS(V12) and BRAF(V600E). These genes included: the cytokine Osteopontin with its receptor CD44 and the chemokines CXCL1/GRO- α (Growth Regulated Oncogene- α), CXCL10/IP-10 (interferon- γ -inducible protein 10), CCL2

(monocyte chemoattractant protein-1). Based on the microarray data, CXCR2, the receptor for CXCL1, and CXCR3, the CXCL10-receptor, were also up-regulated.

We examined genes coding for the chemokines CXCL1/GRO- α and CXCL10/IP-10. A large panel of primary and continuous human thyroid cell lines derived from normal tissue and major types of tumors has been collected in order to validate the array's data in a human model. Most of these cell lines have been characterized for naturally-occurred RET/PTC, RAS or BRAF mutations. This resource has been employed to confirm chemokine and chemokine receptor overexpression (not shown), to correlate this feature to the underlying oncogenic lesion and to perform functional studies.

Autocrine loops that sustain mitogenesis and motility of thyroid cancer cells

Chemokines are small chemotactic cytokines that are subdivided into two main families (α or CXC and β or CC chemokines) on the basis of the relative position of cysteine residues (Dhawan et al.2002). Chemokines bind to 7-transmembrane receptors present in the cell surface that are coupled to G α_i class G proteins and can therefore be inhibited by *Bordetella pertussis* toxin (PTX). Chemokine receptor activation leads to a cascade of cellular events: generation of diacylglycerol and inositol triphosphate, release of intracellular calcium, inhibition of adenylyl cyclase, and activation of several signaling proteins including Janus tyrosine kinase/signal transducers and activators of transcription (Jak/STAT), protein kinase C, phospholipase C, phosphatidylinositol 3-kinase (PI3K) and small GTPases of the Ras and Rho families. This cascades result in the activation of AKT and ERK and in cell polarization, adhesion and migration (Luster et al. 1998; Mellado et al. 2002).

Having shown that mRNA for CXCL1 and CXCL10 are up-regulated in rat and human PTC cell lines, we evaluated whether these chemokines were released in cell supernatants. An ELISA assay demonstrated that CXCL1 and CXCL10 were more abundantly secreted by human PTC cell lines spontaneously carrying the RET/PTC1 rearrangement (TPC1, FB2, BHP2-7) or the BRAF(V600E) mutation (BCPAP, BHP5-16) with respect to P5, a primary culture of normal human thyroid follicular cells (Figure 12).

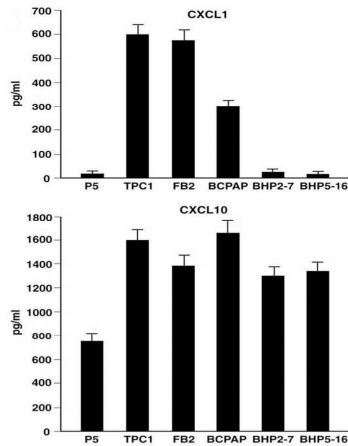


Figure 12: CXCL1 and CXCL10 secretion in human PTC cells was evaluated by ELISA: triplicate determinations (\pm S.D.). Normal thyroid cells (P5) were used as a negative control.

Accordingly, the receptors for the chemokines CXCL1 and CXCL10 (CXCR2 and CXCR3, respectively) were expressed on the cell surface of the PTC cell lines as assessed by flow cytometric analysis (not shown). The up-regulation of two chemokines was also confirmed in a larger set of tumor samples (n. 18) with respect to normal thyroid tissue (Figure 13).

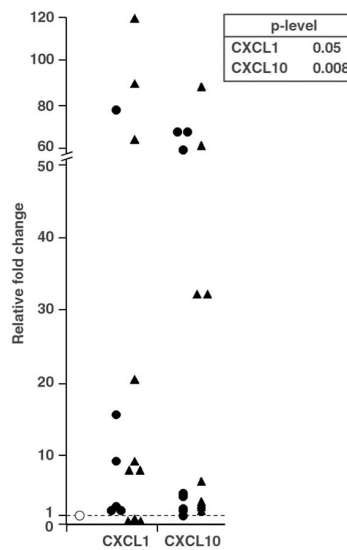


Figure 13: Expression chemokines in human PTC samples versus five normal thyroid tissues by Q-RT-PCR. The PTC samples were characterized for the presence of either a *RET/PTC* rearrangement or a *BRAF(V600E)* mutation. For each target (x-axis), the expression levels values of tumors (y-axis) were calculated relative to the average expression level in normal tissues (TN). All the experiments have been performed in triplicate P value was calculated by the Mann-Whitney Test

To verify the activation of downstream signaling pathways by the two receptors, TPC1 cells, derived from a human PTC carrying the *RET/PTC1* rearrangement, were selected. Cells were stimulated with

recombinant CXCL1 or CXCL10, harvested at different time points, and activation of ERK and AKT was analyzed by phospho-specific antibodies. Both chemokines stimulated a potent ERK and AKT phosphorylation starting after 1 min of treatment; ERK activation was faster than AKT activation (Figure 14).

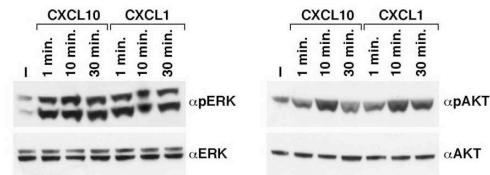


Figure 14: Stimulation with CXCL1 and CXCL10 (100 ng/ml) induced time-dependent ERK and AKT activation in TPC1 cells. Cell lysates were harvested at the indicated time points; western blots were probed with the indicated antibodies.

Since CXCR2 and CXCR3 are expressed and functional in thyroid cells we evaluated their biological role in PTC cells. We measured S-phase entry, upon chemokines stimulation in TPC-1 cells by BrdU incorporation assay. Treatment with recombinant CXCL1 and CXCL10 stimulated DNA synthesis of TPC1 cells. Selective antagonists for CXCR2 (SB225002) and CXCR3 (TAK-779) (White 1998; Gao 2003) and blocking antibodies to chemokines and receptors also inhibited basal proliferation, consistent with the autocrine production of chemokines by these cells (figure 15).

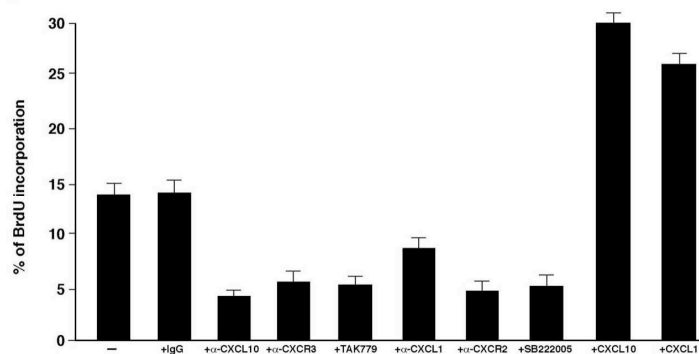


Figure 15: BrdU-incorporation was measured to evaluate S-phase entry upon treatment with CXCL1 or CXCL10 or the indicated inhibitors. Average results of three independent experiments \pm S.D.

Finally, we asked whether chemokines can stimulate cell invasiveness through Matrigel. TPC1 cells displayed low levels of invasiveness in basal conditions; exogenous CXCL1 or CXCL10 induced a strong migratory response. Basal TPC1 migration through Matrigel was inhibited by treatment

with PTX, with selective antagonists (SB225002 and TAK-779) with CXCR2- or CXCR3-blocking antibodies and with CXCL1- or CXCL10-blocking antibodies, but not by non-specific IgG. Cell motility was also blocked by treatment of TPC1 cells with BRAF siRNA and U0126. This effect was not observed when a scrambled control siRNA was used (figure 16).

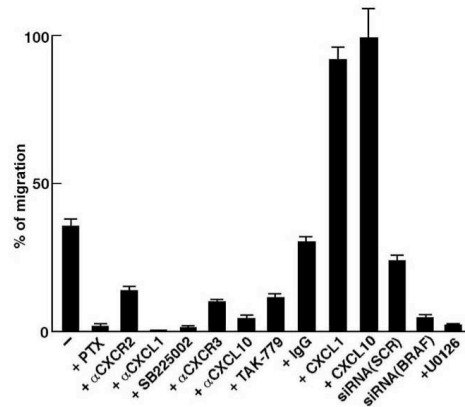


Figure 16: TPC1 cells were seeded in the upper chamber of 8 μ M pore transwells and allowed to migrate for 24 h towards serum-free medium or, a gradient of CXCL1 or CXCL10. Where indicated, cells were preincubated with blocking antibodies, control antibodies, chemical inhibitors, or PTX. The BRAF-ERK pathway was blocked either by using BRAF siRNA or by U0126 treatment.

These data suggested the existence of autocrine loops sustained by CXCL1 and CXCL10 and their receptors that confer mitogenic and motogenic abilities to PTC cells

Role of Osteopontin in Human Papillary Thyroid Carcinomas

The cytokine OPN and its receptor CD44 are major transcriptional targets of RET/PTC3-RAS-BRAF in thyroid cells identified through microarrays screening. In a previous work, we demonstrated that the OPN-CD44 autocrine loop is present and functional in thyroid papillary carcinoma cells (Castellone et al. 2004). OPN is a non-collagenous, sialic acid-rich, and glycosylated phosphoprotein (Butler 1989; Denhardt and Guo 1993). OPN binds to several integrins and to CD44. This protein is involved in normal tissue remodeling processes such as bone resorption, angiogenesis, wound healing and tissue injury as well as certain diseases such as restenosis, atherosclerosis, tumorigenesis and autoimmune diseases (Liaw 1998; Rittling and Novick 1999). OPN expression is upregulated in several cancers and associated with tumor progression and metastasis (Senger et al. 1983; Craig 1990). OPN induces cell adhesion and migration, ECM-invasion, and cell proliferation by interacting with its receptors $\alpha_v\beta_3$ and CD44. CD44 is a member of the immunoglobulin super family that is expressed in most epithelial and non-epithelial cells. Functionally, CD44 binds Hyaluronane in extracellular matrix. CD44 is also an OPN cell surface receptor, and it is frequently overexpressed in neoplastic cells. CD44 pre-mRNA is encoded by 20 exons, which are subjected to alternative splicing. The presence of the v6 exon is required for efficient OPN binding. While CD44s expression does not necessarily convey metastatic potential, CD44 variant isoforms, especially CD44v6, have been identified as markers for metastatic behavior in hepatocellular, breast, colorectal and gastric cancers. Here we investigate whether OPN could be used as a marker of malignancy in papillary thyroid carcinomas.

OPN expression in PTC

We measured OPN expression by immunohistochemistry with an anti-OPN-specific monoclonal antibody in 117 thyroid samples from patients who had undergone surgical resection of the thyroid gland for benign or malignant lesions (not shown).

OPN was virtually undetectable (<10% of cells) in normal thyroid glands (n = 34), follicular adenomas (n = 7), and multinodular goiters (n = 5). In contrast, most of the PTC samples examined (60 of 71), were positive for OPN expression, and positivity was confined to tumor cells. The prevalence and intensity of OPN staining significantly correlated with the presence of lymph node metastases (P = 0.0091) and tumor size (P = 0.0001). Furthermore, 85% (34 of 40) of the classic PTC tumors and 100% (8 of 8) of the tall cell variant PTCs displayed intense OPN immunoreactivity in more than 70% of the cells, whereas PTC-FV tumors were characterized by less intense or negative staining. Finally, in accordance with previous data, classic PTC (n = 40) were invariably positive also to CD44v6-specific monoclonal antibodies.

Protein lysates were harvested from a pool of normal human thyroid tissues and from six classic PTC samples and analysed by immunoblotting. OPN levels were normalized to tubulin. As shown in figure 17 OPN protein was abundantly over-expressed in all carcinomas compared to normal tissues. To determine whether up-regulation occurred at the transcriptional level we examined a small sample set using q-RT-PCR. Levels of OPN transcripts were significantly higher in tumor samples than in normal thyroid tissue (not shown).

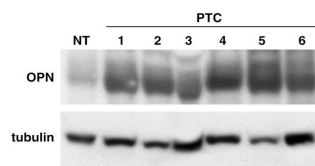


Figure 17: OPN up-regulation in PTC samples. A, OPN protein levels were evaluated by immunoblot in PTC samples and in a pool of five normal thyroid samples (NT). Equal amounts of proteins (100 µg) were immunoblotted with anti-OPN polyclonal antibodies. Antitubulin monoclonal antibody was used as a control for equal loading.

To establish a model system with which to study the role of OPN, we analysed OPN mRNA expression in cultured human thyroid cells. In these experiments we used P5, a primary culture, and a panel of PTC cells lines. As shown by RT-PCR experiment, all the PTC cell lines analyzed overexpressed OPN by more than 10-fold with respect to normal thyrocytes; BCPAP cells were the least positive (not shown). To verify that the up-regulated OPN was indeed secreted by PTC cells, we used an ELISA assay. PTC cells, but not normal P5 cells, secreted abundant OPN in the culture medium. Again, BCPAP cells were the least positive (figure 18)

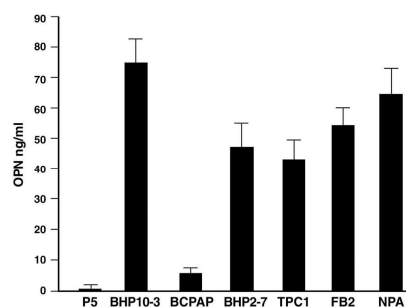


Figure 18: OPN up-regulation in cultured PTC cells. OPN protein secretion by PTC cells was evaluated by ELISA. Normal thyroid cells (P5) were used as the negative control. The results of three independent determinations performed in triplicate ± SD are reported.

We then screened PTC cell lines for CD44 expression by RT-PCR using primers designed on exons 2 and v6. All cancer cells tested, but not normal cells, contained high levels of CD44v6 mRNA (not shown). We therefore used flow-cytometry to determine whether CD44v6 was expressed on the surface of PTC cells. As shown in Figure 19, the TPC1 and BCPAP PTC

cell lines featured homogeneous cell membrane CD44v6 expression, whereas the others displayed varying expression levels of CD44v6.

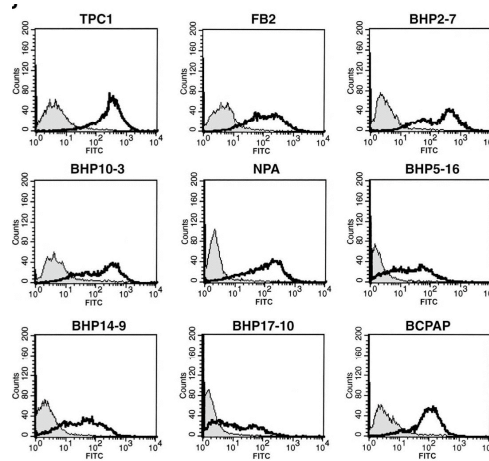


Figure 19: Flow cytometric analysis of cell surface expression of CD44v6 receptor in the indicated PTC cell lines. The shadowed curve is the negative control antibody.

OPN activates intracellular signaling and invasiveness of PTC cells

OPN secretion and cell surface CD44v6 expression reflected the existence of an autocrine OPN-CD44 axis that affected PTC cells. To verify that this axis was functional in human PTC cell lines, we examined cell invasion of Matrigel under basal conditions and in the presence of exogenous recombinant OPN. As shown in Figure 20, OPN induces a strong invasive phenotype in PTC cells in comparison with normal cells. Interestingly, TPC and BCPAP cells, which expressed the highest levels of CD44v6, displayed the best migratory response to OPN.

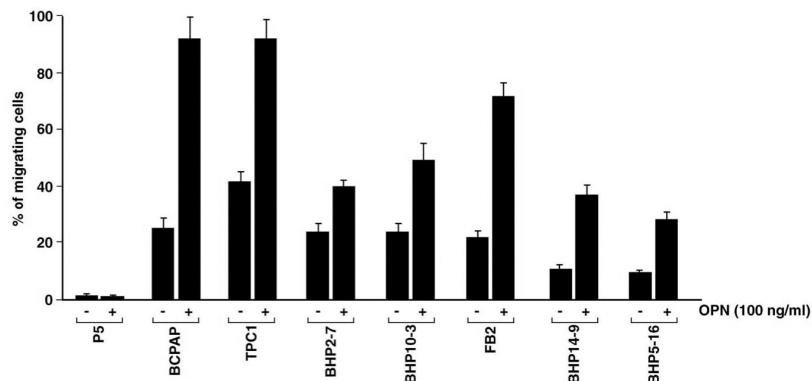


Figure 20: OPN-mediated signaling and Matrigel invasion. A, Matrigel invasion of TPC cells in response to normal culture medium or exogenous recombinant OPN. Cells were incubated for 24 h. Thereafter, filters were fixed and stained. The upper surface was wiped clean, and cells on the lower surface were stained with 0.1% crystal violet. The stained cells were lysed in 10% acetic acid. Invasive ability is expressed as the percentage of migrating cells with respect to the total cell number. Quantification was performed in triplicate samples with an ELISA reader. This figure is representative of three independent experiments.

To evaluate whether OPN was able to induce a biochemical response in PTC cells, we selected BCPAP cells, which express high levels of CD44v6 and relatively low levels of OPN. Cells were harvested at different time points. Cells were subjected to Western Blot analysis and probed respectively with phospho-antibodies against MAPK and Akt. MAPK and Akt were readily activated in stimulated cells (not shown). It has been previously reported that in immortalized liver carcinoma cells (HepG2), OPN up-regulates CD44v6 in a concentration- and time dependent fashion (Gao C et al. 2003). To determine whether this was also the case for thyroid cancer cells, we stimulated BCPAP with OPN and evaluated CD44 expression by Western Blot analysis. As shown in the Figure 21, OPN treatment significantly increased CD44 protein levels.

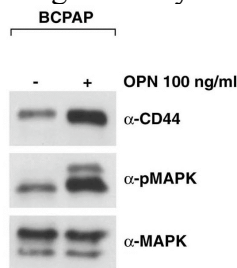


Figure 21: BCPAP cells were stimulated with recombinant OPN for 12 h. Total cell lysates were then prepared and subjected to immunoblot with anti-CD44 antibodies. OPN stimulated CD44 up-regulation and sustained MAPK activation, as shown by staining of the same filter with anti-pMAPK antibodies. The filter was stripped and re-probed with anti-MAPK antibodies to show equal protein loading.

We have shown that OPN stimulates Matrigel invasion and ERK/Akt activation. We sought to determine whether these effects were mediated by the CD44 receptor. To this aim, BCPAP were stimulated with OPN in the presence or the absence of blocking compounds, and downstream signaling and migration ability were evaluated. As shown in figure 22, CD44 functions as an OPN signaling receptor in PTC cells. In fact, pretreatment with CD44 blocking antibodies inhibited MAPK and Akt activation by OPN and also prevented migration through Matrigel. Matrigel invasion induced by OPN is also dependent on the MAPK and Akt pathways.

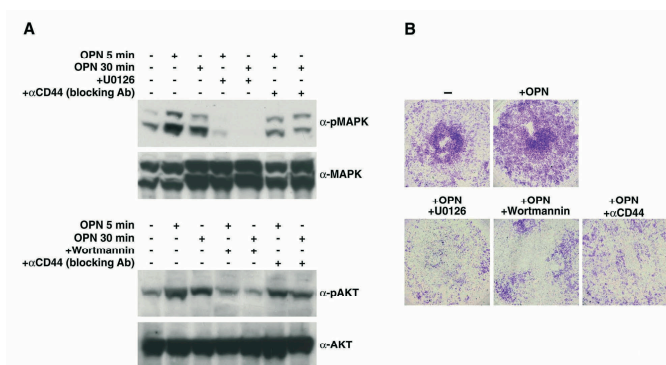


Figure 22: CD44 is involved in OPN-mediated cellular effects. A, Where indicated, cells were preincubated (12 h) with U0126 (10 μ M), wortmannin (100 nM), or CD44-blocking antibody. Total cell lysates were prepared 5 and 30 min after stimulation with the cytokine, as indicated. MAPK and AKT activation was assessed by immunoblot. B,

Cells were preincubated (12 h) with CD44-blocking antibodies, U0126, or wortmannin. Matrigel invasion was analyzed.

Role of CXCR4 in Human Anaplastic Thyroid Carcinomas

CXCR4 is a G protein-coupled receptor (GPCR) that transduces cellular signals for stromal cell derived factor 1 (SDF1), a member of the CXC branch of the chemokine family also designated CXCL12. SDF-1 is chemotactic for B- and T-lymphocyte subsets and is critical for the migration of progenitors during embryologic development of the central nervous, cardiovascular, and hematopoietic systems (Tachibana 1998; Zou 1998). CXCR4 has been shown to have a key role in germ cell migration during embryogenesis and blockade of this receptor in humans results in immobilization of hematopoietic stem cells (Lapidot and Petit 2002). The expression of CXCR4 by mammary carcinoma and other malignancies results in the hijacking of its ability to mediate directed migration resulting in the programming of metastatic spread to target organs that secrete SDF-1 (ie. lymph nodes, bone marrow, lung, and liver). Blockade of CXCR4 with a monoclonal antibody has been reported to inhibit the metastasis of mammary carcinoma cells in a xenografts model in immunodeficient mice (Muller 2001). In a previous report we demonstrated that CXCR4 expression depends on the integrity of the RET/PTC-RAS-BRAF pathway, and that oncogenic activation of each of these proteins can drive CXCR4 overexpression (Castellone et al. 2004). We also found that CXCR4 is expressed and functional in human cell lines derived from papillary thyroid cancers but not in normal thyroid cells. The presence of this receptor has also been confirmed in a set of human PTCs by immunohistochemistry. Anaplastic thyroid carcinoma (ATC) is a rare thyroid cancer type with an extremely poor prognosis that, in some cases, seems to derive from preexisting well differentiated thyroid tumors (WDTC). Here we investigate whether CXCR4 expression is maintained in the progression from WDTC to ATC, and whether it is biologically relevant.

CXCR4 expression in ATC.

Firstly we evaluated CXCR4 mRNA and protein levels in a set of ATC samples versus different samples of normal thyroid tissue. CXCR4 was found to be up-regulated in most of the tumor samples by real time PCR (figure 23).

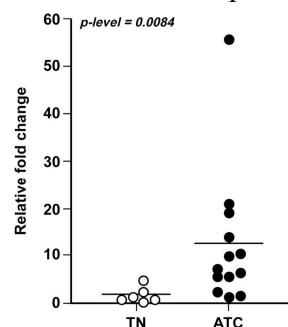


Figure 23: Expression levels of CXCR4 in human ATC samples versus six normal thyroid tissues by real-time RT-PCR. CXCR4 expression levels of tumors (y-axis) are calculated relative to the mean CXCR4 level of normal human thyroid tissues (NT). All experiments have been performed in triplicate, and the average value of the results was plotted on the diagram. P value was calculated with the two-tailed, non-parametric Mann-Whitney test.

To verify whether CXCR4 mRNA overexpression resulted in an increase in the protein levels, we used protein extracts from a different set of ATC samples and 3 normal thyroid tissues in an immunoblot experiment with CXCR4 specific antibodies. As shown in Figure 24, CXCR4 protein levels are higher in ATC samples than in normal thyroid. As a positive control for CXCR4 expression, the ATC cell line ARO was used.

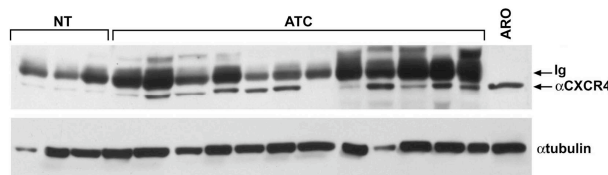


Figure 24: Protein lysates (100 μ g) extracted from the indicated samples underwent western blotting with anti-CXCR4 specific antibodies. Immunocomplexes were revealed by enhanced chemiluminescence. Equal protein loading was ascertained by anti-tubulin immunoblot. NT= normal thyroid tissue; ATC= Anaplastic thyroid carcinoma samples.

Finally, CXCR4 antibodies were used in immunohistochemistry experiments. We evaluated CXCR4 expression in normal thyroid tissues and in a set of ATC samples (n=33). While no CXCR4 expression was detected in normal thyroid tissues, 13 (39%) of the ATC samples scored positive for CXCR4 (not shown). These data indicated that a significant fraction of human ATCs, similarly to other epithelial cancers, features high expression levels of the CXCR4 receptor. Furthermore, they suggested that the increase in CXCR4 levels occurs at the transcriptional level.

Several transgenic mice models of thyroid cancer have been developed by using various oncogenes under the transcriptional control of the thyroid-specific thyroglobulin bovine promoter. Mice expressing either RET/PTC3 (TGPTC3) or TRK/T1 (TGTRK) oncogene (Powell et al. 1998, Russell et al 2000), develop PTC-like tumors; NRAS transgene expression results in follicular tumors that progress to poorly differentiated carcinomas (TGNRAS) (Vitagliano et al. 2006); finally, animals expressing the Simian virus 40 large T antigen (TGSV) present aggressive thyroid cancer with features similar to human ATC (Ledent et al. 1991). To evaluate the expression of CXCR4 in these animal models, we performed western blot analysis with CXCR4 antibodies in different tumor samples of the transgenic mice. Histologic diagnosis of the thyroid lesion was verified before processing of the samples. CXCR4 levels were higher in ATC models than in normal mouse thyroid tissue (not shown). These data, together with previously published (Castellone *et al*, 2004) data suggest that CXCR4 up-regulation is a frequent event in thyroid tumorigenesis and that it may correlates with the malignancy of the disease.

CXCR4 is a functional receptor in human ATC cells

We first identified a suitable cell model to study the role of CXCR4 in ATC. To this aim we tested various normal thyroid and ATC-derived primary and continuous cell lines for CXCR4 expression by western blot analysis.

Normal thyroid cultures displayed low or undetectable CXCR4 expression level, several ATC cell lines featured high levels of the CXCR4 receptor. The increased levels of CXCR4 proteins were associated to an increase in CXCR4 mRNA levels, as assessed by quantitative PCR (Q-PCR) analysis (not shown). To verify the expression of the receptor on the cell surface we performed flow cytometry experiments using a PE-conjugated mouse monoclonal anti-CXCR4 antibody. The percentage of CXCR4 positive cells was determined (figure 25). As shown in the figure both primary (S11T) and continuous ATC cell lines feature membrane expression of CXCR4.

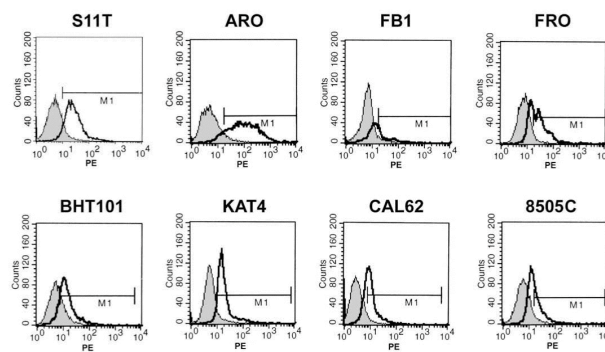


Figure 25: Flow cytometric analysis (FACS) of surface expressed CXCR4 in ATC cells. Subconfluent cells were detached from culture dishes and incubated with phycoerythrin-labeled (PE) antibodies specific for human CXCR4 (R&D Systems, Minneapolis, MN).

SDF-1, was not expressed by ATC cells as assessed by Q-PCR or by ELISA assay (data not shown).

We selected two cell lines, S11T and BHT101 for further experiments. We tested the phosphorylation of two downstream effectors, ERK1/2 and AKT, using phospho-specific antibodies upon stimulation with human recombinant SDF-1 α . SDF-1 α induced rapid and sustained activation of ERK1/2 in both cell lines. AKT activation was also achieved in BHT101 cells upon SDF-1 α treatment, while it was less evident in S11T cells (not shown). Together, these data indicate that CXCR4 is functional in ATC cells.

Biological activity of CXCR4 in ATC cells

To test whether SDF-1 α was able to increase the proliferation rate in these cells, BHT101 and S11T cells were maintained in low serum (2.5%) growth conditions for 24h, and then either left untreated or stimulated with SDF-1 α for 12h. as shown in figure that SDF-1 α consistently enhanced DNA synthesis in both BHT101 and S11T cells. We then used a specific CXCR4 inhibitor, AMD3100 and a small duplex RNA oligo specific for CXCR4, to block this effect. CXCR4 RNA interference was verified by western blot analysis in BHT101 cells (not shown). Normal thyroid cells were insensitive to SDF-1 α stimulation, to CXCR4 silencing and to the effect of AMD3100. As shown in Figure 26, CXCR4 silencing and AMD3100 inhibited SDF-1 α -

mediated BrdU incorporation in ATC cells. When we used the control scrambled siRNA, this inhibitory effect was not observed. The positive effect of SDF-1 α on cell proliferation, measured as S-phase entry, was also observed in other ATC cell lines. To evaluate whether SDF-1 α could stimulate ATC cell growth, we also performed growth curves in low serum (2.5%) conditions. SDF-1 α increased their proliferation rate, and AMD3100 reverted this effect (not shown).

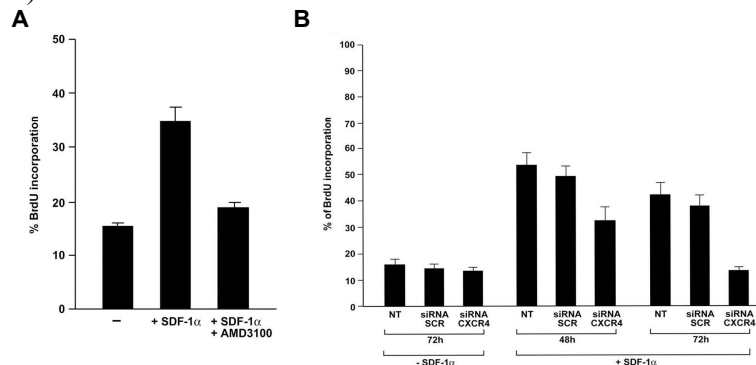


Figure 26: A) BrdU-incorporation was measured to evaluate S-phase entry upon treatment of BHT101 cells with SDF-1 α in the presence or in the absence of the CXCR4 inhibitor AMD3100. B) CXCR4 RNA interference was used to transiently suppress CXCR4 expression in BHT101 cells. BHT101 cells were transfected with small interfering RNAs against CXCR4 (siRNA CXCR4) or control non specific small duplex RNA containing the same nucleotides, but in scrambled fashion (siRNA SCR), and harvested 48 and 72 h later.

AMD3100 inhibits ATC tumor formation in nude mice

It has been previously shown that the CXCR4/SDF-1 α axis plays an important role in the growth and in the metastatic ability of several epithelial cancers. Since we had shown that CXCR4 inhibition blocked SDF1 α -mediated ATC cell growth in culture, and since it has been shown that this chemokine is secreted by stromal tumoral cells (Orimo et al. 2005), we reasoned that SDF-1 α -CXCR4 axis blockade by AMD3100 might inhibit ATC tumor growth. To this aim, we selected BHT101, ARO and KAT4 cells for their ability to respond to SDF-1 α and their ability to form tumors *in vivo* with high efficiency. Nude mice were injected subcutaneously with 5×10^6 cells. When tumors measured approximately 40 mm^3 , mice (n=20 for each cell line) were randomized to receive AMD3100 (1.25 mg/kg/twice a day intraperitoneously) or vehicle 5 days/week for 3-4 weeks. Tumor diameters were measured at regular intervals with caliper. After 21 days, the mean volume of BHT101 tumors in mice treated with AMD3100 was 48 mm^3 , while that of mice treated with vehicle was 620 mm^3 . Tumors induced by ARO and KAT4 reached the volume of 40 mm^3 in only one week. Also in this case AMD3100 was able to inhibit tumor growth, although to a lesser extent. In fact, ARO-induced tumor mean volume at the end of treatment with AMD3100 was 220 mm^3 , while that of mice treated with vehicle was 625 mm^3 . Similar results were also obtained when KAT4 cells were used. In this case, the difference between the mean volume of AMD3100-treated versus vehicle-

treated tumors was not statistically significant after three weeks. However, when treatment was extended for one additional week, AMD3100-treated tumor-mean volume was 180 mm³, while that of mice treated with vehicle was 690 mm³, and the *p* value was 0.039. These data, taken together, demonstrate that treatment with AMD3100 strongly inhibits ATC tumor growth (figure 27).

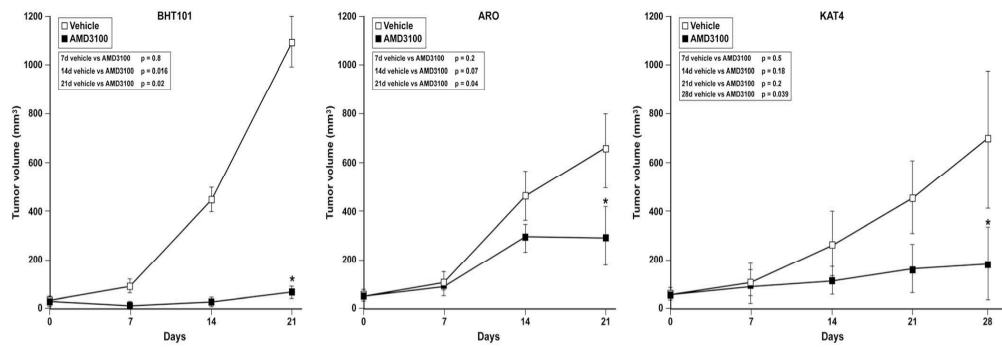


Figure 27: Anti-tumorigenic effects of AMD3100 in ATC cell xenografts. BHT101, ARO and KAT4 cells. All *p* values were two-sided, and differences were statistically significant at *P* < .05.

Role of mast cell infiltrate in PTC

The expression profile of rat thyroid cancer cells transfected with RET/PTC3, HRAS(V12) and BRAF, shows that the three oncogenes induced the expression of a group of genes, including cytokines and chemokines, associated with inflammation and immune response. Among these, chemokines and VEGF have been shown to have a strong chemoattractant potential toward mast cells (Bishoff et al. 2007, Marone et al unpublished observation).

Presence of mast cells in papillary thyroid tumors

We first evaluated by immunohistochemistry the presence of mast cells in 10 normal thyroid tissues and in a set of 96 PTC tissues. The immunostaining of mast cells was performed with a specific mouse monoclonal human anti-tryptase antibody, which specifically stains mast cells. A representative immunostaining is shown in Figure 28 A: the PTC samples displayed the presence of a significant mast cell infiltrate, while the normal tissues did not. Mast cell infiltrate was quantified and the distribution of the mast cell infiltrate in the samples is shown in Figure 28 B. Normal thyroid tissue was characterized by absence or low levels of mast cell infiltrate, while all the PTC samples showed a remarkable mast cell infiltrate. Presence and intensity of mast cell infiltrate did not correlate with clinico-pathological parameters, such as gender, age, etc. Instead, the presence of mast cell infiltrate at the invasion front positively correlated with capsule invasion (figure 28 C).

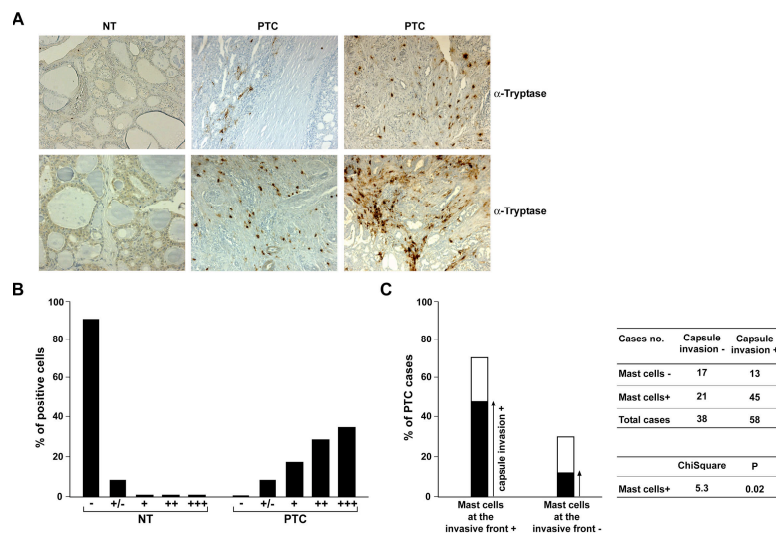


Figure 28: A) Immunohistochemical detection of mast cells presence in normal thyroid tissues and in PTC tumor samples; B) graphic quantification of mast cell infiltration; C) correlation of mast cell invasion front and capsule invasion.

In our laboratory transgenic mice models of PTC have been generated, in which the TRK oncogene is under the transcriptional control of the thyroglobulin promoter (Russel et al. 2000). These mice develop tumors similar to human PTCs. These tumors were analyzed for mast cell infiltrate

with toluidin bleu staining. Thyroid tumors from Tg-TRK transgenic mice showed a significant presence of mast cell infiltrate in comparison to normal control mice thyroid (not shown).

It has been previously shown that the presence of mast cells plays an important role in the growth of several epithelial cancers. To verify whether this is also the case for thyroid cancer, we used xenografts of PTC cells in the presence or in the absence of mast cells in nude mice. To this aim, we have selected the Npa cells derived from a human PTC, for their ability to form tumors in vivo with high efficiency and HMC-1, a human continuous cell line derived from a mastocytosis expressing a constitutively active cKit mutant (Butterfield et al., 1988). Mice were divided into three groups and the cells were injected subcutaneous. The first group was injected with 5×10^6 Npa cells, the second with 1×10^6 HMC-1 cells, and the third was co-injected with 5×10^6 Npa cells and 1×10^6 HMC-1 cells.

As shown in figure 29A, HMC-1 cells alone did not induce tumor formation. In contrast, Npa cell xenografts induced tumor growth with high efficiency. These tumors appeared at 3 weeks after the injection. When Npa were co-injected with HMC-1 cells, tumors occurred earlier and the final volume after 3 weeks was consistently higher than those of the NPA tumors.

End-stage tumors excised from the animals at 6 weeks postinoculation were immunostained for tryptase antigen and the proliferation antigen Ki67, a marker for cycling cells. The immunostaining for tryptase (figure 29B) on mixed xenografts showed that HMC-1 cells were present in these tumors; these data indicate that mast cells survive and proliferate in the presence of PTC cells. On the other hand the immunostaining for Ki67 (figure 29C) indicated an enhanced proliferative index when compared to tumors induced by the Npa cells alone. Thus the presence of mast cells enhanced the proliferation of Npa cells.

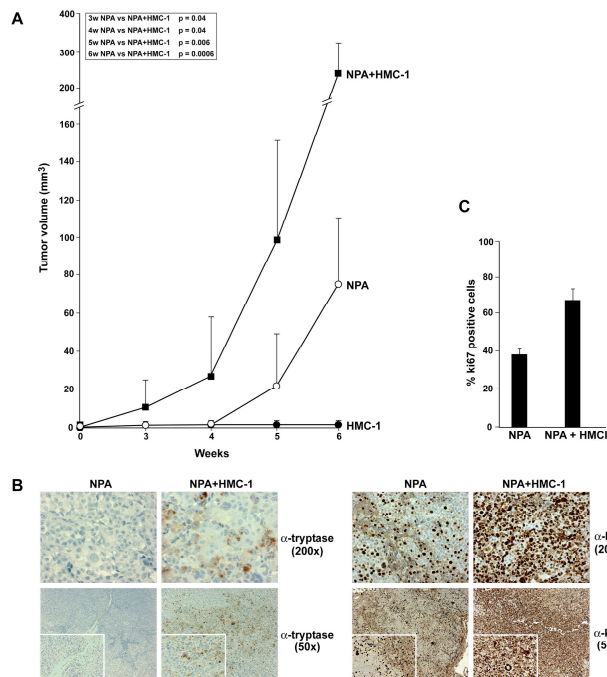


Figure 29: A) mast cell effects on Npa xenografts growth; B) immunostaining of xenografts for tryptase and Ki67 respectively; C) graphic of Ki67 immunostaining.

Then, we asked whether the substantial increase in the tumor size could be attributable to an increase in angiogenesis. To address this question, tumor tissues were also evaluated by using the CD31 antibody and quantitatively assessed for vessel number and diameter. This analysis did not reveal a significant enhancement of vascularization in Npa/HMC-1 compared to Npa tumors. The staining with toluidin bleu, which stains murine mast cells, didn't show the presence of endogenous mast cells in Npa tumors. Thus, mast cells enhanced tumor formation by increasing Npa proliferation. This proliferation does not seem to be a consequence of increased vessel density.

PTC cells action on the mast cells

The immunohistochemical observations suggested a protumorigenic role of mast cells in papillary thyroid carcinomas. To identify the mechanism of recruitment of mast cell in the tumoral site we performed an *in vitro* chemotaxis assay. To this aim, we selected two mast cells lines, HMC-1 and LAD-2. LAD-2 is a continuous cells line that requires SCF for survival and therefore is more similar to primary human mast cells. We tested the ability of conditioned culture media from three PTC cell lines (TPC-1, FB2 and Npa) to induce migration of mast cells through a fibronectin matrix. As shown in figure 30, conditioned culture media from each of the three cell lines were able to induce migration of the HMC-1 and LAD-2 cells; non-conditioned culture medium was used as a negative control.

It has been previously shown that PTC cells are able to produce VEGF-A (Vascular Endothelial Growth Factor A) (Viglietto *et al*, 1995). Furthermore VEGF was one of the genes up-regulated in our gene expression profile experiments. The VEGF family members are secreted dimeric glycoproteins,

consisting of five members VEGF-A, B, C, D and PLGF (placenta growth factor). VEGF-A, a prototype member of a VEGF family, plays a key role in blood vessel growth, induction of vascular permeability, in cardiovascular, haematopoietic and lymphatic development and induction of a leukocyte chemotaxis (Ferrara 2003). Since VEGF-A is a strong chemoattractant for mast cells (Marone *et al*, unpublished observation) we asked whether this factor was responsible for the chemotactic activity. We then blocked VEGF-A activity in PTCs conditioned media with three different blocking antibodies. Figure 30 shows that mast cell chemotaxis is significantly impaired by blocking antibodies to VEGF-A.

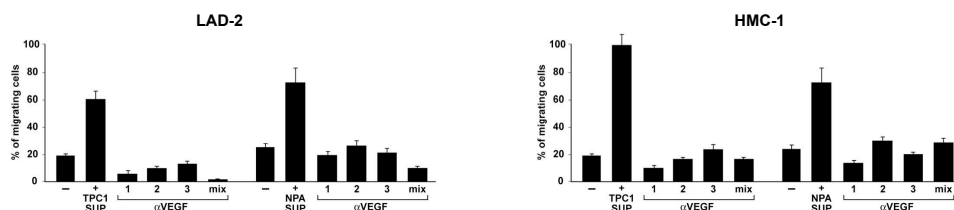


Figure 30: LAD-2 or HMC-1 cells were seeded in the upper chamber of 8 μ M pore transwells and allowed to migrate through fibronectin for 2 h towards serum-free medium or conditioned culture medium from TPC-1 or Npa cell. Where indicated, cells were preincubated with VEGF A blocking antibodies. Thereafter, filters were fixed and stained. The upper surface was wiped clean, and cells on the lower surface were stained with 0.1% crystal violet. The stained cells were lysed in 10% acetic acid. Invasive ability is expressed as the percentage of migrating cells with respect to the total cell number. Quantification was performed in triplicate samples with an ELISA reader. This figure is representative of three independent experiments.

Human mast cells exert their biological functions almost exclusively by humoral immune mechanisms. The array of mediators released by human mast cells is enormous and explains how mast cells can be involved in so many different physiological and pathophysiological functions. Mast cell activation can be achieved by different stimuli and includes: preformed granule release, cytokine and chemokines synthesis and lipid mediators generation.

To evaluate whether PTC conditioned culture media could induce histamine release from mast cells, we used Npa and primary lung mast cells. Figure 31 shows that Npa conditioned culture medium induces histamine release from primary lung mast cells.

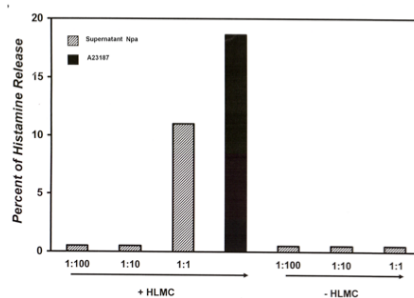


Figure 31: quantification of Histamine release from HLMC stimulated with Npa conditioned culture medium, A23187 calcium ionophore as control.

To verify whether PTC conditioned media could induce transcriptional response in mast cells, we analyzed by Quantitative Real Time Polymerase Chain Reaction (qRT-PCR) the mRNA levels of a set of genes encoding for cytokines and chemokines. Mast cells were incubated for 24 hours with PTC

conditioned culture media, total RNA were extracted and subjected to qPCR. Figure 32 shows that the treatment of mast cells with PTC conditioned culture media significantly up-regulated the mRNA of genes involved in the activation of mast cells: IL-6, GM-CSF, TNF- α , CXCL1/Gro α and CXCL10/IP10. Finally, an ELISA assay demonstrated that CXCL1 and CXCL10 (not shown) are abundantly secreted by HMC-1 and LAD-2 cell lines stimulated with PTC conditioned culture media.

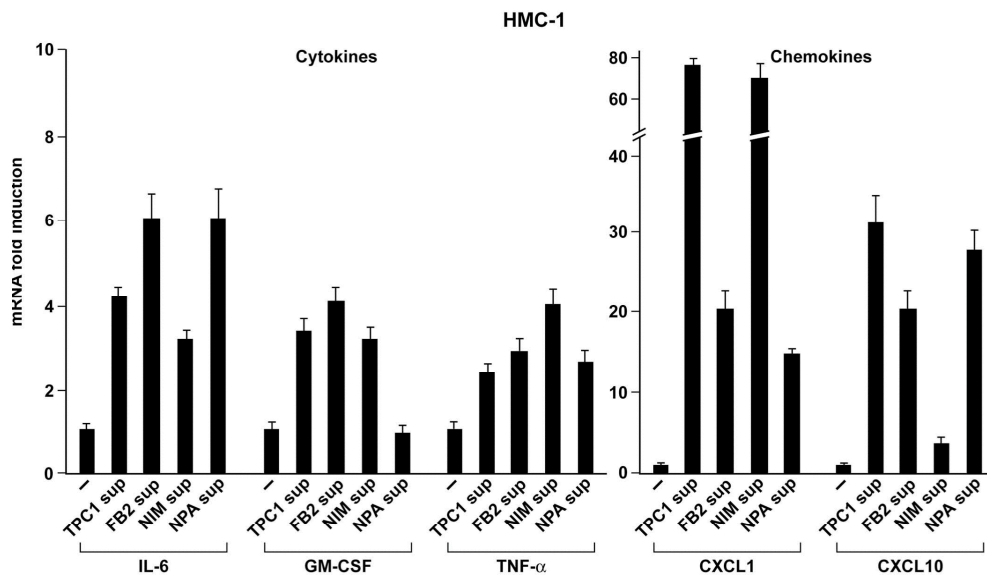


Figure 32: PTC conditioned culture media transcriptional activation of HMC-1; mRNA up-regulation of IL-6, GM-CSF, TNF- α cytokines and CXCL1 and CXCL10.

Mast cells action on PTC cell lines

Then, we asked whether mast cells conditioned culture medium could increase the proliferation rate of PTC cells. To address this point, we measured BrdU incorporation as readout of DNA synthesis after 48h of treatment of PTC cells with HMC-1 and LAD-2 conditioned culture media. Figure 33 shows that treatment with the two conditioned culture media caused an increase in BrdU incorporation rate in PTC cells compared with the non-conditioned medium. The average results of three independent experiments is reported.

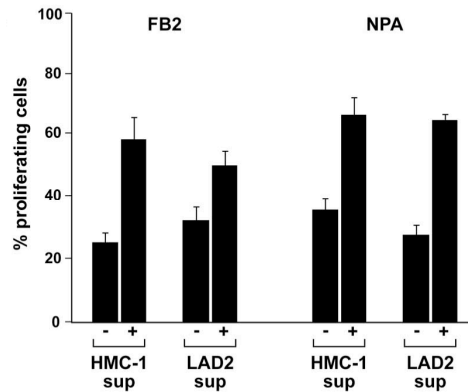


Figure 33: BrdU-incorporation was measured to evaluate S-phase entry upon treatment of FB2 and Npa cells with HMC-1 or LAD-2 conditioned culture media.

Mast cells conditioned culture medium triggers chemotaxis and enhances the invasive behavior of PTC cells

The presence of mast cells at the invasion front correlated with the invasion of the capsule in human PTC. We investigated if mast cells conditioned culture medium was able to enhance migration and extracellular matrix invasion of the PTC cells by using Matrigel chemoinvasion assay. PTC cells (TPC1, FB2, NIM and Npa) were seeded onto the top chamber of transwells, and their ability to invade a reconstituted extracellular matrix (matrigel) toward mast cells conditioned culture medium was evaluated. After 24 h of incubation migrating cells were stained and counted. Figure 34 shows that mast cells conditioned culture media are able to induce a remarkable migration in matrigel of PTC cells, while non-conditioned media were not.

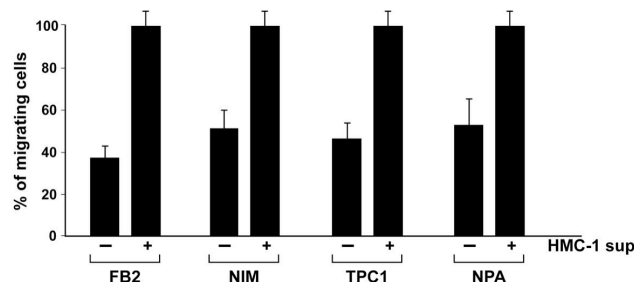


Figure 34: PTC cells were seeded onto upper chamber of 8 μ M pore transwells and allowed to migrate through Matrigel for 24 h towards serum-free medium or conditioned culture medium from HMC-1 cells. Thereafter, filters were fixed and stained. The upper surface was wiped clean, and cells on the lower surface were stained with 0.1% crystal violet. The stained cells were lysed in 10% acetic acid. Invasive ability is expressed as the percentage of migrating cells with respect to the total cell number. Quantification was performed in triplicate samples with an ELISA reader. This figure is representative of three independent experiments.

Identification of mediators of mast cells biological activities

Since Histamine (His) is an important mediator stored in the granules of the mast cells, we asked whether this molecule could mediate mast cell-induced proliferation of PTC cells. To this aim we first verified the expression of the four principal histamine receptors, namely H₁, H₂, H₃, H₄, on PTC cells.

A large panel of PTC cell lines was analysed by RT-PCR the up-regulation of H1 and H2 receptors but not H3 and H4 in PTC cells was found, with respect to normal thyroid cells (not shown). We also confirmed the expression of the H1 and H2 receptors by western blot analysis Figure 35. Protein levels were normalized to tubulin (not shown).

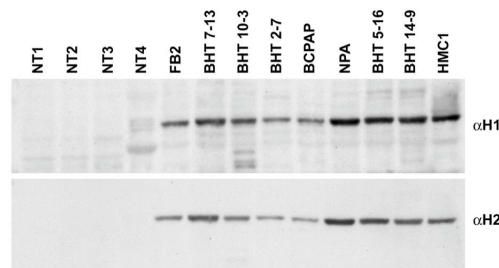


Figure 35: H1 and H2 protein up-regulation in PTC cells, evaluated by immunoblot.

Then, we evaluated the ability of histamine to enhance the proliferation rate of PTC cells lines by performing growth curves. Histamine had a modest but reproducible effect in enhancing PTC cells growth (not shown). BrdU assay on Npa cell treated with Histamine confirmed the results of the growth curves: histamine induces a modest enhancement of S-phase entry Figure 36.

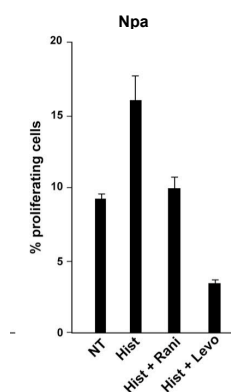


Figure 36: BrdU-incorporation was measured to evaluate S-phase entry upon treatment of Npa cells with Histamine and where indicated Histamine inhibitors Ranitidine or Levocitrizine.

Clearly histamine couldn't account for the strong mitogenic activities of the mast cell conditioned culture medium. We then hypothesized that other mediators might be responsible for those effects. We previously observed that two chemokines, CXCL1/GRO- α and CXCL10/IP10, were important mediators of PTC proliferation and invasive ability and moreover, the PTC conditioned culture medium induces an up-regulation of their expression and secretion in HMC-1 and LAD-2 cells. For these reasons we hypothesized that the combination of histamine with this two chemokines could account for mast cell conditioned media-induced proliferation.

In Figure 37 we show that a combination of histamine and CXCL1/GRO α and CXCL10/IP10 induced thyroid cancer cell proliferation with high efficiency. Indeed in the BrdU proliferation assay we observed that histamine induces 7% of BrdU positive cells, CXCL1/GRO α and CXCL10/IP10 induced 30%; when all the three mediators were added, we obtained an additive effect, with 60% of BrdU positive cells.

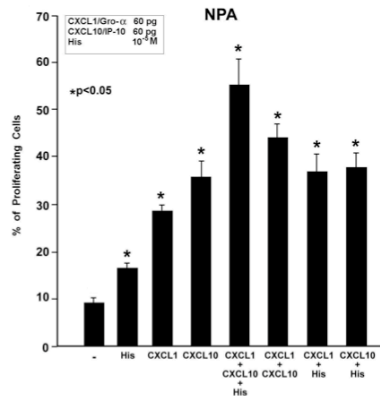


Figure 37: BrdU-incorporation was measured to evaluate S-phase entry upon treatment with Histamine, CXCL1, CXCL10 or in combination. Average results of three independent experiments \pm S.D.

To confirm these results we used blocking antibodies for the two chemokines in immunodepletion experiments. The removal of each chemokine from mast cells conditioned media strongly reduced the proliferation rate of PTC cells; proliferation was completely reverted to basal levels by ablation of the two chemokines. The addition of the recombinant chemokines to the immunodepleted conditioned culture medium carried back the proliferation rate to that of the complete conditioned culture medium (figure 38). Importantly, we also observed that the conditioned media from primary mast cells (HMLC) induce the same enhancement of proliferation in PTC cell (not shown).

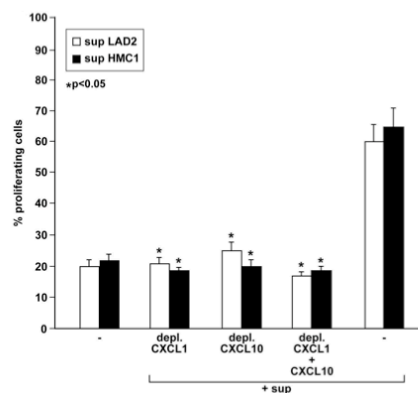


Figure 38: BrdU-incorporation was measured to evaluate S-phase entry upon treatment with HMC-1 or LAD-2 conditioned culture media, were indicated conditioned culture media are immunodepleted for CXCL1, CXCL10 and in combination.

These results suggest that a bidirectional crosstalking between papillary thyroid cancer and mast cells exists. Mast cells recruited in tumor site by PTC cells promote a more severe phenotype by enhancing proliferation and invasive ability of the PTC cancer cells.

DISCUSSION

RET/PTC rearrangements are prevalent in thyroid papillary carcinomas and experimental evidences indicate that they are able to initiate thyroid carcinogenesis, although, very little is known about the mechanisms by which RET/PTC oncogenes transform thyroid follicular cells. Model systems of thyroid follicular cells have been widely used to study growth regulation and neoplastic transformation (Kimura et al. 2003). By using a rat thyroid cell line (PC cells) expressing RET/PTC, HRAS and BRAF oncogenes, we show that these oncogenic proteins belong to the same signaling cascade and are involved in the initiation of PTC carcinogenesis. This pathway starts at the level of RET and, sequentially, triggers RAS, BRAF and ERK stimulation. Consistent with this finding, activating mutations in the three corresponding genes are mutually exclusive in PTC samples (Kimura et al. 2003; Cohen et al. 2003; Soares et al. 2003). In PC thyroid cells, the three activated oncoproteins induce a transformed phenotype together with the stimulation of widely overlapping gene expression signatures. We observed that most of the common targets are under the control of RET/PTC Y1062, this is consistent with the key role of this tyrosine residue to activate the HRAS/ BRAF/ERK pathway. However, the analysis of transcriptional profiles indicates that the three oncoproteins are not completely equivalent. Indeed, in addition to targets common to RET/PTC3, HRAS and BRAF, there were relatively large sets of genes specifically modulated by only one or two of the three oncogenes. Overall, the similarity between transcriptional profiles of HRAS(V12) and BRAF(V600E) thyroid cells was greater than those between RET/PTC3 and HRAS or RET/PTC3 and BRAF cells. This was not unexpected; although the three oncoproteins work together along a single cascade, they are biochemically different, and therefore able to trigger specific signals in addition to the common ones. Molecular genetic evidences nicely support this concept. For instance, BRAF mutations are frequently associated with aggressive thyroid carcinomas, such as poorly differentiated and anaplastic carcinomas, that rarely, if ever, harbor RET/PTC rearrangements (Nikiforova et al. 2003). On the other hand, RAS point-mutations are rare in classic PTC and, instead, characterize PTC of the follicular variant that are rarely affected by mutations in BRAF or RET (Zhu et al. 2003). Consistent with this, PC RAS(V12) and PC BRAF(V600E) cells express genes that are potentially implicated in cancer progression.

Our data show that the RET/PTC-RAS-BRAF signaling cascade stimulates the overexpression of several cytokines and chemokines, i.e., OPN, CCL2, CXCL1 and CXCL10. Interestingly we also found the expression of some receptors for these cytokines such as CD44, OPN receptor, and chemokines CXCR4, CXCR2 and CXCR3, the receptors for SDF1, CXCL1 and CXCL10, respectively. Therefore, several autocrine/paracrine loops may mediate biological activities in PTC that are relevant for the establishment of the neoplastic phenotype, e.g., autonomous proliferation and motility.

Chemokines orchestrate immune reactions, but are also involved in the pathogenesis of several human diseases, such as chronic obstructive pulmonary diseases, asthma and allergic diseases, atherosclerosis and cancer. Interestingly, high levels of some chemokines, such as CXCL8, CXCL12, CXCL9 and CXCL10 have been detected at high levels in the thyroid and in the serum of patients affected by autoimmune thyroid diseases, such as Grave's disease (GD) and Hashimoto's thyroiditis (HT). Since several years an association between autoimmune thyroid diseases and well differentiated thyroid carcinomas has been reported, in particular between HT and papillary thyroid carcinoma (PTC). These observations are sustained by the observation that some cells, in the context of HT, display a RET/PTC rearrangement, which is typical of PTC. Our data, by identifying chemokines and inflammatory mediators as part of the program of gene expression induced by the RET/PTC oncoprotein, support the hypothesis that oncogene activation precedes and causes inflammation.

We show that OPN up-regulation is involved in the invasive phenotype of PTC. Overall, as many as 70% of human PTC are estimated to carry mutations at the level of the RET-RAS-BRAF-ERK signaling cascade (Fagin et al. 2004). We previously reported high levels of OPN and CD44v6 in follicular cells derived from rat thyroid glands and transformed by the RET/PTC oncogene (Castellone et al. 2004). We here show that OPN and CD44v6 up-regulation is a common feature of PTC cells that express the RET/PTC or BRAF V600E oncogenes. This finding suggests that activation of the OPN-CD44v6 axis is one of the end points of the RET-RAS-BRAF-ERK oncogenic cascade. This model is consistent with the idea that in other cell types, OPN expression is induced by the RAS oncogene (Wu et al. 2000, Denhardt et al. 2003) and is dependent on the ERK cascade (Geissinger et al. 2002), and that CD44v6 splicing is under control of the RAS-ERK pathway (Matter et al. 2005). Since OPN is able to induce CD44v6 overexpression (Gao et al. 2003), it is conceivable that in PTC cells, the RET-RAS-BRAF-ERK oncogenic cascade triggers OPN and CD44v6 up-regulation; this leads to OPN-CD44v6 binding, thereby further increasing CD44v6 up-regulation and enhancing ERK and AKT signaling. It is noteworthy that AKT activation is a common feature of aggressive thyroid cancers (Vasko et al. 2004). The foregoing functional autocrine loop may sustain the invasive capability of PTC cells consistently. In this study we show that OPN up-regulation correlates with aggressive clinicopathological features of PTC. Indeed, the presence of lymph node metastases and tumor size both positively correlated with OPN positivity. Thus, OPN might be a diagnostic and prognostic marker for these tumors. Indeed, OPN, which also occurs in blood, has already proven useful as a tumor marker for ovarian (Schorge et al. 2004) and lung (Schneider et al. 2004) carcinomas. Given the low prevalence of OPN overexpression in PTC-FV, our findings anticipate that OPN detection will have a rather low sensitivity in this particular PTC variant. However, our series of PTC-FV is too small to draw firm conclusions. Furthermore, it should be noted that the PTC-

FV were all included in the T1-T2 stages, where the positivity for OPN is less prevalent. Our experiments with CD44-blocking antibodies and ERK kinase and PI3-K inhibitors provide proof of principle that the OPN-CD44v6 pathway may be a molecular target for therapeutic intervention in cases of aggressive PTC.

We previously reported functional expression of CXCR4 in human papillary thyroid cancer (Castellone et al. 2004). Furthermore, Hwang and colleagues showed that an anaplastic cell line, ARO, expressed high levels of functional CXCR4 (Hwang et al. 2003). We screened a large panel of human ATC established and primary cell cultures for CXCR4 expression, both at the mRNA and at the protein level, this receptor is overexpressed in ATC with respect to normal thyroid samples. In contrast, SDF-1 was not detected. The molecular mechanisms underlying CXCR4 up-regulation in ATC are currently unknown. Since we had previously shown that CXCR4 expression was under the control of the RET/PTC-RAS-BRAF-ERK pathway in PTCs (Castellone et al. 2004), and since this pathway is also activated in ATC, we asked whether CXCR4 expression correlated with the BRAF status in ATC. The ATC cell lines that we used in this study had been previously characterized for BRAF mutations. Furthermore, human ATC samples were screened for the presence of BRAF mutations. We found that most of the samples expressed CXCR4, and this expression was present in both the BRAF positive and in the BRAF negative tumors and cell lines. These data suggest that CXCR4 upregulation in ATC is not necessarily linked to the BRAF pathway, and that it can be possibly achieved through different mechanisms. The mechanisms of CXCR4 up-regulation in cancer so far described are various and complex. It has been shown that NF-kappaB positively regulates the expression of CXCR4 (Helbig et al. 2003) in breast cancer cells. Interestingly, NFkB is activated in human thyroid cancer cells (Visconti et al. 1997, Pacifico et al 2004). Transduction of human thyroid cancer cells with the mutant BRAF(V600E) allele induced an increase in NFkB DNA-binding activity (Palona et al. 2006). Thus, it is possible that CXCR4 expression in ATC is sustained by high NFkB activity, which can be the result either of BRAF activation or of the activation of other still undiscovered pathways.

We also show that the CXCR4 expressed on the ATC cell surface is able to transduce biochemical signals into the cell. Indeed, stimulation of ATC cells with recombinant human SDF-1 α activated ERK1/2 and, less consistently, AKT pathways in ATC cells. Moreover, we found that SDF-1 α stimulated cell growth of different ATC cell cultures, which was inhibited by the small CXCR4 inhibitor AMD3100. Given the high rate of mortality of this cancer and the lack of effective therapies, we focused our efforts in the identification of novel potential therapeutic targets in ATC. We found that the treatment with AMD3100 significantly suppressed the development of tumors in different xenograft models of ATC cells in nude mice.

The more dramatic biological effects of CXCR4 inhibition observed in the animals with respect with those observed in cell culture could be explained

by the fact that SDF-1 can act, in tumor microenvironment, at multiple levels. Indeed, tumoral stromal cells, such as fibroblasts and bone marrow derived cells, express high levels of SDF-1 (Orimo et al. 2005), which can directly enhance the growth of epithelial tumoral cells and can recruit endothelial progenitors, thus favoring angiogenesis. However, when we analyzed xenograft tumors for CD31-positive tumor capillaries, we found that there were no differences in vessel density of AMD3100-treated versus untreated tumors. Preliminary data suggest that AMD3100 activity in xenografts correlates better with a proapoptotic than with an antiproliferative activity (Guarino et al., unpublished observation). Our findings are in accord with previous reports regarding the use of CXCR4 inhibitors in brain tumor models (Rubin et al 2003, Yang et al. 2007). Although treatment of ATC xenografts with AMD3100 did not induce a complete regression of tumors, we observed a strong reduction in growth rate, which was more dramatic in the case of BHT101 xenografts. It is conceivable that the combination of conventional anticancer therapies with CXCR4 targeting would display a stronger antineoplastic effect. Given the strong antitumor activity of AMD3100, newer generation compounds have been developed, such as AMD3465. This compound differs from the bicyclam AMD3100 in that it is a monocyclam endowed with greater solubility in water, higher affinity for CXCR4 and a potent anti-tumor activity (Yang et al. 2007). Although these compounds are effective in inhibiting various cancers, long-term sustained dosing of AMD3100 displayed certain toxicity (Hendrix et al. 2004). For this reason further studies, aimed at understanding the effects of long-term administration of CXCR4 inhibitors, must be pursued. Despite these considerations, our data, together with several other reports, strongly indicate that the inhibition of this pathway should be actively evaluated as a novel anticancer therapy.

PTC is associated with a striking chronic inflammatory reaction in about 30% of cases (Rosai 1992; Scarpino et al. 2000). Chemokines secreted by tumor cells can recruit leukocytes (macrophages, dendritic cells, T cells and

natural killer cells) to tumor sites. We have shown that RET/PTC/RAS/BRAF oncogenes in PTC induced an “inflammatory program” that, among other effects, can trigger rapid recruitment of inflammatory cells to the tumor site. Recent studies have demonstrated that mast cells, a component of innate immunity, are present in several tumors, (Ribatti et al. 1999, Vacca et al. 2001, Tosato et al. 2004, Coussens et al. 1999, Soucek et al. 2007) We found that human PTCs display an intense mast cells infiltrate, which is not present in normal thyroid. Mast cell infiltrate positively correlated with invasive ability of PTCs, but not with vessel density. This result is in contrast with other observations showing that in several cancer types mast cell infiltrate correlates with increased angiogenesis (Coussens et al. 1999, Soucek et al. 2007). Our data instead support a role of mast cells in PTC cell proliferation. Not only mast cell induced cell growth in vivo and in vitro, but also stimulated PTC cell invasion. Mast cell, once activated, can secrete a plethora of growth factors, angiogenic factor, pro-inflammatory molecules. The activation of mast cells can be activated through various stimuli. The nature of these stimuli in our model system is currently unknown, and will be the object of further investigation. The activity of mast cells on thyroid cancer cells has been investigated through mast cells conditioned media stimulation of PTC cell. These experiments showed that chemokines (CXCL1 and CXCL10) contained in mast cell conditioned media together with histamine, strongly induced PTC cell proliferation. These results indicate that mast cell infiltrate promote proliferation and invasive ability of PTC. These data also suggest that the inhibition of chemokines, by blocking both autocrine loops and mast cell released factors, might be a potential therapy for these carcinomas. Furthermore, therapies that block mast cell degranulation or cytokine synthesis could also be of potential interest in these cancers. Our data, although indicating a role for mast cells in PTC formation, also raise new questions. When are mast cells recruited in PTC formation? In some model systems, such as those proposed by Coussens (Junakur et al. 2006), mast cell infiltrate is found at very early stages. Whether this is the case also for PTC is currently under investigation. Are mast cells necessary for PTC cancer formation? Experiments in which mast cells deficient mice (Kit^{-/-}) will be crossed with PTC-prone mice clarify this issue.

CONCLUSIONS

Our findings, taken together, indicate that oncogenes typically activated in human PTCs induce a common transcriptional signature characterized by the presence of genes encoding for inflammatory factors, such as cytokines and chemokines. Interestingly, the receptors for some of these ligands are also overexpressed, thus generating autocrine loops that sustain PTC growth and invasive ability; these data suggest that these soluble mediators and/or their receptors can be targeted by novel therapeutic agents for the treatment of thyroid carcinomas. In support of this, we identify CXCR4 as potential target of ATC anticancer therapy and suggest that AMD3100, or other specific CXCR4 inhibitors, should be developed and tested for the therapy of human ATC. Finally, our data support the occurrence of a complex interplay between mast cells and PTC cells, whereby PTC cells support mast cell recruitment, survival and activation, and mast cells sustain PTC cell proliferation and invasive ability.

REFERENCES

- Airaksinen M.S. et al. GDNF family neurotrophic factor signaling: four masters, one servant? *Mol. Cell Neurosci.* 1999;13; 313-325.
- Balkwill F, Cancer and the chemokine network. *Nat Rev Cancer* 2004; 4, 540-550
- Balkwill F, and Mantovani A. Inflammation and cancer: back to Virchow? *Lancet* 2001;357: 539-545.
- Baron JA and Sandler RS. Nonsteroidal anti-inflammatory drugs and cancer prevention. *Ann Rev Med* 2000: 51: 511-523
- Beaven MA Histamine, *N Engl J Med* 1976; 294, 1, 30-36
- Bishoff SC Role of mast cells in allergic and non-allergic immune responses: comparison of human and murine data. *Nat Rev Immunol* 2007; 7, 93-104
- Borrello MG, Alberti L, Fischer A, Degl'innocenti D, Ferrario C, Gariboldi M, Marchesi F, Allavena P, Greco A, Collini P, Pilotti S, Cassinelli G, Bressan P, Fugazzola L, Mantovani A, Pierotti MA. Induction of a proinflammatory program in normal human thyrocytes by the RET/PTC1 oncogene. *Proc Nat Acad Sci U.S.A.* 2005; 102: 14825-14830
- Brandi ML, Gagel RF, Angeli A, Bilezikian JP, Beck-Peccoz P, Bordi C, Conte-Devolx B, Falchetti A, Gheri RG, Libroia A, Lips CJ, Lombardi G, Mannelli M, Pacini F, Ponder BA, Raue F, Skogseid B, Tamburrano G, Thakker RV, Thompson NW, Tomassetti P, Tonelli F, Wells SA Jr, Marx SJ. Guidelines for diagnosis and therapy of MEN type 1 and type 2. *J Clin Endocrinol Metab.* 2001 Dec;86(12):5658-71. Review
- Bunone G, Vigneri P, Mariani L, Butò S, Collini, P., Pilotti, S., Pienotti, M.A., Borganzone, I. Expression of angiogenesis stimulators and inhibitors in human thyroid tumors and correlation with clinical pathological features. *Am J Pathol* 1999; 155: 1967-76
- Burnet FM. Cancer – a Biological Approach. *Br Med J* 1957; 1: 841-847
- Burnet FM. Immunological factors in the process of carcinogenesis. *Br Med Bull* 1964 20: 154-158
- Burnet FM. Immunological surveillance in neoplasia. *Transplant Rev* 1971 7: 3-25

Butler WT. The nature and significance of osteopontin. *Connect Tissue Res.* 1989; 23(2-3): 123-36. Review.

Butterfield JH, Weiler D, Dewald G, Gleich GJ. Establishment of an immature mast cell line from a patient with mast cell leukaemia. *Leuk Res* 1988; 12: 345

Carlomagno F, Salvatore G, Cirafici AM, De Vita G, Melillo RM, de Franciscis V, Billaud M, Fusco A, Santoro M. The different RET-activating capability of mutations of cysteine 620 or cysteine 634 correlates with the multiple endocrine neoplasia type 2 disease phenotype. *Cancer Res.* 1997 Feb 1;57(3):391-5

Cascieri MA, Springer M. The chemokine/chemokine-receptor family: potential and progress for therapeutic intervention. *Curr Opin Chem Biol* 2000; 4: 420-427

Castellone MD, Cirafici AM, De Vita G, De Falco V, Malorni L, Tallini G, Fagin JA, Fusco A, Melillo RM, Santoro M. Ras-mediated apoptosis of PC CL 3 rat thyroid cells induced by RET/PTC oncogenes. *Oncogene.* 2003 Jan 16;22(2):246-55.

Castellone MD, Guarino V, De Falco V, Carlomagno F, Basolo F, Faviana P, Kruhoffer M, Orntoft T, Russell JP, Rothstein JL, Fusco A, Santoro M, Melillo RM. Functional expression of the CXCR4 chemokine receptor is induced by RET/PTC oncogenes and is a common event in human papillary thyroid carcinomas. *Oncogene* 2004; Aug 5; 23(35):5958-67.

Castellone MD, Celetti A, Guarino V, Cirafici AM, Basolo F, Giannini R, Medico E, Kruhoffer M, Orntoft TF, Curcio F, Fusco A, Melillo RM, Santoro M. Autocrine stimulation by osteopontin plays a pivotal role in the expression of the mitogenic and invasive phenotype of RET/PTC-transformed thyroid cells. *Oncogene.* 2004; Mar 18; 23(12):2188-96.

Coge F, Guenin SP, Rique H, Boutin JA, Galizzi JP. Structure and expression of the human histamine H4-receptor gene. *Biochem Biophys Res Commun* 2001; 284: 301-309

Cohen Y, Xing M, Mambo E, Guo Z, Wu G, Trink B, Beller U, Westra WH, Ladenson PW, Sidransky D. BRAF mutation in papillary thyroid carcinoma. *J Natl Cancer Inst* 2003;95:625-7.

Coussens LM, Raymond WW, Bergers G, Laig-Webster M, Behrendysen O, Werb Z, Caughey GH, Hanahan D. Inflammatory mast cells up-regulate angiogenesis during squamous epithelial carcinogenesis. *Genes Dev* 1999; 13: 1382-1397

Coussens LM. and Werb Z. Inflammatory cells and cancer: think different! *J Exp Med* 2001; 193: 23-26

Coussens LM, Werb Z. Inflammation and cancer. *Nature* 2002; 420: 860-867

Craig AM, Bowden GT, Chambers AF, Spearman MA, Greenberg AH, Wright JA, McLeod M, Denhardt DT. Secreted phosphoprotein mRNA is induced during multi-stage carcinogenesis in mouse skin and correlates with the metastatic potential of murine fibroblasts. *Int J Cancer*. 1990; Jul 15; 46(1):133-7.

Crocker J, Smith PJ. A quantitative study of mast cells in Hodgkin's disease. *J Clin Pathol* 1984 37: 519-22

Curcio F, Ambesi-Impiombato FS, Perrella G, Coon HG. Long-term culture and functional characterization of follicular cells from adult normal human thyroids. *Proc Natl Acad Sci U S A*. 1994 Sep 13;91(19):9004-8.

Davies H, Bignell GR, Cox C, Stephens P, Edkins S, Clegg S, Teague J, Woffendin H, Garnett MJ, Bottomley W, Davis N, Dicks E, Ewing R, Floyd Y, Gray K, Hall S, Hawes R, Hughes J, Kosmidou V, Menzies A, Mould C, Parker A, Stevens C, Watt S, Hooper S, Wilson R, Jayatilake H, Gusterson BA, Cooper C, Shipley J, Hargrave D, Pritchard-Jones K, Maitland N, Chenevix-Trench G, Riggins GJ, Bigner DD, Palmieri G, Cossu A, Flanagan A, Nicholson A, Ho JW, Leung SY, Yuen ST, Weber BL, Seigler HF, Darrow TL, Paterson H, Marais R, Marshall CJ, Wooster R, Stratton MR, Futreal PA. Mutations of the BRAF gene in human cancer. *Nature* 2002 .Jun 27;417(6892):949-54.

de Paulis A, Ciccarelli A, de Crescenzo G, Cirillo R, Patella V, Marone G. Cyclosporin H is a potent and selective competitive antagonist of human basophil activation by N-formil-methionyl-leucyl- phenylalanine. *J Allergy Clin Immunol* 1996; 98: 152-64

de Paulis, A, Prevete N, Fiorentino I, Walls AF, Curto M, Petraroli A, Castaldo V, Ceppa P, Fiocca R, Marone G. Basophils infiltrate human gastric mucosa at sites of *Helicobacter pylori* infection, and exhibit chemotaxis in response to *H. pylori*-derived peptide Hp(2-20). *J Immunol* 2004; 172: 7734-43

de Paulis A, Prevete N, Fiorentino I, Rossi FW, Staibano, S, Montuori N, Ragno P, Longobardi A, Liccardo B, Genovese A, Ribatti D, Walls A, F.,

- Marone G. Expression and functions of the vascular endothelial growth factors and their receptors in human basophils. *J Immunol* 2006 177: 7322-7331
- De Visser KE, Eichten A, Coussens LM. Paradoxical roles of the immune system during cancer development, *Nat Rev Cancer* 2006; 6: 24 - 37
- Denhardt DT, Guo X. Osteopontin: a protein with diverse functions. *FASEB J*. 1993 Dec;7(15):1475-82. Review.
- Dhawan P, and Richmond A. Role of CXCL1 in tumorigenesis of melanoma. *J Leukoc. Biol.* 2002 72:9-18.
- Di Pasquale M, Rothstein JL, Palazzo JP. Pathologic features of Hashimoto's-associated papillary thyroid carcinoma. *Hum Pathol* 2001; 32: 24-30
- Donghi R, Longoni A, Pilotti S, Michieli P, Della Porta G, Pierotti MA. Gene p53 mutations are restricted to poorly differentiated and undifferentiated carcinomas of the thyroid gland. *J Clin Invest.* 1993 Apr;91(4):1753-60.
- Drosten M, Pützer BM. Mechanisms of Disease: cancer targeting and the impact of oncogenic RET for medullary thyroid carcinoma therapy. *Nat Clin Pract Oncol.* 2006 Oct;3(10):564-74. Review
- Dunn GP, Old LJ, Schreiber RD. The immunobiology of cancer immunosurveillance and immunoediting. *Immunity* 2004; 21: 137-148
- Ehrlich P. Ueber den jetzigenStand der Karzinomforshung. *Ned. Tijdschr. Geneesk* 1909; 5: 273-290.
- Eisenberg BL, Hensley SD. Thyroid cancer with coexistent Hashimoto's thyroiditis. Clinical assessment and management. *Arch Surg* 1989; 124: 1045-7
- Fagin JA, Matsuo K, Karmakar A, Chen DL, Tang SH, Koeffler HP. High prevalence of mutations of the p53 gene in poorly differentiated human thyroid carcinomas. *J Clin Invest.* 1993 Jan;91(1):179-84.
- Fagin JA. How thyroid tumors start and why it matters: kinase mutants as targets for solid cancer pharmacotherapy. *J Endocrinol.* 2004 Nov;183(2):249-56. Review.
- Ferrara N. The role of vascular endothelial growth factor in pathological angiogenesis. *Breast Cancer Res Treat* 1995; 36: 127-137
- Ferrara N, Gerber HP, LeCouter J. The biology of VEGF and its receptors. *Nat Med.* 2003 Jun;9(6):669-76. Review.

Ferrara N, Hillan KJ, Novotny W. Bevacizumab (Avastin), a humanized anti-VEGF monoclonal antibody for cancer therapy. *Biochem Biophys Res Commun* 2005; 333: 328-335

Folkman J. Angiogenesis and angiogenesis inhibition: an overview. In *Regulation of Angiogenesis*, pp. 1-8. Eds ID Goldberg & E. M. Rosen 1997; Basel, Boston, Berlin: Birkhauser

Fujisawa N, Hayashi S, Kurdowska A, Carr FK, Miller EJ. Inhibition of Gro- α -induced human endothelial cell proliferation by the α -chemokine inhibitor antileukinate. *Cytokine* 1999; 11: 231-238

Fusco A, Berlingieri MT, Di Fiore PP, Portella G, Grieco M, Vecchio G. One- and two-step transformations of rat thyroid epithelial cells by retroviral oncogenes. *Mol Cell Biol.* 1987 Sep;7(9):3365-70.

Galli SJ, Nakae S, Tsay M. Mast cells in the development of adaptive immune responses. *Nat Rev Immunol* 2005; 6: 135-142

Gantner F, Sakai K, Tusche MW, Cruikshank WW, Center DM, Bacon KB. Histamine h(2) and h(4) receptors control histamine-induced interleukin-16 release from human CD8(+) cells. *J Pharmacol Exp Ther* 2002; 303: 300-307

Gao P, Zhou XY, Yashiro-Ohtani Y, Yang YF, Sugimoto N, Ono S, Nakanishi T, Obika S, Imanishi T, Egawa T, Nagasawa T, Fujiwara H, Hamaoka T. The unique target specificity of a nonpeptide chemokine receptor antagonist: selective blockade of two Th1 chemokine receptors CCR5 and CXCR3. *J Leukoc Biol.* 2003 Feb;73(2):273-80

García-Rostán G, Costa AM, Pereira-Castro I, Salvatore G, Hernandez R, Hermsem MJ, Herrero A, Fusco A, Cameselle-Teijeiro J, Santoro M. Mutation of the PIK3CA gene in anaplastic thyroid cancer. *Cancer Res.* 2005 Nov 15;65(22):10199-207

Garcia-Rostan G, Zhao H, Camp RL, Pollan M, Herrero A, Pardo J, Wu R, Carcangiu ML, Costa J, Tallini G. ras mutations are associated with aggressive tumor phenotypes and poor prognosis in thyroid cancer. *J Clin Oncol.* 2003 Sep 1;21(17):3226-35.

Geissinger E, Weisser C, Fischer P, Scharl M, Wellbrock C. Autocrine stimulation by osteopontin contributes to antiapoptotic signalling of melanocytes in dermal collagen. *Cancer Res.* 2002 Aug 15;62(16):4820-8.

- Gerard C, Rollins BJ. Chemokines and disease. *Nat Immunol* 2001; 2: 108-115
- Gilfillan AM and Tzaczyk C. Integrated signalling pathways for mast-cell activation. *Nat Rev Immunol* 2006; 6: 218-30
- Gruber BL, Marchese MJ, Kew R. Angiogenic factors stimulate mast-cell migration. *Blood* 1995; 86: 2488-2493
- Hallgren J, Pejler G. Biology of mast cell tryptase. An inflammatory mediator. *FEBS J.* 2006 May;273(9):1871-95. Review.
- Hanahan D, Weimberg RA. The hallmarks of cancer. *Cell* 2000; 100: 57-70
- Hanahan D, and Folkman J. Patterns and emerging mechanisms of the angiogenic switch during tumorigenesis. *Cell* 1996; 86, 353-364
- Helbig G, Christopherson KW 2nd, Bhat-Nakshatri P, Kumar S, Kishimoto H, Miller KD, Broxmeyer HE, Nakshatri H. NF-kappaB promotes breast cancer cell migration and metastasis by inducing the expression of the chemokine receptor CXCR4. *J Biol Chem.* 2003 Jun 13;278(24):21631-8.
- Hendrix CW, Collier AC, Lederman MM, Schols D, Pollard RB, Brown S, Jackson JB, Coombs RW, Glesby MJ, Flexner CW, Bridger GJ, Badel K, MacFarland RT, Henson GW, Calandra G; AMD3100 HIV Study Group. Safety, pharmacokinetics, and antiviral activity of AMD3100, a selective CXCR4 receptor inhibitor, in HIV-1 infection. *J Acquir Immune Defic Syndr.* 2004 Oct 1;37(2):1253-62.
- Hingorani SR, Jacobetz MA, Robertson GP, Herlyn M, Tuveson DA. Suppression of BRAF(V599E) in human melanoma abrogates transformation. *Cancer Res.* 2003 Sep 1;63(17):5198-202.
- Hofstra CL, Desai PJ, Thurmond RL, Fung-Leung WP. Histamine H4 receptor mediates chemotaxis and calcium mobilization of mast cells. *J Pharmacol Exp Ther* 2003; 305: 1212-1221
- Hwang JH, Hwang JH, Chung HK, Kim DW, Hwang ES, Suh JM, Kim H, You KH, Kwon OY, Ro HK, Jo DY, Shong M. CXC chemokine receptor 4 expression and function in human anaplastic thyroid cancer cells. *J Clin Endocrinol Metab.* 2003 Jan;88(1):408-16.
- Iwashita T, Kato M, Murakami H, Asai N, Ishiguro Y, Ito S, Iwata Y, Kawai K, Asai M, Kurokawa K, Kajita H, Takahashi M. Biological and biochemical properties of Ret with kinase domain mutations identified in multiple

endocrine neoplasia type 2B and familial medullary thyroid carcinoma. *Oncogene*. 1999 Jul 1;18(26):3919-22.

Jangi SM, Pérez JL, Ochoa-Lizarralde B, Martin-Ruiz I, Asumendi A, Pérez-Yarza G, Gardeazabal J, Diaz-Ramon JL, Boyano MD. H1 histamine receptor antagonists induce genotoxic and caspase-2-dependent apoptosis in human melanoma cells. *Carcinogenesis* 2006; 27: 1787-1796

Jhiang S.M. The RET proto-oncogene in human cancers. *Oncogene*. 2000; 19; 5590-5597.

Junankar SR, Eichten A, Kramer A, de Visser KE, Coussens LM. Analysis of immune cell infiltrates during squamous carcinoma development. *J Invest Dermatol Symp Proc*. 2006 Sep;11(1):36-43.

Katoh R, Miyagi E, Kawaoi A, Hemmi A, Komiyama A, Oyama T, Shibuya M. Expression of vascular endothelial growth factor (VEGF) in human thyroid neoplasms. *Hum Pathol* 1999; 30: 891-7

Kawamoto Y, Takeda K, Okuno Y, Yamakawa Y, Ito Y, Taguchi R, Kato M, Suzuki H, Takahashi M, Nakashima I. Identification of RET autophosphorylation sites by mass spectrometry. *J Biol Chem* 2004;279:1421324.

Kimura ET, Nikiforova MN, Zhu Z, Knauf JA, Nikiforov YE, Fagin JA. High prevalence of BRAF mutations in thyroid cancer: genetic evidence for constitutive activation of the RET/PTC-RAS-BRAF signalling pathway in papillary thyroid carcinoma. *Cancer Res*. 2003; 63;1454-1457.

Kirshenbaum AS, Akin C, Wu Y, Rottem M, Goff JP, Beaven MA, Rao VK, Metcalfe DD. Characterization of novel stem cell factor responsive human mast cell lines LAD1 and 2 established from a patient with mast cell sarcoma/leukaemia; activation following aggregation of FcεRI or FcγRI. *Leuk Res* 2003; 27: 677-82

Klein M, Picard E, Vignaud JM, Marie B, Bresler L, Toussaint B, Weryha G, Duprez, A, Leclère, J. Vascular endothelial growth factor gene and protein: strong expression in thyroiditis and thyroid carcinoma. *J Endocrin* 1999; 161: 41-49

Klein M, Vignaud JM, Hennequin V, Toussaint B, Bresler L, Plénat F, Leclère J, Duprez A, Weryha G. Increased expression of the vascular endothelial growth factor is a pejorative prognosis marker in papillary thyroid carcinoma. *J Clin Endocrin Metab* 2001; 86: 656-658

Kroll TG, Sarraf P, Pecciarini L, Chen CJ, Mueller E, Spiegelman BM, Fletcher JA. PAX8-PPAR γ 1 fusion oncogene in human thyroid carcinoma. *Science* 2000;289(5483):1357-60.

Lapidot T, Petit I. Current understanding of stem cell mobilization: the roles of chemokines, proteolytic enzymes, adhesion molecules, cytokines, and stromal cells. *Exp Hematol*. 2002 Sep;30(9):973-81. Review.

Ledent C, Dumont J, Vassart G, Parmentier M. Thyroid adenocarcinomas secondary to tissue-specific expression of simian virus-40 large T-antigen in transgenic mice. *Endocrinology*. 1991 Sep;129(3):1391-401.

Lernmark A. Autoimmune diseases: are markers ready for prediction? *J Clin Invest*. 2001 Oct;108(8):1091-6. Review.

Levi R, Allan G. Histamine-mediated cardiac effects. In Bristow M.R., ed. *Drug-induced heart diseases*; vol.5. Amsterdam: Elsevier/ North Holland 1980; 377-95

Levi R, Smith NCE. Histamine H₃-Receptors: a new frontier in myocardial ischemia. *J Pharmacol Exp Ther* 1999; 292: 825-830

Lin EY, Nguyen AV, Russell RG, Pollard JW. Colony-stimulating factor 1 promotes progression of mammary tumors to malignancy. *J Exp Med* 2001; 193: 727-740

Liaw L, Birk DE, Ballas CB, Whitsitt JS, Davidson JM, Hogan BL. Altered wound healing in mice lacking a functional osteopontin gene (*spp1*). *J Clin Invest*. 1998 Apr 1;101(7):1468-78.

Lorenzo MJ, Gish GD, Houghton C, Stonehouse TJ, Pawson T, Ponder BA, Smith DP. RET alternate splicing influences the interaction of activated RET with the SH2 and PTB domains of Shc, and the SH2 domain of Grb2. *Oncogene*. 1997 Feb 20;14(7):763-71.

Luster AD. Chemokines--chemotactic cytokines that mediate inflammation. *N. Engl. J. Med*. 1998; **338**:436-445.

Malumbres M, Barbacid M. RAS oncogenes: the first 30 years. *Nat Rev Cancer* 2003;3(6):459-65.

Mantovani A, Allavena P, Sozzani S, Vecchi A, Locati M, Sica A. Chemokines in the recruitment and shaping of the leucocyte infiltrate of tumors. *Semin Cancer Biol* 2004; 14: 155-60

Marone G, Triggiani M, de Paulis A. Mast cells and basophils: friends as well as foes in bronchial asthma? *Trends Immunol* 2005; 26: 25-31

Marone G, Triggiani M, Genovese A, de Paulis A. Role of human mast cells and basophils in bronchial asthma. *Adv Immunol* 2005; 88: 97-106

Mechler C, Bounacer A, Suarez H, Saint Frison M, Magois C, Aillet G, Gaulier A. Papillary thyroid carcinoma: 6 cases from 2 families with associated lymphocytic thyroiditis harbouring RET/PTC rearrangements. *Br J Cancer* 2001; 85: 1831-7

Meininger C. Mast cells and tumor-associated angiogenesis. In *Human basophils and mast cells: Clinical aspects*. ed. G.Marone 1995; pp. 238-256. Karger, Basel, Switzerland

Melillo RM, Santoro M, Ong SH, Billaud M, Fusco A, Hadari YR, Schlessinger J, Lax I. Docking protein FRS2 links the protein tyrosine kinase RET and its oncogenic forms with the mitogen-activated protein kinase signaling cascade. *Mol Cell Biol*. 2001 Jul;21(13):4177-87.

Melillo R.M, Castellone, M.D, Guarino, V, De Falco V, Cirafici AM, Salvatore G, Chiazzo F, Basolo F, Giannini R, Kruhoffer M, Orntoft T, Fusco A. and Santoro M. The RET/PTC-RAS-BRAF linear signalling cascade mediates the motile and mitogenic phenotype of thyroid cancer cells. *J Clin Invest* 2005; 115: 1068-1081

Mellado M, Rodriguez-Frade JM, Manes S. and Martinez-AC. Chemokine signaling and functional responses: the role of receptor dimerization and TK pathway activation. *Annu. Rev. Immunol*. 2001; **19**:397-421.

Metz M, and Maurer M. Mast cells – key effector cells in immune responses. *Trends Immunol* 2007; 28: 234-241

Müller A, Homey B, Soto H, Ge N, Catron D, Buchanan ME, McClanahan T, Murphy E, Yuan W, Wagner SN, Barrera JL, Mohar A, Verástegui E, Zlotnik A. Involvement of chemokine receptors in breast cancer metastasis. *Nature*. 2001 Mar 1;410(6824):50-6.

Nakayama T, Yao L and Tosato G. Mast cell-derived angiopoietin-1 plays a critical role in the growth of plasma cell tumors. *J Clin Invest* 2004; 114: 1317-1325

Nikiforova MN, Kimura ET, Gandhi M, Biddinger PW, Knauf JA, Basolo F, Zhu Z, Giannini R, Salvatore G, Fusco A, Santoro M, Fagin JA, Nikiforov YE. BRAF mutations in thyroid tumors are restricted to papillary carcinomas and anaplastic or poorly differentiated carcinomas arising from papillary carcinomas. *J Clin Endocrinol Metab* 2003;88(11):5399-404.

Norrby K, and Wooley DE. Role of mast cells in mitogenesis and angiogenesis in normal tissue and tumor tissue. *Adv Biosci* 1993; 89: 71-115.

Orimo A, Gupta PB, Sgroi DC, Arenzana-Seisdedos F, Delaunay T, Naeem R, Carey VJ, Richardson AL, Weinberg RA. Stromal fibroblasts present in invasive human breast carcinomas promote tumor growth and angiogenesis through elevated SDF-1/CXCL12 secretion. *Cell*. 2005 May 6;121(3):335-48.

Ott RA, McCall AR, Jarosz H, Armin A, Lawrence AM, Paloyan E. The incidence of thyroid carcinoma in Hashimoto's thyroiditis. *Am Surg* 1987; 53: 442-445

Pacifico F, Mauro C, Barone C, Crescenzi E, Mellone S, Monaco M, Chiappetta G, Terrazzano G, Liguoro D, Vito P, Consiglio E, Formisano S, Leonardi A. Oncogenic and anti-apoptotic activity of NF-kappa B in human thyroid carcinomas. *J Biol Chem*. 2004 Dec 24;279(52):54610-9.

Pandey A, Liu X, Dixon JE, Di Fiore PP, Dixit VM. Direct association between the Ret receptor tyrosine kinase and the Src homology 2-containing adapter protein Grb7. *J Biol Chem* 1996;271:10607-10.

Pellicci G, Troglio F, Bodini A, Melillo RM, Pettirossi V, Coda L, De Giuseppe A, Santoro M, Pelicci PG. The neuron-specific Rai (ShcC) adaptor protein inhibits apoptosis by coupling Ret to the phosphatidylinositol 3-kinase/Akt signaling pathway. *Mol Cell Biol*. 2002 Oct;22(20):7351-63.

Pisanu A, Piu S, Cois A, Uccheddu A. Coexisting Hashimoto's thyroiditis with differentiated thyroid cancer and benign thyroid disease: indications for thyroidectomy. *Chir Ital* 2003; 55: 365-372

Powell DJ Jr, Russell J, Nibu K, Li G, Rhee E, Liao M, Goldstein M, Keane WM, Santoro M, Fusco A, Rothstein JL. The RET/PTC3 oncogene: metastatic solid-type papillary carcinomas in murine thyroids. *Cancer Res*. 1998 Dec 1;58(23):5523-8.

Powell DJ, Eisenlohr LC, Rothstein JL. A thyroid tumor-specific antigen formed by the fusion of two self proteins. *J Immunol* 2003; 170: 861-869

Prussin C. and Metcalfe DD. IgE, mast cells, basophils, and eosinophils. *J Allergy Clin Immunol* 2006; 117: 450-455

Puxeddu E, Knauf JA, Sartor M.A, Mitsutake N, Smith EP, Medvedovic M, Tomlinson CR., Moretti S, Fagin JA. RET/PTC-induced gene expression in thyroid PCCL3 reveals early activation of genes involved in regulation of the immune response. *Endocr Relat Cancer* 2005; 12: 319-334

Qu Z, Liebler JM, Powers MR, Galey T, Ahmadi P, Huang XN, Ansel JC, Butterfield, JH, Planck SR, Rosenbaum JT. Mast cells are a major source of basic fibroblast growth factor in chronic inflammation and cutaneous hemangioma. *Am J Pathol* 1995; 147: 564-573

Reber L, Da Silva CA, Frossard N. Stem cell factor and its receptor c-Kit as targets for inflammatory diseases. *Eur J Pharmacol* 2006; 533: 327-340

Rhoden KJ, Unger K, Salvatore G, Yilmaz Y, Vovk V, Chiappetta G, Qumsiyeh MB, Rothstein JL, Fusco A, Santoro M, Zitzelsberger H, Tallini G. RET/papillary thyroid cancer rearrangement in nonneoplastic thyrocytes: follicular cells of Hashimoto's thyroiditis share low-level recombination events with a subset of papillary carcinoma. *J Clin Endocrinol Metab.* 2006 Jun;91(6):2414-23. Epub 2006 Apr 4.

Ribatti D, Vacca A, Nico B, Quondamatteo F, Ria R, Minischetti M, Marzullo A, Herken R, Roncali L, Dammacco F. Bone marrow angiogenesis and mast cell density increase simultaneously with progression of human multiple myeloma. *Br J Cancer* 1999; 79: 451-455

Ribatti D, Finato N, Crivellato E, Marzullo A, Mangieri D, Nico B, Vacca A, Beltrami CA. Neovascularization and mast cells with tryptase activity increase simultaneously with pathologic progression in human endometrial cancer. *Am. J Obstet Gynecol* 2006; 193: 1961-1965

Rittling SR, Novick KE. Osteopontin expression in mammary gland development and tumorigenesis. *Cell Growth Differ.* 1997 Oct;8(10):1061-9.

Ron E, Kleinerman RA, Boice JD Jr, LiVolsi VA, Flannery JT, Fraumeni JF Jr. A population-based case-control study of thyroid cancer. *J Natl Cancer Inst.* 1987 Jul;79(1):1-12.

Rosai J. The 1991 Fred W. Stewart Award. 14th recipient of the Fred W. Stewart Award: Javier Arias Stella, M.D. *Am J Surg Pathol.* 1992 Jun;16(6):632.

Rosai J. Rosai and Ackerman's Surgical Pathology ed. Mostby 2005 NY USA.

Rüegg C. Leukocytes, inflammation, and angiogenesis in cancer: fatal attractions. *J Leuk Biol* 2006; 80: 682-684

Russell JP, Powell DJ, Cunnane M, Greco A, Portella G, Santoro M, Fusco A, Rothstein JL. The TRK-T1 fusion protein induces neoplastic transformation of thyroid epithelium. *Oncogene*. 2000 Nov 23;19(50):5729-35.

Santoro M, Carlomagno F, Romano A, Bottaro DP, Dathan NA, Grieco M, Fusco A, Vecchio G, Matoskova B, Kraus MH, et al. Activation of RET as a dominant transforming gene by germline mutations of MEN2A and MEN2B. *Science*. 1995 Jan 20;267(5196):381-3.

Santoro M, Grieco M, Melillo RM, Fusco A, Vecchio G. Molecular defects in thyroid carcinomas: role of the RET oncogene in thyroid neoplastic transformation. *Eur J Endocrinol*. 1995 Nov;133(5):513-22. Review

Santoro M, Melillo RM, Carlomagno F, Vecchio G, Fusco A. Minireview: RET: Normal and Abnormal Functions. *Endocrinology* 2004; 145(12):5448-51.

Scarpino S, Stoppacciaro A, Ballerini F, Marchesi M, Prat M, Stella MC, Sozzani S, Allavena P, Mantovani A, Ruco LP. Papillary carcinoma of the thyroid: hepatocyte growth factor (HGF) stimulates tumor cells to release chemokines active in recruiting dendritic cells. *Am J Pathol*. 2000 Mar;156(3):831-7.

Schall, T.J., Bacon, K.B. Chemokines, leukocyte trafficking, and inflammation. *Curr Opin Immunol* 1994; 6: 865-873

Schlicker E, Malinowska B, Kathmann M, Gohert M. Modulation of neurotransmitter release via histamine H3 heteroreceptors. *Fundam Clin Pharmacol* 1994; 8: 128-137

Schorge JO, Drake RD, Lee H, Skates SJ, Rajanbabu R, Miller DS, Kim JH, Cramer DW, Berkowitz RS, Mok SC. Osteopontin as an adjunct to CA125 in detecting recurrent ovarian cancer. *Clin Cancer Res*. 2004 May 15;10(10):3474-8.

Schneider S, Yochim J, Brabender J, Uchida K, Danenberg KD, Metzger R, Schneider PM, Salonga D, Hölscher AH, Danenberg PV. Osteopontin but not osteonectin messenger RNA expression is a prognostic marker in curatively resected non-small cell lung cancer. *Clin Cancer Res*. 2004 Mar 1;10(5):1588-96.

Sclafani AP, Valdes M, Cho H. Hashimoto's thyroiditis and carcinoma of the thyroid: optimal management. *Laryngoscope* 1993; 103: 845-849

Segal K, Ben-Bassat M, Avraham A, Har-El G, Sidi J. Hashimoto's thyroiditis and carcinoma of the thyroid gland. *Int Surg* 1985; 70: 205-209

Senger DR, Asch BB, Smith BD, Perruzzi CA, Dvorak HF. A secreted phosphoprotein marker for neoplastic transformation of both epithelial and fibroblastic cells. *Nature*. 1983 Apr 21;302(5910):714-5.

Siraganian RP. An automated continuous-flow system for the extraction and fluorometric analysis of histamine. *Anal Biochem* 1974; 57: 383-394

Smirnova IO, Kvetnoi IM, Smirnova ON, Antonova I.V. Mast cells in photolesion of the skin and basal cell cancer associated with it. *Ark Patol* 2005; 67: 26-29

Soares P, Trovisco V, Rocha AS, Lima J, Castro P, Preto A, Maximo V, Botelho T, Seruca R, Sobrinho-Simoes M. BRAF mutations and RET/PTC rearrangements are alternative events in the etiopathogenesis of papillary thyroid carcinoma. *Oncogene* 2003; 22; 4578-4580.

Soucek L, Lawlor ER, Soto D, Shehors K, Swigart LB, Evan GI. Mast cells are required for angiogenesis and macroscopic expansion of Myc-induced pancreatic islet tumors. *Nat Med*. 2007 Oct; 13(10):1211-8..

Tachibana K, Hirota S, Iizasa H, Yoshida H, Kawabata K, Kataoka Y, Kitamura Y, Matsushima K, Yoshida N, Nishikawa S, Kishimoto T, Nagasawa T. The chemokine receptor CXCR4 is essential for vascularization of the gastrointestinal tract. *Nature*. 1998 Jun 11;393(6685):591-4.

Takahashi K, Tanaka S, Furuta K, Ichikawa A. Histamine H2 receptor-mediated modulation of local cytokine expression in a mouse experimental tumour model. *Biochem Biophys Res Commun* 2002; 297: 1205-1210

Takeshita K, Sakai K, Bacon KB, Gantner, F. Critical role of histamine H4 receptor in leukotriene B4 production and mast cell-dependent neutrophil recruitment induced by zymosan in vivo. *J Pharmacol Exp Ther* 2003; 307: 1072-1078

Thomas L. Discussion. In *cellular and Humoral Aspects of the Hypersensitive States*. H.S. Lawrence, ed. 1959; New York: Hoeber-Harper: 529-532

Thomas L. On immunosurveillance in human cancer. *Yale J Biol Med* 1982; 55: 329-333.

Vacca A, Ribatti D, Roccaro A.M, Frigeri A, Dammacco F. Bone marrow angiogenesis in patients with active multiple myeloma. *Semin Oncol* 2001; 28: 543-550

Van Wanrooij EJA, Happé H, Hauer AD, de Vos P, Imanishi T, Fujiwara H, van Berkel TJC, Kuiper J. HIV entry inhibitor TAK-779 attenuates atherogenesis in low-density lipoprotein receptor-deficient mice. *Atheroscler Thromb Vasc Biol* 2005 25: 2642-7

Van Weering DH. and Bos JL. Signal transduction by the receptor tyrosine kinase Ret. *Recent Results Cancer Res.* 1998; 154; 271-281.

Vannier E, Miller LC, Dinarello CA. Histamine suppresses gene expression and synthesis of tumor necrosis factor α via histamine H₂ receptors. *J Exp Med* 1991; 174: 281-284

Vasko V, Saji M, Hardy E, Kruhlak M, Larin A, Savchenko V, Miyakawa M, Isozaki O, Murakami H, Tsushima T, Burman KD, De Micco C, Ringel MD. Akt activation and localisation correlate with tumour invasion and oncogene expression in thyroid cancer. *J Med Genet.* 2004 Mar;41(3):161-70.

Viglietto, G, Maglione D, Rimbaldi M, Cerutti J, Romano A, Trapasso F, Fedele M, Ippolito P, Chiappetta G, Botti G. Upregulation of vascular endothelial growth factor (VEGF) and downregulation of placental growth factor (PlGF) associated with malignancy in human thyroid tumors and cell lines. *Oncogene* 1995; 11: 1569-1579

Visconti R, Cerutti J, Battista S, Fedele M, Trapasso F, Zeki K, Miano MP, de Nigris F, Casalino L, Curcio F, Santoro M, Fusco A. Expression of the neoplastic phenotype by human thyroid carcinoma cell lines requires NFkappaB p65 protein expression. *Oncogene.* 1997 Oct 16;15(16):1987-94.

Vitagliano D, Portella G, Troncone G, Francione A, Rossi C, Bruno A, Giorgini A, Coluzzi S, Nappi TC, Rothstein JL, Pasquinelli R, Chiappetta G, Terracciano D, Macchia V, Melillo RM, Fusco A, Santoro M. Thyroid targeting of the N-ras(Gln61Lys) oncogene in transgenic mice results in follicular tumors that progress to poorly differentiated carcinomas. *Oncogene.* 2006 Aug 31;25(39):5467-74.

Vogelstein B, Fearon ER, Hamilton SR, Kern SE, Preisinger AC, Leppert M, Nakamura Y, White R, Smits AM, Bos JL. Genetic alterations during colorectal-tumor development. *N Engl J Med.* 1988 Sep 1;319(9):525-32.

Westphal E. Uber mastzellen. In *Farbenanalytische Untersuchungen zur Histologie und Klinik des Blutes: gesammelte Mitt(h)eilungen* ed. P. Ehrlich 1891; Vol.1, p.17. Hirschwald Press, Berlin, Germany

Widdowson KL, Elliott JD, Veber DF, Nie H, Rutledge MC, McClelland BW, Xiang JN, Jurewicz AJ, Hertzberg RP, Foley JJ, Griswold DE, Martin L, Lee JM, White JR, Sarau HM. Evaluation of potent and selective small-molecule antagonists for the CXCR2 chemokine receptor. *J Med Chem.* 2004 Mar 11;47(6):1319-21.

Williams ED, Doniach I, Bjarnason O, Michie W. Thyroid cancer in an iodide rich area: a histopathological study. *Cancer.* 1977 Jan;39(1):215-22.

Williams CS, Mann M, DuBois RN. The role of cyclooxygenases in inflammation, cancer, and development. *Oncogene* 1999; 18: 7908-7916

Williams D. Cancer after nuclear fallout: lessons from the Chernobyl accident. *Nat Rev Cancer.* 2002 Jul;2(7):543-9. Review.

Willis, R.A. *The spread of tumors in the human body*, Butterworth & Co., London. In *Pathologic Basis of Disease*, Robbins. Sixth edition: Cotran Kumar Collins, W.B. Saunders Company, Philadelphia 1952; Pennsylvania, U.S.A

Wirtschafter, A, Schmidt R, Rosen, D, Kundu N, Santoro M, Fusco A, Mulhaupt H, Atkins JP, Rosen MR, Keane WM, Rothstein JL. Expression of the RET/PTC fusion gene as a marker for papillary carcinoma in Hashimoto's thyroiditis. *Laryngoscope* 1997; 107: 95-100

White JR, Lee JM, Young PR, Hertzberg RP, Jurewicz AJ, Chaikin MA, Widdowson K, Foley JJ, Martin LD, Griswold DE, Sarau HM. Identification of a potent, selective non-peptide CXCR2 antagonist that inhibits interleukin-8-induced neutrophil migration. *J Biol Chem.* 1998 Apr 24;273(17):10095-8.

Xu B Yoshimoto K, Miyauchi A, Kuma S, Mizusawa N, Hirokawa M, Sano T. Cribiform-morular variant of papillary thyroid carcinoma: a pathological and molecular genetic study with evidence of frequent somatic mutations in exon 3 of the beta-catenin gene. *J Pathol.* 2003; 199; 58-67.

Yang L, Jackson E, Woerner BM, Perry A, Piwnica-Worms D, Rubin JB. Blocking CXCR4-mediated cyclic AMP suppression inhibits brain tumor growth in vivo. *Cancer Res.* 2007 Jan 15;67(2):651-8.

Zitvogel L, Tesniere A, Kroemer G. Cancer despite immunosurveillance: immunoselection and immunosubversion. *Nat Rev Immunol* 2006; 6: 715- 727

Zhu Z, Gandhi M, Nikiforova MN, Fischer AH, Nikiforov YE. Molecular profile and clinical-pathologic features of the follicular variant of papillary thyroid carcinoma. An unusually high prevalence of ras mutations. *Am J Clin Pathol* 2003;120(1):71-7.

Zou YR, Kottmann AH, Kuroda M, Taniuchi I, Littman DR. Function of the chemokine receptor CXCR4 in haematopoiesis and in cerebellar development. *Nature*. 1998 Jun 11; 393(6685): 595-9.

ACKNOWLEDGEMENTS

This study was performed at the University of Naples Federico II, Italy, Department of Molecular and Cellular Biology and Patology and Istituto di Endocrinologia ed Oncologia Sperimentale “G. Salvatore”. This work has been supervised by Professor Rosa Marina Melillo.

I wish to thank many persons who helped me during my PhD research. First of all I would like to thank my supervisor, Prof. Rosa Marina Melillo, who gave me the support and trust I needed to finish my PhD thesis. A special tank goes to the IEOS research groups of Rosa Marina Melillo, Francesca Carlomagno and Angela Celetti for reciprocal help, sharing, ideas, stimulating discussion and technical support.

I am presenting my warmest gratitude to all contributors in this thesis. My thanks go to Professor Massimo Santoro and to his working group at the University of Naples, for encouraging my interest in medical research.

I acknowledge with gratitude professor Giancarlo Vecchio coordinator of the International Doctorate Program, University of Naples Federico II for his support during these years.

I also had a pleasant work experience at the Astma and Allergy Center (Johns Hopkins University) in the laboratory of Professor Casolaro. I wish to thank all the people of the laboratory for their kindness and hospitality, in particular I am indebted to Prof. Vincenzo Casolaro and Professor Cristiana Stellato for his continuous encouragement and for the exiting exchange of ideas.

Biological Role and Potential Therapeutic Targeting of the Chemokine Receptor CXCR4 in Undifferentiated Thyroid Cancer

Valentina De Falco,¹ Valentina Guarino,¹ Elvira Avilla,¹ Maria Domenica Castellone,¹ Paolo Salerno,¹ Giuliana Salvatore,² Pinuccia Faviana,³ Fulvio Basolo,³ Massimo Santoro,¹ and Rosa Marina Melillo¹

¹Dipartimento di Biologia e Patologia Cellulare e Molecolare c/o Istituto di Endocrinologia ed Oncologia Sperimentale del CNR "G. Salvatore," Facolta' di Medicina e Facolta' di Scienze Biotechnologiche dell'Universita' "Federico II"; ²Dipartimento di Studi delle Istituzioni e dei Sistemi Territoriali, Universita' "Parthenope," Naples, Italy and ³Dipartimento di Chirurgia, Universita' di Pisa, Pisa, Italy

Abstract

Anaplastic thyroid carcinoma (ATC) is a rare thyroid cancer type with an extremely poor prognosis. Despite appropriate treatment, which includes surgery, radiotherapy, and chemotherapy, this cancer is invariably fatal. CXCR4 is the receptor for the stromal cell-derived factor-1 (SDF-1)/CXCL12 chemokine and it is expressed in a variety of solid tumors, including papillary thyroid carcinoma. Here, we show that ATC cell lines overexpress CXCR4, both at the level of mRNA and protein. Furthermore, we found that CXCR4 was overexpressed in ATC clinical samples, with respect to normal thyroid tissues by real-time PCR and immunohistochemistry. Treatment of ATC cells with SDF-1 induced proliferation and increase in phosphorylation of extracellular signal-regulated kinases and protein kinase B/AKT. These effects were blocked by the specific CXCR4 antagonist AMD3100 and by CXCR4 RNA interference. Moreover, AMD3100 effectively reduced tumor growth in nude mice inoculated with different ATC cells. Thus, we suggest that CXCR4 targeting is a novel potential strategy in the treatment of human ATC. [Cancer Res 2007;67(24):1-9]

Introduction

Thyroid cancer accounts for the majority of endocrine neoplasms worldwide (1). Malignant tumors derived from the thyroid gland include well-differentiated thyroid carcinomas (WDTC; papillary and follicular) and undifferentiated or anaplastic thyroid carcinomas (ATC). Another group of cancers falls between these two types, the so-called poorly differentiated thyroid carcinomas (PDC). WDTC represents >90% of all thyroid cancers, whereas ATC accounts for approximately 2% to 5% of them (2-4). WDTC management requires surgery and adjuvant radioactive iodine (5, 6). Whereas most of the patients with WDTC have an excellent prognosis, those that present with PDC or ATC have a poor prognosis. PDC displays intermediate biological and clinical features between WDTC and ATC. Indeed, these tumors display high propensity to recur and metastasize. Furthermore, they tend to a progressive dedifferentiation, which leads to the decrease in the levels of the sodium iodide symporter. As a consequence of this,

these tumors are unable to concentrate iodine and become resistant to radiometabolic therapy (4, 7). ATC is the most malignant thyroid tumor and one of the more fatal human malignancy with a median survival from the time of diagnosis of only 4 to 12 months (8, 9). ATC is more frequent in iodine-deficient areas and can be associated with other thyroid disorders. These tumors arise at a mean age of 55 to 65 years, are more common in women, and present usually as a rapidly growing mass, localized in the anterior neck area, which rapidly metastasizes at lungs, bone, and brain. Treatment of ATC with surgery, radiotherapy, and chemotherapy, alone or in combination, shows little or no effect on patient's survival (10). For these reasons, novel treatment strategies are urgently needed. Unlike the WDTC, the molecular mechanisms underlying the development of human ATC are largely unknown. Genetic rearrangements of the RET and TRKA tyrosine kinase receptors, point mutations of the BRAF serine-threonine kinase or, less frequently, RAS mutations, are typically found in papillary thyroid carcinoma (PTC). Rearrangements of PPAR γ or RAS point mutations are instead found in human FTC (11, 12). Among these genetic alterations, RAS or BRAF point mutations are detected at low frequency in ATC, suggesting that some ATC may arise from a preexisting WDTC, whereas others arise *de novo* (12, 13). Inactivating point mutations of the p53 tumor suppressor and activating point mutations of the β -catenin or the PIK3CA are also found in ATC (13, 14).

In the attempt to better characterize human ATC at the molecular level, we aimed to study the involvement of chemokine and chemokine receptors in these tumors. Chemokines are small secretory proteins that were initially reported to control the recruitment and the activation of immune cells in inflammation (16). These molecules exert their action through binding to a group of seven-transmembrane G protein-coupled receptors. All chemokine receptors initiate signal transduction by activating a member of the Gi family of G proteins which, on receptor activation, dissociates into α and $\beta\gamma$ subunits. The G α subunit inhibits adenylyl cyclase, whereas the G $\beta\gamma$ dimer activates the phospholipase C β and the phosphatidylinositol 3-kinase pathways, with the activation of downstream signaling. It has becoming clear recently that chemokines are also involved in cancer cell migration, survival, and growth (17). Not only chemokines regulate some important features of cancer cells but are also involved in the regulation of tumor angiogenesis and leukocyte recruitment (17). In particular, the chemokine receptor CXCR4 and its ligand stromal cell-derived factor-1 (SDF-1)/CXCL12 have been implicated in the metastatic spread of breast cancer cells (18). CXCR4 is one of the

Requests for reprints: Rosa Marina Melillo, Istituto di Endocrinologia ed Oncologia Sperimentale del CNR, via S. Pansini 5, 80131 Naples, Italy. Phone: 39-081-7463603; Fax: 39-081-7463603; E-mail: rosmelil@unina.it.

©2007 American Association for Cancer Research.
doi:10.1158/0008-5472.CAN-07-0899

most important chemokine receptors for cancer cells. Indeed, it is expressed in a great number of human solid and hematologic cancers, including breast, prostate, brain, colon, and lung cancer (19, 20). We and others previously reported the overexpression and functional activity of CXCR4 in thyroid cancer (21, 22). In this report, we show that human ATC cells express high levels of CXCR4 and that the CXCR4-SDF-1/CXCL12 axis sustains the growth of ATC cells. Finally, we provide evidences that targeting CXCR4 might be exploited as a novel anticancer therapy for human ATC.

Materials and Methods

Cell lines. Human primary cultures of normal thyroid and ATC cells were obtained from F. Curcio (P5, P5-2N, P5-3N, P5-4N, and HTU8) and H. Zitzelsberger (S11T, S77T, and S14T) and cultured as described previously (23). Primary cultures of ATC were also a kind gift of H. Zitzelsberger. Of these, only the S11T displays a BRAF(V600E) mutation in heterozygosis.⁴ Human thyroid papillary cancer cell lines TPC1, FB2, and NIM have been described previously (24–26). TPC1 and FB2 cells harbor a RET/PTC1 rearrangement. NPA87 cells derive from a PDC and harbor a BRAF(V600E) mutation in homozygosis (23). The anaplastic cells ARO, KAT4, BHT101, and FB1 cells harbor a BRAF(V600E) mutation in heterozygosis; 8505C and FRO harbor a BRAF(V600E) mutation in homozygosis (23); and CAL62 cells express wild-type BRAF but mutant NRAS allele. Continuous cell lines were maintained in DMEM supplemented with 10% fetal bovine serum, 1% penicillin-streptomycin, and 1% glutamine.

RNA extraction and reverse transcription PCR. Total RNA was isolated by the RNeasy kit (Qiagen) and subjected to on-column DNase digestion with the RNase-free DNase set (Qiagen) according to the manufacturer's instructions. The quality of RNA was verified by electrophoresis through 1% agarose gel and visualized with ethidium bromide. RNA (1 µg) from each sample was reverse transcribed with the QuantiTect Reverse Transcription (Qiagen) using an optimized blend of oligo(dT) and random primers according to the manufacturer's instructions. To design a quantitative reverse transcription-PCR (RT-PCR) assay, we used the Human ProbeLibrary system (Exiqon). Briefly, Exiqon provides 90 human prevalidated Taqman probes (8–9 nucleotides long) that recognize ~99% of human transcripts in the RefSeq database at the National Center for Biotechnology Information. The ProbeFinder assay design software (available online)⁵ was used to design primer pairs and probes. All fluorogenic probes were dual labeled with FAM at 5'-end and with a black quencher at the 3'-end. Primer pairs and PCR conditions are available on request. Quantitative RT-PCR was performed in a Chromo 4 Detector (MJ Research) in 96-well plates using a final volume of 20 µL. For each PCR, 8 µL of 2.5× RealMasterMix Probe ROX (Eppendorf AG), 200 nmol/L of each primer, 100 nmol/L probe, and cDNA generated from 50 ng of total RNA were used. PCRs were performed in triplicate and fold changes were calculated with the following formula: $2^{-(\text{sample 1 } \Delta Ct - \text{sample 2 } \Delta Ct)}$, where ΔCt is the difference between the amplification fluorescent thresholds of the mRNA of interest and the mRNA of RNA polymerase 2 used as an internal reference.

Immunohistochemistry. Retrospectively collected archival thyroid tissue samples from patients affected by ATCs were retrieved from the files of the Pathology Department of the University of Pisa on informed consent. Sections (4 µm thick) of paraffin-embedded samples were stained with H&E for histologic examination to ensure that the samples fulfilled the diagnostic criteria required for the identification of ATC. Normal thyroid tissue samples were also retrieved from the files of the Pathology Department of the University of Pisa.

For immunohistochemistry, paraffin sections (3–5 µm) were dewaxed in xylene, dehydrated through graded alcohols, and blocked with 5%

nonimmune mouse serum in PBS with 0.05% sodium azide for 5 min. Mouse monoclonal antibody against CXCR4 (clone 12G5; R&D Systems) was added at 1:1,000 dilution for 15 min. After incubation with biotinylated anti-mouse secondary antibody for 15 min followed by streptavidin-biotin complex for 15 min (Catalyzed Signal Amplification System, DAKO), sections were developed for 5 min with 0.05% 3,3'-diaminobenzidine tetrahydrochloride and 0.01% hydrogen peroxide in 0.05 mol/L Tris-HCl buffer (pH 7.6), counterstained with hematoxylin, dehydrated, and mounted.

Protein studies. Immunoblotting experiments were performed according to standard procedures. Briefly, cells were harvested in lysis buffer [50 mmol/L HEPES (pH 7.5), 150 mmol/L NaCl, 10% glycerol, 1% Triton X-100, 1 mmol/L EGTA, 1.5 mmol/L MgCl₂, 10 mmol/L NaF, 10 mmol/L sodium pyrophosphate, 1 mmol/L Na₂VO₄, 10 µg/mL aprotinin, 10 µg/mL leupeptin] and clarified by centrifugation at 10,000 × *g*. For protein extraction from human tissues, snap-frozen samples were immediately homogenized in lysis buffer by using the Mixer Mill apparatus (Qiagen). Protein concentration was estimated with a modified Bradford assay (Bio-Rad). Antigens were revealed by an enhanced chemiluminescence detection kit (Amersham). Anti-CXCR4 antibodies were from Abcam Ltd. For the evaluation of mitogen-activated protein kinase (MAPK) and AKT activity on SDF-1α triggering, BHT101 and S11T cells were serum deprived for 12 h and then stimulated with human recombinant SDF-1α (R&D Systems) for the indicated time. Anti-phosphorylated p44/42 MAPK, anti-p44/42 MAPK, anti-phosphorylated AKT, and anti-AKT antibodies were from New England Biolabs. Anti-tubulin monoclonal antibody was from Sigma Chemical. Secondary anti-mouse and anti-rabbit antibodies coupled to horseradish peroxidase were from Bio-Rad.

Flow cytometric analysis. Subconfluent cells were detached from culture dishes with a solution of 0.5 mmol/L EDTA and then washed thrice in PBS buffer. After saturation with 1 µg of human IgG/10⁵ cells, cells were incubated for 20 min on ice with phycoerythrin (PE)-labeled antibodies specific for human CXCR4 (R&D Systems) or isotype control antibody. After incubation, unreacted antibody was removed by washing cells twice in PBS buffer. Cells resuspended in PBS were analyzed on a FACSCalibur cytofluorimeter using the CellQuest software (Becton Dickinson). Analyses were performed in triplicate. In each analysis, a total of 10⁴ events were calculated.

Cell proliferation. S-phase entry was evaluated by bromodeoxyuridine (BrdUrd) incorporation and indirect immunofluorescence. Cells were grown on coverslips, kept in 2.5% serum for 24 h, and then treated with recombinant SDF-1α (100 ng/mL) for 48 h. BrdUrd was added at a concentration of 10 µmol/L for the last 1 h. Subsequently, cells were fixed in 3% paraformaldehyde and permeabilized with 0.2% Triton X-100. BrdUrd-positive cells were revealed with Texas red-conjugated secondary antibodies (Jackson ImmunoResearch Laboratories, Inc.). Cell nuclei were identified by Hoechst staining. Fluorescence was visualized with a Zeiss 140 epifluorescent microscope.

For growth curves, cells were plated at a density of 0.5 × 10⁵ in low-serum conditions (2.5%) and counted at the indicated time points.

RNA interference. Small inhibitor duplex RNAs targeting human CXCR4 have been described previously (27) and were chemically synthesized by Prologo. Sense strand for human CXCR4 small interfering RNA (siRNA) targeting was the following: 5'-GAGGGGAUCAGCAGUAUAC-3'.

Small duplex RNAs containing the same nucleotides, but in scrambled fashion (siRNA SCR), were used as a negative control. For siRNA transfection, ATC cells were grown under standard conditions. The day before transfection, cells were plated in six-well dishes at 50% to 60% confluency. Transfection was performed using 5 to 15 µg of duplex RNA and 6 µL of Oligofectamine reagent (Invitrogen). Cells were harvested at 48 and 72 h after transfection and analyzed for protein expression and biological activity.

Xenografts in nude mice. Mice were housed in barrier facilities and 12-h light-dark cycles and received food and water *ad libitum* at the Dipartimento di Biologia e Patologia Cellulare e Molecolare (University of Naples "Federico II," Naples, Italy). This study was conducted in accordance with Italian regulations for experimentation on animals. All manipulations were performed while mice were under isoflurane gas anesthesia. No mouse

⁴ G. Salvatore, unpublished observation.

⁵ <http://www.probelibrary.com>

showed signs of wasting or other signs of toxicity. BHT101, ARO, or KAT4 cells (5×10^6 per mouse) were inoculated s.c. into the right dorsal portion of 4-week-old male BALB/c *nu/nu* mice (The Jackson Laboratory). When tumors measured 40 mm³, mice were randomized to receive AMD3100 ($n = 10$; 1.25 mg/kg/twice daily) or vehicle alone ($n = 10$; PBS) by i.p. injection for 5 consecutive days per week for 3 to 4 weeks. Tumor diameters were measured at regular intervals with calipers. Tumor volumes (V) were calculated with the following formula: $V = A \times B^2 / 2$ (A = axial diameter; B = rotational diameter). Tumors were excised and fixed overnight in neutral buffered formalin and processed by routine methods.

Statistical analysis. To compare CXCR4 mRNA levels in normal thyroid tissues versus ATC samples, we used the Mann-Whitney nonparametric test and the GraphPad InStat software, v.3.0b. To compare ATC xenograft growth in AMD3100-treated versus untreated animals, we used the unpaired Student's *t* test (normal distributions and equal variances) and the GraphPad InStat software, v.3.0b. All *P* values were two sided, and differences were considered statistically significant at $P < 0.05$.

Results

CXCR4 is overexpressed in surgical samples of human ATC.

We compared CXCR4 mRNA levels in a set of ATC samples ($n = 15$)

versus different samples of normal thyroid tissue ($n = 5$). As shown in Fig. 1A, CXCR4 mRNA was found to be up-regulated in most of the tumor samples (11 of 15). When we performed statistical analysis, the differences in the expression levels of CXCR4 between tumors and normal thyroid tissues were statistically significant ($P = 0.0084$; Fig. 1A).

To verify whether CXCR4 mRNA overexpression resulted in an increase in the protein levels, we used protein extracts from a different set of ATC samples and three normal thyroid tissues in an immunoblot experiment with CXCR4-specific antibodies. As shown in Fig. 1B, CXCR4 protein levels were higher in ATC samples than in normal thyroid. As a positive control for CXCR4 expression, the ATC cell line ARO was used.

Finally, CXCR4 antibodies were used in immunohistochemical experiments. We evaluated CXCR4 expression in normal thyroid tissues and a set of ATC samples ($n = 33$). Whereas no CXCR4 expression was detected in normal thyroid tissues, 13 (39%) of the ATC samples scored positive for CXCR4. A representative CXCR4 immunostaining is shown in Fig. 1C. These data indicate that a significant fraction of human ATCs, similarly to other epithelial

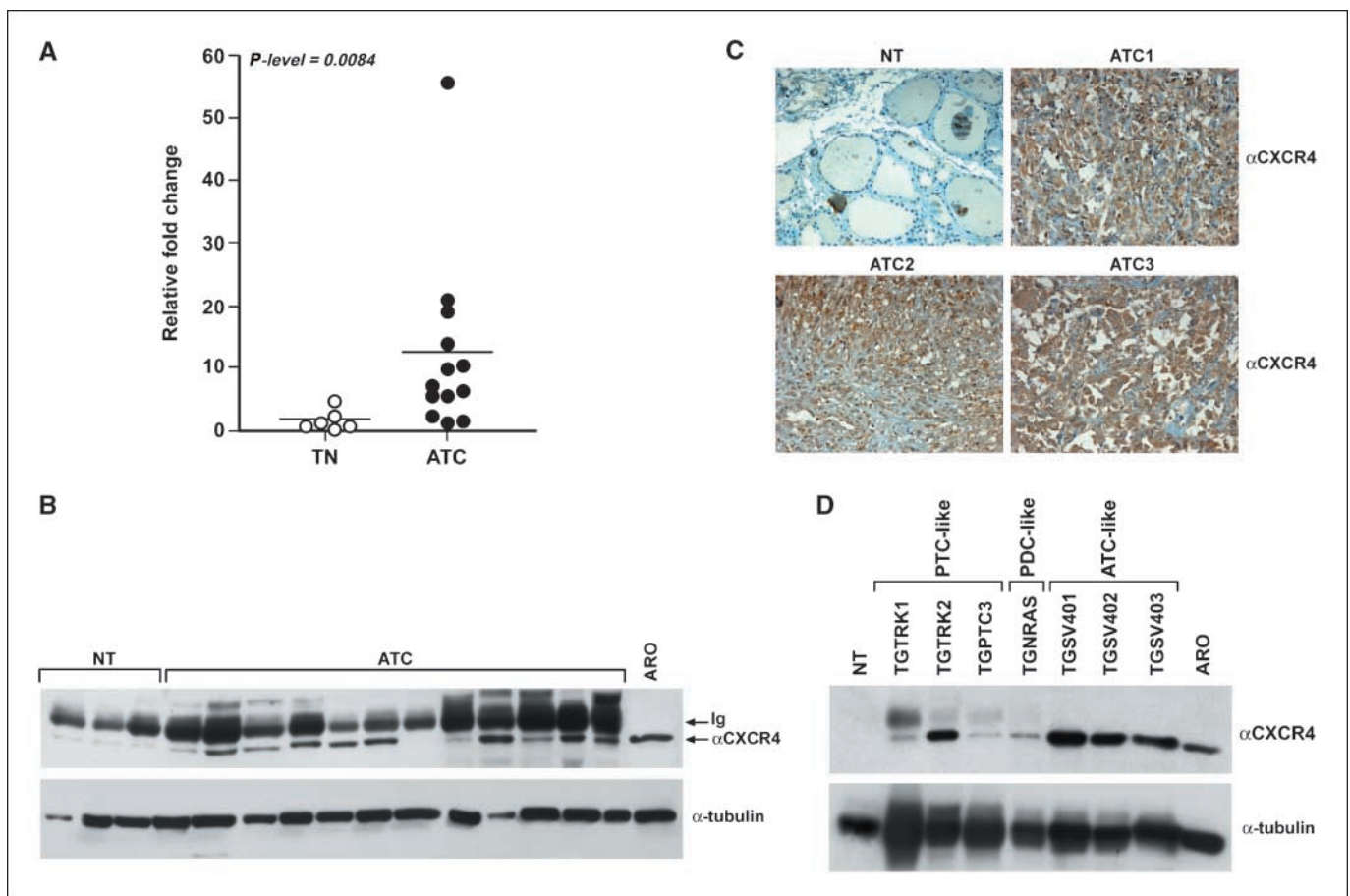


Figure 1. A, expression levels of CXCR4 in human ATC samples versus six normal thyroid tissues by real-time RT-PCR. CXCR4 expression levels of tumors (Y axis) are calculated relative to the mean CXCR4 level of normal human thyroid tissues (NT). All experiments have been performed in triplicate, and the average value of the results was plotted on the diagram. *P* value was calculated with the two-tailed, nonparametric Mann-Whitney test. B, protein lysates (100 μ g) extracted from the indicated samples underwent Western blotting with anti-CXCR4-specific antibodies. Immunocomplexes were revealed by enhanced chemiluminescence. Equal protein loading was ascertained by anti-tubulin immunoblot. C, immunohistochemical staining for CXCR4 of formalin-fixed, paraffin-embedded ATCs. Tissue samples from normal thyroid or ATC were incubated with a mouse monoclonal anti-CXCR4 antibody. ATCs show a strong immunoreactivity for CXCR4, whereas normal thyroid tissue is negative. Representative pictures of normal and pathologic positive samples are shown. Isotype control was also performed (data not shown). D, the expression levels of CXCR4 protein were analyzed in thyroid tumor samples from transgenic mice models. Tumor tissues were snap frozen and immediately homogenized by using the Mixer Mill apparatus in lysis buffer. Equal amounts of proteins were immunoblotted and stained with anti-CXCR4 polyclonal antibodies (Abcam). ATC-like samples displayed a more intense immunoreactivity for CXCR4. As a control for equal loading, the anti- α -tubulin monoclonal antibody was used.

cancers, feature high expression levels of the CXCR4 receptor. Furthermore, they suggest that the increase in CXCR4 levels occurs at the transcriptional level.

CXCR4 is highly expressed in animal models of ATC. Several transgenic mice model of thyroid cancer have been developed by using various oncogenes under the transcriptional control of the thyroid-specific thyroglobulin bovine promoter. Depending on the specific transgene, these mice develop carcinomas that resemble, for cytologic and histologic features, human PTC, FTC, or ATC. In particular, mice expressing either RET/PTC3 (TGPTC3) or TRK/T1 (TGTRK) oncogene develop PTC-like tumors (28, 29). NRAS transgene expression results in follicular tumors that progress to poorly differentiated carcinomas (TGNRS; ref. 27). Finally, animals expressing the SV40 large T antigen (TGSV) present aggressive thyroid cancer with features similar to human ATC (30). To evaluate the expression of CXCR4 in these animal models, we extracted proteins from different tumor samples of the different transgenic lines and performed Western blot analysis with CXCR4 antibodies. Histologic diagnosis of the thyroid lesion was verified before processing of the samples. As shown in Fig. 1D, CXCR4

levels were higher in ATC models than in normal mouse thyroid tissue. PTC samples displayed intermediate levels of CXCR4. These data, together with previously published data (21, 22), suggest that CXCR4 up-regulation is a frequent event in thyroid tumorigenesis and that it correlates with the malignancy of the disease.

CXCR4 is a functional receptor in human ATC cells. To study the role of CXCR4 in human ATC, we first needed to identify a suitable cell model. To this aim, various normal thyroid and ATC-derived primary cultures and continuous cell lines were tested for CXCR4 expression by Western blot analysis. As shown in Fig. 2A and B, whereas normal thyroid cultures displayed low or undetectable CXCR4 expression levels, several ATC cell lines featured high levels of the CXCR4 receptor. In particular, of 10 ATC cell lines, 7 displayed high expression levels of CXCR4. In the case of ATC cells, the increased levels of CXCR4 proteins were associated to an increase in CXCR4 mRNA levels as assessed by quantitative PCR analysis (Fig. 2C). We then asked whether this receptor was expressed on the cell surface. To this aim, we performed flow cytometry experiments using a PE-conjugated mouse monoclonal anti-CXCR4 antibody. The percentage of CXCR4-positive cells was

F2

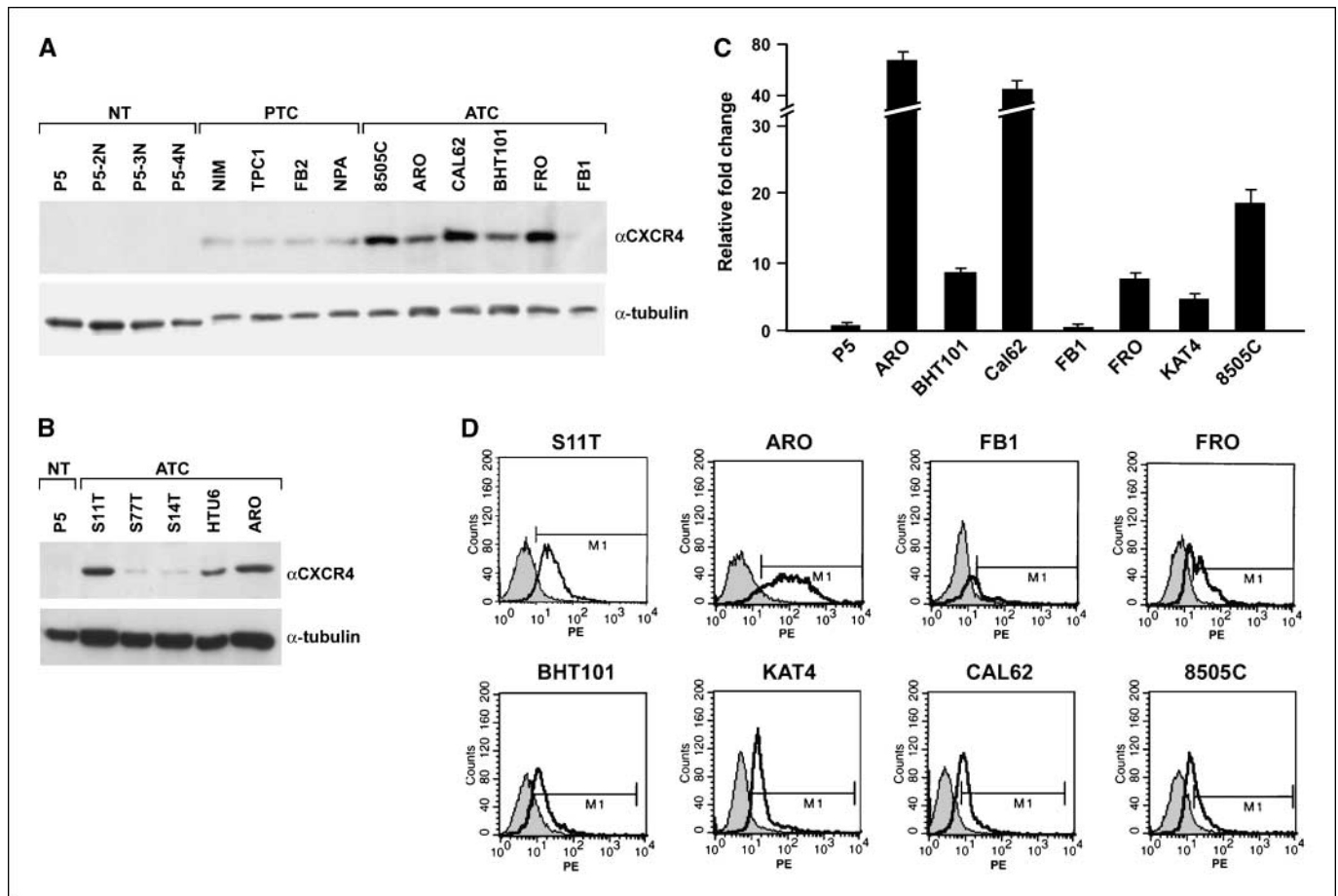
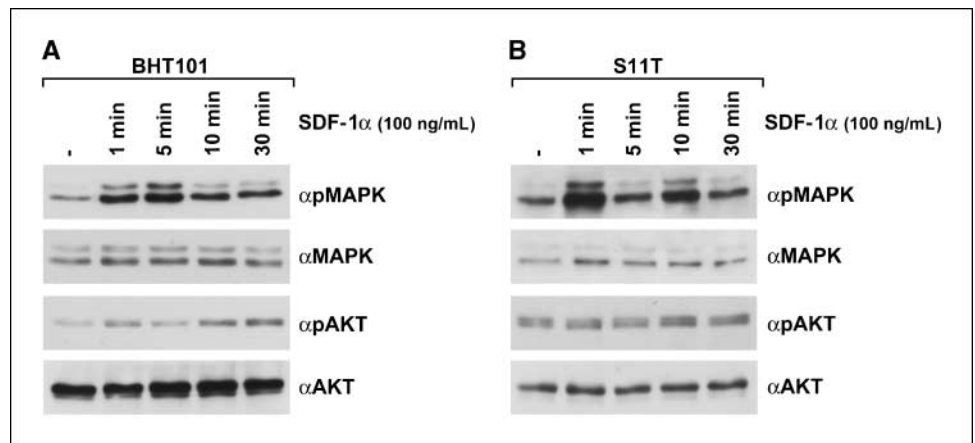


Figure 2. A, CXCR4 up-regulation in cell lines derived from human thyroid carcinomas was evaluated by immunoblot with a polyclonal anti-CXCR4 antibody. The expression levels of CXCR4 protein were analyzed in the P5 human primary thyroid cells, and in the indicated cell lines, derived from human PTCs (NIM, TPC1, FB2, and NPA) or from human ATCs (8505C, ARO, CAL62, BHT101, FRO, and FB1). B, ATC-derived (S11T, S77T, S14T, and HTU8) and normal thyroid primary culture (P5) were screened for CXCR4 expression by Western blot analysis with the polyclonal anti-CXCR4 antibody. As a control for equal loading, the anti- α -tubulin monoclonal antibody was used. C, expression levels of CXCR4 in human ATC cells versus the P5 normal thyroid culture were evaluated by real-time RT-PCR analysis. CXCR4 expression levels of ATC cell lines (Y axis) are calculated relative to the expression level in the normal human cell culture P5. All experiments were performed in triplicate, and the average value of the results was plotted on the diagram. SDs were smaller than 25% in all the cases (data not shown). D, flow cytometric analysis (fluorescence-activated cell sorting) of surface-expressed CXCR4 in ATC cells. Subconfluent cells were detached from culture dishes and incubated with PE-labeled antibodies specific for human CXCR4.

Figure 3. A and B, protein extracts from the indicated cell lines were subjected to immunoblotting with anti-phosphorylated p44/42 MAPK (α pMAPK) and with anti-phosphorylated AKT (α pAKT) antibodies. The blots were reprobed with anti-p44/42 and anti-AKT antibodies for normalization.



determined. As shown in Fig. 2D, CXCR4 was expressed in almost all the ATC cell lines tested, with the exception of the FB1 cells. The ARO cells, which in a previous report were shown to feature high CXCR4 levels (21), were included as a positive control. In contrast, normal thyroid cells did not express CXCR4 (data not shown). SDF-1, the CXCR4 ligand, was not expressed by ATC cells as assessed by quantitative PCR or ELISA assay (data not shown).

We selected two cell lines, S11T and BHT101, for further experiments. First, we tested the ability of recombinant SDF-1 α to stimulate signal transduction in ATC cells. It has been previously reported that stimulation of CXCR4 induces the activation of several kinase cascades mainly through the activation of the G β γ subunit of the Gi protein (31, 32). We therefore tested the phosphorylation of two downstream effectors, extracellular signal-regulated kinase (ERK) 1/2 and AKT, using phosphorylated-specific antibodies. To this aim, cells were serum starved for 12 h and then stimulated with SDF-1 α for different time points. As shown in Fig. 3A and B, SDF-1 α induced rapid and sustained activation of ERK1/2 in both cell lines. AKT activation was also achieved in BHT101 cells on SDF-1 α treatment, whereas it was less evident in S11T cells. Together, these data indicate that CXCR4 is functional in ATC cells. Activation of ERK1/2 and AKT was observed in virtually all the ATC cell lines expressing CXCR4, whereas normal thyroid cells, which do not express CXCR4, did not display these effects (data not shown).

Biological activity of CXCR4 in ATC cells. To further test the functional responsiveness of CXCR4 in ATC, we stimulated these cells with SDF-1 α and evaluated its ability to induce cell proliferation. To this aim, BHT101 and S11T cells were maintained in low-serum (2.5%) growth conditions for 24 h and then either left untreated or stimulated with SDF-1 α for 12 h. As a measure of DNA synthesis, we counted BrdUrd-positive cells on a 1-h BrdUrd pulse. As shown in Fig. 4, SDF-1 α consistently enhanced DNA synthesis in both BHT101 and S11T cells. We then used a specific CXCR4 inhibitor, AMD3100, to block this effect. AMD3100 is a competitive antagonist of SDF-1 α , but it also displays partial agonist activity (33). Normal thyroid cells were insensitive to SDF-1 α stimulation and to the effect of AMD3100 (data not shown). As shown in Fig. 4A, AMD3100 inhibited SDF-1 α -mediated BrdUrd incorporation in ATC cells. The positive effect of SDF-1 on cell proliferation, measured as S-phase entry, was also observed in other ATC cell lines (Fig. 5C). To evaluate whether SDF-1 α could stimulate ATC cell growth, we also performed growth curves in low-serum (2.5%) conditions. As shown in Fig. 4B, the stimulation of BHT101 with

SDF-1 α increased their proliferation rate, and AMD3100 reverted this effect. SDF-1 α was also able to increase the proliferation rate of three different ATC cell lines, KAT4, CAL62, and ARO, which express CXCR4, but was unable to do so on FB1 cells, which we previously reported to be devoid of CXCR4 (Fig. 4B). AMD3100 alone did not have any effect on ATC cells (data not shown).

To exclude off-target effects of AMD3100 and to directly determine the role of CXCR4 on ATC cell proliferation, we used small duplex RNA oligos to knock down CXCR4. CXCR4 RNA interference was verified by Western blot analysis in BHT101 cells (Fig. 5A). We then transfected CXCR4 siRNAs into BHT101, KAT4, CAL62, and 8505C cells. CXCR4 silencing substantially impaired SDF-1 α -induced S-phase entry in all the ATC cells but had no effect on BrdUrd incorporation in the absence of the chemokine, as shown in Fig. 5. When we used the control scrambled siRNA, this inhibitory effect was not observed. Furthermore, scrambled oligos had no effect on CXCR4 protein levels (Fig. 5A).

AMD3100 inhibits ATC tumor formation in nude mice. It has been previously shown that the CXCR4/SDF-1 axis plays an important role in the growth and in the metastatic ability of several epithelial cancers (20). Because we had shown that CXCR4 inhibition blocked SDF-1 α -mediated ATC cell growth in culture, and because it has been shown that this chemokine is secreted by stromal tumoral cells (34), we reasoned that SDF-1 α -CXCR4 axis blockade by AMD3100 might inhibit ATC tumor growth. To this aim, we selected BHT101, ARO, and KAT4 cells for their ability to respond to SDF-1 α and their ability to form tumors *in vivo* with high efficiency. Nude mice were injected s.c. with 5×10^6 cells. When tumors measured ~ 40 mm³, mice ($n = 20$ for each cell line) were randomized to receive AMD3100 (1.25 mg/kg/twice daily i.p.) or vehicle 5 days per week for 3 to 4 weeks. Tumor diameters were measured at regular intervals with caliper. After 21 days, the mean volume of BHT101 tumors in mice treated with AMD3100 was 48 mm³, whereas that of mice treated with vehicle was 620 mm³. Representative experiments are shown in Fig. 6A and B. Tumors induced by ARO and KAT4 reached the volume of 40 mm³ in only 1 week. In addition, in this case, AMD3100 was able to inhibit tumor growth, although to a lesser extent. In fact, ARO-induced tumor mean volume at the end of treatment with AMD3100 was 220 mm³, whereas that of mice treated with vehicle was 625 mm³. Similar results were also obtained when KAT4 cells were used. In this case, the difference between the mean volume of AMD3100-treated versus vehicle-treated tumors was not statistically significant after 3 weeks. However, when treatment

was extended for 1 additional week, AMD3100-treated tumor mean volume was 180 mm³, whereas that of mice treated with vehicle was 690 mm³, and the *P* value was 0.039 (Fig. 6A). These data, taken together, show that treatment with AMD3100 strongly inhibits ATC tumor growth.

Discussion

Despite ATC is a rare disease, it is one of the most aggressive human cancers (9). Although various therapeutic strategies have been exploited to slow down the growth of this tumor, none of

these treatments improved survival (10). The molecular pathways implicated in this disease are poorly understood, and this hampers the application of novel rational therapeutic strategies. Genetic alterations found in ATC are inactivating mutations of the p53 tumor suppressor and activating mutations of β -catenin, RAS, BRAF, and PIK3CA (11). Recently, molecular genetic alterations of FHIT have been also detected in ATC (35). Among the genes involved in ATC, BRAF serine-threonine kinase has been exploited as a potential therapeutic target (23).

Most epithelial cancers feature high levels of expression of the chemokine receptor CXCR4 (20). This receptor has been widely

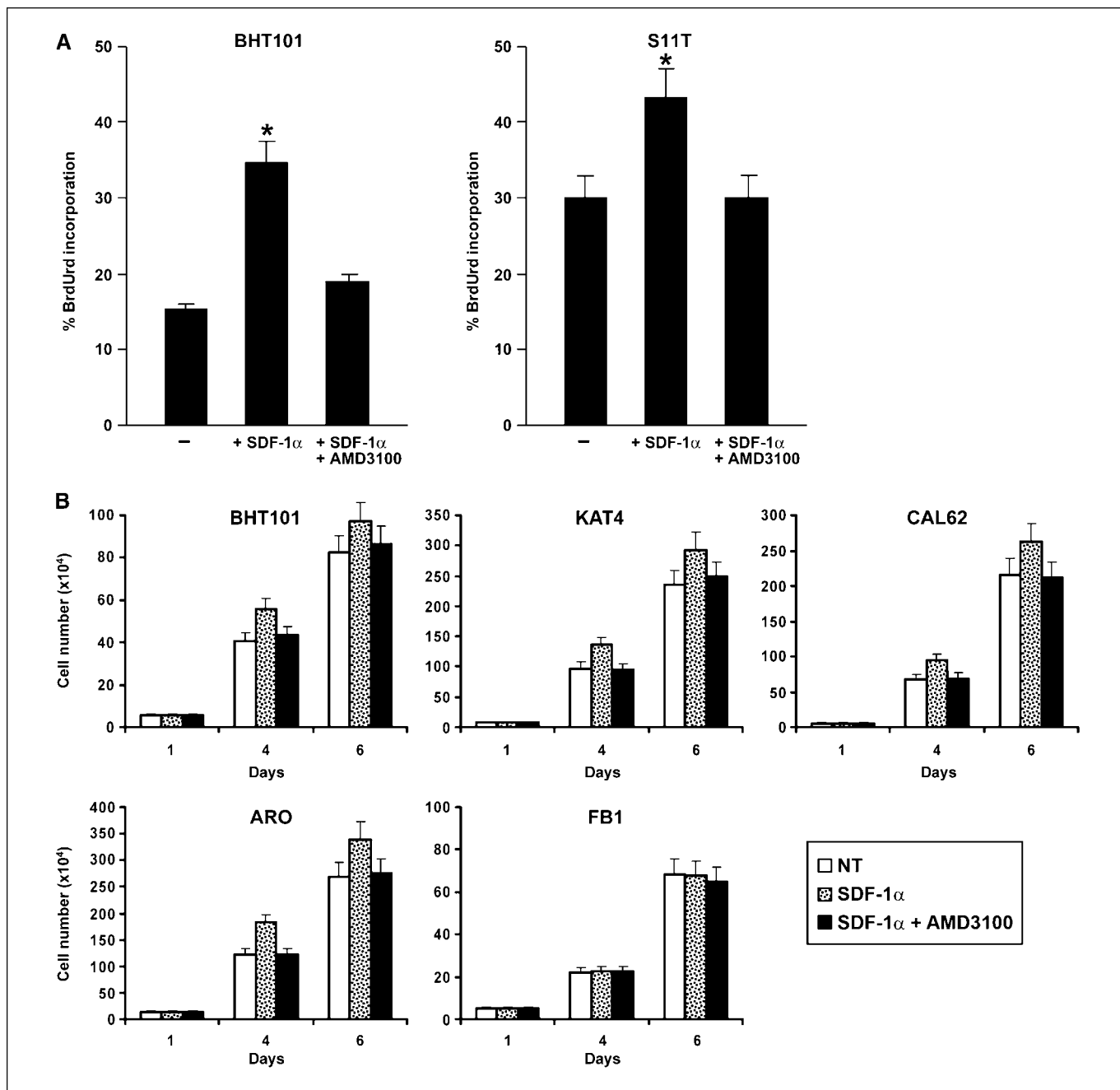


Figure 4. A, BrdUrd incorporation was measured to evaluate S-phase entry on treatment of BHT101 and S11T cells with SDF-1 α in the presence or absence of the CXCR4 inhibitor AMD3100. Columns, average results of three independent experiments; bars, SD. *P* < 0.05. B, the indicated cell lines were plated at the same density (5×10^4) in 2.5% serum, harvested, and counted at the indicated time points. Columns, average results of at least three independent determinations; bars, SD.

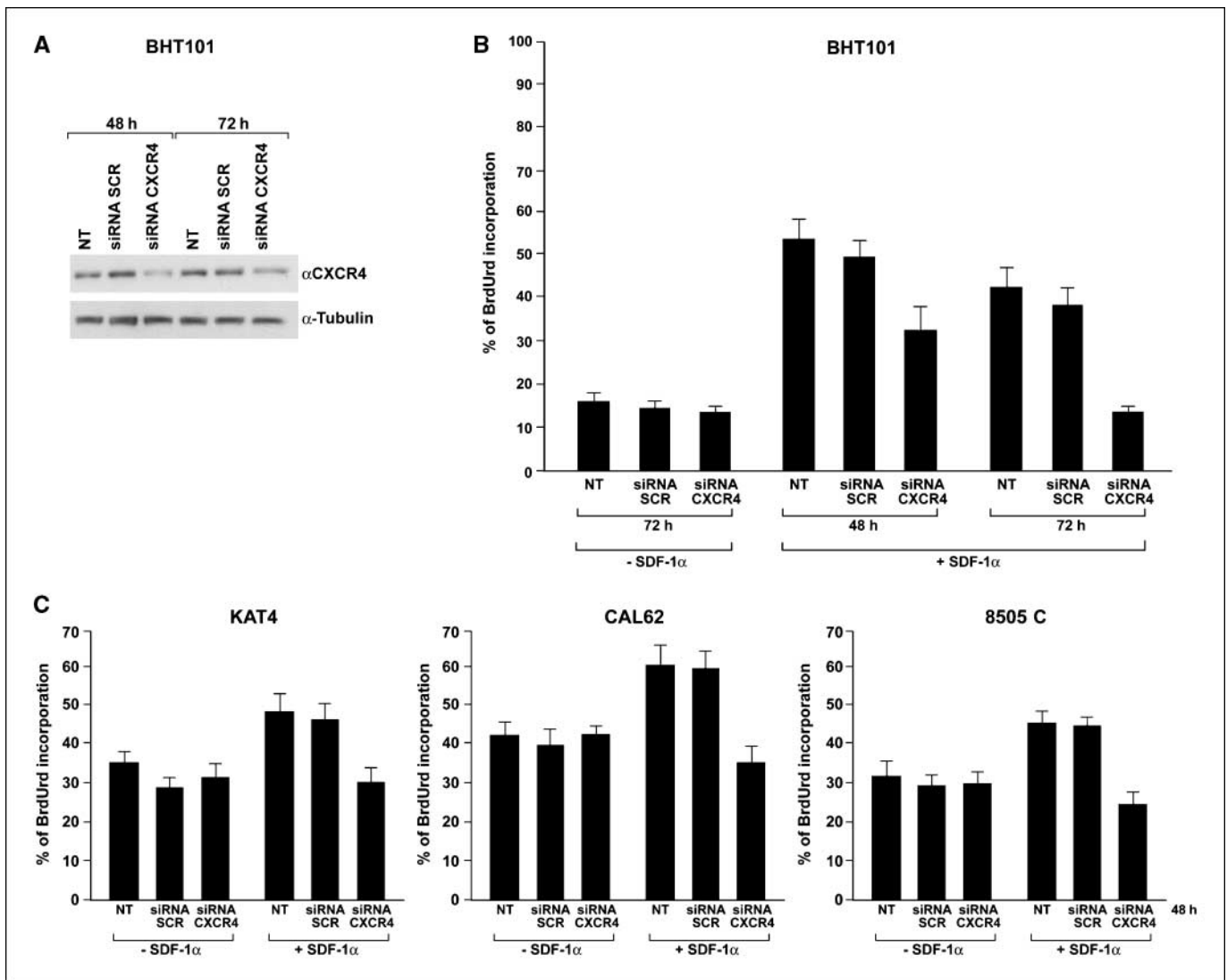


Figure 5. A, CXCR4 RNA interference was used to transiently suppress CXCR4 expression in BHT101 cells. BHT101 cells were transfected with siRNAs against CXCR4 (*siRNA CXCR4*) or control nonspecific small duplex RNA containing the same nucleotides, but in scrambled fashion (*siRNA SCR*), and harvested 48 and 72 h later. Protein lysates were subjected to immunoblotting with anti-CXCR4 and anti-tubulin antibodies. Control siRNA did not affect CXCR4 protein levels. B, CXCR4 RNA interference (*siRNA CXCR4*) in BHT101 cells inhibited SDF-1 α -stimulated S-phase entry as evaluated by BrdUrd incorporation assay. Control siRNA (*siRNA SCR*) did not inhibit DNA synthesis. Unstimulated BHT101 cells were not affected by siRNA transfection. C, CXCR4 RNA interference (*siRNA CXCR4*) inhibited S-phase entry in SDF-1 α -stimulated KAT4, CAL62, and 8505C. ATC cells were transfected with siRNAs against CXCR4 (*siRNA CXCR4*) or control siRNA (*siRNA SCR*) and harvested 48 h later. Control siRNA did not inhibit DNA synthesis. Unstimulated cells were not affected by siRNA transfection.

studied because its expression contributes to several phenotypes of cancer cells, such as the ability to grow, survive, and spread throughout the body. On the contrary, most epithelial cancers do not express SDF-1, the unique CXCR4 ligand, whereas SDF-1 is produced in high amounts in specific body districts. It has been suggested that the role of this chemokine in cancer is mainly to attract cancer cells to these districts (18). In support of this hypothesis, it has been shown that SDF-1 is produced in several metastatic sites. Recently, it has also been suggested that tumoral stroma secretes high amounts of SDF-1, supporting the concept that this chemokine is pivotal in sustaining local protumorigenic events, such as growth and survival of cancer cells (34). Furthermore, the expression of SDF-1 by stromal cancer cells directly recruits endothelial progenitors that are required for tumor angiogenesis (19). As most epithelial and hematopoietic malignancies, also thyroid cancer expresses high levels of CXCR4.

We previously reported functional expression of CXCR4 in human papillary thyroid cancer (22). Furthermore, Hwang et al. (21) showed that an anaplastic cell line, ARO, expressed high levels of functional CXCR4. In this report, we analyzed human ATC samples for CXCR4 expression. We also screened a large panel of human ATC established and primary cell cultures for CXCR4 expression. We show that, both at the mRNA and at the protein level, this receptor is overexpressed in ATC with respect to normal thyroid samples. In contrast, SDF-1 was not detected. The molecular mechanisms underlying CXCR4 up-regulation in ATC are currently unknown. Because we had previously shown that CXCR4 expression was under the control of the RET/PTC-RAS-BRAF-ERK pathway in PTCs (22), and because this pathway is also activated in ATC, we asked whether CXCR4 expression correlated with the BRAF status in ATC. The ATC cell lines that we used in this study had been previously characterized for BRAF mutations.

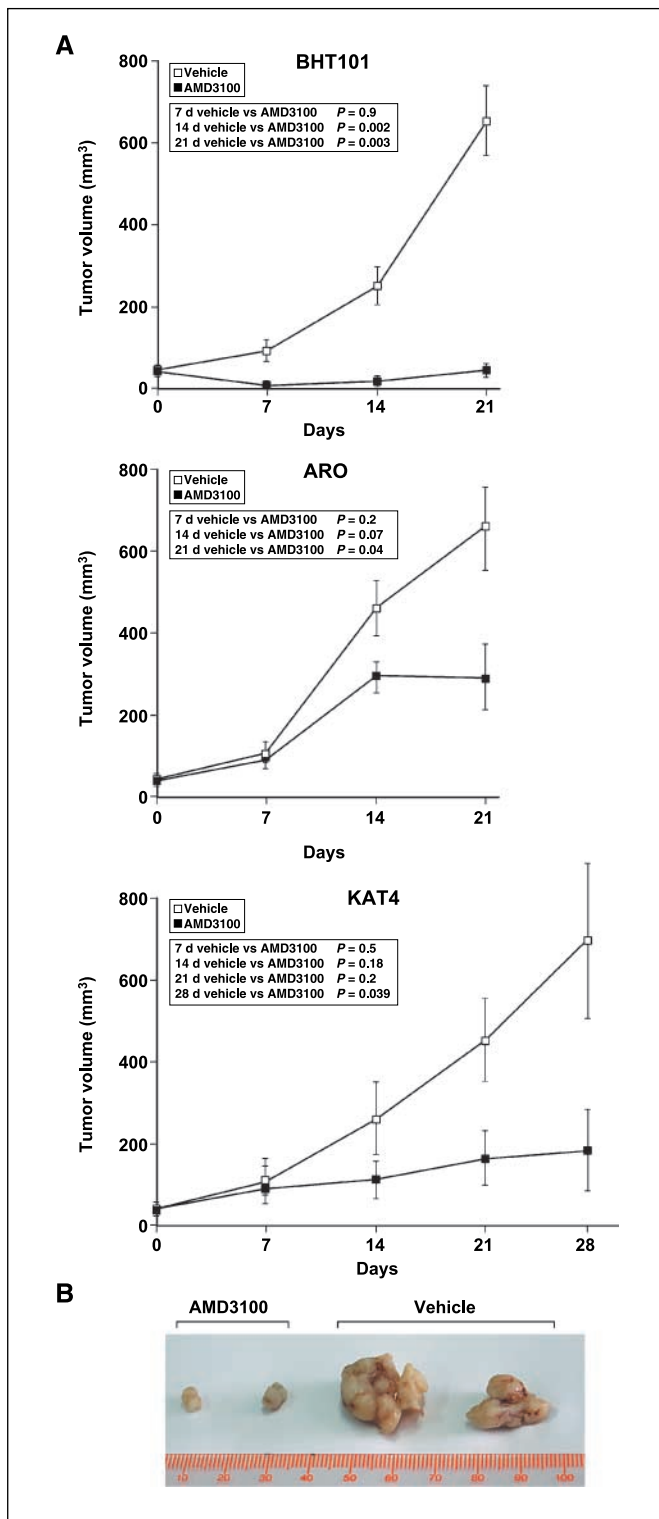


Figure 6. A, antitumor effects of AMD3100 in ATC cell xenografts. BHT101, ARO, and KAT4 cells (5×10^6 per mouse) were injected s.c. into the right dorsal portion of BALB/c athymic mice. When tumors measured 40 mm^3 , mice were randomized to two groups (10 mice per group) to receive AMD3100 or vehicle (PBS) by i.p. injection. Treatment was given for 5 consecutive days per week for 3 to 4 wks (day 1 is the treatment starting day). Tumor diameters were measured with calipers and tumor volumes were calculated. Unpaired Student's *t* test (normal distributions and equal variances) was applied. All *P* values were two sided, and differences were statistically significant at $P < 0.05$. B, tumors were excised and photographed. Two representative examples of BHT101 xenografts are shown.

Furthermore, human ATC samples were screened for the presence of BRAF mutations.⁶ We found that most of the samples expressed CXCR4, and this expression was present in both the BRAF-positive and in the BRAF-negative tumors and cell lines. These data suggest that CXCR4 up-regulation in ATC is not necessarily linked to the BRAF pathway and that it can be possibly achieved through different mechanisms. The mechanisms of CXCR4 up-regulation in cancer thus far described are various and complex. It has been shown that nuclear factor- κ B (NF- κ B) positively regulates the expression of CXCR4 (36) in breast cancer cells. Interestingly, NF- κ B is activated in human thyroid cancer cells (37, 38). Interestingly, transduction of human thyroid cancer cells with the mutant BRAF(V600E) allele induced an increase in NF- κ B DNA-binding activity (39). Thus, it is possible that CXCR4 expression in ATC is sustained by high NF- κ B activity, which can be the result either of BRAF activation or of the activation of other still undiscovered pathways.

We also show that the CXCR4 expressed on the ATC cell surface is able to transduce biochemical signals into the cell. Indeed, stimulation of ATC cells with recombinant human SDF-1 α activated ERK1/2 and, less consistently, AKT pathways in ATC cells. Moreover, we found that SDF-1 α stimulated cell growth of different ATC cell cultures, which was inhibited by the small CXCR4 inhibitor AMD3100. Given the high rate of mortality of this cancer and the lack of effective therapies, we focused our efforts in the identification of novel potential therapeutic targets in ATC. We found that the treatment with AMD3100 significantly suppressed the development of tumors in different xenograft models of ATC cells in nude mice.

The more dramatic biological effects of CXCR4 inhibition observed in the animals with respect with those observed in cell culture could be explained by the fact that SDF-1 can act, in tumor microenvironment, at multiple levels. Indeed, tumoral stromal cells, such as fibroblasts and bone marrow-derived cells, express high levels of SDF-1 (34), which can directly enhance the growth of epithelial tumoral cells and can recruit endothelial progenitors, thus favoring angiogenesis. However, when we analyzed xenograft tumors for CD31-positive tumor capillaries, we found that there were no differences in vessel density of AMD3100-treated versus untreated tumors. Preliminary data suggest that AMD3100 activity in xenografts correlates better with a proapoptotic than with an antiproliferative activity.⁷ Our findings are in accord with previous reports about the use of CXCR4 inhibitors in brain tumor models (40, 41). Although treatment of ATC xenografts with AMD3100 did not induce a complete regression of tumors, we observed a strong reduction in growth rate, which was more dramatic in the case of BHT101 xenografts. It is conceivable that the combination of conventional anticancer therapies with CXCR4 targeting would display a stronger antineoplastic effect. Given the strong antitumor activity of AMD3100, newer-generation compounds have been developed, such as AMD3465. This compound differs from the bicyclam AMD3100 in that it is a monocyclam endowed with greater solubility in water, higher affinity for CXCR4, and a potent antitumor activity (41). Although these compounds are effective in inhibiting various cancers, long-term sustained dosing of

⁶ F. Basolo and P. Faviana, unpublished observations.

⁷ V. Guarino et al., unpublished observation.

AMD3100 displayed a certain toxicity (42). For this reason, further studies, aimed at understanding the effects of long-term administration of CXCR4 inhibitors, must be pursued. Despite these considerations, our data, together with several other reports, strongly indicate that the inhibition of this pathway should be actively evaluated as a novel anticancer therapy.

In conclusion, in this report, we identify CXCR4 as another potential target of ATC anticancer therapy and suggest that AMD3100, or other specific CXCR4 inhibitors, should be developed and tested for the therapy of human ATC.

References

- De Lellis RA, Williams ED. Thyroid and parathyroid tumors. In: De Lellis RA, Lloyd RV, Heitz PU, Eng C, editors. World Health Organization classification of tumors: tumors of the endocrine organs. Lyons (France): IARC Press; 2004. p. 51–6.
- Sherman SI. Thyroid carcinoma. *Lancet* 2003;361:501–11.
- Slough CM, Randolph GW. Workup of well-differentiated thyroid carcinoma. *Cancer Control* 2006;13:99–105.
- Rosai J. Poorly differentiated thyroid carcinoma: introduction to the issue, its landmarks, and clinical impact. *Endocr Pathol* 2004;15:293–6.
- Vini L, Harmer C. Management of thyroid cancer. *Lancet Oncol* 2002;3:407–14.
- Pacini F, Schlumberger M, Dralle H, Elisei R, Smit JW, Wiersinga W; European Thyroid Cancer Taskforce. European consensus for the management of patients with differentiated thyroid carcinoma of the follicular epithelium. *Eur J Endocrinol* 2006;154:787–803.
- Patel KN, Shaha AR. Poorly differentiated and anaplastic thyroid cancer. *Cancer Control* 2006;13:119–28.
- Pasieka JL. Anaplastic thyroid cancer. *Curr Opin Oncol* 2003;15:78–83.
- Are C, Shaha AR. Anaplastic thyroid carcinoma: biology, pathogenesis, prognostic factors, and treatment approaches. *Ann Surg Oncol* 2006;13:453–64.
- Veness MJ, Porter GS, Morgan GJ. Anaplastic thyroid carcinoma: dismal outcome despite current treatment approach. *ANZ J Surg* 2004;74:559–62.
- Kondo T, Ezzat S, Asa SL. Pathogenetic mechanisms in thyroid follicular-cell neoplasia. *Nat Rev Cancer* 2006;6:292–306.
- Nikiforov YE. Genetic alterations involved in the transition from well-differentiated to poorly differentiated and anaplastic thyroid carcinomas. *Endocr Pathol* 2004;15:319–27.
- Garcia-Rostan G, Costa AM, Pereira-Castro I, et al. Mutation of the PIK3CA gene in anaplastic thyroid cancer. *Cancer Res* 2005;65:10199–207.
- Garcia-Rostan G, Tallini G, Herrero A, D'Aquila TG, Carcangiu ML, Rimm DL. Frequent mutation and nuclear localization of β -catenin in anaplastic thyroid carcinoma. *Cancer Res* 1999;59:1811–5.
- Quiros RM, Ding HG, Gattuso P, Prinz RA, Xu X. Evidence that one subset of anaplastic thyroid carcinomas are derived from papillary carcinomas due to BRAF and p53 mutations. *Cancer* 2005;103:2261–8.
- Rossi D, Zlotnik A. The biology of chemokines and their receptors. *Annu Rev Immunol* 2000;18:217–42.
- Zlotnik A. Chemokines and cancer. *Int J Cancer* 2006;119:2026–9.
- Muller A, Homey B, Soto H, et al. Involvement of chemokine receptors in breast cancer metastasis. *Nature* 2001;410:50–6.
- Burger JA, Kipps TJ. CXCR4: a key receptor in the crosstalk between tumor cells and their microenvironment. *Blood* 2006;107:1761–7.
- Balkwill F. The significance of cancer cell expression of the chemokine receptor CXCR4. *Semin Cancer Biol* 2004;14:171–9.
- Hwang JH, Hwang JH, Chung HK, et al. CXC chemokine receptor 4 expression and function in human anaplastic thyroid cancer cells. *J Clin Endocrinol Metab* 2003;88:408–16.
- Castellone MD, Guarino V, De Falco V, et al. Functional expression of the CXCR4 chemokine receptor is induced by RET/PTC oncogenes and is a common event in human papillary thyroid carcinomas. *Oncogene* 2004;23:5958–67.
- Salvatore G, De Falco V, Salerno P, et al. BRAF is a therapeutic target in aggressive thyroid carcinoma. *Clin Cancer Res* 2006;12:1623–9.
- Carlomagnò F, Vitagliano D, Guida T, et al. Efficient inhibition of RET/papillary thyroid carcinoma oncogenic kinases by 4-amino-5-(4-chloro-phenyl)-7-(*t*-butyl)-pyrazolo[3,4-*d*]pyrimidine (PP2). *J Clin Endocrinol Metab* 2003;88:1897–902.
- Basolo F, Giannini R, Toniolo A, et al. Establishment of a non-tumorigenic papillary thyroid cell line (FB-2) carrying the RET/PTC1 rearrangement. *Int J Cancer* 2002;97:608–14.
- Inokuchi N, Zeki K, Morimoto I, et al. Stimulatory effect of interleukin-1 α on proliferation through a Ca²⁺/calmodulin-dependent pathway of a human thyroid carcinoma cell line, NIM 1. *Jpn J Cancer Res* 1995;86:670–6.
- Vitagliano D, Portella G, Troncone G, et al. Thyroid targeting of the N-ras(Gln61Lys) oncogene in transgenic mice results in follicular tumors that progress to poorly differentiated carcinomas. *Oncogene* 2006;25:5467–74.
- Powell DJ, Jr., Russell J, Nibu K, et al. The RET/PTC3 oncogene: metastatic solid-type papillary carcinomas in murine thyroids. *Cancer Res* 1998;58:5523–8.
- Russell JP, Powell DJ, Cunnane M, et al. The TRK-T1 fusion protein induces neoplastic transformation of thyroid epithelium. *Oncogene* 2000;19:5729–35.
- Ledent C, Dumont J, Vassart G, Parmentier M. Thyroid adenocarcinomas secondary to tissue-specific expression of simian virus-40 large T-antigen in transgenic mice. *Endocrinology* 1991;129:1391–401.
- Ganju RK, Brubaker SA, Meyer J, et al. The α -chemokine, stromal cell-derived factor-1 α , binds to the transmembrane G-protein-coupled CXCR-4 receptor and activates multiple signal transduction pathways. *J Biol Chem* 1998;273:23169–75.
- Peng SB, Peek V, Zhai Y, et al. Akt activation, but not extracellular signal-regulated kinase activation, is required for SDF-1 α /CXCR4-mediated migration of epitheloid carcinoma cells. *Mol Cancer Res* 2005;3:227–36.
- De Clercq E. Potential clinical applications of the CXCR4 antagonist bicyclam AMD3100. *Mini Rev Med Chem* 2005;5:805–24.
- Orimo A, Gupta PB, Sgroi DC, et al. Stromal fibroblasts present in invasive human breast carcinomas promote tumor growth and angiogenesis through elevated SDF-1/CXCL12 secretion. *Cell* 2005;121:335–48.
- Pavelic K, Dedivitis RA, Kapitanovic S, et al. Molecular genetic alterations of FHIT and p53 genes in benign and malignant thyroid gland lesions. *Mutat Res* 2006;599:45–57.
- Helbig G, Christopherson KW II, Bhat-Nakshatri P, et al. NF- κ B promotes breast cancer cell migration and metastasis by inducing the expression of the chemokine receptor CXCR4. *J Biol Chem* 2003;278:21631–8.
- Visconti R, Cerutti J, Battista S, et al. Expression of the neoplastic phenotype by human thyroid carcinoma cell lines requires NF κ B p65 protein expression. *Oncogene* 1997;15:1987–94.
- Pacifico F, Mauro C, Barone C, et al. Oncogenic and anti-apoptotic activity of NF- κ B in human thyroid carcinomas. *J Biol Chem* 2004;279:54610–9.
- Palona I, Namba H, Mitsutake N, et al. BRAFV600E promotes invasiveness of thyroid cancer cells through nuclear factor κ B activation. *Endocrinology* 2006;147:5699–707.
- Rubin JB, Kung AL, Klein RS, et al. A small-molecule antagonist of CXCR4 inhibits intracranial growth of primary brain tumors. *Proc Natl Acad Sci U S A* 2003;100:13513–8.
- Yang L, Jackson E, Woerner BM, Perry A, Piwnicka-Worms D, Rubin JB. Blocking CXCR4-mediated cyclic AMP suppression inhibits brain tumor growth *in vivo*. *Cancer Res* 2007;67:651–8.
- Hendrix CW, Collier AC, Lederman MM, et al. AMD3100 HIV Study Group. Safety, pharmacokinetics, and antiviral activity of AMD3100, a selective CXCR4 receptor inhibitor, in HIV-1 infection. *J Acquir Immune Defic Syndr* 2004;37:1253–62.

Acknowledgments

Received 3/7/2007; revised 7/26/2007; accepted 9/28/2007.

Grant support: Associazione Italiana per la Ricerca sul Cancro and E.C. Contract 03695 (GenRisk-T). V. De Falco was a fellow of the Dipartimento di Biologia e Patologia Cellulare e Molecolare of the University of Naples. V. Guarino was a fellow of the Associazione Italiana per la Ricerca sul Cancro.

The costs of publication of this article were defrayed in part by the payment of page charges. This article must therefore be hereby marked *advertisement* in accordance with 18 U.S.C. Section 1734 solely to indicate this fact.

We thank F. Curcio for the P5 and HTU8 cells; H. Zitzelsberger for the S11T, S77T, and S147T; J. Dumont for animals expressing the SV40 transgene; and S. Sequino for excellent assistance in animal care and manipulation.

OPN/CD44v6 overexpression in laryngeal dysplasia and correlation with clinical outcome

S Staibano¹, F Merolla², D Testa³, R Iovine⁴, M Mascolo¹, V Guarino², MD Castellone², M Di Benedetto¹, V Galli⁴, S Motta³, RM Melillo², G De Rosa¹, M Santoro² and A Celetti^{*,2}

¹Dipartimento di Scienze Biomorfologiche e Funzionali, Università di Napoli 'Federico II', Naples, Italy; ²Dipartimento di Biologia e Patologia Cellulare e Molecolare, Università di Napoli 'Federico II', Istituto di Endocrinologia ed Oncologia Sperimentale del CNR, Naples, Italy; ³Clinica Otorinolaringoiatrica, Seconda Università di Napoli, Naples, Italy; ⁴Dipartimento Assistenziale di Otorinolaringoiatria e Scienze Affini, Università di Napoli 'Federico II', Naples, Italy

Laryngeal dysplasia is a common clinical concern. Despite major advancements, a significant number of patients with this condition progress to invasive squamous cell carcinoma. Osteopontin (OPN) is a secreted glycoprotein, whose expression is markedly elevated in several types of cancers. We explored OPN as a candidate biomarker for laryngeal dysplasia. To this aim, we examined OPN expression in 82 cases of dysplasia and in hyperplastic and normal tissue samples. OPN expression was elevated in all severe dysplasia samples, but not hyperplastic samples, with respect to matched normal mucosa. OPN expression levels correlated positively with degree of dysplasia ($P = 0.0094$) and negatively with disease-free survival ($P < 0.0001$). OPN expression was paralleled by cell surface reactivity for CD44v6, an OPN functional receptor. CD44v6 expression correlated negatively with disease-free survival, as well ($P = 0.0007$). Taken as a whole, our finding identify OPN and CD44v6 as predictive markers of recurrence or aggressiveness in laryngeal intraepithelial neoplasia, and overall, point out an important signalling complex in the evolution of laryngeal dysplasia.

British Journal of Cancer (2007) **97**, 1545–1551. doi:10.1038/sj.bjc.6604070 www.bjcancer.com

Published online 6 November 2007

© 2007 Cancer Research UK

Keywords: OPN; SCC; dysplasia; marker

Laryngeal squamous cell carcinoma (LSCC) is the most common type of head and neck squamous cell carcinoma (HNSCC). LSCC accounts for 1–2% of all malignancies diagnosed worldwide (Vokes *et al*, 1993; Licitra *et al*, 2003; Mao *et al*, 2004). Notwithstanding primary prevention, screening, surgical treatment, and radiotherapy, the long-term survival rate of LSCC patients has remained substantially unchanged in the last two decades (Hoffman *et al*, 1998). Survival of the patients depends on the stage of the disease; therefore, early detection and timely therapy are essential (Vokes *et al*, 1993; Hoffman *et al*, 1998; Licitra *et al*, 2003; Mao *et al*, 2004).

Laryngeal squamous cell carcinoma usually develops in a multistep process: normal mucosa – dysplasia (laryngeal intraepithelial neoplasia, LIN) – LSCC *in situ* – invasive LSCC (Rosai *et al*, 1992; Tabor *et al*, 2002; Zuckerman, 2002; Johnson, 2003). Dysplasia is characterised by increased cell growth, cellular atypia (nuclear and nucleolar abnormalities, altered nuclear/cytoplasmic ratio, and altered cytoplasmic differentiation), and architectural alteration of the epithelium. Conventionally, the dysplastic changes are graded as mild (LIN I: dysplasia limited to the basal third of the epithelium, few mitoses), moderate (LIN II: dysplasia involving the lower two-thirds of the epithelium, marked nuclear changes, prominent nucleoli, mitoses in the parabasal, and

intermediate layers), and severe (LIN III: dysplasia involving more than two-thirds of the epithelial thickness, nuclear pleomorphism and hyperchromasia, prominent nucleoli, cell crowding, and atypical mitoses). Often, severe dysplasia and *in situ* carcinoma are grouped in the same category (Rosai *et al*, 1992; Tabor *et al*, 2002; Zuckerman, 2002; Johnson, 2003). Early forms of dysplasia may be reversible if the initial stimuli (like smoke and volatile irritating substances) are removed, while severe dysplasia, if left untreated, is regarded as a precancerous lesion (Rosai *et al*, 1992; Tabor *et al*, 2002; Zuckerman, 2002; Johnson, 2003). For patients with mild or moderate dysplasia, the reported rate of progression to invasive cancer is up to 11.5 and 45%, respectively. In severe dysplasia, higher rates of progression are commonly reported (Rosai *et al*, 1992; Tabor *et al*, 2002; Zuckerman, 2002; Johnson, 2003). The molecular events that induce the evolution of dysplasia to carcinoma are still unknown (Cowan *et al*, 1992; Zuckerman, 2002; Perez-Ordóñez *et al*, 2006).

Osteopontin (OPN), also known as SPP1 (secreted phosphoprotein 1), is a highly acidic calcium-binding glycosylated phosphoprotein (Weber, 2001; Rittling and Chambers, 2004; Rangaswami *et al*, 2006). OPN can function both as cell adhesion molecule and as cytokine. It binds to the cell surface receptors α - or β 1-containing integrins and CD44v6 (Weber, 2001; Rittling and Chambers, 2004; Rangaswami *et al*, 2006), thereby supporting proliferation, chemotaxis, attachment, and migration of many cell types. CD44 is a cell surface glycoprotein that is involved in regulating cell–cell and cell–matrix interactions, migration, and tumour growth and progression (Ponta *et al*, 2003). CD44 is

*Correspondence: Dr A Celetti; E-mail: celetti@unina.it

Received 18 July 2007; revised 1 October 2007; accepted 9 October 2007; published online 6 November 2007

expressed as a standard receptor (CD44s) and in multiple splice isoforms (CD44v), whose expression is altered during tumour growth and progression. Expression of the 'v6' variant exon of CD44 is necessary for OPN binding (Ponta *et al*, 2003). OPN is overexpressed in many human tumours, for example, colon, breast, liver, prostate, gastric, ovarian, lung, thyroid, and kidney carcinomas (Agrawal *et al*, 2002; Kang *et al*, 2003; Ye *et al*, 2003; Schorge *et al*, 2004; Donati *et al*, 2005; Guarino *et al*, 2005; Matusan *et al*, 2006).

We recently reported that OPN and CD44v6 are overexpressed in full-blown LSCC (Celetti *et al*, 2005). Here, we have investigated the role of the OPN/CD44v6 axis in laryngeal dysplasia.

MATERIALS AND METHODS

Study population

Patients (82 cases: 77 men and 5 women) underwent surgery at the Otolaryngology Department of the University Federico II of Naples between January 1993 and December 2001. The patients' age ranged from 23 to 83 years, with a mean of 62.46 years. Paraffin blocks were retrieved from the files of the Department of Biomorphological and Functional Sciences, Pathology Section, University Federico II of Naples. Each patient agreed to and signed a consent for the treatment of clinical data and tissues for diagnostic and research purposes, according to the guidelines of the Institutional Ethic Committee. For all the patients, clinicopathologic and follow-up data were recorded (Table 1). Before surgery, patients underwent otolaryngological, fiberoptic, and radiological evaluation. The mean follow-up time was 10.1 years (range: 8–13 years). Follow-up consisted in clinical and radiological evaluation at 3-month intervals for the first year and 6-months intervals thereafter. At completion of follow-up, patients were subdivided into alive with absence of relapse (no); alive with evidence of recurrent disease (LIN); and alive with progression of disease to LSCC (SCC).

After surgical resection, tissues were fixed in 10% neutral buffered formalin and embedded in paraffin blocks. Sections (4- μ m thick) were stained with haematoxylin–eosin for histological examination. The pathologic analysis was performed in a blinded fashion to the clinical informations. The cytological evaluation was according to standard criteria (Evans *et al*, 1986; Gale *et al*, 2000; Tabor *et al*, 2003).

Table 1 Clinicopathological features of studied laryngeal intraepithelial neoplasia (LIN) patients

Characteristics	Total (%)
No. of subjects	
Male	77 (94)
Female	5 (6)
Disease site	
Glottis–hypoglottis	43 (53)
Supraglottis	39 (47)
Degree of dysplasia	
Mild	21 (47)
Moderate	8 (19)
Severe	53 (64)
Relapse	
No	35 (43)
LIN	10 (12)
SCC	37 (45)

SCC = squamous cell carcinoma.

Immunohistochemistry

Four-micromolar thick serial sections, mounted on poly-L-lysine-coated glass slides, were dewaxed, rehydrated through multiple graded ethanol solutions, treated with 3% hydrogen peroxide for 5 min to inactivate endogenous peroxidases, and washed in distilled water. After antigen retrieval (microwave oven 5 min \times 3 times, in 1% citrate buffer), nonspecific binding was blocked by incubation (2 h at room temperature) with 1.5% blocking serum. Slides were first incubated with anti-OPN (final concentration: 5 μ g ml⁻¹) (10A16; Assay Designs, Ann Arbor, MI, USA) or anti-CD44v6 (dilution of 1:100) (NCL-CD44v6, clone VFF-7; Novocastra Laboratories Ltd, Newcastle upon Tyne, UK) monoclonal antibodies and then with biotinylated anti-IgG and the premixed avidin–biotin complex (overnight at 4°C) (Vectastain ABC kits; Vector Laboratories, Burlingame, CA, USA). The immune reaction was revealed with 0.06 mmol l⁻¹ diaminobenzidine (DAB-DAKO, Carpinteria, CA, USA) and 2 mmol l⁻¹ hydrogen peroxide. Finally, slides were counterstained with haematoxylin and coverslipped with a synthetic mounting media. Control slides in the presence of preimmune serum were included for each staining as an additional negative control. Anti-OPN antibody was preincubated with a fivefold molar excess of OPN peptide to ascertain specificity of the reaction.

The results of the immunohistochemical staining were evaluated separately and in a blinded fashion by two pathologists. Five representative microscopic areas at \times 400 magnification were randomly selected for examination. Expression of OPN was semiquantitatively assessed as percentage of positive cells with respect to the total number of epithelial cells. The samples were assigned to one of the four following categories: 0 (absence of positive cells); + (<10% of positive cells); ++ (10–50% of positive cells); and +++ (>50% of positive cells). Staining of CD44v6 was classified as 'lower' (lower third) (L), 'lower and middle' (up to two-thirds of the thickness of the epithelium) (M), and 'full thickness' (F).

Statistical analysis

The Pearson's χ^2 test was used to assess the statistical significance of the frequency distribution of all categories of OPN or CD44v6 expression by degree of dysplasia or by relapse. Differences were significant with *P*-value <0.05.

Nonparametric Spearman's correlation coefficient method was used to assess the statistical significance of the correlation between OPN expression vs CD44v6 positivity. A test was run for all the patients' cohort combined or grouped by degree of dysplasia or by type of relapse. Correlations were significant when *P*-value was <0.05. Disease-free survival curves of the patients were calculated using the Kaplan–Meier method, and analysis was performed by the log-rank test. Differences were significant when *P*<0.05. In this analysis, a group of 31 patients has been censored for lack of data. Statistical analysis was performed using the JMP software program (version 5.1.1; SAS Institute Inc., Austin, TX, USA).

RESULTS

Immunohistochemical detection of OPN and CD44v6 in laryngeal dysplasia

Eighty-two laryngeal samples with different degree of dysplasia (Table 1) and the matched normal mucosa were tested for OPN expression by immunohistochemistry with an anti-OPN-specific monoclonal antibody. Representative stainings are shown in Figure 1, and the entire data set is reported in Table 2. OPN was virtually undetectable (<2.0% of the cells) in normal tissue (*n*=10). Dysplastic areas showed different degrees of OPN positivity. In most (76%) of mild dysplasia cases, only few cells

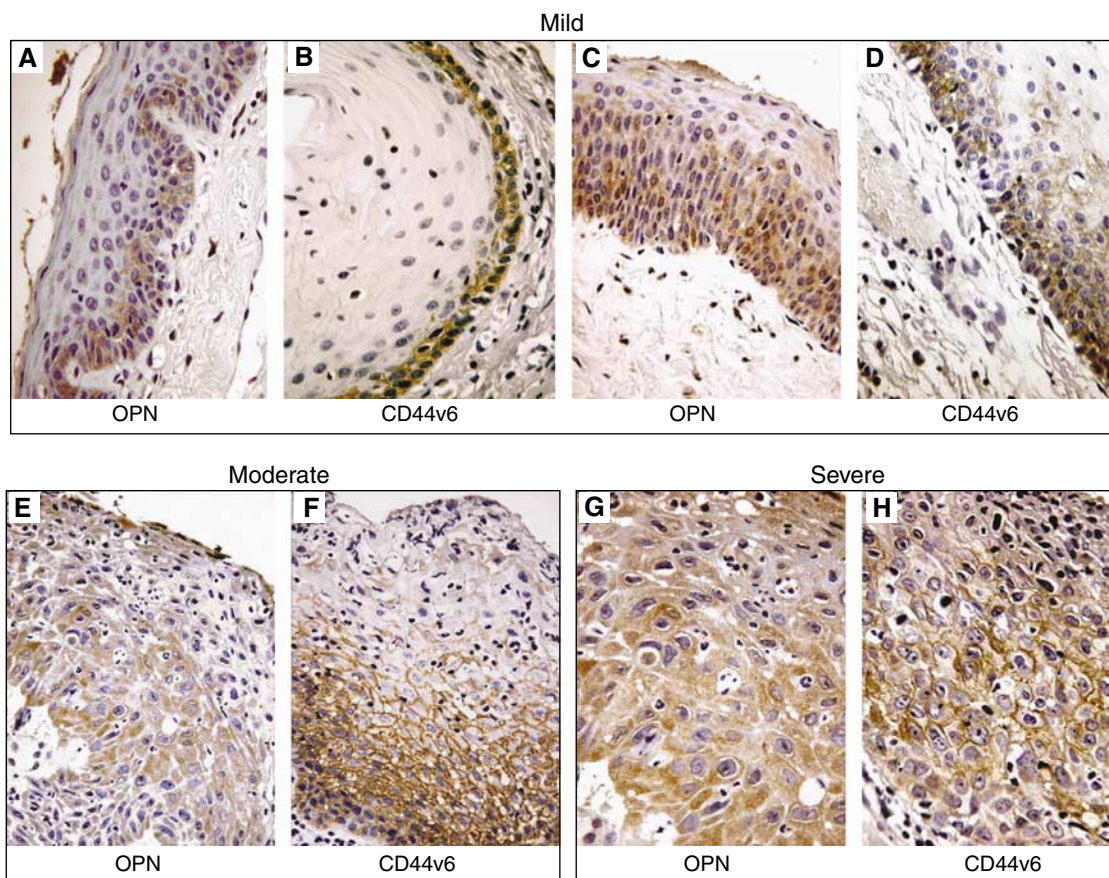


Figure 1 (A and B) A representative case of mild degree dysplasia showing weak immunostaining for OPN (A) and CD44v6 positivity restricted to the lower third of the epithelium (B) (× 150). (C and D) Another mild dysplasia sample showing stronger immunostaining for both the markers (× 150). (E and F) A representative case of moderate dysplasia showing a strong immunostaining for OPN (E) and a CD44v6 positivity involving the lower two-thirds of the epithelium (F) (× 250). (G and H) A case of high-grade dysplasia showing strong immunostaining for OPN (G) and CD44v6 positivity up to the upper third of the epithelium (H) (× 400).

Table 2 OPN and CD44v6 positivity in laryngeal intraepithelial neoplasia at different degree

LIN	OPN positivity ^a	CD44v6 positivity ^a
Mild (21)	16/21 (+)	16/21 (L)
	1/21 (++)	2/21 (M)
	4/21 (+++)	3/21 (F)
Moderate (8)	3/8 (+)	2/8 (L)
	1/8 (++)	3/8 (M)
	4/8 (+++)	3/8 (F)
Severe (53)	16/53 (+)	15/53 (L)
	11/53 (++)	12/53 (M)
	26/53 (+++)	26/53 (F)

OPN=osteopontin. ^aOsteopontin and CD44v6 expression were assessed by immunohistochemistry and scored respectively as follows: + = < 10% positive cells; ++ = 10–50% positive cells; and +++ = 50–100% positive cells; L=lower; M = lower and middle; and F = full-thickness involvement of the epithelial layers.

(+) were positive (Figure 1A), while 50% of moderate and severe dysplasia samples had intense (+++) OPN staining (Figures 1E and G). Only 20% cases of mild dysplasia were highly positive for OPN (+++); interestingly, in these samples, OPN expression coexisted with a diffuse CD44v6 staining (see below) (Figures 1C and D).

The samples were also analysed for the expression of CD44v6, the receptor that is involved in OPN binding (Table 2). Only basal cells (L category) were CD44v6 positive in 76% of mild dysplasia

samples (Figure 1B). Instead, in moderate dysplasia, CD44v6 positivity was found in the basal two-thirds (M category) (Figure 1F) or even full thickness (F category) of the epithelium. Finally, 50% of severe dysplasia samples showed a full-thickness (F category) CD44v6 staining (Figure 1H). The association between OPN and CD44v6 immunoreactivity resulted significant when analysed by the Spearman's rank correlation test (Table 3A). The frequency distribution of OPN positivity or CD44v6 immunoreactivity by degree of dysplasia resulted highly significant at Pearson's χ^2 test (Table 4A).

Foci of squamous metaplasia of laryngeal cylindrical-cell-lined areas were almost constantly present in our samples. Metaplastic areas ($n=20$) were almost constantly negative for OPN and CD44v6 staining (Figures 2A and B). Only in few (5%) cases, we observed an intense (+++) OPN staining paralleled by full-thickness CD44v6 positivity in the squamous metaplastic cells (Figures 2C and D). Although the ultimate statistical relevance of this finding is still to be verified on larger series of cases, it is interesting to note that these OPN- and CD44v6-positive metaplasia areas were found in patients with a history of development of SCC at the follow-up.

OPN and CD44v6 expression levels in laryngeal dysplasia negatively correlate with disease-free survival

The disease-free survival rate in patients affected by laryngeal dysplasia negatively correlated with intense OPN staining and full-thickness CD44v6 positivity. As shown by the Kaplan–Meier

survival curves reported in Figure 3A, the 8-years disease-free survival was 94 and 91% for OPN (+)- and OPN (++)-positive cases, respectively, and 33% for OPN (+++)-positive cases (two-sided log-rank test, $P < 0.0001$; Figure 4A). Relative to CD44v6 expression, the probability of recurrence was 94 and 75% for cases that showed basal (L), or basal and middle (M) staining, respectively, and 38% for patient that had full-thickness (F) positivity (two-sided log-rank test, $P = 0.007$; Figure 4B).

Table 3A Correlation of osteopontin and CD44v6 expression in all laryngeal intraepithelial neoplasia (LIN) patients combined or grouped by degree of dysplasia

LIN	r_s	P_s
Combined (82)	0.8231	<0.0001
Mild (21)	0.9941	<0.0001
Moderate (8)	0.2622	=0.5304
Severe (53)	0.7957	<0.0001

Note: Correlation between osteopontin and CD44v6 expression in LIN patients analysed by Spearman's rank correlation test. Correlation coefficient (r_s) and P_s are shown ($P_s < 0.05$ was considered significant).

Table 3B Correlation of osteopontin and CD44v6 expression in all laryngeal intraepithelial neoplasia (LIN) patients combined or grouped by relapse

Relapse	r_s	P_s
Combined (82)	0.8231	<0.0001
no (35)	0.8133	<0.0001
LIN (10)	0.5976	=0.0734
SCC (37)	-0.7892	<0.0001

SCC = squamous cell carcinoma. Note: Absence of relapse (no), recurrence of dysplasia (LIN), progression to carcinoma (SCC). Correlation between osteopontin and CD44v6 expression in LIN patients analysed by Spearman's rank correlation test. Correlation coefficient (r_s) and P_s are shown ($P_s < 0.05$ was considered significant).

At the Pearson's test, the frequency distribution of OPN and CD44v6 expression levels were significantly correlated with relapse (Table 4B).

Moreover, the correlation between OPN and CD44v6 expression in patients with absence of relapse, with recurrence of dysplasia, or with progression to LSCC resulted very significant at the Spearman's rank correlation test (Table 3B). Finally, the contingency analysis showed that the frequency distribution of OPN by CD44v6 were highly significant in combined or grouped types of relapse (Table 4C).

DISCUSSION

An in-depth understanding of the factors involved in the initial steps of LSCC development will facilitate the prevention and diagnosis of this condition. Currently, histological grading and the

Table 4 Pearson's test

	χ^2	P
A. Contingency analysis of osteopontin (OPN) and CD44v6 positivity by degree of dysplasia		
OPN	13.425	0.0094
CD44v6	16.198	0.0028
B. Contingency analysis of OPN and CD44v6 positivity by relapse (no, LIN, SCC)		
OPN	21.780	<0.0002
CD44v6	9.567	0.0484
C. Contingency analysis of OPN positivity by CD44v6 expression in all laryngeal intraepithelial neoplasia combined or grouped by relapse		
Combined (82)	73.026	<0.0001
No (35)	32.694	<0.0001
LIN (10)	10.000	0.0067
SCC (37)	34.857	<0.0001

LIN = laryngeal intraepithelial neoplasia; SCC = squamous cell carcinoma. Note: Absence of relapse (no), recurrence of dysplasia (LIN), and progression to carcinoma (SCC).

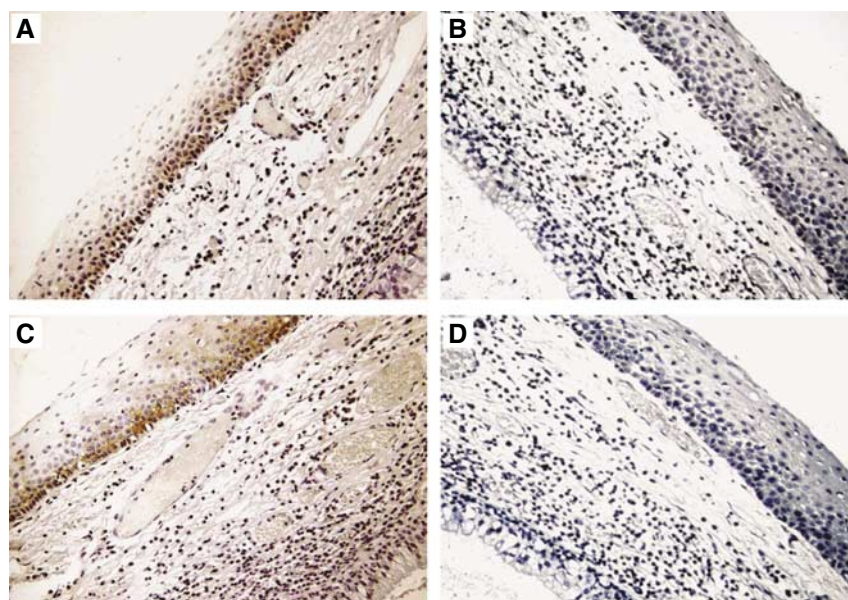


Figure 2 (A and C) A representative case of mild degree dysplasia showing weak immunostaining for OPN (A) and CD44v6 positivity restricted to the lower third of the epithelium (C) ($\times 150$). (B and D) The same samples as in (A) negative for OPN immunostaining after incubation with isotype control antiserum (B) ($\times 150$), and the same sample as in (C) negative for CD44v6 immunostaining after incubation with isotype control antiserum (D) ($\times 150$).

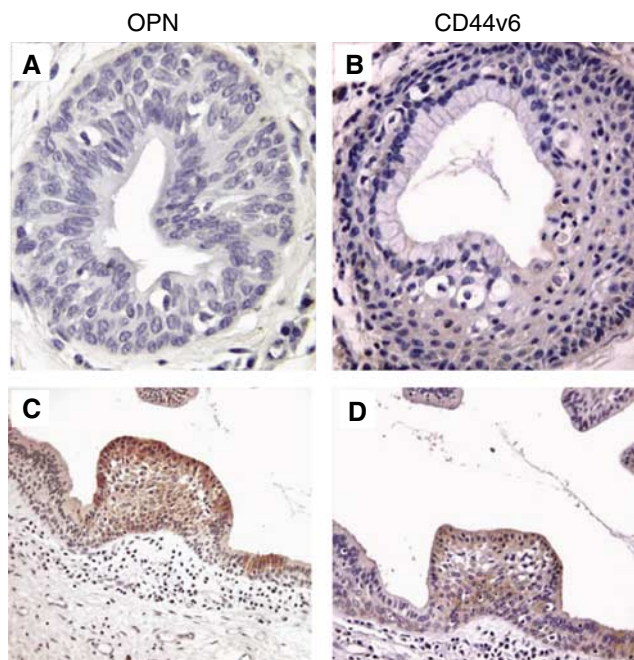


Figure 3 (A and B) An area of incomplete squamous metaplasia, negative for OPN (A), and CD44v6 (B) immunostaining ($\times 250$). (C and D) Another case of incomplete squamous metaplasia (patient with a history of laryngeal SCC), showing an intense OPN (C) and CD44v6 (D) immunostaining ($\times 106$).

topographical extension of laryngeal dysplasia are used to predict the risk for cancer and to determine the treatment strategy (Rosai *et al*, 1992; Zuckerberg, 2002; Johnson, 2003). Although significant efforts have been made to identify molecular markers of the clinical outcome of premalignant laryngeal lesion, still neither single nor combination of markers is accepted in clinical practice (Tabor *et al*, 2002).

We have previously reported that both OPN and CD44v6 are highly expressed in invasive LSCC (Celetti *et al*, 2005). Here, we have explored whether the same ligand/receptor pair is involved in the premalignant phases as well. To this aim, we have investigated OPN and CD44v6 in a set of laryngeal dysplasia samples and correlated their expression level to histological grading and clinical outcome. Both OPN and CD44v6 were consistently overexpressed in dysplastic but not hyperplastic or metaplastic mucosa. Dysplasia, in particular high-grade dysplasia, is regarded as a preneoplastic condition (Rosai *et al*, 1992). Importantly, OPN/CD44v6 overexpression was significantly correlated with the degree of dysplasia, type of recurrence, and reduced disease-free survival. Taken together, these findings suggest that OPN signalling through CD44v6 may play a role in the establishment of dysplastic changes in the laryngeal epithelium. Interestingly, it has been recently reported that genetic deletion of OPN in transgenic mice did not change the rate of hyperplasia formation but caused a reduction of benign papilloma formation after the two-stage skin chemical carcinogenesis protocol; thus, also in this experimental model system, OPN is involved in the early phases of tumorigenesis (Hsieh *et al*, 2006).

Osteopontin is able to engage several cell surface receptors, including integrins and CD44 variants. In particular, OPN binds CD44 proteins that contain v6-encoded sequences, and OPN/CD44v6 binding has been implicated in carcinogenesis (Ponta *et al*, 2003). Here, we show that OPN expression levels were paralleled by intense expression of CD44v6; at contingency analysis, the frequency distribution of OPN expression by CD44v6 positivity resulted highly significant at Pearson's test;

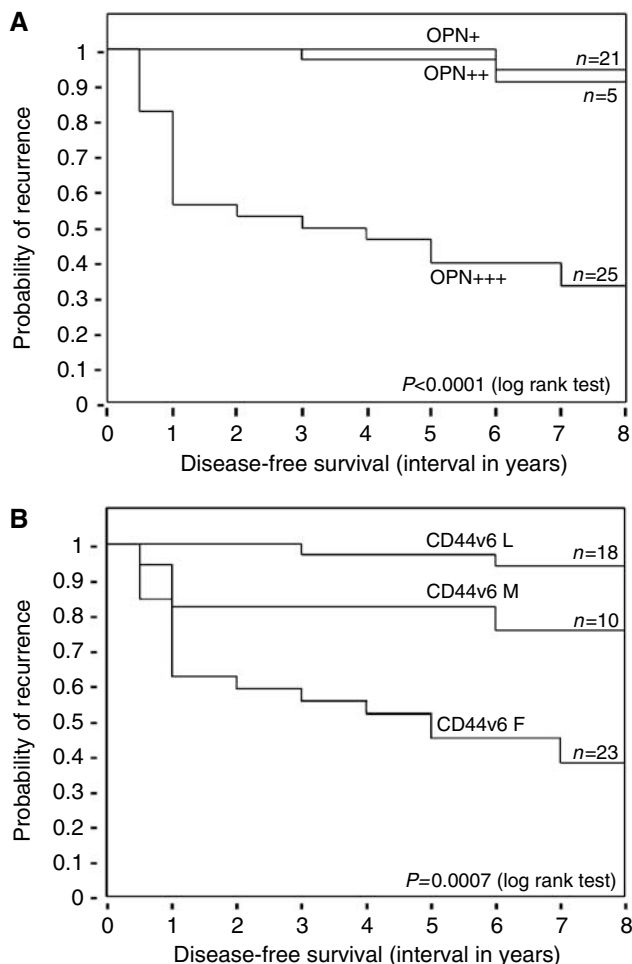


Figure 4 Osteopontin and CD44v6 staining in laryngeal dysplasia negatively correlates with disease-free survival. Kaplan–Meier survival plots for patients grouped on the basis of the OPN (A) or CD44v6 (B) expression level. (A) Patients were stratified into three categories (+ ($n=21$), ++ ($n=5$), and +++ ($n=25$)) based on OPN immunostaining intensity. (B) Patients were stratified into three categories (L ($n=18$), M ($n=10$), and F ($n=23$)) based on the thickness of CD44v6 staining. The *P*-value was determined by a two-sided log-rank test.

moreover, the association between OPN and CD44v6 immunoreactivity was highly significant at the Spearman's correlation coefficient test, suggesting that CD44v6 is at least one of the functional OPN receptors in laryngeal dysplasia.

To investigate whether the OPN/CD44v6 overexpression was causally related with dysplasia, cytological changes induced by OPN stimulation of primary human keratinocytes, obstructed by CD44 blockade, have been observed (Celetti A *et al*, in preparation). Addressing CD44 as a functional receptor for OPN would be important to explore the molecular mechanism underlying dysplastic changes induced by the OPN/CD44 axis. It is known that CD44 triggering stimulates diverse signalling pathways, including activation of ERK (Bourguignon *et al*, 2005), RAC (Teramoto *et al*, 2005), and RHO (Bourguignon *et al*, 2003), as well as secretion of soluble factors, like cytokines and metalloproteinases (Zhang *et al*, 2002; Bourguignon *et al*, 2003; Murphy *et al*, 2005). These pathways are potentially involved in dysplastic changes induced by OPN/CD44v6.

A model for the initiation and progression of colorectal cancer has become a paradigm for other human solid tumours (Fearon and Vogelstein, 1990). Like colorectal cancer, HNSCC is thought to

progress through a series of well-defined clinical and histopathological stages. While not all of the specific mutations required for progression have been delineated, a working molecular model has been proposed (Silverman, 2003). The loss of chromosomal regions 3p and 9p21 are among the first identified genetic changes (Mao et al, 1996; Sanz-Ortega et al, 2003). In particular, loss-of-heterozygosity (LOH) at 9p21 in conjunction with promoter hypermethylation results in the inactivation of the *CDKN2A* gene, coding for the cyclin-dependent kinase inhibitor 2A (p16INK4). This alteration occurs prior to the development of histologic atypia and is associated with the transition from normal to hyperplastic/metaplastic mucosa (Papadimitrakopoulou et al, 2001; Sanz-Ortega et al, 2003). Subsequent LOH at 17p with mutation of the *TP53* tumour suppressor gene is associated with progression to dysplasia (Boyle et al, 1993). The overexpression of the EGF receptor is also an early event in carcinogenesis (Rubin Grandis et al, 1998). Amplification and overexpression of the *CCND1* gene, encoding cyclin D1 is a common late event in HNSCC formation

(Michalides et al, 1995; Izzo et al, 1998; Chatrath et al, 2006). Our findings suggest that the upregulation of the OPN/CD44v6 axis is an additional early event during the progression of laryngeal dysplasia. Thus, early immunocytochemical detection of OPN and CD44v6 can be exploited to set a screening test for laryngeal dysplasia. Moreover, perturbation of OPN/CD44v6 signalling may represent a promising novel strategy to prevent progression of laryngeal preneoplastic lesions.

ACKNOWLEDGEMENTS

We thank Giancarlo Vecchio for continuous support. We are grateful to JA Gilder for text editing. This study was supported by the Associazione Italiana per la Ricerca sul Cancro (AIRC), the NOGEC (Naples OncoGenomic Center), and the Italian Ministero della Salute.

REFERENCES

- Agrawal D, Chen T, Irby R, Quackenbush J, Chambers AF, Szabo M, Cantor A, Coppola D, Yeatman TJ (2002) Osteopontin identified as lead marker of colon cancer progression, using pooled sample expression profiling. *J Natl Cancer Inst* **94**: 513–521
- Bourguignon LY, Gilad E, Rothman K, Peyollier K (2005) Hyaluronan-CD44 interaction with IQGAP1 promotes Cdc42 and ERK signaling leading to actin binding, Elk-1/estrogen receptor transcriptional activation and ovarian cancer progression. *J Biol Chem* **280**: 11961–11972
- Bourguignon LY, Singleton PA, Zhu H, Diedrich F (2003) Hyaluronan-mediated CD44 interaction with RhoGEF and Rho kinase promotes Grb2-associated binder-1 phosphorylation and phosphatidylinositol 3-kinase signaling leading to cytokine (macrophage-colony stimulating factor) production and breast tumor progression. *J Biol Chem* **278**: 29420–29434
- Boyle JO, Hakim J, Koch W, van der Riet P, Hruban RH, Roa RA, Correo R, Eby YJ, Ruppert JM, Sidransky D (1993) The incidence of p53 mutations increases with progression of head and neck cancer. *Cancer Res* **53**: 4477–4480
- Celetti A, Testa D, Staibano S, Merolla F, Guarino V, Castellone MD, Iovine R, Mansueto G, Somma P, De Rosa G, Galli V, Melillo RM, Santoro M (2005) Overexpression of the cytokine osteopontin identifies aggressive laryngeal squamous cell carcinomas and enhances carcinoma cell proliferation and invasiveness. *Clin Cancer Res* **11**: 8019–8027
- Chatrath P, Scott IS, Morris LS, Davies RJ, Bird K, Vowler SL, Coleman N (2006) Immunohistochemical estimation of cell cycle phase in laryngeal neoplasia. *Br J Cancer* **95**: 314–321
- Cowan JM, Beckett MA, Ahmed-Swan S, Weichselbaum RR (1992) Cytogenetic evidence of the multistep origin of head and neck squamous cell carcinomas. *J Natl Cancer Inst* **84**: 793–797
- Donati V, Boldrini L, Dell'Omodarme M, Prati MC, Faviana P, Camacci T, Lucchi M, Mussi A, Santoro M, Basolo F, Fontanini G (2005) Osteopontin expression and prognostic significance in non-small cell lung cancer. *Clin Cancer Res* **11**: 6459–6465
- Evans DMD, Hudson EA, Brown CL, Boddington MM, Hughes HE, Mackenzie EF, Marshall T (1986) Terminology in gynecological cytopathology: report of the working party of the British Society for Clinical Cytology. *J Clin Pathol* **39**: 933–944
- Fearon ER, Vogelstein B (1990) A genetic model for colorectal tumorigenesis. *Cell* **61**: 759–767
- Gale N, Kambic V, Michaels L, Cardesa A, Hellquist H, Zidar N, Poljak M (2000) The Ljubljana classification: a practical strategy for the diagnosis of laryngeal precancerous lesions. *Adv Anat Pathol* **7**: 240–251
- Guarino V, Faviana P, Salvatore G, Castellone MD, Cirafici AM, De Falco V, Celetti A, Giannini R, Basolo F, Melillo RM, Santoro M (2005) Osteopontin is overexpressed in human papillary thyroid carcinomas and enhances thyroid carcinoma cell invasiveness. *J Clin Endocrinol Metab* **90**: 5270–5278
- Hoffman HT, Karnell LH, Funk GF, Robinson RA, Menck HR (1998) The National Cancer Data Base report on cancer of the head and neck. *Arch Otolaryngol Head Neck Surg* **124**: 951–962
- Hsieh YH, Juliana MM, Hicks PH, Feng G, Elmets C, Liaw L, Chang PL (2006) Papilloma development is delayed in osteopontin-null mice: implicating an antiapoptosis role for osteopontin. *Cancer Res* **66**: 7119–7127
- Izzo JG, Papadimitrakopoulou VA, Li XQ, Ibarguen H, Lee JS, Ro JY, El-Naggar A, Hong WK, Hittelman WN (1998) Dysregulated cyclin D1 expression early in head and neck tumorigenesis: *in vivo* evidence for an association with subsequent gene amplification. *Oncogene* **17**: 2313–2322
- Johnson FL (2003) Management of advanced premalignant laryngeal lesions. *Curr Opin Otolaryngol Head Neck Surg* **11**: 462–466
- Kang Y, Siegel PM, Shu W, Drobnjak M, Kakonen SM, Cordón-Cardo C, Guise TA, Massagué J (2003) A multigenic program mediating breast cancer metastasis to bone. *Cancer Cell* **3**: 537–549
- Licitra L, Bernier J, Grandi C, Locati L, Merlano M, Gatta G, Lefebvre JL (2003) Cancer of the larynx. *Crit Rev Oncol Hematol* **147**: 65–80
- Mao L, Hong WK, Papadimitrakopoulou VA (2004) Focus on head and neck cancer. *Cancer Cell* **5**: 311–316
- Mao L, Lee JS, Fan YH (1996) Frequent microsatellite alterations at chromosomes 9p21 and 3p14 in oral premalignant lesions and their value in cancer risk assessment. *Nat Med* **6**: 682–685
- Matusan K, Dordevic G, Stipic D, Mozetic V, Lucin K (2006) Osteopontin expression correlates with prognostic variables and survival in clear cell renal cell carcinoma. *J Surg Oncol* **94**: 325–331
- Michalides R, van Veelen N, Hart A, Loftus B, Wientjens E, Balm A (1995) Overexpression of cyclin D1 correlates with recurrence in a group of forty-seven operable squamous cell carcinomas of the head and neck. *Cancer Res* **55**: 975–978
- Murphy JF, Lennon F, Steele C, Kelleher D, Fitzgerald D, Long AC (2005) Engagement of CD44 modulates cyclooxygenase induction, VEGF generation, and cell proliferation in human vascular endothelial cells. *FASEB J* **19**: 446–448
- Papadimitrakopoulou VA, Izzo J, Mao L, Keck J, Hamilton D, Shin DM, El-Naggar A, den Hollander P, Liu D, Hittelman WN, Hong WK (2001) Cyclin D1 and p16 alterations in advanced premalignant lesions of the upper aerodigestive tract: role in response to chemoprevention and cancer development. *Clin Cancer Res* **7**: 3127–3134
- Perez-Ordóñez B, Beauchemin B, Jordan RC (2006) Molecular biology of squamous cell carcinoma of the head and neck. *J Clin Pathol* **59**: 445–453
- Ponta H, Sherman L, Herrlich PA (2003) CD44: from adhesion molecules to signalling regulators. *Nat Rev Mol Cell Biol* **4**: 33–45
- Rangaswami H, Bulbule A, Kundu GC (2006) Osteopontin: role in cell signaling and cancer progression. *Trends Cell Biol* **16**: 79–87
- Rittling SR, Chambers AF (2004) Role of osteopontin in tumour progression. *Br J Cancer* **90**: 1877–1881
- Rosai J, Carcangiu ML, DeLellis RA (1992) *Atlas of Tumor Pathology – Tumors of the Larynx, 3rd series*. Washington: Armed Forces Institute of Pathology
- Rubin Grandis J, Melhem MF, Gooding WE, Day R, Holst VA, Wagener MM, Drening SD, Twardy DJ (1998) Levels of TGF- α and EGFR

- protein in head and neck squamous cell carcinoma and patient survival. *J Natl Cancer Inst* **90**: 824–832
- Sanz-Ortega J, Valor C, Saez MC, Ortega L, Sierra E, Poch J, Hernández S, Sanz-Esponera J (2003) 3p21, 5q21, 9p21 and 17p13 allelic deletions accumulate in the dysplastic spectrum of laryngeal carcinogenesis and precede malignant transformation. *Histol Histopathol* **18**: 1053–1057
- Schorge JO, Drake RD, Lee H, Skates SJ, Rajanbabu R, Miller DS, Kim JH, Cramer DW, Berkowitz RS, Mok SC (2004) Osteopontin as an adjunct to CA125 in detecting recurrent ovarian cancer. *Clin Cancer Res* **10**: 3474–3478
- Silverman S (2003) *Oral Cancer Hamilton*. Ontario: BD Dekker
- Tabor MP, Braakhuis BJ, van der Wal JE, van Diest PJ, Leemans CR, Brakenhoff RH, Kummer JA (2003) Comparative molecular and histological grading of epithelial dysplasia of the oral cavity and the oropharynx. *J Pathol* **199**: 354–360
- Tabor MP, Brakenhoff RH, Ruijter-Schippers HJ, Van Der Wal JE, Snow GB, Leemans CR, Braakhuis BJ (2002) Multiple head and neck tumours frequently originate from a single preneoplastic lesion. *Am J Pathol* **161**: 1051–1060
- Teramoto H, Castellone MD, Malek RL, Letwin N, Frank B, Gutkind JS, Lee NH (2005) Autocrine activation of an osteopontin–CD44–Rac pathway enhances invasion and transformation by H-RasV12. *Oncogene* **24**: 489–501
- Vokes EE, Weichselbaum RR, Lippman SM, Hong WK (1993) Head and neck cancer. *N Engl J Med* **328**: 184–194
- Weber GF (2001) The metastasis gene osteopontin: a candidate target for cancer therapy. *Biochim Biophys Acta* **1552**: 61–85
- Ye QH, Qin LX, Forgues M, He P, Kim JW, Peng AC, Simon R, Li Y, Robles AI, Chen Y, Ma ZC, Wu ZQ, Ye SL, Liu YK, Tang ZY, Wang XW (2003) Predicting hepatitis B virus-positive metastatic hepatocellular carcinomas using gene expression profiling and supervised machine learning. *Nat Med* **9**: 416–423
- Zhang Y, Thant AA, Machida K, Ichigotani Y, Naito Y, Hiraiwa Y, Senga T, Sohara Y, Matsuda S, Hamaguchi M (2002) Hyaluronan-CD44s signaling regulates matrix metalloproteinase-2 secretion in a human lung carcinoma cell line QG90. *Cancer Res* **62**: 3962–3965
- Zuckerberg L (2002) The molecular basis of dysplasia. *Semin Diagn Pathol* **19**: 48–53

Overexpression of the Cytokine Osteopontin Identifies Aggressive Laryngeal Squamous Cell Carcinomas and Enhances Carcinoma Cell Proliferation and Invasiveness

Angela Celetti,¹ Domenico Testa,² Stefania Staibano,³ Francesco Merolla,¹ Valentina Guarino,¹ Maria Domenica Castellone,¹ Renata Iovine,² Gelsomina Mansueto,³ Pasquale Somma,³ Gaetano De Rosa,³ Vieri Galli,² Rosa Marina Melillo,¹ and Massimo Santoro¹

Abstract Purpose: Osteopontin is a secreted cytokine that binds to the cell surface CD44v6 receptor. We studied osteopontin and CD44v6 expression in laryngeal squamous cell carcinomas and correlated osteopontin expression levels with clinicopathologic tumor features.

Experimental Design: We used immunohistochemistry, immunoblotting, and reverse transcription-PCR to study osteopontin expression in 58 laryngeal squamous cell carcinomas. Cultured squamous carcinoma cells were treated with exogenous osteopontin or with RNA interference to knockdown osteopontin expression.

Results: Osteopontin expression was higher in all the invasive carcinomas than in patient-matched normal mucosa. Its expression levels were significantly correlated with tumor stage and grade and with the presence of lymph node and distant metastases. Osteopontin positivity was negatively correlated with overall survival ($P = 0.03$). Osteopontin expression was paralleled by intense cell surface reactivity for CD44v6. Treatment of squamous carcinoma cells with recombinant osteopontin sharply increased proliferation and Matrigel invasion in comparison with the untreated cells parallel to activation of the mitogen-activated protein kinase/extracellular signal-regulated kinase kinase/mitogen-activated protein kinase signaling cascade. Osteopontin knockdown by RNA interference, anti-CD44 antibodies, and mitogen-activated protein kinase/extracellular signal-regulated kinase kinase inhibition prevented these effects.

Conclusions: These results identify osteopontin as a marker and a potential therapeutic target in cases of aggressive laryngeal squamous cell carcinomas.

Head and neck squamous cell carcinoma (HNSCC) is the sixth most frequent cancer. Laryngeal squamous cell carcinoma (LSCC) is the most common HNSCC (1–3). Notwithstanding primary prevention, screening, surgical treatment, and radiotherapy, the long-term survival rate of LSCC patients has remained substantially unchanged in the last two decades (4, 5). Stage and

histologic grade are prognostic factors in LSCC but do not always distinguish between high-risk and low-risk patients (1–5). Various biological prognostic markers have been identified for LSCC and other HNSCC types: mutation in the *p53* tumor suppressor gene (6), amplification of cyclin D1 (7, 8), overexpression of the epidermal growth factor receptor (9) and vascular endothelial growth factor (10), and reduced expression of the CIP/KIP cell cycle inhibitory proteins (11). However, little is known about the molecular mechanisms that govern the establishment and maintenance of the LSCC neoplastic phenotype.

Osteopontin, also known as secreted phosphoprotein 1, is a highly acidic calcium-binding glycosylated phosphoprotein. It is a cytokine (early T lymphocyte antigen-1 or interleukin-28) that regulates T helper cell-1 function (12, 13). In addition, osteopontin binds to the cell surface receptors α_v - or β_1 -containing integrins and CD44 (14, 15), thereby supporting chemotaxis, attachment, and migration of many epithelial cell types (16, 17). CD44 is expressed as a standard receptor (CD44s) and in multiple splice isoforms (CD44v), whose expression is altered during tumor growth and progression. Expression of the v6 variant exon of CD44 is necessary for osteopontin binding (18). CD44 splice variants are thought to be correlated with invasive growth and metastasis in many tumor types (18). Osteopontin is overexpressed in many human tumors (e.g., colon, breast, liver, prostate, gastric, ovarian, and lung carcinomas; refs. 19–22).

Authors' Affiliations: ¹Istituto di Endocrinologia ed Oncologia Sperimentale del Consiglio Nazionale delle Ricerche/Dipartimento di Biologia e Patologia Cellulare e Molecolare, ²Dipartimento Assistenziale di Otorinolaringoiatria e Scienze Affini, and ³Dipartimento di Scienze Biomorfologiche e Funzionali, University of Naples "Federico II," Naples, Italy

Received 3/22/05; revised 8/5/05; accepted 8/24/05.

Grant support: Associazione Italiana per la Ricerca sul Cancro, Progetto Strategico Oncologia of the Consiglio Nazionale delle Ricerche/Ministero dell'Istruzione, dell'Università e della Ricerca, Italian Ministero della Salute, Centro Regionale di Competenza Genomic for Applied Research, and Naples Oncogenomic Center (M. Santoro) and BioGeM scrl fellowships (MDC and VG).

The costs of publication of this article were defrayed in part by the payment of page charges. This article must therefore be hereby marked *advertisement* in accordance with 18 U.S.C. Section 1734 solely to indicate this fact.

Note: D. Testa and S. Staibano contributed equally to the work.

Requests for reprints: Massimo Santoro, Dipartimento di Biologia e Patologia Cellulare e Molecolare, University of Naples "Federico II," via S. Pansini 5, 80131 Naples, Italy. Phone: 39-81-7463056; Fax: 39-81-7463037; E-mail: masantor@unina.it.

© 2005 American Association for Cancer Research.
doi:10.1158/1078-0432.CCR-05-0641

We have explored osteopontin expression in LSCC. Our results indicate that osteopontin is a promising molecular marker for LSCC risk assessment. At cellular level, osteopontin binding to CD44v6 promoted SCC cell growth and invasion.

Materials and Methods

Tumors. Archival tumor samples from 58 patients (57 males and 1 female) with laryngeal cancer were retrieved from the files of the Department of Biomorphological and Functional Sciences, Pathology Section, University of Naples "Federico II," after having obtained informed consent. Clinicopathologic data were recorded (Table 1). Patients underwent surgery at the Institute of Otolaryngology, University of Naples "Federico II," between 1997 and 2001. The study was approved by the institutional review board committee. The patients' age ranged between 43 and 83 years, with a mean of 64.7 years. Patients underwent otolaryngologic examination, fiberoptic study, and radiological evaluation and were treated by surgery alone, except for patients with locally advanced tumors (T₄), who received postsurgical radiation therapy. The patients underwent a median of 60 months' follow-up, which consisted of clinical and radiological evaluation at 3-month intervals for the first year and at 6-month intervals thereafter. After surgical resection, tissues were fixed in 10% neutral buffered formalin and embedded in paraffin blocks. Sections (4 μm thick) were stained with H&E. Histologic grading and tumor-node-metastasis classification were done according to the recommendations of the International Union Against Cancer (23, 24). The pathologic analysis was done in a blinded manner with respect to the patients' clinical data. For five patients, a 10-μm-thick section was processed for dissection. Paraffin was removed by treatment with xylene for 3 hours at room temperature followed by tissue rehydration through multiple graded ethanol solutions and distilled water. The cancerous

region was identified microscopically; normal and tumor tissues were dissected with a sterile 30-gauge hypodermic needle. The collected samples (~120,000 cells) were placed into 1.5-mL microcentrifuge tubes and processed for RNA extraction.

Immunohistochemistry. Serial tumor sections (4 μm thick) were mounted on poly-L-lysine-coated glass slides. After antigen retrieval, the slides were incubated with anti-osteopontin (5 μg/mL; 10A16, Assay Designs, Ann Arbor, MI) or anti-CD44 (1:100; NCL-CD44v6, clone VFF-7, Novocastra Laboratories Ltd., Newcastle upon Tyne, United Kingdom) monoclonal antibodies (mAb). The sections were incubated (overnight at 4°C) with the primary antibody, biotinylated anti-IgG, and the premixed avidin-biotin complex (Vectastain ABC kits, Vector Laboratories, Burlingame, CA). The immune reaction was revealed with 0.06 mmol/L 3,3'-diaminobenzidine (DAKO, Carpinteria, CA) and 2 mmol/L H₂O₂. The slides were counterstained with hematoxylin. Anti-osteopontin antibody was preincubated with a 5-fold molar excess of osteopontin peptide to ascertain the specificity of the reaction. Control slides, stained with preimmune serum, were included as an additional negative control. The results of the immunohistochemical staining were evaluated separately by two investigators in a blinded manner. The percentage of positive tumor cells was determined by examining at least five representative microscope areas at a ×400 magnification. For osteopontin, samples were assigned to one of the four following categories: 0, absence of positive cells; +, <10% of positive cells; ++, 10% to 50% of positive cells; and +++, >50% of positive cells. Immunohistochemical staining for CD44v6 was expressed as "basal" or "full thickness" based on the epithelium layers stained.

Cell lines. Human normal epidermal keratinocytes (HNEK; neonatal) were cultured in keratinocyte growth medium according to the recommendation of the manufacturer (Cambrex, East Rutherford, NJ). HN and BHY cell lines were derived from a human oral cavity SCC (25), CAL27 and CAL33 cell lines were from human tongue SCC (26), and Hep2 cells were from a LSCC (27); KB are epidermoid cancer cells (28). Tumor cells were maintained in DMEM supplemented with 10% fetal bovine serum, 2 mmol/L L-glutamine, and 100 units/mL penicillin-streptomycin (Life Technologies, Paisley, PA). For cell treatments, recombinant mouse osteopontin protein was from R&D Systems (Minneapolis, MN). U0126 was from Calbiochem (San Diego, CA). Blocking CD44 mAbs were purified from the KM81 hybridoma cell line (TIB-241, American Type Culture Collection, Manassas, VA; ref. 29). For blocking experiments, cells were preincubated for 30 minutes with the KM81 mAb (10 μg/mL) at 37°C, 5% CO₂.

RNA extraction and reverse transcription-PCR. Tissue samples were snap frozen in liquid nitrogen and stored at -80°C before RNA extraction. Tissues were homogenized using a Mixer Mill Homogenizer (Qiagen, Crawley, West Sussex, United Kingdom). Total RNA from the indicated cell cultures and from frozen tissue samples was prepared using the RNeasy Mini kit (Qiagen) according to the manufacturer's instructions. Only tissue samples containing >70% neoplastic cells were used. Total RNA (2.5 μg) was retrotranscribed into cDNA by using the GeneAmp RNA PCR Core kit (Applied Biosystems, Foster City, CA). PCR amplification was done using 2.5 μL of the reverse transcription product in a reaction volume of 25 μL. To exclude DNA contamination, each PCR reaction was also done on untranscribed RNA. The levels of the housekeeping β-actin transcript served as a control of equal RNA loading. Primers were designed with the Primer 3 program (http://www-genome.wi.mit.edu/cgi-bin/primer/primer3_www.cgi) and synthesized by MWG Biotech (Ebersberg, Germany). Primer sequences were osteopontin forward 5'-AGGAGGAGGCAGAGCACA-3', osteopontin reverse 5'-CTGGTATGGCAGGTTGATG-3', CD44 (exon 2) forward 5'-GCTTTCAATAGCACCTTGCC-3', CD44 (exon3) reverse 5'-GTTGT-TTGCTGCACAGATGG-3', CD44 (exon v6) reverse 5'-GTTGCCAAAC-CACTGTTCCCT-3', β-actin forward 5'-TGCCTGACATTAAGGAGAAG-3', and β-actin reverse 5'-GCTCGTAGCTCTTCTCCA-3'. Reverse transcription-PCR (RT-PCR) products were loaded on a 2% agarose gel and stained with 0.5 μg/mL ethidium bromide, and the corresponding

Table 1. Clinicopathologic features of studied laryngeal cancer patients

Characteristics	Total (%)
No. subjects	
Male	57 (98)
Female	1 (2)
Disease site	
Glottis-hypoglottis	43 (74)
Supraglottis	15 (26)
Histologic differentiation	
G ₁	19 (33)
G ₂	21 (36)
G ₃	18 (31)
Stage	
T ₁	9 (16)
T ₂	19 (33)
T ₃ /T ₄	30 (52)
Lymph nodes	
N ₊	15 (26)
N ₀	25 (43)
N _x	18 (31)
Metastasis	
M ₀	27 (46)
Bone	4 (7)
Lung	8 (14)
Brain	1 (2)
M _x	18 (31)

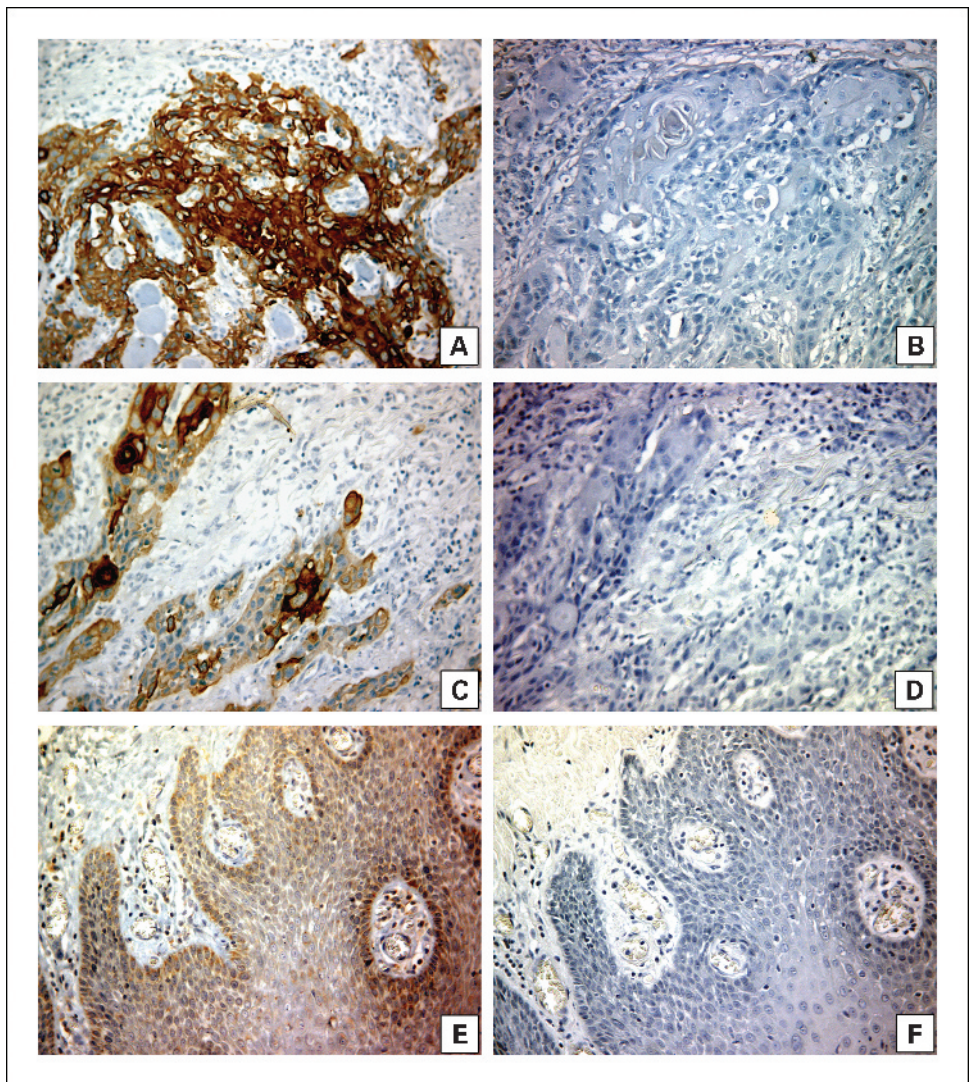


Fig. 1. Immunohistochemical detection of osteopontin in laryngeal carcinomas. *A*, an infiltrating LSCC (G₂, N₊, M₀) showing intense (+++) osteopontin staining ($\times 106$). *B*, the same sample as in (*A*): no signal was detected after preincubation with a molar excess of osteopontin-blocking peptide. *C*, an infiltrating LSCC (G₃, N₀, M₀) showing (++) osteopontin immunoreactivity ($\times 106$); *D*, the same sample as in (*C*) after preincubation with a molar excess of osteopontin-blocking peptide. *E*, hyperplastic epithelium (without dysplasia) negative for osteopontin staining ($\times 150$). *F*, the same sample as in (*E*) after preincubation with osteopontin-blocking peptide.

image was saved with the Typhoon 8600 laser scanning system (Amersham Pharmacia Biotech, Buckinghamshire, United Kingdom). The density and width of each band were quantified using the ImageQuant 5.0 (Amersham Pharmacia Biotech).

Protein studies. Immunoblotting experiments were done according to standard procedures. For tissue protein extraction, samples were snap frozen and homogenized in lysis buffer by using the Mixer Mill apparatus (Qiagen). Protein concentration was estimated with a modified Bradford assay (Bio-Rad, Hercules, CA). Antigens were revealed by an enhanced chemiluminescence detection kit (Amersham Pharmacia Biotech). Anti-osteopontin goat polyclonal antibody (K20) and rabbit polyclonal anti-CD44 (H300) were from Santa Cruz Biotechnology (Santa Cruz, CA). Monoclonal anti- α -tubulin was from Sigma-Aldrich (St. Louis, MO). Anti-phosphorylated mitogen-activated protein kinase/extracellular signal-regulated kinase (ERK) kinase (MEK) 1/2 (Ser²¹⁷/Ser²²¹), anti-phosphorylated p44/42 mitogen-activated protein kinase (Thr²⁰²/Tyr²⁰⁴; ERK), and anti-p44/42 mitogen-activated protein kinase were from Cell Signaling Technology, Inc. (Beverly, MA).

Flow cytometric analysis. Subconfluent cells (1×10^6) were detached from culture dishes. After saturation with $1 \mu\text{g}$ human IgG per 10^5 cells, cells were incubated for 20 minutes on ice with antibodies specific for human CD44v6 (R&D Systems) or isotype control antibody. After incubation, unreacted antibody was removed. Cells were then

incubated (30 minutes, 4°C) with $100 \mu\text{L}$ fluorescein-conjugated goat anti-mouse IgG/M (Jackson ImmunoResearch, West Grove, PA) and analyzed on a FACSCalibur cytofluorimeter using the CellQuest software (Becton Dickinson, San Jose, CA). Analyses were done in triplicate. In each analysis, a total of 10^4 events were calculated.

Chemoinvasion. The cell suspension (1×10^5 cells per well) was added to the upper chamber of Transwell cell culture chambers on a prehydrated polycarbonate membrane filter of 8- μm pore size (Costar, Cambridge, MA) coated with $35 \mu\text{g}$ Matrigel (Collaborative Research, Inc., Bedford, MA). The lower chamber was filled with complete medium, and when required, purified recombinant osteopontin was added at the concentration of 100 ng/mL . To inhibit Matrigel invasion, cells were preincubated with $10 \mu\text{g/mL}$ CD44-blocking antibodies (KM81) or with $10 \mu\text{mol/L}$ U0126. After 24-hour incubation at 37°C, nonmigrating cells on the upper side of the filter were wiped off and migrating cells on the reverse side of the filter were stained with 0.1% crystal violet in 20% methanol for 15 minutes and photographed. The stained cells were lysed in 10% acetic acid. Triplicate samples were analyzed at 570 nm with an ELISA reader (model 550 microplate reader, Bio-Rad). The results were expressed as percentage of migrating cells.

Bromodeoxyuridine incorporation. Cells were seeded on glass coverslips and bromodeoxyuridine (BrdUrd) was added to the cell culture medium at a final concentration of $100 \mu\text{g/mL}$ (BrdUrd Labeling and

Detection kit, Boehringer Mannheim, Mannheim, Germany). After 1-hour incubation, cells were fixed with 70% ethanol/50 mmol/L glycine (pH 2.0). Coverslips were incubated with anti-BrdUrd mouse mAb and with a FITC-conjugated anti-mouse antibody. All coverslips were counterstained in PBS containing Hoechst 33258 (final concen-

Table 2. Osteopontin positivity in laryngeal carcinomas

Characteristics (no. samples)	Osteopontin positivity*
Disease site	
Glottis-hypoglottis (43)	22/43 (+++) 16/43 (++) 3/43 (+) 2/43 (0)
Supraglottis (15)	7/15 (+++) 5/15 (++) 1/15 (+) 2/15 (0)
Stage	
T ₁ (9)	3/9 (++) 2/9 (+) 4/9 (0)
T ₂ (19)	7/19 (+++) 10/19 (++) 2/19 (+)
T ₃ /T ₄ (30)	22/30 (+++) 8/30 (++)
Grade	
G ₁ (19)	4/19 (+++) 8/19 (++) 3/19 (+) 4/19 (0)
G ₂ (21)	11/21 (+++) 9/21 (++) 1/21 (+)
G ₃ (18)	14/18 (+++) 4/18 (++)
Lymph node metastases	
N ₊ (15)	9/15 (+++) 6/15 (++)
N ₀ (25)	6/25 (+++) 9/25 (++) 8/25 (+) 2/25 (0)
N _x (18)	
Distant metastases	
M ₊ (13)	12/13 (+++) 1/13 (++)
M ₀ (27)	7/27 (+++) 12/27 (++) 4/27 (+) 4/27 (0)
M _x (18)	

*Osteopontin expression was assessed by immunohistochemistry and scored as follows: 0, absence of positive cells; +, <10% positive cells; ++, 10% to 50% positive cells; and +++, 50% to 100% positive cells.

Table 3. Correlation of osteopontin expression and clinicopathologic characteristics of laryngeal carcinomas

Osteopontin positivity	r _s	P
Tumor stage	0.6230	<0.0001
Grade	0.5169	<0.0001
Node	0.4391	<0.0046
Distant metastases	0.7821	<0.0001

NOTE: Correlation between osteopontin expression and tumor stage, grade, node, and distant metastases analyzed by the Spearman rank correlation test: correlation coefficient (r_s) and P_s are shown (P_s < 0.05 were considered significant).

tration, 1 µg/mL; Sigma-Aldrich), rinsed in water and mounted in Moviol on glass slides. The fluorescent signal was visualized with an epifluorescent microscope (Axioskop 2, Zeiss) interfaced with the image analyzer software Axiovision (Zeiss, Gottingen, Germany).

RNA silencing. Small inhibitor duplex RNAs targeting human osteopontin were designed with a small interfering RNA (siRNA) selection program available online at <http://jura.wi.mit.edu/siRNAext/> and were chemically synthesized by PROLIGO (Boulder, CO). Sense strand for siRNA targeting was (osteopontin siRNA) 5'-AAGCAG-CUUUACAACAAAUACCC-3'. As a control, a nonspecific siRNA duplex containing the same nucleotides but in irregular sequence (scrambled) was used. The day before transfection, 1 × 10⁵ cells were plated in 35-mm dishes in DMEM supplemented with 10% fetal bovine serum and without antibiotics. Transfection was done using 360 pmol siRNA and 18 µL Oligofectamine reagent (Invitrogen, Groningen, the Netherlands)

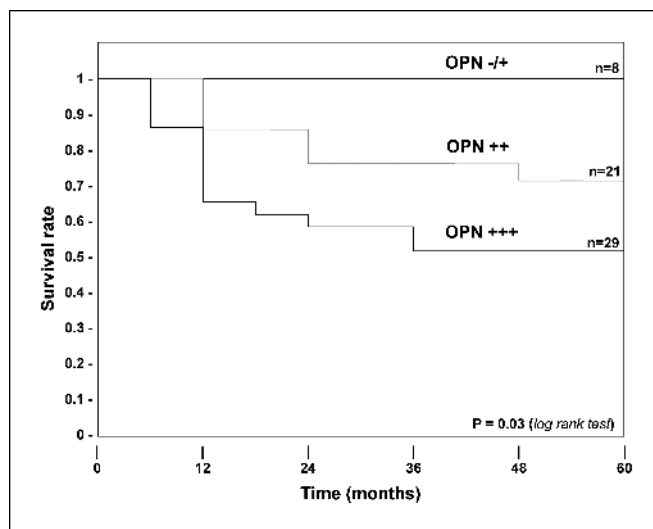


Fig. 2. Osteopontin staining negatively correlates with LSCC patient survival. Kaplan-Meier survival plots for LSCC patients grouped by the level of expression of osteopontin (OPN). LSCC tumoral samples were stratified in three categories [0/+ (n = 8), ++ (n = 21), and +++ (n = 29)] based on intensity of osteopontin immunostaining. P was determined by a two-sided log-rank test. For patients whose tumors had osteopontin (++) immunostain, the 2- and 5-year overall survival rates were 76.19% [95% confidence interval (95% CI), 56.53-95.87%] and 71.40% (95% CI, 48.53-94.27%), respectively. For patients whose tumors had osteopontin (+++) immunostain, the 2- and 5-year overall survival rates were 58.60% (95% CI, 35.85-81.35%) and 51.70% (95% CI, 26.41-76.99%), respectively. All patients whose tumors had osteopontin (0/+) stain were still alive at the end of the study.

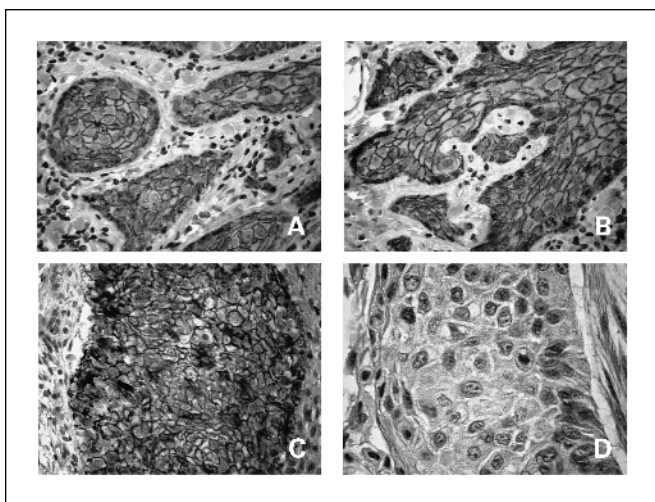


Fig. 3. Expression of CD44v6 in LSCC. *A*, an infiltrating LSCC (G₂, N₀, M₀) strongly immunoreactive for CD44v6 ($\times 150$). *B*, full thickness CD44v6 positivity in a G₂, N₊, M₀ LSCC sample ($\times 150$). *C*, full thickness CD44v6 positivity in a G₂, N₀, M₀ LSCC sample ($\times 400$). *D*, LSCC: absence of signal in the presence of preimmune serum ($\times 400$).

following the manufacturer's instruction. Cells were kept in 2.5% serum and BrdUrd incorporation was measured 48 hours after transfection.

Statistical analysis. Statistical evaluation of the data was done with a two-tailed Student's *t* test when simple comparison between two groups was required; χ^2 test was used to establish the statistical significance of distributions. Nonparametric Spearman's correlation coefficient method was used to assess the statistical significance of the correlation between clinicopathologic characteristics of tumor and osteopontin expression. Survival curves of the patients were calculated using the Kaplan-Meier method and analysis was done by the log-rank test. Differences were significant at $P < 0.05$. Statistical analysis was done using the JMP software program version 5.1.1 (SAS Institute, Inc., Austin, TX).

Results

Immunohistochemical detection of osteopontin up-regulation in laryngeal squamous cell carcinomas. Fifty-eight larynx carcinomas at different grades of malignancy and the corresponding normal tissues (Table 1) were tested for osteopontin expression by immunohistochemistry with an anti-osteopontin-specific mAb. Representative immunohistochemical stainings are shown in Fig. 1 and the entire data set is reported in Table 2. Osteopontin was virtually undetectable ($<2.0\%$ of cells) in normal tissues ($n = 58$; data not shown). Hyperplastic epithelia ($n = 20$) were also constantly negative for osteopontin staining (Fig. 1E; data not shown). In contrast, 93% (54 of 58) of the tumor samples were osteopontin positive (Fig. 1A and C). The signal was confined to tumor cells. The specificity of signal was shown by competition with a molar excess of osteopontin-blocking peptide (Fig. 1B, D, and F). Overall, 37% of T₂ tumors and 73% of T₃/T₄ tumors showed intense (+++) osteopontin immunostaining. Moreover, osteopontin immunostaining was intense (+++) in 21%, 52%, and 78% of G₁, G₂, and G₃ tumors, respectively. Finally, 60% of tumors with lymph node metastases and 92% of tumors with distant metastases had intense osteopontin staining. Accordingly, metastatic tissues were intensely osteo-

pontin positive (data not shown). Thus, osteopontin reactivity was correlated with tumor stage ($P < 0.0001$) and grade ($P < 0.0001$) and with the presence of lymph node ($P < 0.0046$) and distant ($P < 0.0001$) metastases (Table 3). Importantly, the 5-year survival rate for LSCC patients was negatively correlated with intense osteopontin staining. Five-year survival was 71.40% for osteopontin-positive cases (++) and 51.70% for osteopontin-positive cases (+++) as shown by the Kaplan-Meier survival curves reported in Fig. 2 ($P = 0.03$, two-sided log-rank test).

The interaction of osteopontin with the CD44 cell surface receptor has been implicated in many signal transduction pathways. CD44 pre-mRNA is encoded by 20 exons. The constant 5'-terminal five exons encode the NH₂-terminal extracellular portion of the CD44 protein, whereas the constant 3'-terminal five exons encode the transmembrane and the short cytosolic tail of the protein. An additional 10 exons (variants v1-v10) are alternatively spliced and encode the extracellular membrane-proximal stem structure (18). Cancer cells often overexpress CD44 variants that include a variable number of "v" exons. The v6 exon has been reported to be important for efficient osteopontin binding (18). Thus, we sought to verify whether CD44v6 molecules were expressed in LSCC. LSCC samples ($n = 58$) were constantly CD44v6 positive at immunohistochemistry (representative samples are shown in Fig. 3A-C). In tumors, CD44v6-positive cells showed full thickness staining, whereas only basal cells were CD44v6 positive in normal stratified epithelium (data not shown).

Osteopontin and CD44 up-regulation in laryngeal squamous cell carcinomas at protein and mRNA level. Protein lysates were harvested from selected high-stage/grade snap-frozen LSCC samples (T₃, G₃; $n = 10$) and from the corresponding adjacent normal mucosa from the same patients, and osteopontin protein levels were examined by immunoblotting. As shown in Fig. 4A, the osteopontin protein ($M_r \sim 60,000$) was abundantly expressed in all carcinomas but was barely detectable in matched normal tissues (Fig. 4A). To determine whether up-regulation occurred at transcriptional level, we subjected the same LSCC

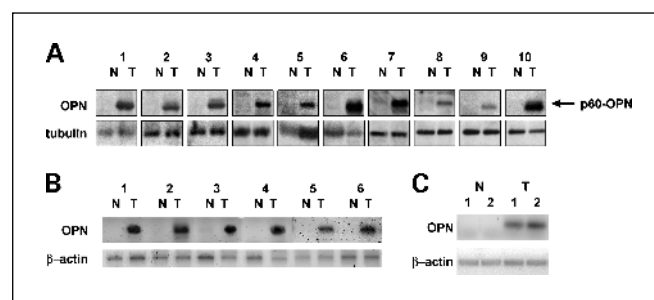


Fig. 4. Osteopontin up-regulation in LSCC samples at the protein and mRNA levels. *A*, levels of osteopontin protein were evaluated by immunoblot in LSCC and in adjacent normal epithelium: T, tumoral sample; N, normal epithelium. Anti- α -tubulin were used for normalization. Representative of three independent experiments. *B*, semiquantitative RT-PCR (25 cycles) was done to detect osteopontin mRNA levels in the indicated LSCC samples and in adjacent normal epithelium. β -Actin mRNA detection was used for normalization. Band intensity was calculated by phosphorimaging. Representative of three independent experiments. *C*, RT-PCR (28 cycles) was done on purified cells from two representative samples of LSCC (sample 1: G₃, N₊, M₀; sample 2: G₂, N₀, M₀) and from the corresponding normal cells after microscope-guided manual dissection.

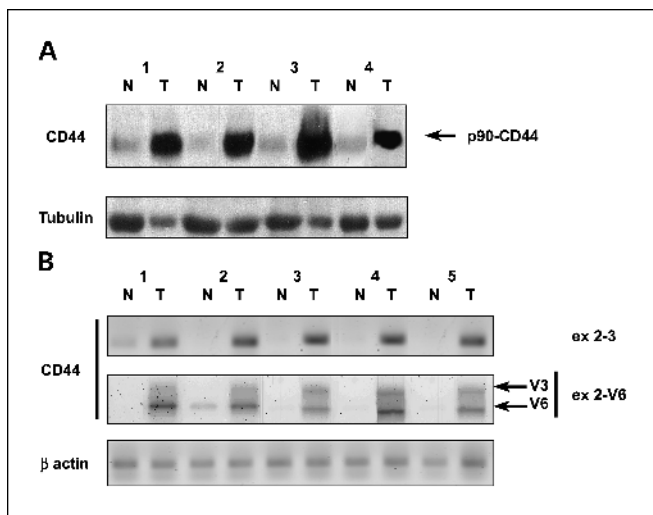


Fig. 5. CD44 up-regulation in LSCC samples. *A*, equal amounts of proteins (100 μg) from LSCC tumor samples and adjacent normal epithelium underwent Western blotting with an anti-CD44 antibody. Anti-α-tubulin was used for normalization. Representative of three independent experiments. *B*, semiquantitative RT-PCR (25 cycles) was used to detect mRNA levels of CD44 variants in LSCC samples. Band intensity was calculated by phosphorimaging. Amplimers mapping on exons 2 and 3 were used to detect all CD44 mRNA species, whereas the exon 2-v6 primer pair was used to detect variant mRNA species containing exon v6. In LSCC, the latter primer pair amplified two major products of 734 and 876 bp containing, along with standard exons 2 to 5, exon v6 or both exon v3 and v6 as proven by subsequent Southern hybridization with exon-specific probes (data not shown). β-Actin mRNA detection was used for normalization. Representative of three independent experiments.

samples ($n = 10$) to RT-PCR. Osteopontin mRNA was abundantly overexpressed at mRNA level in tumors with respect to adjacent normal mucosa from the same patients (Fig. 4B; data not shown). Phosphorimaging analysis of band intensity indicated that osteopontin mRNA was 15 ± 3 -fold higher in LSCC samples than in the normal tissue counterpart. To validate the results, we analyzed osteopontin mRNA levels in purified dissected tumor cells from five representative high-stage/grade LSCC samples and corresponding normal cells by RT-PCR; the representative samples shown in Fig. 4C showed that osteopontin mRNA accumulation was restricted to tumor cells.

We next examined CD44 expression in LSCC (T_3, G_3) samples ($n = 10$) using immunoblotting. An intense broad band of a relative molecular mass of 90 kDa was detected in tumors (Fig. 5A; data not shown). In contrast, CD44 was weakly expressed ($<10 \pm 3$ -fold compared with LSCC samples) in normal tissue counterparts (Fig. 5A). Then, we used different combinations of amplimers in RT-PCR experiments with RNA extracted from LSCC (T_3, G_3) samples ($n = 10$). LSCC overexpressed CD44 mRNA species containing the v6 or both v3 and v6 variant exons (Fig. 5B; data not shown).

Osteopontin and CD44v6 overexpression in squamous cell carcinoma cell lines. We evaluated osteopontin expression in six cultured human SCC lines. A primary culture of HNEK was used as a control. Osteopontin protein and mRNA expression was >7-fold higher in SCC than in normal cells (Fig. 6A and B). Moreover, all the SCC cell lines featured high levels (>10-fold with respect to HNEK) of standard and v6-containing CD44 species (Fig. 6C and D). All the cell lines featured abundant cell surface CD44v6 expression by flow cytometry (Fig. 6E; data not shown).

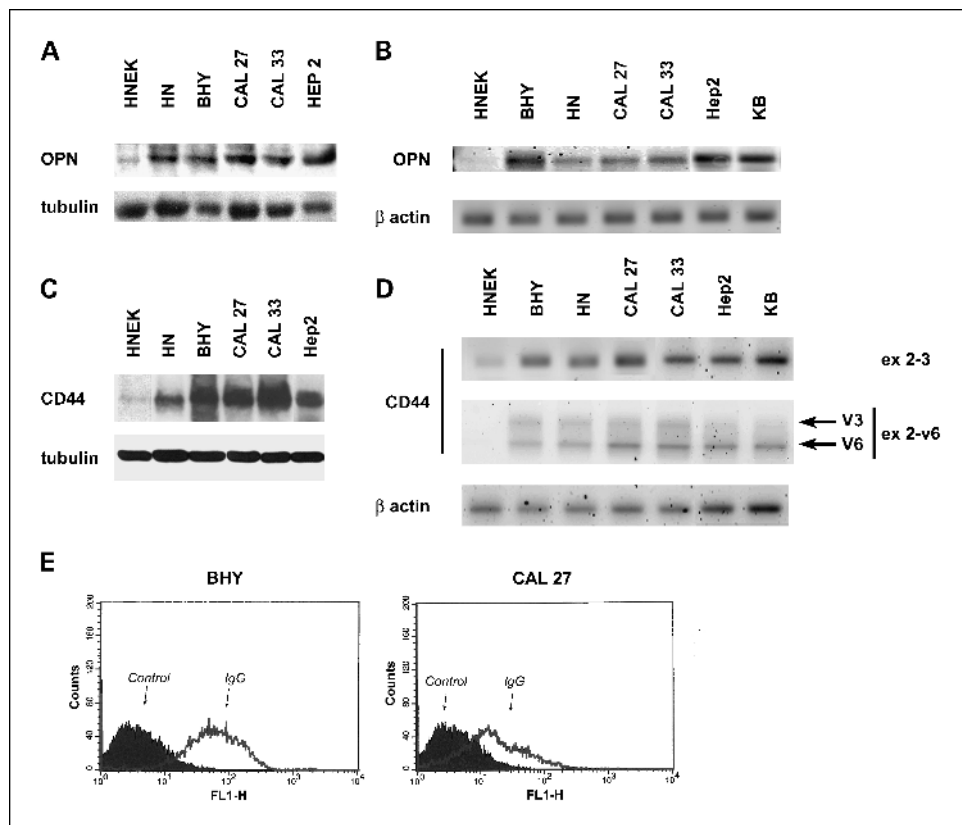
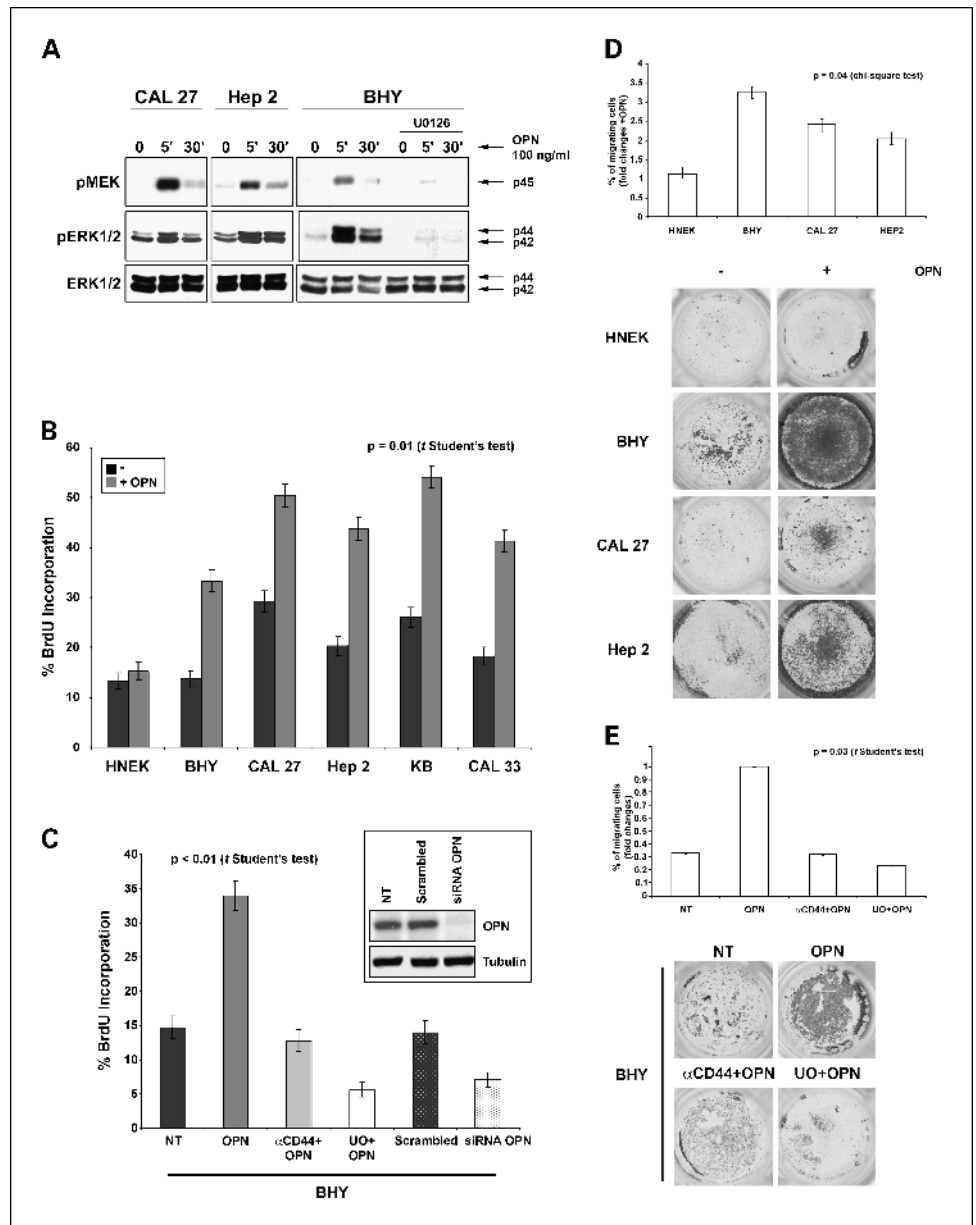


Fig. 6. Osteopontin and CD44 up-regulation in cultured SCC cells. *A*, osteopontin protein levels were evaluated by immunoblot in the indicated cell lines. Anti-α-tubulin was used for normalization. *B*, semiquantitative RT-PCR (25 cycles) was used to detect osteopontin mRNA levels in the indicated cell lines. β-Actin mRNA detection was used for normalization. Band intensity was calculated by phosphorimaging. *C*, CD44 protein levels were determined by immunoblot. *D*, semiquantitative RT-PCR (25 cycles) was done (see Fig. 5 legend) to detect CD44 mRNA levels in the indicated cell lines. *E*, flow cytometric analysis of cell surface expression of CD44v6 in the indicated cell lines. Black histogram, negative control antibody.

Fig. 7. Osteopontin-mediated signaling, growth, and Matrigel invasion in SCC cells. **A**, total cell lysates were prepared at various time points after stimulation of SCC cells, washed in serum-free medium, with recombinant osteopontin (100 ng/mL). Immunoblots were probed with the indicated phosphospecific antibodies. Anti-ERK was used for normalization. **B**, after starvation, the indicated cell lines were treated (48 hours) or not with exogenous recombinant osteopontin (100 ng/mL). Cells were exposed to BrdUrd for 1 hour, and cells were fixed and processed for immunofluorescence. Average results of three independent experiments in which at least 400 cells were counted; bars, 95% CI. **C**, BrdUrd incorporation was evaluated in BHY cells, washed in serum-free medium, in response to osteopontin (100 ng/mL) with and without U0126 (10 μ mol/L) or KM81 CD44-blocking mAb (10 μ g/mL). NT, not treated cells. Moreover, osteopontin knockdown was obtained by transient transfection with siRNA (*inset*). Mock-transfected cells and cells transfected with scrambled siRNA served as a control. BrdUrd was evaluated in transfected cells. All experiments were carried out in triplicate. Bars, 95% CI. **D**, Matrigel invasion of the various SCC cells in response to normal culture medium or exogenous recombinant osteopontin. The percentage of migrating cells was quantified with an ELISA reader. Top, average results of three independent experiments; bars, 95% CI. Bottom, representative micrographs. **E**, cells were preincubated with U0126 (10 μ mol/L) or CD44-blocking antibody (10 μ g/mL) and Matrigel invasion was analyzed as described in (**D**).



Osteopontin activates intracellular signaling, growth, and invasiveness of squamous cell carcinoma cells. Various SCC cell lines, washed in serum-free medium, were stimulated with exogenous recombinant osteopontin and harvested at different time points. Protein lysates were probed with phosphorylated MEK and phosphorylated ERK (ERK1/2) antibodies. MEK and ERK were readily activated in osteopontin-stimulated cells, peaking at 5 to 15 minutes (Fig. 7A), but not in normal HNEK cells (data not shown). We then examined the ability of SCC cells to synthesize DNA in basal conditions and in the presence of exogenous recombinant osteopontin. Osteopontin stimulated DNA synthesis in SCC cells, washed in serum-free medium, but not in normal HNEK cells ($P = 0.01$, two tailed Student's t test). Thus, we asked whether osteopontin expression was required for the growth of SCC cells. BrdUrd incorporation was obtained in triplicate after BHY and CAL27 cell transfection with osteopontin or scrambled siRNA. The transient silencing

of osteopontin (Fig. 7C, *inset*) significantly inhibited the growth of BHY cells, whereas the negative control siRNA had virtually no effect (Fig. 7C; data not shown). To determine whether the CD44 receptor mediated these events, we treated BHY, after washing in serum-free medium, with exogenous osteopontin after CD44 blockade with specific antibodies or chemical ERK blockade by the U0126 MEK inhibitor. Activation of MEK and ERK was virtually abrogated by pretreatment with U0126 (Fig. 7A). Stimulation of cell proliferation by osteopontin was obstructed by both anti-CD44 and U0126 (Fig. 7C). We next examined the ability of SCC cells to invade Matrigel in basal conditions and in the presence of exogenous osteopontin. Treatment with osteopontin induced a strong migratory response of tumor cells but not of normal HNEK cells ($P = 0.04$, χ^2 test; Fig. 7D). Treatment with CD44-blocking antibodies or U0126 sharply inhibited these effects ($P = 0.03$, two tailed Student's t test; Fig. 7E).

Discussion

Here, we show that osteopontin expression was closely correlated with advanced stage, high grade, metastatic disease, and poor survival of LSCC. This is in accordance with our observation that osteopontin affected the signaling and the mitogenic and motile phenotypes of carcinoma cells. Thus, although larger, prospective studies are needed to elucidate the relevance of osteopontin status versus other prognostic factors, our data suggest that osteopontin expression could be exploited as a predictor of outcome in LSCC patients. Interestingly, osteopontin plasma levels have been associated with treatment outcome and survival of HNSCC patients (30).

After its identification as a protein secreted by neoplastic cells (31), osteopontin has been detected in several human tumor types (i.e., gliomas and lung, prostate, gastric, esophageal, and ovarian carcinomas; refs. 16, 17, 19, 20). Osteopontin is also a major determinant of breast (21) and liver (22) cancer metastatization. Numerous growth factors (32), the RAS (33) and SRC (34) oncogenes, and the tumor suppressor p53 (35) regulate the expression of osteopontin. Many of these oncogenic proteins are involved in the pathogenesis of HNSCC (1) and thus might be responsible for osteopontin deregulation in such a tumor type. Osteopontin is able to engage several receptors, including integrins and CD44 variants, and thus may stimulate diverse signaling pathways and influence cellular events that, in turn, favor tumorigenesis and metastasis (16, 17). In particular, osteopontin binds CD44 proteins that contain v6-encoded sequences (14, 15), and osteopontin-CD44v6 binding has been implicated in carcinogenesis (16–18). In agreement with a report of CD44 (the standard

CD44 variant in that case) expression in HNSCC (36), we show that osteopontin up-regulation is paralleled by intense expression of CD44 (in particular, CD44v6) in LSCC tissue samples as well as in a panel of SCC cell lines. Thus, CD44v6 is a candidate receptor for osteopontin in LSCC cells. Accordingly, CD44 blockade obstructed osteopontin-mediated cellular effects. CD44 activates a wealth of signaling proteins, among which ERK (37), RAC (38), and RHO (39), as well as secretion of cytokines (40), angiogenic factors, and metalloproteinases (41). This could explain the effects exerted by the osteopontin-CD44v6 axis. On the other hand, osteopontin induces CD44v6 overexpression (42). Of note, our experiments show that osteopontin-CD44v6 binding mediates the effects occurring in SCC cells, but they do not exclude that interactions between osteopontin and integrins (16–18) and between CD44, hyaluronan (16–18), and other membrane receptors, such as members of the MET and ERBB family (43–45), are involved in the osteopontin-CD44 axis as well.

In conclusion, the results of this study suggest that patients affected by LSCC that express high levels of osteopontin protein may be more prone to a poor outcome than patients with low osteopontin-expressing LSCC. Thus, therapies targeted at the molecular mechanism (e.g., ligands that antagonize the interaction of osteopontin with CD44 or antibodies directed against osteopontin and CD44) may prove useful in LSCC patients.

Acknowledgments

We thank L. Vitiello and L. Racioppi for fluorescence-activated cell sorting analysis and Jean Gilder for text editing.

References

- Mao L, Hong WK, Papadimitrakopoulou VA. Focus on head and neck cancer. *Cancer Cell* 2004;5:311–6.
- Licitra L, Bernier J, Grandi C, et al. Cancer of the larynx. *Crit Rev Oncol Hematol* 2003;47:65–80.
- Vokes EE, Weichselbaum RR, Lippman SM, Hong WK. Head and neck cancer. *N Engl J Med* 1993;328:184–94.
- Hoffman HT, Karnell LH, Funk GF, Robinson RA, Menck HR. The National Cancer Data Base report on cancer of the head and neck. *Arch Otolaryngol Head Neck Surg* 1998;124:951–62.
- Tabor MP, Brakenhoff RH, Ruijter-Schippers HJ, et al. Multiple head and neck tumours frequently originate from a single preneoplastic lesion. *Am J Pathol* 2002;161:1051–60.
- Shin DM, Lee JS, Lippman SM, et al. p53 expressions: predicting recurrence and second primary tumors in head and neck squamous cell carcinoma. *J Natl Cancer Inst* 1996;88:519–29.
- Bellacosa A, Almadori G, Cavallo S, et al. Cyclin D1 gene amplification in human laryngeal squamous cell carcinomas: prognostic significance and clinical implications. *Clin Cancer Res* 1996;2:175–80.
- Pignataro L, Pruner G, Carboni N, et al. Clinical relevance of cyclin D1 protein overexpression in laryngeal squamous cell carcinoma. *J Clin Oncol* 1998;9:3069–77.
- Rubin Grandis J, Melhem MF, Gooding WE, et al. Levels of TGF- α and EGFR protein in head and neck squamous cell carcinoma and patient survival. *J Natl Cancer Inst* 1998;90:824–32.
- Smith BD, Smith GL, Carter D, Sasaki CT, Haffty BG. Prognostic significance of vascular endothelial growth factor protein levels in oral and oropharyngeal squamous cell carcinoma. *J Clin Oncol* 2000;18:2046–52.
- Pruner G, Pignataro L, Carboni N, et al. Clinical relevance of expression of the CIP/KIP cell-cycle inhibitors p21 and p27 in laryngeal cancer. *J Clin Oncol* 1999;17:3150–9.
- Ashkar S, Weber GF, Panoutsakopoulou V, et al. Eta-1 (osteopontin): an early component of type-1 (cell-mediated) immunity. *Science* 2000;287:860–4.
- Chabas D, Baranzini SE, Mitchell D, et al. The influence of the proinflammatory cytokine, osteopontin on autoimmune demyelinating disease. *Science* 2001;294:1731–5.
- Weber GF, Ashkar S, Glimcher MJ, Cantor H. Receptor-ligand interaction between CD44 and osteopontin (Eta-1). *Science* 1996;271:509–12.
- Katagiri YU, Sleeman J, Fujii H, et al. CD44 variants but not CD44s cooperate with β_1 -containing integrins to permit cells to bind to osteopontin independently of arginine-glycine-aspartic acid, thereby stimulating cell motility and chemotaxis. *Cancer Res* 1999;59:219–26.
- Rittling SR, Chambers AF. Role of osteopontin in tumor progression. *Br J Cancer* 2004;90:1877–81.
- Weber GF. The metastasis gene osteopontin: a candidate target for cancer therapy. *Biochim Biophys Acta* 2001;1552:61–85.
- Ponta H, Sherman L, Herrlich PA. CD44: from adhesion molecules to signalling regulators. *Nat Rev Mol Cell Biol* 2003;4:33–45.
- Agrawal D, Chen T, Irby R, et al. Osteopontin identified as lead marker of colon cancer progression, using pooled sample expression profiling. *J Natl Cancer Inst* 2002;94:513–21.
- Schorge JO, Drake RD, Lee H, et al. Osteopontin as an adjunct to CA125 in detecting recurrent ovarian cancer. *Clin Cancer Res* 2004;10:3474–8.
- Kang Y, Siegel PM, Shu W, et al. A multigenic program mediating breast cancer metastasis to bone. *Cancer Cell* 2003;3:537–49.
- Ye QH, Qin LX, Forgues M, et al. Predicting hepatitis B virus-positive metastatic hepatocellular carcinomas using gene expression profiling and supervised machine learning. *Nat Med* 2003;9:416–23.
- Hermanek P, Sobin LH. Larynx. In: Hermanek P, Sobin LH, editors. *TNM classification of malignant tumors*. Berlin (Germany): Springer-Verlag; 1987. p. 25–8.
- Rosai J, Carcangiu ML, DeLellis RA. Atlas of tumor pathology—tumors of the larynx, 3rd series. Washington: Armed Force Institute of Pathology; 1992.
- Kawamata H, Nakashiro K, Uchida D, Harada K, Yoshida H, Sato M. Possible contribution of active MMP2 to lymph-node metastasis and secreted cathepsin L to bone invasion of newly established human oral-squamous-cancer cell lines. *Int J Cancer* 1997;70:120–7.
- Gioanni J, Fischel JL, Lambert JC, et al. Two new human tumor cell lines derived from squamous cell carcinomas of the tongue: establishment, characterization and response to cytotoxic treatment. *Eur J Cancer Clin Oncol* 1988;24:1445–55.
- Moore AE, Sabachewsky L, Toolan HW. Culture characteristics of four permanent lines of human cancer cells. *Cancer Res* 1955;15:598–602.
- Eagle H. Propagation in a fluid medium of a human epidermoid carcinoma, strain KB. *Proc Soc Exp Biol Med* 1955;89:362–4.
- Weiss JM, Renkl AC, Maier CS, et al. Osteopontin is involved in the initiation of cutaneous contact hypersensitivity by inducing Langerhans and dendritic cell migration to lymph nodes. *J Exp Med* 2001;194:1219–29.

30. Le QT, Sutphin PD, Raychaudhuri S, et al. Identification of osteopontin as a prognostic marker for head and neck squamous cell carcinomas. *Clin Cancer Res* 2003;9:31–2.
31. Senger DR, Wirth DF, Hytnes RO. Transformed mamalian cells secrete specific proteins and phosphoproteins. *Cell* 1979;16:885–93.
32. Medico E, Gentile A, Lo Celso C, et al. Osteopontin is an autocrine mediator of hepatocyte growth factor-induced invasive growth. *Cancer Res* 2001;61:5861–8.
33. Wu Y, Denhardt DT, Rittling SR. Osteopontin is required for full expression of the transformed phenotype by the ras oncogene. *Br J Cancer* 2000;83:156–63.
34. Chackalaparampil I, Peri A, Nemir M, et al. Cells *in vivo* and *in vitro* from osteopetrotic mice homozygous for c-src disruption show suppression of synthesis of osteopontin, a multifunctional extracellular matrix protein. *Oncogene* 1996;12:1457–67.
35. Morimoto I, Sasaki Y, Ishida S, Imai K, Tokino T. Identification of the osteopontin gene as a direct target of TP53. *Genes Chromosomes Cancer* 2002;3:270–8.
36. Liu M, Lawson G, Delos M, et al. Prognostic value of cell proliferation markers, tumour suppressor proteins and cell adhesion molecules in primary squamous cell carcinoma of the larynx and hypopharynx. *Eur Arch Otorhinolaryngol* 2003;260:28–34.
37. Bourguignon LY, Gilad E, Rothman K, Peyollier K. Hyaluronan-CD44 interaction with IQGAP1 promotes Cdc42 and ERK signaling leading to actin binding, Elk-1/estrogen receptor transcriptional activation and ovarian cancer progression. *J Biol Chem* 2005;280:11961–72.
38. Teramoto H, Castellone MD, Malek RL, et al. Autocrine activation of an osteopontin-CD44-Rac pathway enhances invasion and transformation by H-RasV12. *Oncogene* 2005;24:489–501.
39. Bourguignon LY, Singleton PA, Zhu H, Diedrich F. Hyaluronan-mediated CD44 interaction with Rho-GEF and Rho kinase promotes Grb2-associated binder-1 phosphorylation and phosphatidylinositol 3-kinase signaling leading to cytokine (macrophage-colony stimulating factor) production and breast tumor progression. *J Biol Chem* 2003;278:29420–34.
40. Murphy JF, Lennon F, Steele C, Kelleher D, Fitzgerald D, Long A. Engagement of CD44 modulates cyclooxygenase induction, VEGF generation, and cell proliferation in human vascular endothelial cells. *FASEB J* 2005;19:446–8.
41. Zhang Y, Thant AA, Machida K, et al. Hyaluronan-CD44s signaling regulates matrix metalloproteinase-2 secretion in a human lung carcinoma cell line QG90. *Cancer Res* 2002;62:3962–5.
42. Gao C, Guo H, Downey L, Marroquin C, Wei J, Kuo PC. Osteopontin-dependent CD44v6 expression and cell adhesion in HepG2 cells. *Carcinogenesis* 2003;24:1871–8.
43. Orian-Rousseau V, Chen L, Sleeman JP, Herrlich P, Ponta H. CD44 is required for two consecutive steps in HGF/c-Met signaling. *Genes Dev* 2002;16:3074–86.
44. Ghatak S, Misra S, Toole BP. Hyaluronan constitutively regulates ErbB2 phosphorylation and signaling complex formation in carcinoma cells. *J Biol Chem* 2005;280:8875–83.
45. Tuck AB, Hota C, Wilson SM, Chambers AF. Osteopontin-induced migration of human mammary epithelial cells involves activation of EGF receptor and multiple signal transduction pathways. *Oncogene* 2003;22:1198–205.

Osteopontin Is Overexpressed in Human Papillary Thyroid Carcinomas and Enhances Thyroid Carcinoma Cell Invasiveness

Valentina Guarino, Pinuccia Faviana, Giuliana Salvatore, Maria Domenica Castellone, Anna Maria Cirafici, Valentina De Falco, Angela Celetti, Riccardo Giannini, Fulvio Basolo, Rosa Marina Melillo, and Massimo Santoro

Dipartimento di Biologia e Patologia Cellulare e Molecolare, Università di Napoli Federico II, Istituto di Endocrinologia ed Oncologia Sperimentale del Consiglio Nazionale delle Ricerche (V.G., G.S., M.D.C., A.M.C., V.D.F., A.C., R.M.M., M.S.), Naples, Italy; and Dipartimento di Oncologia, Università di Pisa (P.F., R.G., F.B.), Pisa, Italy

Context: The transmembrane glycoprotein CD44v6 is overexpressed in most papillary thyroid carcinomas (PTC). We previously reported that osteopontin (OPN), a secreted glycoprotein that functions as a ligand for CD44v6, is overexpressed in thyrocytes transformed by the RET/PTC oncogene.

Objective: In this study we asked whether OPN is overexpressed in human PTC samples, and whether its expression correlates with clinical and histological features of the tumors. Furthermore, we wanted to establish the functional role of the CD44-OPN axis in thyroid tumorigenesis.

Design: Thyroid samples from 117 patients who had undergone surgical resection of the thyroid gland for benign or malignant lesions were collected. OPN and CD44 expressions were evaluated by immunohistochemistry with specific monoclonal antibodies. OPN expression was correlated with different PTC histological variants, lymph node metastasis, and PTC size.

Results: In this study we show that OPN is overexpressed in human PTCs with respect to normal thyroid tissue, follicular adenomas, and multinodular goiters ($P < 0.05$). The prevalence and intensity of OPN staining were significantly correlated with the presence of lymph node metastases ($P = 0.0091$) and tumor size ($P = 0.0001$). We also show that treatment of human PTC cells with recombinant exogenous OPN stimulated Matrigel invasion and activated the ERK and V-AKT murine thymoma viral oncogene homolog 1/protein kinase B; signaling pathways. Blockage of anti-CD44 antibodies prevented these effects.

Conclusions: Given its prevalence and its correlation with aggressive features of human PTCs, we suggest that OPN might be used as a diagnostic and prognostic marker for these tumors. Furthermore, given the role of the OPN-CD44v6 axis in PTC cells, we suggest that CD44 and/or OPN may be molecular targets for therapeutic intervention in aggressive PTCs. (*J Clin Endocrinol Metab* 90: 5270–5278, 2005)

THYROID TUMORS ARE the most common malignancies of the endocrine system; their annual incidence is estimated to be 122,000 cases worldwide (1). Papillary thyroid carcinomas (PTC) far outnumber the other morphological subtypes (2). The incidence of PTC has increased worldwide. For instance, there were an estimated 22,000 new cases in the United States in 2004 vs. 10,000 cases in 1980 (1). The past decade has witnessed significant advances in our understanding of thyroid carcinogenesis at the molecular level. Hallmarks of PTC are chromosomal translocations or inversions that cause the recombination of the tyrosine kinase domain of the RET receptor to heterologous genes, thereby generating RET/PTC chimeric oncogenes (3). Similar rearrangements of the NTRKA receptor occur in a smaller fraction of PTC (4). The activating V600E mutation in the BRAF serine/threonine kinase, present in 36–69% of PTC cases, is the most frequent genetic change in PTC (5–12). Very re-

cently, the oncogenic AKAP9-BRAF fusion has been found in radiation-induced PTC (13). RAS point mutations are infrequent in PTC and are restricted to aggressive subtypes (14) and to the follicular variant of PTC (15). Various lines of evidence indicate that the formation of BRAF and RET/PTC oncogenes is the first step of thyroid carcinogenesis: 1) these oncoproteins recreate the disease in transgenic animals; 2) they are activated in the early stages of tumor development; and 3) radiation has been implicated in the oncogenic activation of both of them (16). Activation of the serine/threonine V-AKT murine thymoma viral oncogene homolog 1/protein kinase B (AKT/PKB) kinase is another common feature of human PTC (17).

Despite the link between these oncogenes and PTC, little is known about the molecular mechanisms that control the establishment and maintenance of the PTC neoplastic phenotype. Using oligonucleotide microarrays, we previously found that osteopontin (OPN) is among the transcripts most strongly induced by RET/PTC in thyroid follicular cells (18). OPN, also known as SPP1 (secreted phosphoprotein 1), was first identified as a noncollagenous bone matrix protein. Subsequently, it was shown that OPN is indeed a cytokine, and that it regulates cell trafficking within the immune system (19, 20). OPN binds to the cell surface receptors α_v - or β_1 -containing integrins and CD44 (21). CD44 is a cell surface

First Published Online July 5, 2005

Abbreviations: AKT/PKB, V-AKT murine thymoma viral oncogene homolog 1/protein kinase B; FV, Follicular variant; OPN, osteopontin; PI3-K, phosphatidylinositol 3-kinase; PTC, papillary thyroid carcinoma; Q-RT-PCR, quantitative (real-time) RT-PCR.

JCEM is published monthly by The Endocrine Society (<http://www.endo-society.org>), the foremost professional society serving the endocrine community.

glycoprotein that can be expressed as a standard receptor (CD44s) and as multiple splice isoforms (CD44v) whose expression is altered during tumor growth and progression. Expression of the v6 variant exon is required for efficient OPN binding (21, 22). Under normal conditions, only CD44s is expressed on the cell surface of nonproliferating thyrocytes, whereas CD44v6 is invariably overexpressed in PTC samples (23–26). OPN is expressed in numerous human tumors, including colon, breast, prostate, gastric, ovarian, and lung carcinomas. In addition, OPN expression often correlates with a poor prognosis (27).

In our previous work we proposed that RET/PTC signaling triggered the formation of an autocrine axis involving OPN and its receptor, CD44. An intact kinase activity and the integrity of tyrosine 1062 of RET were required for the up-regulation of both OPN and CD44. Furthermore, we showed that addition of exogenous OPN or transduction of OPN through a lentiviral vector in RET/PTC1-expressing rat thyroid cells stimulated mitogenesis, survival, and motility (18). To validate these observations and to assess the role of OPN expression in human thyroid tumors, we collected human PTC tumor samples and studied OPN and CD44 expression. Furthermore, we used human PTC cell lines characterized for the presence of the RET/PTC1 rearrangement or BRAF (V600E) mutation. In this study we show that OPN is consistently overexpressed in human PTC samples, and that OPN-induced CD44 stimulation activates the ERK and AKT/PKB signaling pathways, thereby sustaining Matrigel invasion of human PTC cell lines.

Patients and Methods

Tumors

Archival thyroid samples from 117 patients were retrieved from the files of the Department of Oncology of University of Pisa (Pisa, Italy). Informed consent was obtained from the patients, and the study was approved by the institutional review board committee. Tumor size, extrathyroid invasion, node metastasis, associated thyroid lesions, and metastatic deposits were recorded. After surgical resection, tissues were fixed in 10% neutral buffered formalin and embedded in paraffin blocks. Sections (4 μ m thick) were stained with hematoxylin and eosin for histological examination. The nuclear and architectural features were evaluated to ensure that the samples fulfilled the diagnostic criteria required for the identification of PTC (enlarged nuclei with fine dusty chromatin, nuclear grooves, single or multiple micro/macronucleoli, and intranuclear inclusions) (28, 29). The final histological diagnoses of the carcinomas were: classic papillary (n = 40), follicular variant PTC (PTC-FV; n = 23), and tall cell variant PTC (n = 8). In addition, 34 normal thyroid samples, seven follicular adenomas, and five multinodular goiters were examined.

Immunohistochemistry

Formalin-fixed and paraffin-embedded 4- to 5- μ m-thick tumor sections were deparaffinized, placed in a solution of absolute methanol and 0.3% hydrogen peroxide for 30 min, and treated with blocking serum for 20 min. The slides were incubated overnight with anti-OPN or anti-CD44 monoclonal antibodies, with biotinylated anti-IgG, and finally with pre-mixed avidin-biotin complex (Vectostain ABC kits, Vector Laboratories, Inc., Burlingame, CA). Anti-OPN IgG₁ mouse monoclonal (10A16) was obtained from Assay Designs (Ann Arbor, MI), and anti-CD44v6 IgG₁ mouse monoclonal (NCL-CD44v6, clone VFF-7) was purchased from Novocastra Laboratories Ltd. (Newcastle upon Tyne, UK). The immune reaction was revealed with 0.06 mmol/liter diaminobenzidine (DAB-Dako, DakoCytomation, Carpinteria, CA) and 2 mmol/liter hydrogen peroxide. The slides were counterstained with hematoxylin. As a neg-

ative control, tissue slides were incubated with isotype-matched IgG₁ control antibodies. The OPN immunostaining was mostly localized in the cytoplasm. Staining intensity was scored semiquantitatively into different grades on an arbitrary scale from 0–3: grade 0, no detectable immunostaining; 1+, weak staining; 2+ moderate staining; and 3+, strong staining intensity. For each sample, the percentage of positive cells for OPN staining was also evaluated.

Cell lines and plasmids

Human primary cultures of thyroid cells (P5) were obtained from F. Curcio (Dipartimento di Patologia e Medicina Sperimentale e Clinica, Università di Udine, Udine, Italy) and cultured as previously described (30). Human RET/PTC1-positive (TPC1, FB2, BHP2-7, BHP7-13, and BHP10-3) and BRAF V600E-positive (NPA and BCPAP) PTC cell lines were described previously (5, 31). BHP5-16, BHP14-9, and BHP17-10 were shown by direct sequencing to harbor the BRAF V600E mutation at the heterozygous level (Salvatore, G., V. Guarino, T. Nappi, F. Carlomagno, R. M. Melillo, and M. Santoro, unpublished observations). PTC cells were maintained in DMEM supplemented with 10% fetal bovine serum, 2 mM L-glutamine, and 100 U/ml penicillin-streptomycin (Invitrogen Life Technologies, Inc., Paisley, PA).

RNA extraction and RT-PCR

Total RNA from the indicated cell cultures and from snap-frozen tissue samples was prepared using the RNeasy Mini Kit (Qiagen, Crawley, UK) and subjected to on-column deoxyribonuclease digestion with the ribonuclease-free deoxyribonuclease set (Qiagen) following the manufacturer's instructions. Only tissue samples containing more than 70% neoplastic cells were used. The quality of RNA from each sample was verified by electrophoresis through 1% agarose gel. Total RNA (2.5 μ g) was denatured, and cDNA was synthesized using the GeneAmp RNA PCR Core Kit system (Applied Biosystems, Foster City, CA) following the manufacturer's instructions. PCR was amplified using 2.5 μ l reverse transcriptase product in a reaction volume of 25 μ l with primer pairs specific for the gene studied. To exclude DNA contamination, each PCR was also performed with untranscribed RNA. The levels of the house-keeping β -actin transcript were used as a control for equal RNA loading. Primers were designed with the Primer 3 program (www.genome.wi.mit.edu/cgi-bin/primer/primer3_www.cgi) and synthesized by MWG (Ebersberg, Germany). Primer sequences were as follows: OPN forward, 5'-AGGAGGAGGCAGAGCAC-3'; OPN reverse, 5'-CTGGTATG-GCACAGGTGATG-3'; CD44 (exon 2) forward, 5'-GCTTTC AATAG-CACCTTGCC-3'; CD44 (exon v6) reverse, 5'-GTTGCCAAACCACTGT-TCCT; β -actin forward, 5'-TGCCTGACATTAAGGAGAAG-3'; and β -actin reverse, 5'-GCTCGTAGCTCTTCTCCA-3'.

Each RT-PCR product was loaded on 2% agarose gel, stained with ethidium bromide (0.5 μ g/ml), and the corresponding image was saved by the Typhoon 8600 laser scanning system (Amersham Biosciences, Little Chalfont, UK). The density and width of each band were quantified using ImageQuant 5.0 (Amersham Biosciences). OPN expression in the different cell lines was expressed as the fold increase with respect to normal P5 thyroid cells (=1) after normalization for β -actin expression.

Quantitative (real-time) RT-PCR (Q-RT-PCR) was performed by using the SYBR Green PCR MasterMix (Applied Biosystems) in the iCycler apparatus (Bio-Rad Laboratories, Munich, Germany). Amplification reactions (25 μ l final reaction volume) contained 200 nM of each primer, 3 mM MgCl₂, 300 μ M deoxy-NTPs, 1 \times SYBR Green PCR buffer, 0.1 U/ μ l AmpliTaq Gold DNA polymerase, 0.01 U/ μ l Amp Erase, ribonuclease-free water, and 2 μ l cDNA samples. We performed 80 cycles of melting to verify the absence of nonspecific products. In all cases, the melting curve confirmed that a single product was generated. Amplification was monitored by measuring the increase in fluorescence caused by SYBR Green binding to double-stranded DNA. Fluorescent threshold values were measured in triplicate, and fold changes were calculated by the formula: $2^{-(\text{sample 1 } \Delta C_T - \text{sample 2 } \Delta C_T)}$, where ΔC_T is the difference between the amplification fluorescent thresholds of the mRNA of interest and the β -actin mRNA. Primer sequences were as follows: OPN forward, 5'-ATCCATGTGGTCATGGCTTT-3'; OPN reverse, 5'-GAAGGAGCT-GAAGGAGCTGA-3'; β -actin forward, 5'-TGCCTGACATTAAG-GAGAAG-3'; and β -actin reverse, 5'-GCTCGTAGCTCTTCTCCA-3'.

Protein studies

Immunoblotting experiments were performed according to standard procedures. Briefly, cells were harvested in lysis buffer [50 mM HEPES (pH 7.5), 150 mM NaCl, 10% glycerol, 1% Triton X-100, 1 mM EGTA, 1.5 mM MgCl₂, 10 mM sodium fluoride, 10 mM sodium pyrophosphate, 1 mM Na₃VO₄, 10 μg aprotinin/ml, and 10 μg leupeptin/ml] and clarified by centrifugation at 10,000 × *g*. For protein extraction from human tissues, samples were snap-frozen and immediately homogenized in lysis buffer in the Mixer Mill apparatus (Qiagen). Protein concentration was estimated with a modified Bradford assay (Bio-Rad Laboratories). Antigens were revealed by an enhanced chemiluminescence detection kit (ECL, Amersham Biosciences). Anti-OPN goat polyclonal antibody (K20) and rabbit polyclonal anti-CD44 (H300) were obtained from Santa Cruz Biotechnology, Inc. (Santa Cruz, CA). Monoclonal anti- α -tubulin was purchased from Sigma-Aldrich Corp. (St. Louis, MO). Anti-phospho-p44/42 MAPK (ERK) and anti-p44/42 MAPK, anti-phospho-AKT, and anti-AKT antibodies were obtained from New England Biolabs (Beverly, MA). Secondary antimouse and antirabbit antibodies coupled to horseradish peroxidase were purchased from Bio-Rad Laboratories. Where indicated, densitometric analysis of the immunoreactive bands was performed by phosphorimager scanning (Typhoon, Amersham Biosciences) and analyzed using ImageQuant 5.0 software. Protein levels were expressed as fold increases with respect to normal thyroid samples (=1) after normalization for tubulin expression.

ELISA

Thyroid cells (3 × 10⁵) were plated in six-well dishes, allowed to grow to 70% confluence, and then serum-deprived for 24 h. Culture media were centrifuged at 2000 rpm at 4°C to remove detached cells and debris. Attached cells were lysed, and total protein concentration was evaluated by a modified Bradford assay (Bio-Rad Laboratories), as described above. OPN levels in culture supernatants were measured using a quantitative immunoassay ELISA kit (QuantiKine assay, R&D Systems, Inc., Minneapolis, MN) following the manufacturer's instructions. Triplicate samples were analyzed at 490 nm with an ELISA reader (model 550 microplate reader, Bio-Rad Laboratories). OPN levels, expressed in nanograms per milliliter, were adjusted considering total protein levels of the grown cells.

Flow cytometric analysis

Subconfluent cells were detached from culture dishes with a solution of 0.5 mM EDTA, then washed three times in PBS buffer. After saturation with 1 μg human IgG/10⁵ cells, cells were incubated for 20 min on ice with antibodies specific for human CD44v6 (R&D Systems, Inc.) or isotype control antibody. After incubation, unreacted antibody was removed by washing cells twice in PBS buffer. Cells were then incubated (30 min, 4°C) with 100 μl fluorescein-conjugated goat antimouse IgG/M (Jackson ImmunoResearch Laboratories, Inc., West Grove, PA). Cells resuspended in PBS were analyzed on a FACSCalibur cytofluorometer using CellQuest software (BD Biosciences, San Jose, CA). Analyses were performed in triplicate. In each analysis, a total of 10⁴ events were calculated.

Chemoinvasion

In vitro invasiveness through Matrigel was assayed using Transwell cell culture chambers as described previously (18). Briefly, confluent cell monolayers were harvested with trypsin/EDTA and centrifuged at 800 × *g* for 10 min. The cell suspension (1 × 10⁵ cells/well) was added to the upper chamber of a prehydrated polycarbonate membrane filter with a pore size of 8 μm (Costar, Cambridge, MA) coated with 35 μg Matrigel (Collaborative Research, Inc., Bedford, MA). The lower chamber was filled with complete medium, and when required, purified recombinant OPN (R&D Systems, Inc.) was added at a concentration of 100 ng/ml. To inhibit Matrigel invasion, cells were preincubated with 5 μg/ml CD44-blocking antibodies (KM81 hybridoma, TIB-241, American Type Culture Collection, Manassas, VA) (32). Alternatively, cells were treated for 12 h with U0126 (10 μM) or wortmannin (100 nM; Upstate Biotechnology, Inc., Charlottesville, VA). Cells were then incubated at 37°C in a humidified incubator in 5% CO₂ and 95% air for 24 h.

Nonmigrating cells on the upper side of the filter and Matrigel were wiped off, and migrating cells on the reverse side of the filter were stained with 0.1% crystal violet in 20% methanol for 15 min and photographed. The stained cells were lysed in 10% acetic acid. Triplicate samples were analyzed at 570 nm with an ELISA reader (model 550 microplate reader, Bio-Rad Laboratories). The results were expressed as the percentage of migrating cells.

Statistical analysis

Statistical analysis (Statistica, StatSoft, Tulsa, OK) was performed using 2 × 2 tables (χ^2); differences were significant at *P* < 0.05.

Results

Immunohistochemical determination of OPN expression in PTC

We measured OPN expression by immunohistochemistry with an anti-OPN-specific monoclonal antibody in 117 thyroid samples from patients who had undergone surgical resection of the thyroid gland for benign or malignant lesions. Representative immunohistochemical stainings are shown in Fig. 1, and the entire dataset is reported in Table 1. OPN was virtually undetectable (<10% of cells) in normal thyroid glands (n = 34), follicular adenomas (n = 7), and multinodular goiters (n = 5). In contrast, most of the PTC samples examined (60 of 71), were positive for OPN expression, and positivity was confined to tumor cells (Table 1). As shown in Table 2, the prevalence and intensity of OPN staining were significantly correlated with the presence of lymph node metastases (*P* = 0.0091) and tumor size (*P* = 0.0001). Furthermore, 85% (34 of 40) of the classic PTC tumors and 100% (eight of eight) of the tall cell variant PTC tumors displayed intense (2+ /3+) OPN immunoreactivity in more than 70% of the cells, whereas PTC-FV tumors were characterized by less intense or negative staining. Finally, in accordance with previous data (23–26), classic PTC (n = 40) were invariably positive also to CD44v6-specific monoclonal antibodies (Fig. 1H and data not shown).

Immunoblot and PCR analysis of OPN expression in PTC

Protein lysates were harvested from a pool of normal human thyroid tissues and from six classic PTC samples and analyzed by immunoblotting. Densitometric analysis of the blots was performed, and OPN levels were normalized to tubulin. As shown in Fig. 2A, the OPN protein (molecular mass, ~65,000) was abundantly expressed in all carcinomas, but was barely detectable in normal tissue. To obtain an additional assessment of OPN up-regulation and to determine whether up-regulation occurred at the transcriptional level, we examined a small sample set using Q-RT-PCR. As shown in Fig. 2B, the levels of OPN transcripts were significantly higher (8- to 22-fold) in tumor samples than in normal thyroid tissue.

To verify these findings and to establish a model system with which to study the role of OPN up-regulation, we analyzed OPN mRNA expression in cultured human thyroid cells. In these experiments we used a primary culture of normal thyroid follicular cells (P5) (30) and a panel of PTC cell lines characterized for the presence of RET/PTC rearrangements (TPC1, FB2, BHP2-7, BHP7-13, and BHP10-3) or the V600E mutation in BRAF (BHP5-16, BHP14-9, BHP17-10,

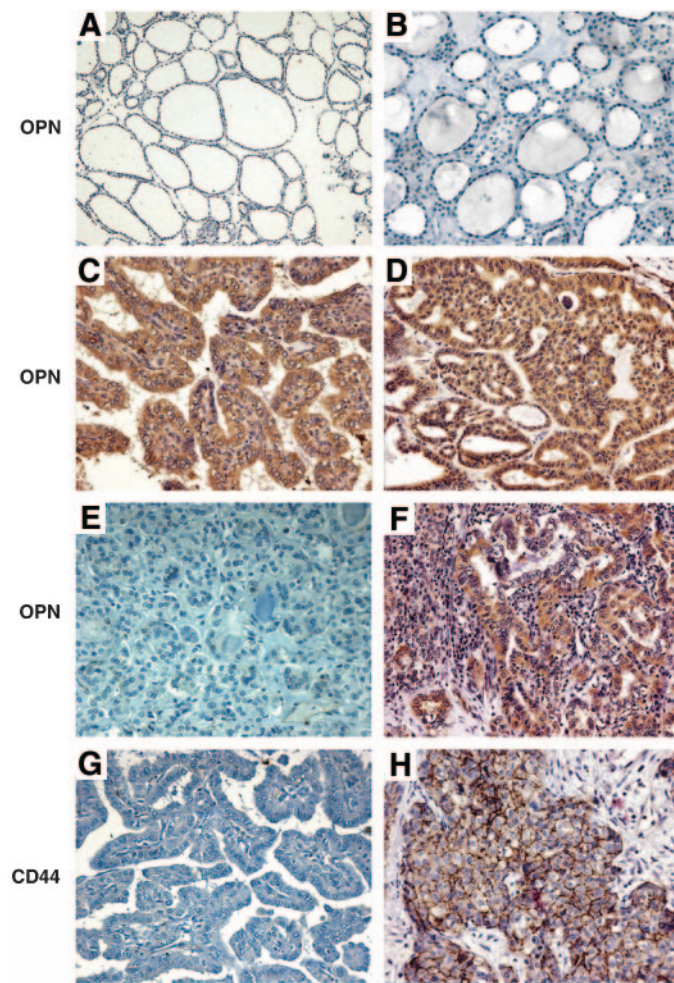


FIG. 1. Immunohistochemical detection of OPN and CD44 in thyroid samples. Tissue samples from normal thyroid (A and B), primary PTC (C and D), and a PTC node metastasis (F) were incubated with a mouse monoclonal anti-OPN antibody. PTC samples showed intense immunoreactivity for OPN. In PTC samples, intense immunoreactivity was also seen with CD44v6 antibodies (H). Negative controls were performed in all PTC cases using isotype control antibodies (E and G). Magnification: A, C, E, and H, $\times 100$; B, D, F, and G, $\times 200$.

NPA, and BCPAP) (5, 31) (Salvatore, G., unpublished observations). As shown by the RT-PCR experiment, all the PTC cell lines analyzed overexpressed OPN by more than 10-fold with respect to normal thyrocytes; BCPAP cells were the least positive (Fig. 3A). Thus, OPN up-regulation correlated with the presence of the two most common genetic alterations in PTC, *i.e.* the RET/PTC and BRAF mutations (16). To verify that the up-regulated OPN was indeed secreted by PTC cells, we used an ELISA to examine conditioned medium harvested from the various cell lines. PTC cells, but not normal P5 cells, secreted abundant OPN in the culture medium (Fig. 3B). Again, BCPAP cells were the least positive.

CD44 is an OPN cell surface receptor, and it is frequently overexpressed in neoplastic cells. CD44 pre-mRNA is encoded by 20 exons, which are subject to alternative splicing. The constant 5'-terminal five exons encode the N-terminal extracellular domain of the protein, whereas the constant

TABLE 1. OPN positivity in thyroid lesions

Histology	No. of cases	OPN positivity no. of cases (%) ^a	
		>10% (1+/3+)	<10% (0/1+)
PTC	71	60 (84.5) ^b	11 (15.5)
Microfollicular adenoma	4		4 (100)
Macrofollicular adenoma	3		3 (100)
Multinodular goiter	5		5 (100)
Normal	34		34 (100)

^a The OPN immunostaining was mostly localized in the cytoplasm. Cytoplasmic staining intensity was scored semiquantitatively as described in *Patients and Methods*. The percentage of OPN-positive cells was estimated. The samples were divided in two groups (>10% and <10% of positive cells). The intensity of OPN staining was graded into the following categories: 0, no signal; 1+, weak; 2+, moderate; 3+, strong. The number of positive cells invariably correlated with stain intensity.

^b OPN positivity (>10% cells) in PTC *vs.* the other lesions: $P < 0.05$ [2×2 tables (χ^2)].

3'-terminal five exons encode the transmembrane and the short cytosolic tail. An additional 10 exons (variant v1–v10 exons) are alternatively spliced and encode the extracellular membrane-proximal stem structure (21, 22). Cancer cells often overexpress CD44 variants that differ in the number of v exons. The presence of the v6 exon is required for efficient OPN binding (21, 22). Consequently, we screened PTC cell lines for CD44 expression by RT-PCR using primers designed on exons 2 and v6. As shown in Fig. 4A, all cancer cells tested, but not normal cells, contained high levels of CD44v6 mRNA. To enable cells to bind OPN, CD44v6 must be expressed on the cell surface. We therefore used flow cytometry to determine whether CD44v6 was expressed on the surface of PTC cells. As shown in Fig. 4B, the TPC1 and BCPAP PTC cell lines featured homogeneous cell membrane CD44v6 expression, whereas the others displayed varying expression levels of CD44v6.

OPN activates intracellular signaling and invasiveness of PTC cells

OPN protein secretion and cell surface CD44v6 expression reflected the existence of an autocrine/paracrine OPN-CD44 axis that affected PTC cells. To verify that this axis was functional in human PTC cell lines, we examined cell invasion of Matrigel under basal conditions and in the presence of exogenous recombinant OPN. To this aim, we treated normal P5 and PTC-derived cell lines with exogenous OPN and evaluated the number of migrating cells. As shown in Fig. 5A, OPN induced a strong migratory response in all PTC, but not in normal cells. Interestingly, the TPC1 and BCPAP cells, which expressed the highest levels of CD44v6, displayed the best migratory response to OPN. To verify whether OPN was able to induce a biochemical response in PTC cells, we selected BCPAP cells, which express high levels of CD44v6 and relatively low levels of OPN. Cells were stimulated with exogenous recombinant OPN and harvested at different time points. Protein lysates were probed with antiphospho-MAPK (ERK) and antiphospho-AKT/PKB antibodies. As shown in Fig. 5B, both p44/42 MAPK and AKT were readily activated in OPN-stimulated cells; they peaked at 5–15 min. It has been previously reported that in immortalized liver carcinoma cells (HepG2), OPN up-regulated

TABLE 2. Correlation between OPN positivity and clinicopathological features in PTC

T (no.) ^{a,b}	Node metastases (no.) ^c	Subtype (no.) ^d	OPN-positivity no. of cases ^e			
			>70% (2+/3+)	30–70% (1+/2+)	10–29% (1+)	<10% (0–1+)
T1–T2 (32)	Yes (7)	Classic (3)	3			
		Tall-cell (0)				
	No (25)	Follicular (4)	6	1	2	1
		Classic (6)				
T3–T4 (39)	Yes (25)	Tall-cell (0)	15	2		
		Follicular (19)				
		Classic (17)				
	No (14)	Tall-cell (8)	10	4		
		Follicular (0)				
		Classic (14)				
		Tall-cell (0)				
		Follicular (0)				

^a T was defined as follows: TX, primary tumor cannot be assessed; T0, no evidence of primary tumor; T1, the tumor is 2 cm (slightly less than an inch) or smaller; T2, tumor is between 2 and 4 cm (slightly less than 2 inches); T3, tumor is larger than 4 cm or has slightly grown outside the thyroid; T4a, tumor of any size and has grown beyond the thyroid gland to invade nearby tissues of the neck; T4b, tumor has grown either back to the spine or into nearby large blood vessels.

^b OPN positivity (>10% cells) in T1–T2 *vs.* T3–T4 PTC samples: $P = 0.0001$ [2×2 tables (χ^2)].

^c OPN positivity (>10% cells) in N(+) *vs.* N(-) PTC samples: $P = 0.0091$ [2×2 tables (χ^2)].

^d Weak or no OPN positivity (<10% cells) in FV *vs.* other PTC variants: $P < 0.0001$ [2×2 tables (χ^2)].

^e The OPN immunostaining was mostly localized in the cytoplasm. Cytoplasmic staining intensity was scored semiquantitatively. The percentage of OPN-positive cells was estimated and the samples were divided in four groups. The intensity of OPN staining was graded into the following categories: 0, no signal; 1+, weak; 2+, moderate; 3+, strong. The number of positive cells invariably correlated with stain intensity; for instance, a high fraction of positive cells (>70%) was paralleled by moderate-strong (2+/3+) stain intensity, whereas a reduced fraction of positive cells (<10%) was paralleled by weak staining.

plasma membrane CD44v6 protein expression in a concentration- and time-dependent fashion (33). To determine whether this was also the case for thyroid cancer cells, we stimulated BCPAP with OPN and evaluated CD44 expression by Western blot analysis. As shown in Fig. 5C, OPN treatment significantly increased CD44 protein levels. Such

an up-regulation reasonably occurred at a posttranscriptional level, because it was not detected at the mRNA level (not shown).

To evaluate whether the CD44 receptor mediated invasiveness of thyroid cancer cells, we treated CD44-blocked BCPAP cells with exogenous OPN (for 5 or 30 min). As

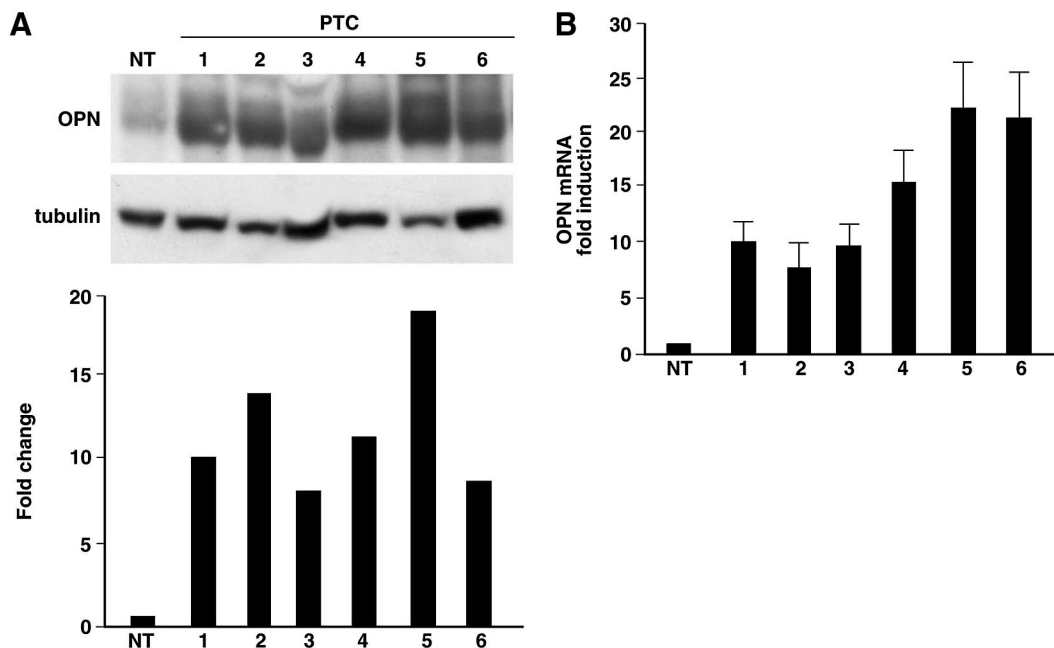


FIG. 2. OPN up-regulation in PTC samples. **A**, OPN protein levels were evaluated by immunoblot in PTC samples and in a pool of five normal thyroid samples (NT). Equal amounts of proteins (100 μ g) were immunoblotted with anti-OPN polyclonal antibodies. Antitubulin monoclonal antibody was used as a control for equal loading. Densitometric analysis was performed with the Typhoon 8600 laser scanning system and the ImageQuant 5.0 software (Amersham Biosciences), and data are shown in the *bar graph*. Each *column* represents the relative fold change with respect to the normal thyroid (NT) sample expression (=1). **B**, Q-RT-PCR was used to calculate OPN mRNA fold induction in six independent PTC tumor samples with respect to a pool of four normal thyroids. The results are the average of three independent experiments \pm SD.

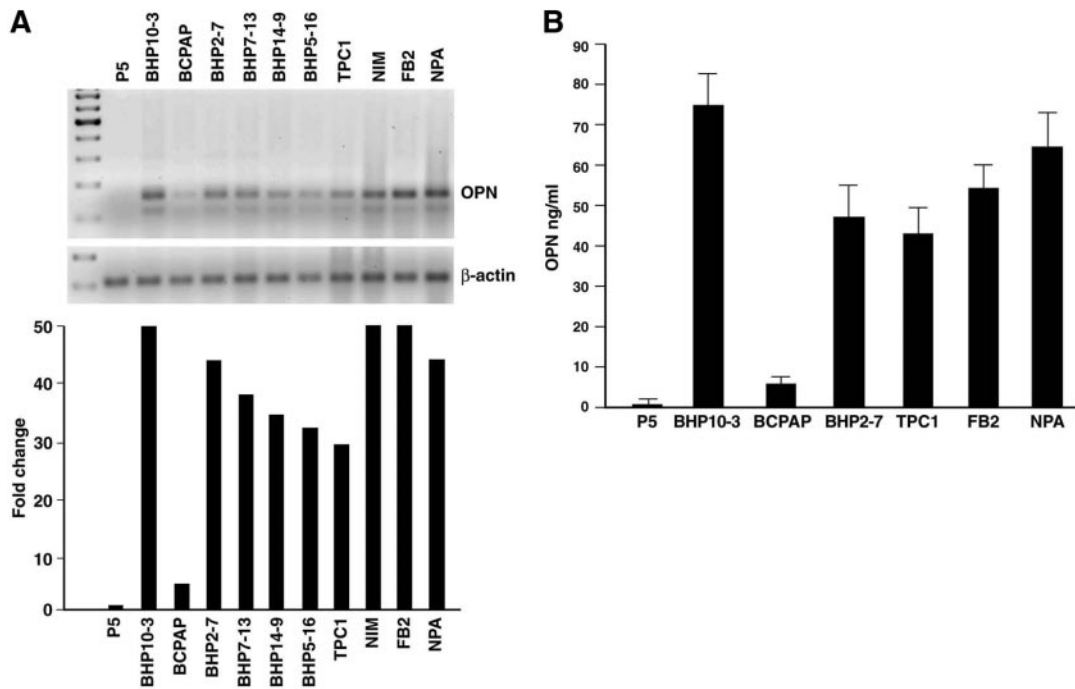


FIG. 3. OPN up-regulation in cultured PTC cells. A, Semiquantitative RT-PCR (25 cycles) was performed to evaluate OPN mRNA levels in the indicated cell lines; β -actin mRNA detection was used for normalization. Band intensity was calculated by phosphorimaging and expressed as the fold change with respect to P5 normal thyroid cells (=1) in the lower panel. This figure is representative of three independent experiments. B, OPN protein secretion by PTC cells was evaluated by ELISA. Normal thyroid cells (P5) were used as the negative control. The results of three independent determinations performed in triplicate \pm SD are reported.

shown in Fig. 6A, p44/42 MAPK and AKT activation was attenuated by pretreatment with CD44-blocking antibodies. CD44 blockade also prevented migration through Matrigel

(Fig. 6B). These observations show that CD44 functions as an OPN-signaling receptor in PTC cells. To investigate whether intracellular signaling was involved in Matrigel invasion

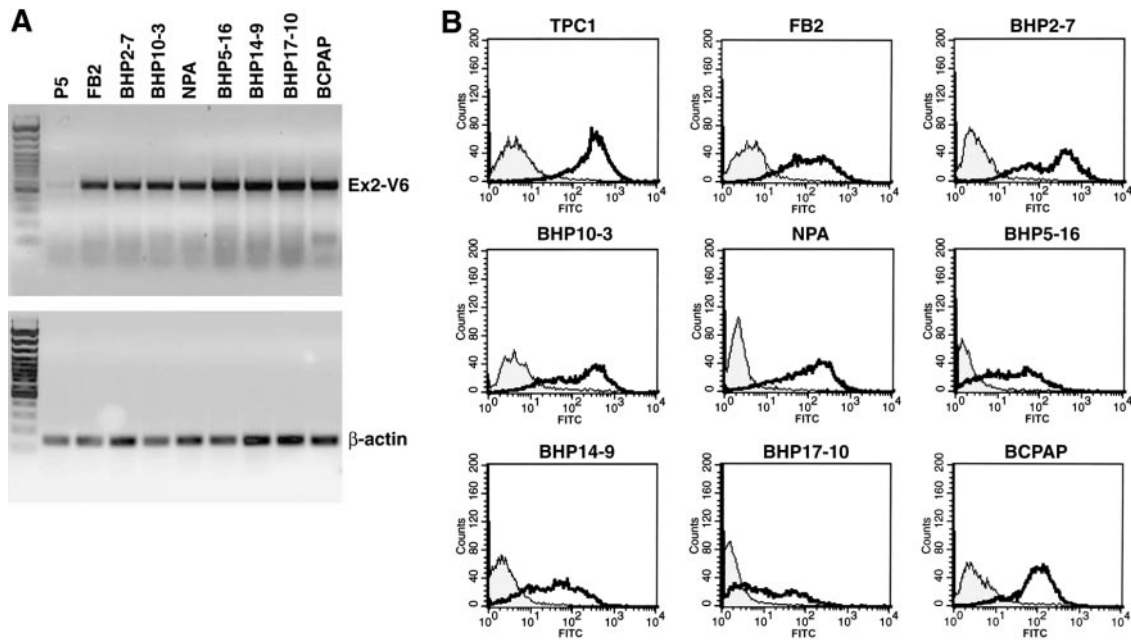


FIG. 4. CD44v6 up-regulation in cultured PTC cells. A, Semiquantitative RT-PCR (25 cycles) was performed to evaluate mRNA levels of the exon v6-containing CD44 variant in the indicated cell lines. Semiquantitative RT-PCR (25 cycles) was performed to evaluate mRNA levels of the exon v6-containing CD44 variant in the indicated cell lines. Amplimers mapping on exons 2 and v6 were used. The exon 2-v6 primer pair amplified one product of 780 bp, containing exons 2–5 and exon v6, as demonstrated by subsequent Southern hybridization with exon-specific probes (not shown). β -Actin mRNA detection was used for normalization. This figure is representative of three independent experiments. B, Flow cytometric analysis of cell surface expression of CD44v6 receptor in the indicated PTC cell lines. The shadowed curve is the negative control antibody.

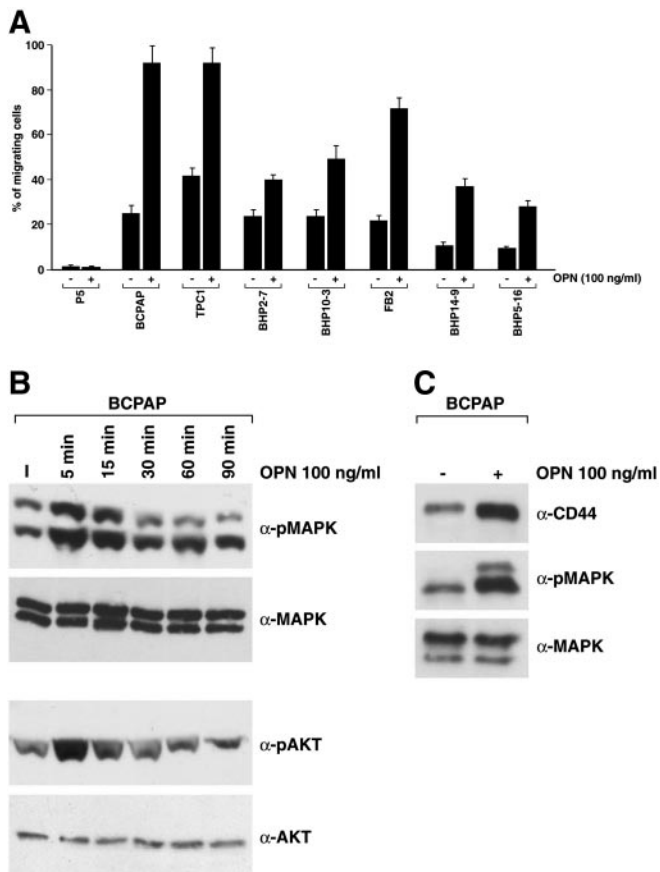


FIG. 5. OPN-mediated signaling and Matrigel invasion. **A**, Matrigel invasion of TPC cells in response to normal culture medium or exogenous recombinant OPN. Cells were incubated for 24 h. Thereafter, filters were fixed and stained. The upper surface was wiped clean, and cells on the lower surface were stained with 0.1% crystal violet. The stained cells were lysed in 10% acetic acid. Invasive ability is expressed as the percentage of migrating cells with respect to the total cell number. Quantification was performed in triplicate samples with an ELISA reader. This figure is representative of three independent experiments. **B**, Total cell lysates were prepared at various time points after stimulation of BCPAP cells with recombinant OPN. Western blots were probed with the indicated phospho-specific antibodies. Anti-MAPK and anti-AKT were used for normalization. **C**, BCPAP cells were stimulated with recombinant OPN for 12 h. Total cell lysates were then prepared and subjected to immunoblot with anti-CD44 antibodies. OPN stimulated CD44 up-regulation and sustained MAPK activation, as shown by staining of the same filter with anti-pMAPK antibodies. The filter was stripped and reprobed with anti-MAPK antibodies to show equal protein loading.

mediated by the OPN-CD44 axis, we used U0126, an inhibitor of the MAPK pathway (MEK1/2), and wortmannin, an inhibitor of the phosphatidylinositol 3-kinase (PI3-K)/AKT pathway. As shown in Fig. 6B, both compounds sharply inhibited (15 ± 5 -fold) Matrigel invasion in parallel with MAPK and AKT blockade (Fig. 6A).

Discussion

OPN is overexpressed in many tumor types (21, 27). The expression of OPN is induced by various signaling proteins that are constitutively active in tumors: growth factors such as the hepatocyte growth factor (34, 35), oncogenes such as

RAS (36) and SRC (37), and tumor promoters such as 12-*O*-tetradecanoyl phorbol 13-acetate (38).

In this study we show that OPN up-regulation is involved in the invasive phenotype of PTC. Overall, as many as 70% of human PTC are estimated to carry mutations at the level of the RET-RAS-BRAF-MAPK signaling cascade (16). We previously reported high levels of OPN and CD44v6 in follicular cells derived from rat thyroid glands and transformed by the RET/PTC oncogene (18). We now show that OPN and CD44v6 up-regulation is a common feature of PTC cells that express the RET/PTC or BRAF V600E oncogenes. This finding suggests that activation of the OPN-CD44v6 axis is one of the end points of the RET-RAS-BRAF-MAPK oncogenic cascade. This model is consistent with the idea that in other cell types, OPN expression is induced by the RAS oncogene (36, 39) and is dependent on the MAPK cascade (40), and that CD44v6 splicing is under control of the RAS-MAPK pathway (41).

Our findings could also clarify the role played by overexpression of CD44v6 in PTC (22–26). CD44 is able to activate a wealth of signaling proteins, such as ERK (42), RAC (43), and RHO (44), leading to cell adhesion and migration, angiogenesis (45), and the secretion of cytokines (44) and metalloproteinases (46). Given the finding that OPN is able to induce CD44v6 overexpression (33), it is conceivable that in PTC cells, the RET-RAS-BRAF-MAPK oncogenic cascade triggers OPN and CD44v6 up-regulation; this leads to OPN-CD44v6 binding, thereby further increasing CD44v6 up-regulation and enhancing MAPK and AKT signaling. It is noteworthy that AKT activation is a common feature of aggressive thyroid cancers (17). The foregoing functional autocrine loop may sustain the invasive capability of PTC cells. Although our experiments demonstrate that OPN-CD44v6 binding mediates cellular effects in thyroid carcinoma cells, they do not exclude that other interactions between OPN and integrins (21, 27) and between CD44, hyaluronan (22), and other membrane receptors such as MET and ERBB2 (47, 48) may be involved in the effects exerted by the OPN-CD44 axis in PTC. Intriguingly, both MET (49) and ERBB2 (50) are overexpressed in PTC. Normal and cancer thyroid cells have been reported to express several integrin receptors, among which the fibronectin receptors α_3/β_1 , α_v/β_3 , and α_v/β_5 (51, 52). Furthermore, immunohistochemistry demonstrated altered expression of $\alpha_v\beta_3$ in human PTC (52). Using real-time RT-PCR, we found expression of the α_v , β_3 , and β_5 , but not of β_1 , integrin in our PTC cell lines, including BCPAP (Guarino, V., A. Celetti, R. M. Melillo, and M. Santoro, unpublished observations).

In this study we show that OPN up-regulation correlates with aggressive clinicopathological features of PTC. Indeed, the presence of lymph node metastases and tumor size both positively correlated with OPN positivity. Thus, OPN might be a diagnostic and prognostic marker for these tumors. Indeed, OPN, which also occurs in blood, has already proven useful as a tumor marker for ovarian (53) and lung (54) carcinomas. Given the low prevalence of OPN overexpression in PTC-FV, our findings anticipate that OPN detection will have a rather low sensitivity in this particular PTC variant. However, our series of PTC-FV is too small to draw firm conclusions. Furthermore, it should be noted that the

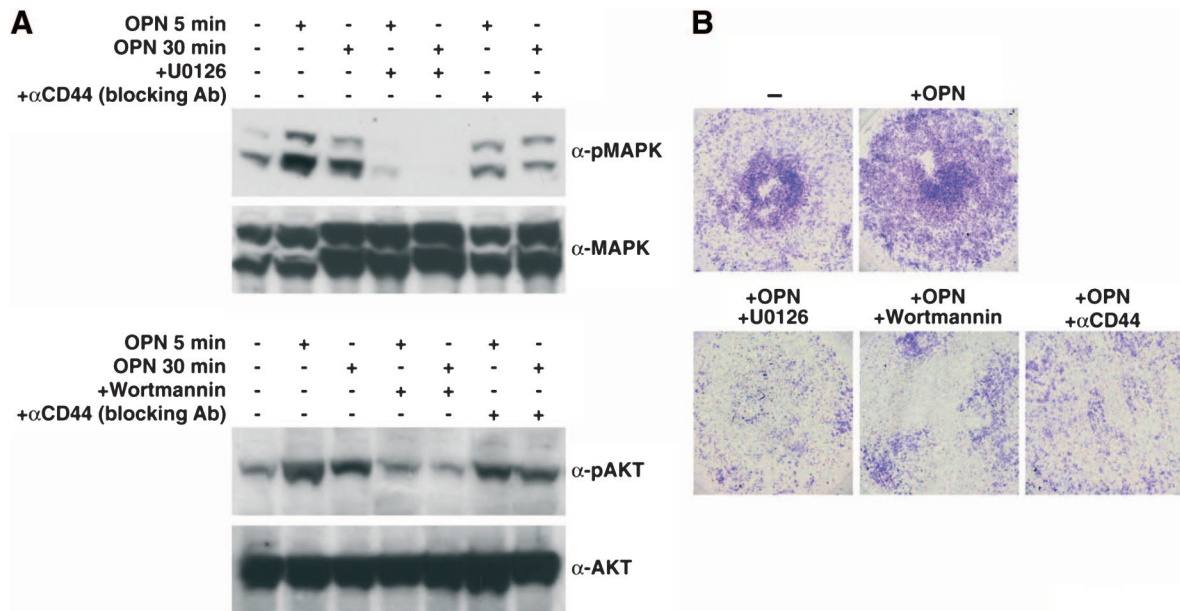


FIG. 6. CD44 is involved in OPN-mediated cellular effects. A, Where indicated, cells were preincubated (12 h) with U0126 (10 μ M), wortmannin (100 nM), or CD44-blocking antibody (KM81 hybridoma; α CD44). Total cell lysates were prepared 5 and 30 min after stimulation with the cytokine, as indicated. MAPK and AKT activation was assessed by immunoblot. B, Cells were preincubated (12 h) with CD44-blocking antibodies, U0126, or wortmannin. Matrigel invasion was analyzed as described in Fig. 5. When required, the lower chamber of Transwells contained the blocking antibody or the inhibitor. The percentage of migrating cells was quantified in triplicate samples with an ELISA reader.

PTC-FV were all included in the T1-T2 stages, where the positivity for OPN is less prevalent. The MAPK kinase and PI3-K pathways could be targets for thyroid cancer therapy (16, 55). Our experiments with CD44-blocking antibodies and MAPK kinase and PI3-K inhibitors provide proof of principle that the OPN-CD44v6 pathway may be a molecular target for therapeutic intervention in cases of aggressive PTC.

Acknowledgments

We are grateful to F. Curcio for the P5 primary thyroid culture, and to J. M. Hershman for the BHP cell lines. We are grateful to L. Vitiello and L. Racioppi for FACS analysis. We thank Jean Gilder for text editing.

Received February 7, 2005. Accepted June 28, 2005.

Address all correspondence and requests for reprints to: Dr. Massimo Santoro, Dipartimento di Biologia e Patologia Cellulare e Molecolare, Facoltà di Medicina e Chirurgia, Università di Napoli Federico II, via S. Pansini 5, 80131 Naples, Italy. E-mail: masantor@unina.it.

This work was supported by the Associazione Italiana per la Ricerca sul Cancro, the Progetto Strategico Oncologia of the Consiglio Nazionale delle Ricerche/Ministero dell'Istruzione dell'Università e della Ricerca, the Italian Ministero della Salute, the Centro Regionale di Competenza Genomic for Applied Research, and the Naples OncoGenomic Center). M.D.C. and V.G. were recipients of BioGem scar.l. fellowships.

References

- DeLellis RA, Williams ED 2004 Thyroid and parathyroid tumors. In: DeLellis LA, Lloyd RV, Heitz PU, Eng C, eds Tumours of endocrine organs: World Health Organization classification of tumors. Geneva: World Health Organization; 51–56
- Sherman SI 2003 Thyroid carcinoma. *Lancet* 361:501–511
- Santoro M, Carlomagno F, Melillo RM, Fusco A 2004 Dysfunction of the RET receptor in human cancer. *Cell Mol Life Sci* 61:2954–2964
- Alberti L, Carniti C, Miranda C, Roccatto E, Pierotti MA 2003 RET and NTRK1 proto-oncogenes in human diseases. *J Cell Physiol* 195:168–186
- Kimura ET, Nikiforova MN, Zhu Z, Knauf JA, Nikiforov YE, Fagin JA 2003 High prevalence of BRAF mutations in thyroid cancer: genetic evidence for constitutive activation of the RET/PTC-RAS-BRAF signaling pathway in papillary thyroid carcinoma. *Cancer Res* 63:1454–1457
- Soares P, Trovisco V, Rocha AS, Lima J, Castro P, Preto A, Maximo V, Botelho T, Seruca R, Sobrinho-Simoes M 2003 BRAF mutations and RET/PTC rearrangements are alternative events in the etiopathogenesis of PTC. *Oncogene* 22:4578–4580
- Cohen Y, Xing M, Mambo E, Guo Z, Wu G, Trink B, Beller U, Westra WH, Ladenson PW, Sidransky D 2003 BRAF mutation in papillary thyroid carcinoma. *J Natl Cancer Inst* 95:625–627
- Xu X, Quiros RM, Gattuso P, Ain KB, Prinz RA 2003 High prevalence of BRAF gene mutation in papillary thyroid carcinomas and thyroid tumor cell lines. *Cancer Res* 63:4561–4567
- Namba H, Nakashima M, Hayashi T, Hayashida N, Maeda S, Rogounovitch TI, Ohtsuru A, Saenko VA, Kanematsu T, Yamashita S 2003 Clinical implication of hot spot BRAF mutation, V599E, in papillary thyroid cancers. *J Clin Endocrinol Metab* 88:4393–4397
- Fukushima T, Suzuki S, Mashiko M, Ohtake T, Endo Y, Takebayashi Y, Sekikawa K, Hagiwara K, Takenoshita S 2003 BRAF mutations in papillary carcinomas of the thyroid. *Oncogene* 22:6455–6457
- Nikiforova MN, Kimura ET, Gandhi M, Biddinger PW, Knauf JA, Basolo F, Zhu Z, Giannini R, Salvatore G, Fusco A, Santoro M, Fagin JA, Nikiforov YE 2003 BRAF mutations in thyroid tumors are restricted to papillary carcinomas and anaplastic or poorly differentiated carcinomas arising from papillary carcinomas. *J Clin Endocrinol Metab* 88:5399–5404
- Xing M, Vasko V, Tallini G, Larin A, Wu G, Udelsman R, Ringel MD, Ladenson PW, Sidransky D 2004 BRAF T1796A transversion mutation in various thyroid neoplasms. *J Clin Endocrinol Metab* 89:1365–1368
- Ciampi R, Knauf JA, Kerler R, Gandhi M, Zhu Z, Nikiforova MN, Rabes HM, Fagin JA, Nikiforov YE 2005 Oncogenic AKAP9-BRAF fusion is a novel mechanism of MAPK pathway activation in thyroid cancer. *J Clin Invest* 115:94–101
- Garcia-Rostan G, Zhao H, Camp RL, Pollan M, Herrero A, Pardo J, Wu R, Carcangiu ML, Costa J, Tallini G 2003 ras mutations are associated with aggressive tumor phenotypes and poor prognosis in thyroid cancer. *J Clin Oncol* 21:3226–3235
- Zhu Z, Gandhi M, Nikiforova MN, Fischer AH, Nikiforov YE 2003 Molecular profile and clinical-pathologic features of the follicular variant of papillary thyroid carcinoma. An unusually high prevalence of ras mutations. *Am J Clin Pathol* 120:71–77
- Fagin JA 2004 How thyroid tumors start and why it matters: kinase mutants as targets for solid cancer pharmacotherapy. *J Endocrinol* 183:249–256
- Vasko V, Saji M, Hardy E, Krullak M, Larin A, Savchenko V, Miyakawa M, Isozaki O, Murakami H, Tsushima T, Burman KD, De Micco C, Ringel MD 2004 Akt activation and localisation correlate with tumour invasion and oncogene expression in thyroid cancer. *J Med Genet* 41:161–170
- Castellone MD, Celetti A, Guarino V, Cirafici AM, Basolo F, Giannini R, Medico E, Kruhoffer M, Orntoft TF, Curcio F, Fusco A, Melillo RM, Santoro M 2004 Autocrine stimulation by osteopontin plays a pivotal role in the

- expression of the mitogenic and invasive phenotype of RET/PTC-transformed thyroid cells. *Oncogene* 23:2188–2196
19. Ashkar S, Weber GF, Panoutsakopoulou V, Sanchirico ME, Jansson M, Zawaideh S, Rittling SR, Denhardt DT, Glimcher MJ, Cantor H 2000 Eta-1 (osteopontin): an early component of type-1 (cell-mediated) immunity. *Science* 287:860–864
 20. Chabas D, Baranzini SE, Mitchell D, Bernard CC, Rittling SR, Denhardt DT, Sobel RA, Lock C, Karpuz M, Pedotti R, Heller R, Oksenberg JR, Steinman L 2001 The influence of the proinflammatory cytokine, osteopontin, on auto-immune demyelinating disease. *Science* 294:1731–1735
 21. Weber GF 2001 The metastasis gene osteopontin: a candidate target for cancer therapy. *Biochim Biophys Acta* 1552:61–85
 22. Ponta H, Sherman L, Herrlich PA 2003 CD44: from adhesion molecules to signalling regulators. *Nat Rev Mol Cell Biol* 4:33–45
 23. Ermak G, Jennings T, Robinson L, Ross JS, Figge J 1996 Restricted patterns of CD44 variant exon expression in human papillary thyroid carcinoma. *Cancer Res* 56:1037–1042
 24. Ermak G, Gerasimov G, Troshina K, Jennings T, Robinson L, Ross JS, Figge J 1995 Deregulated alternative splicing of CD44 messenger RNA transcripts in neoplastic and nonneoplastic lesions of the human thyroid. *Cancer Res* 55:4594–4598
 25. Chhieng DC, Ross JS, McKenna BJ 1997 CD44 immunostaining of thyroid fine-needle aspirates differentiates thyroid papillary carcinoma from other lesions with nuclear grooves and inclusions. *Cancer* 81:157–162
 26. Bartolazzi A, Gasbarri A, Papotti M, Bussolati G, Lucante T, Khan A, Inohara H, Marandino F, Orlandi F, Nardi F, Vecchione A, Tecce R, Larsson O, Thyroid Cancer Study Group 2001 Application of an immunodiagnostic method for improving cooperative diagnosis of nodular thyroid lesions. *Lancet* 357:1644–1650
 27. Rittling SR, Chambers AF 2004 Role of osteopontin in tumour progression. *Br J Cancer* 90:1877–1881
 28. Hedinger C, Williams ED, Sobin LH 1989 The WHO histological classification of thyroid tumors: a commentary on the ed. 2. *Cancer* 63:908–911
 29. Rosai J, Carcangiu ML, DeLellis RA 1992 Atlas of tumor pathology: tumors of the thyroid gland, 3rd series. Washington DC: Armed Force Institute of Pathology; 1–343
 30. Curcio F, Ambesi-Impombato FS, Perrella G, Coon HG 1994 Long-term culture and functional characterization of follicular cells from adult normal human thyroids. *Proc Natl Acad Sci USA* 91:9004–9008
 31. Vitagliano D, Carlomagno F, Motti ML, Viglietto G, Nikiforov YE, Nikiforova MN, Hershman JM, Ryan AJ, Fusco A, Melillo RM, Santoro M 2004 Regulation of p27Kip1 protein levels contributes to mitogenic effects of the RET/PTC kinase in thyroid carcinoma cells. *Cancer Res* 64:3823–3829
 32. Miyake K, Medina KL, Hayashi S, Ono S, Hamaoka T, Kincade PW 1990 Monoclonal antibodies to Pgp-1/CD44 block lympho-hemopoiesis in long-term bone marrow cultures. *J Exp Med* 171:477–488
 33. Gao C, Guo H, Downey L, Marroquin C, Wei J, Kuo PC 2003 Osteopontin-dependent CD44v6 expression and cell adhesion in HepG2 cells. *Carcinogenesis* 24:1871–1878
 34. Medico E, Gentile A, Lo Celso C, Williams TA, Gambarotta G, Trusolino L, Comoglio PM 2001 Osteopontin is an autocrine mediator of hepatocyte growth factor-induced invasive growth. *Cancer Res* 61:5861–5868
 35. Gallego MI, Bierie B, Hennighausen L 2003 Targeted expression of HGF/SF in mouse mammary epithelium leads to metastatic adenocarcinomas through the activation of multiple signal transduction pathways. *Oncogene* 22:8498–8508
 36. Wu Y, Denhardt DT, Rittling SR 2000 Osteopontin is required for full expression of the transformed phenotype by the ras oncogene. *Br J Cancer* 83:156–163
 37. Chackalaparampil I, Peri A, Nemir M, Mckee MD, Lin PH, Mukherjee BB, Mukherjee AB 1996 Cells in vivo and in vitro from osteopetrotic mice homozygous for c-src disruption show suppression of synthesis of osteopontin, a multifunctional extracellular matrix protein. *Oncogene* 12:1457–1467
 38. Su L, Mukherjee AB, Mukherjee BB 1995 Expression of antisense osteopontin RNA inhibits tumor promoter-induced neoplastic transformation of mouse JB6 epidermal cells. *Oncogene* 10:2163–2169
 39. Denhardt DT, Mistretta D, Chambers AF, Krishna S, Porter JF, Raghuram S, Rittling SR 2003 Transcriptional regulation of osteopontin and the metastatic phenotype: evidence for a Ras-activated enhancer in the human OPN promoter. *Clin Exp Metastasis* 20:77–84
 40. Geissinger E, Weisser C, Fischer P, Scharl M, Wellbrock C 2002 Autocrine stimulation by osteopontin contributes to antiapoptotic signalling of melanocytes in dermal collagen. *Cancer Res* 62:4820–4828
 41. Matter N, Herrlich P, Konig H 2002 Signal-dependent regulation of splicing via phosphorylation of Sam68. *Nature* 420:691–695
 42. Bourguignon LY, Gilad E, Rothman K, Peyollier K 2005 Hyaluronan-CD44 interaction with IQGAP1 promotes Cdc42 and ERK signaling leading to actin binding, Elk-1/estrogen receptor transcriptional activation and ovarian cancer progression. *J Biol Chem* 280:11961–11972
 43. Teramoto H, Castellone MD, Malek RL, Letwin N, Frank B, Gutkind JS, Lee NH 2005 Autocrine activation of an osteopontin-CD44-Rac pathway enhances invasion and transformation by H-RasV12. *Oncogene* 24:489–501
 44. Bourguignon LY, Singleton PA, Zhu H, Diedrich F 2003 Hyaluronan-mediated CD44 interaction with RhoGEF and Rho kinase promotes Grb2-associated binder-1 phosphorylation and phosphatidylinositol 3-kinase signaling leading to cytokine (macrophage-colony stimulating factor) production and breast tumor progression. *J Biol Chem* 278:29420–29434
 45. Murphy JF, Lennon F, Steele C, Kelleher D, Fitzgerald D, Long A 2005 Engagement of CD44 modulates cyclooxygenase induction, VEGF generation, and cell proliferation in human vascular endothelial cells. *FASEB J* 19:446–448
 46. Zhang Y, Thant AA, Machida K, Ichigotani Y, Naito Y, Hiraiwa Y, Senga T, Sahara Y, Matsuda S, Hamaguchi M 2002 Hyaluronan-CD44s signaling regulates matrix metalloproteinase-2 secretion in a human lung carcinoma cell line QG90. *Cancer Res* 62:3962–3965
 47. Oriani-Rousseau V, Chen L, Sleeman JP, Herrlich P, Ponta H 2002 CD44 is required for two consecutive steps in HGF/c-Met signaling. *Genes Dev* 16:3074–3086
 48. Ghatak S, Misra S, Toole BP 2005 Hyaluronan constitutively regulates ErbB2 phosphorylation and signaling complex formation in carcinoma cells. *J Biol Chem* 280:8875–8883
 49. Di Renzo MF, Olivero M, Ferro S, Prat M, Bongarzone I, Pilotti S, Belfiore A, Costantino A, Vigneri R, Pierotti MA, Comoglio P 1992 Overexpression of the c-MET/HGF receptor gene in human thyroid carcinomas. *Oncogene* 7:2549–2553
 50. Kato S, Kobayashi T, Yamada K, Nishii K, Sawada H, Ishiguro H, Itoh M, Funahashi H, Nagasaka A 2004 Expression of erbB receptors mRNA in thyroid tissues. *Biochim Biophys Acta* 1673:194–200
 51. Vitale M, Bassi V, Illario M, Fenzi G, Casamassima A, Rossi G 1994 Loss of polarity and de novo expression of the β_1 family of integrins in thyroid tumors. *Int J Cancer* 59:185–190
 52. Illario M, Cavallo AL, Monaco S, Di Vito E, Mueller F, Marzano LA, Troncione G, Fenzi G, Rossi G, Vitale M 2005 Fibronectin-induced proliferation in thyroid cells is mediated by $\alpha_5\beta_3$ integrin through Ras/Raf-1/MEK/ERK and calcium/CaMKII signals. *J Clin Endocrinol Metab* 90:2865–2873
 53. Schorge JO, Drake RD, Lee H, Skates SJ, Rajanbabu R, Miller DS, Kim JH, Cramer DW, Berkowitz RS, Mok SC 2004 Osteopontin as an adjunct to CA125 in detecting recurrent ovarian cancer. *Clin Cancer Res* 10:3474–3478
 54. Schneider S, Yochim J, Brabender J, Uchida K, Danenberg KD, Metzger R, Schneider PM, Salonga D, Holscher AH, Danenberg PV 2004 Osteopontin but not osteonectin messenger RNA expression is a prognostic marker in curatively resected non-small cell lung cancer. *Clin Cancer Res* 10:1588–1596
 55. Kada F, Saji M, Ringel MD 2004 Akt: a potential target for thyroid cancer therapy. *Curr Drug Targets Immune Endocr Metab Disord* 4:181–185

JCEM is published monthly by The Endocrine Society (<http://www.endo-society.org>), the foremost professional society serving the endocrine community.

ORIGINAL PAPER

RAI(ShcC/N-Shc)-dependent recruitment of GAB1 to RET oncoproteins potentiates PI3-K signalling in thyroid tumorsValentina De Falco^{1,3}, Valentina Guarino^{1,3}, Luca Malorni¹, Anna Maria Cirafici¹, Flavia Troglio², Marco Erreni², Giuliana Pelicci², Massimo Santoro¹ and Rosa Marina Melillo^{*1}¹Istituto di Endocrinologia ed Oncologia Sperimentale del CNR 'G. Salvatore', clo Dipartimento di Biologia e Patologia Cellulare e Molecolare, Via S. Pansini 5, 80131 Naples, Italy; ²Department of Experimental Oncology, European Institute of Oncology, Milan, Italy

RAI, also named ShcC/N-Shc, one of the members of the Shc proteins family, is a substrate of the RET receptor tyrosine kinase. Here, we show that RAI forms a protein complex with both RET/MEN2A and RET/PTC oncoproteins. By coimmunoprecipitation, we found that RAI associates with the Grb2-associated binder1 (GAB1) adapter. This association is constitutive, but, in the presence of RET oncoproteins, both RAI and GAB1 are tyrosine-phosphorylated, and the stoichiometry of this interaction remarkably increases. Consequently, the p85 regulatory subunit of phosphatidylinositol-3 kinase (PI-3K) is recruited to the complex, and its downstream effector Akt is activated. We show that human thyroid cancer cell lines derived from papillary or medullary thyroid carcinoma (PTC or MTC) carrying, respectively, RET/PTC and RET/MEN2A oncoproteins express RAI proteins. We also show that human PTC samples express higher levels of RAI, when compared to normal thyroid tissue. In thyroid cells expressing RET/PTC1, ectopic expression of RAI protects cells from apoptosis; on the other hand, the silencing of endogenous RAI by small inhibitory duplex RNAs in a PTC cell line that expresses endogenous RET/PTC1, increases the rate of spontaneous apoptosis. These data suggest that RAI is a critical substrate for RET oncoproteins in thyroid carcinomas.

Oncogene advance online publication, 6 June 2005;
doi:10.1038/sj.onc.1208776

Keywords: thyroid tumor; RET oncogenes; RAI and GAB1 adaptors

Introduction

The family of Shc-like proteins includes three members: Shc, SLI (ShcB/ScK) and RAI (ShcC/N-Shc) (Cattaneo and Pelicci, 1998; Luzi *et al.*, 2000). It has been shown that while Shc is ubiquitously expressed, the other two members, RAI and SLI, are predominantly expressed in

neural tissues (O'Bryan *et al.*, 1996; Pelicci *et al.*, 1996; Nakamura *et al.*, 1998). In support of their role in the developing brain, it has been shown that null mutations of both RAI and SLI in mice results in a loss of sympathetic neurons. In particular, neurons of the superior cervical ganglia (SCG) are significantly reduced in number in the double-knockout mice, a phenotype that resembles that induced by the knockout of RET tyrosine kinase receptor (Sakai *et al.*, 2000). Accordingly, we showed that RAI is a physiological substrate of the RET receptor, and that it potentiates RET-mediated activation of phosphatidylinositol 3-kinase (PI3-K) and RET-dependent survival of neuronal cells. We also defined the molecular determinants of this interaction, which is mediated by tyrosine 1062 of RET and the phosphotyrosine binding (PTB) domain of RAI (Pelicci *et al.*, 2002).

The *RAI* gene codes for two proteins, p64 RAI and p52 RAI, as a consequence of alternative initiation codon usage. These proteins, like the other members of the Shc-like family, share a similar PTB-CH1-SH2 domains modular structure (Luzi *et al.*, 2000; Ravichandran, 2001). The PTB and SH2 domains are phospho-tyrosine-recognition modules common to several different proteins with similar functions. The CH1 region contains tyrosine-phosphorylation residues and several SH3 binding sites. For these features, RAI proteins have been implicated in signal transduction mediated by tyrosine kinase receptors (Nakamura *et al.*, 1996; O'Bryan *et al.*, 1998; Pelicci *et al.*, 2002; Liu and Meakin, 2002; Nakazawa *et al.*, 2002). While RAI and Shc share many common properties, specific features of RAI-mediated signalling have been identified. First, RAI transduces Grb2-SOS-RAS-dependent ERK activation less efficiently than Shc, because it binds less efficiently Grb2. Furthermore, RAI has three novel tyrosine phosphorylation sites that are not present in Shc. These sites represent potential docking sites for signalling adapters, one of which has been identified as the CRK protein. These data implicate that recruitment of RAI may result in specific signalling output and consequent biological activities (Nakamura *et al.*, 2002).

The receptor tyrosine kinase RET is specifically activated by members of the GDNF family of ligands, which are involved in the control of neuronal survival

*Correspondence: RM Melillo; E-mail: rosmelil@unina.it

³These authors contributed equally to this study

Received 21 December 2004; revised 12 April 2005; accepted 15 April 2005

and differentiation, kidney development, and spermatogonial cell fate. These ligands bind RET through GPI-anchored coreceptors (Santoro *et al.*, 2004). *RET* genetic alterations are responsible for the occurrence of two thyroid malignancies, the medullary (MTC) and the papillary thyroid carcinomas (PTC). These tumors arise, respectively, from the parafollicular C-cells and from the epithelial follicular cells of the thyroid gland. Germline point mutations in RET cause MTC in the context of three related dominantly inherited tumor syndromes, multiple endocrine neoplasia type 2A (MEN2A), multiple endocrine neoplasia type 2B (MEN2B) and familial medullary thyroid carcinoma (FMTC). RET point mutations are also found in a fraction of sporadic MTCs (Santoro *et al.*, 2004). PTC is the most common endocrine malignancy. In a remarkable fraction of these tumors, chromosomal aberrations involving chromosome 10 are present. Following these aberrations, the intracellular kinase domain of RET is rearranged with heterologous genes, generating the so-called RET/PTC oncogenes (Pierotti, 2001; Nikiforov, 2002). RET/PTC1 and RET/PTC3 are the most frequent isolates. Both MTC- and PTC-associated RET genetic alterations have a gain-of-function effect, resulting in constitutive kinase activation and oncogenic conversion. Activation of RET either by ligand triggering or by oncogenic conversion initiates most of the signalling pathways activated by tyrosine kinases, such as the RAS/RAF/ERK and the PI3-K/Akt pathways (Santoro *et al.*, 2004). Several groups have shown the central role of tyrosine 1062 of RET in signal transduction. This residue is the binding site for several different signalling adaptors, such as Shc, RAI, IRS1/2, FRS2, Dok and Enigma (Hayashi *et al.*, 2000). Activation of PI3-K has been shown to depend on Y1062 of RET through the formation of a Shc/Grb2/GAB1 complex and consequent recruitment and activation of the p85 subunit of the PI3-K (Besset *et al.*, 2000; Segouffin-Cariou and Billaud, 2000). Furthermore, it has been shown that GAB1 is necessary not only for Akt activation but also Rac1 activation and lamellipodia formation (Maeda *et al.*, 2004). In this study, we examined involvement of RAI in human PTC and MTC cell lines derived from these tumor histotypes, by evaluating expression and tyrosine-phosphorylation of this protein. Furthermore, we have studied how RAI couples the PI3-K/Akt pathway to oncogenic RET. We characterized molecular complexes containing RET, RAI and the GAB1 adapter and showed that these complexes lead to the activation of the PI3-K/Akt pathway and cell survival.

Results

An RAI/GAB1 complex links Ret to the p85 subunit of PI3-K and Akt activation

We had previously shown that RAI is able to complex with p85, the regulatory subunit of the PI3-kinase, *in vivo*, both in the presence and in the absence of RET

(Pelicci *et al.*, 2002). However, the molecular mechanism for p85 recruitment by RAI remains unclear. We had also observed that RAI coprecipitated other phosphoproteins of unknown identity. Among the different phosphoproteins, a band of 115kDa, a molecular weight compatible with the adapter protein GAB1, was detected (not shown). GAB1 is a likely candidate for p85 recruitment since it has several tyrosine residues that function as docking sites for p85 (Gu and Neel, 2003). To study whether RAI-recruitment of p85 was indeed mediated by GAB1, we first investigated whether RAI, GAB1 and p85 were able to form stable complexes *in vivo*. To this aim, we used 293 cells transiently transfected with different combinations of cDNAs encoding RAI, GAB1 and oncogenic RET/MEN2A. In a first set of experiments, we showed a complex between RAI and GAB1 by reciprocal coimmunoprecipitation and Western blotting (Figure 1a). This interaction was constitutive, since it occurred also in the absence of RET, but it is strongly potentiated in the presence of RET/MEN2A. Furthermore, RAI and GAB1 are tyrosine-phosphorylated only in the presence of RET/MEN2A (Figure 1a). To show that also RET/PTC was able to recruit RAI-GAB1 complex, 293 cells were transiently transfected with RAI, GAB1 and RET/PTC1. Also, in this case, reciprocal coimmunoprecipitation of RAI and GAB1 showed the presence of a RAI-GAB1 complex, which was enhanced by RET/PTC1 (Figure 1b). Phosphotyrosine staining of anti-GAB1 immunoprecipitates showed that GAB1 was tyrosine-phosphorylated only when RET/PTC1 was coexpressed (data not shown). Since it has been described that Shc recruits GAB through Grb2 (Besset *et al.*, 2000; Segouffin-Cariou and Billaud, 2000), we asked whether this was also the case for RAI. To this aim, we evaluated the GAB1 ability to bind a mutant of RAI, RAI 3F, in which the consensus sequences for Grb2 (Y304) and Crk binding (Y221, Y222) have been converted to phenylalanine. As shown in Figure 1c, RAI 3F retains the ability to bind GAB1 despite the lack of tyrosine phosphorylation *in vivo* (not shown). It has been shown that the CH1 domain of RAI has additional tyrosines (Y259, Y260 and Y286) that are sites of phosphorylation *in vivo*. In particular, Y286 is a binding site for CRK (Nakamura *et al.*, 2002). To investigate whether these tyrosines were involved in RAI/GAB1 interaction, we generated the mutant RAI 6F, derived from RAI 3F, in which we introduced the Y259F, Y260F and Y286F mutations. Also, this mutant retains its ability to bind GAB1, as shown by the coimmunoprecipitation experiment in Figure 1c. Furthermore, these mutants retained their ability to bind GAB1 also in the absence of RET (data not shown). We were unable to detect any Grb2-RAI association *in vivo* by reciprocal immunoprecipitation, while we could detect both Grb2-Shc and Grb2-GAB1 interactions (not shown).

One of the consequences of p85 recruitment could be the activation of the PI3-K, which leads to the activation of the serine-threonine kinase Akt (Pelicci *et al.*, 2002). To evaluate whether Akt was activated, 293 cells were cotransfected with RET/PTC1 or RET/MEN2A with

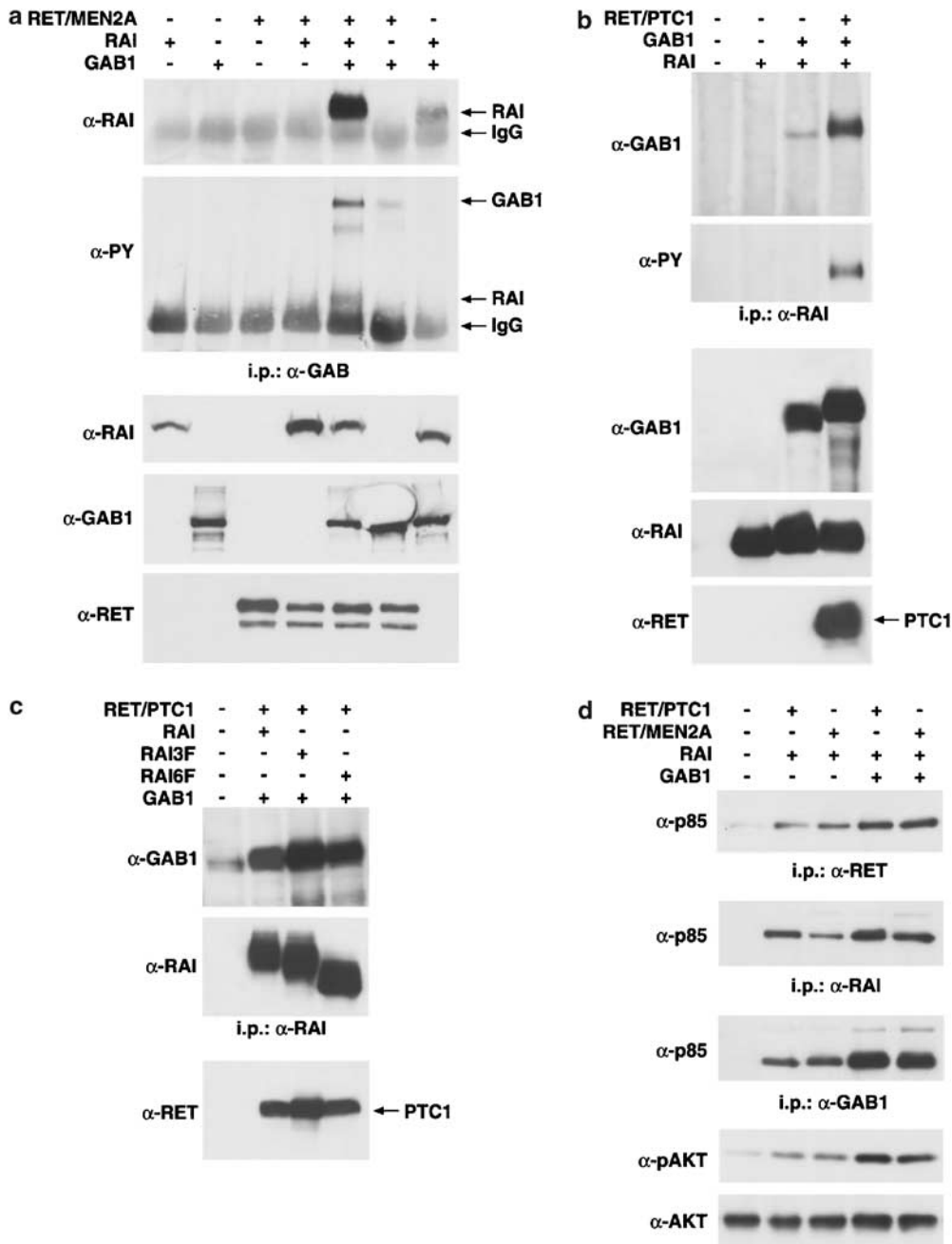


Figure 1 RET oncoproteins induce RAI/GAB1 interaction and tyrosine phosphorylation. (a) 293 cells were cotransfected with cDNAs encoding different combinations of RAI, GAB1 and RET/MEN2A, as indicated. Cell lysates were immunoprecipitated with anti-GAB1 antibodies, and immunoblotted with antiphosphotyrosine (PY) and anti-RAI antibodies. Total cell lysates of the corresponding transfections were immunoblotted with anti-RAI, anti-GAB1 and anti-RET antibodies. (b) 293 cells were cotransfected with cDNAs encoding different combinations of RAI, GAB1 and RET/PTC1, as indicated. Cell lysates were immunoprecipitated with anti-RAI antibodies, and immunoblotted with anti-PY and anti-GAB1 antibodies. Total cell lysates of the corresponding transfections were immunoblotted with anti-RAI, anti-GAB1 and anti-RET antibodies. (c) RAI/GAB1 interaction does not depend on RAI-CH1 tyrosine phosphorylation. RAI mutants in residues Y221, Y222, Y304 (RAI 3F), and in residues Y221, Y222, Y259, Y260, Y286, Y304 (RAI 6F) were coexpressed with GAB1 and, where indicated, RET/MEN2A. Lysates were immunoprecipitated with anti-RAI antibodies and immunoblotted with anti-PY and anti-GAB1 antibodies. (d) RET oncoproteins recruitment of p85 and Akt activation are enhanced by RAI and GAB1. The cell lysates from the indicated transfections were immunoprecipitated with anti-RET, anti-RAI and anti-GAB1 antibodies and probed with anti-p85 antibodies. Total protein lysates were probed with anti-phospho Akt antibodies. Anti-Akt antibodies were used as a control for equal protein loading

RAI in the absence or in the presence of GAB1. The amounts of p85 recruited in the complex were then evaluated by immunoprecipitation with anti-RET, anti-

RAI and anti-GAB1 antibodies. Furthermore, the levels of endogenous Akt activation were evaluated by Western blotting with anti-phosphoAkt antibodies.

As shown in Figure 1d, the coexpression of RET oncoproteins with RAI induced Akt activation, which was further potentiated when GAB1 was present. GAB1 overexpression also potentiated p85 recruitment (Figure 1d).

Molecular determinants of RAI-GAB1 interaction

To investigate the molecular mechanisms underlying the interaction of RAI with GAB1, we performed *in vitro* binding assays. To this aim, the PTB, CH1 and SH2 domains of RAI were expressed as recombinant GST-fusion proteins in bacteria. Purified proteins were used for pull-down assays in which each GST-protein was incubated with lysates from 293 cells transiently transfected with GAB1 both in the absence and in the presence of activated RET (RET/MEN2A). As shown in Figure 2a, two regions of RAI are involved in GAB1 binding: the CH1 region, which binds GAB1 irrespective of the presence of RET/MEN2A, and the SH2 domain, which binds GAB1 only when it is phosphorylated by RET/MEN2A. These data suggest that the constitutive interaction between RAI and GAB1 observed in the *in vivo* coimmunoprecipitation experiments (Figure 1a) is mediated by the CH1 domain of RAI, and that this interaction can be further stabilized by tyrosine phosphorylation of GAB1 through the engagement of another domain of RAI, the SH2. GAB1 lacks a classical PTB domain, but it contains a noncanonical PTB domain, the so-called MBD or c-Met binding domain, which mediates the interaction with the c-Met receptor. To investigate whether this region of GAB1 is involved in the interaction with RAI, we performed pull-down assays using GST-recombinant proteins fused to either wild-type GAB1 or its MBD domain (GST-GAB1 and GST-MBD). Purified proteins were incubated with cell lysates from 293 cells transfected with RAI both in the absence and in the presence of activated RET (RET/MEN2A). As shown in Figure 2b, GST-GAB1 was able to recruit RAI, both in the presence and in the absence of RET. This interaction was potentiated when RAI was tyrosine phosphorylated by RET/MEN2A. GST-MBD, on the other hand, was able to bind RAI only when RET/MEN2A was coexpressed. By using anti-RET or antiphosphotyrosine antibodies, RET/MEN2A was always detected in complex with RAI (data not shown). To verify equal loading, the coomassie staining of GST-fusion proteins used for pull-down experiments is shown (Figure 2a and b).

To assess whether the constitutive interaction between RAI and GAB1 is direct or mediated by other protein adapters, we performed a Far Western overlay assay using recombinant GST-GAB1 fusion protein. 293 cells were transfected with RAI, and RAI immunoprecipitates and total lysates were probed with unphosphorylated GST-GAB1. Consistent with previous data, GST-GAB1 recognized RAI in RAI immunoprecipitates and in total lysates (Figure 2c). These data show that RAI and GAB1 are constitutively complexed in the cell and that the constitutive RAI/GAB1 interaction is mediated by the CH1 domain of RAI.

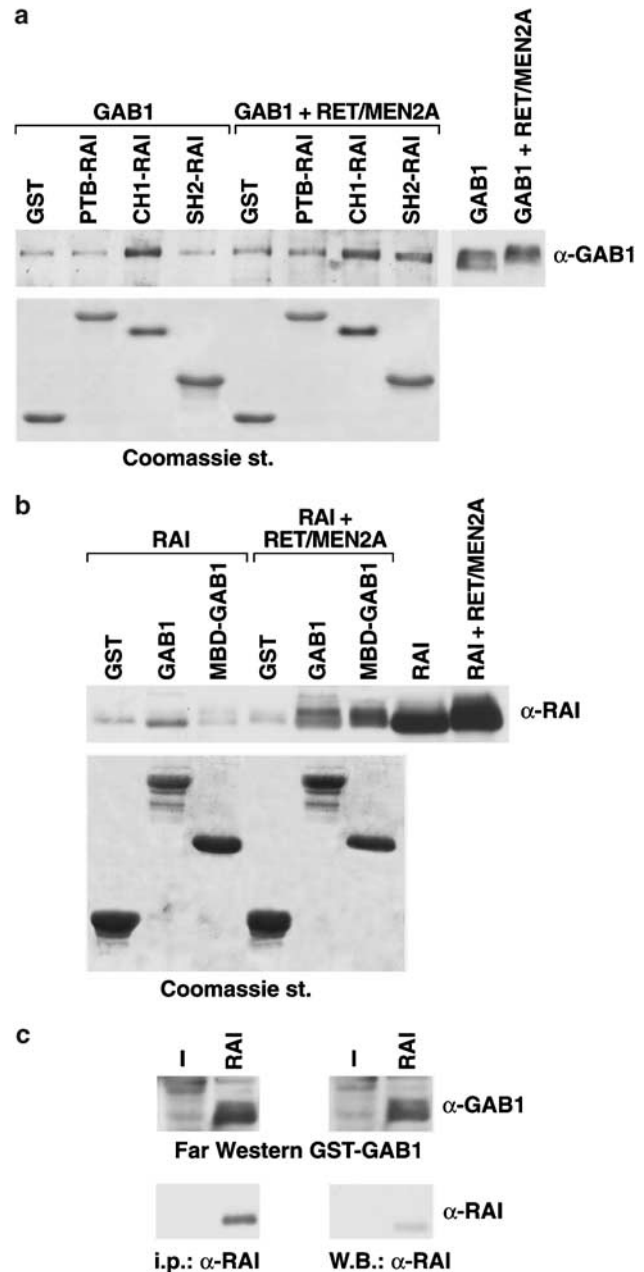


Figure 2 Molecular determinants of RAI/GAB1 interaction. **(a)** RAI/GAB1 interaction is mediated by the CH1 and SH2 domains of RAI. *In vitro* binding experiments with immobilized GST, GST-PTB-RAI, GST-RAI-CH1 and GST-RAI-SH2 (respectively, GST, PTB-RAI, CH1-RAI and SH2-RAI) and protein lysates from 293 cells transfected with GAB1 in the presence or absence of RET/MEN2A. Bound proteins were revealed by probing the filter with anti-GAB1 antibodies. GST-fusion protein were visualized by Coomassie staining of the filters. **(b)** The MBD domain of GAB1 is sufficient to bind RAI in the presence of RET/MEN2A. 293 cells transfected with RAI or RAI and RET/MEN2A plasmids were lysed and incubated with GST, GST-GAB1 or GST-MBD-GAB1 (respectively, GST, GAB1 and MBD-GAB1). Bound proteins were revealed by probing the filter with anti-RAI antibodies. Equal loading of GST-fusion protein was assessed by Coomassie staining of the filters. **(c)** RAI and GAB1 binding is direct. 293 cells were transfected with the indicated cDNAs. Anti-RAI immunoprecipitated lysates or total protein lysates were analysed by Far Western blotting with the GST-GAB1 fusion protein. Filters were re-probed with anti-RAI and anti-PY antibodies

Ectopic RAI expression induces survival of RET/PTC1 expressing thyroid cells

To study the role of RAI in thyroid cells, we selected the PC RET/PTC1 rat thyroid cells. This cell line derives from PC Cl 3 rat thyroid epithelial cells, which are a very well established model system to study oncogenic transformation in a thyroid cell setting. Furthermore, these cells express very low levels of endogenous RAI proteins. PC RET/PTC1 cells were transduced with a RAI retroviral vector to obtain the RET/PTC1-RAI cells. RAI and RET/PTC1 expression were verified by immunoblot. We show that also in this system RAI coprecipitated with RET and was constitutively tyrosine-phosphorylated (Figure 3a). As a consequence of RAI expression, Akt phosphorylation increased (not shown). We then sought to examine whether RAI induced survival of thyroid cells. Thyroid transformed cells were treated with a strong apoptotic stimulus, diethyl maleate (DEM) (Celetti *et al.*, 2004). In these conditions, we compared RET/PTC1 to RET/PTC1-

RAI cells and the apoptotic rate was evaluated by the terminal deoxynucleotidyl transferase-mediated desoxyuridine triphosphate nick end-labelling (TUNEL) assay, as described (Castellone *et al.*, 2003). As shown in Figure 3c, RAI overexpression significantly reduced DEM-mediated apoptosis.

We have shown that RAI can recruit the p85 subunit of the PI3-K through GAB1. To investigate whether RAI-GAB1 interaction is required to activate the PI3-K/Akt pathway, and consequently, to induce survival in thyroid cells, we used expression vectors encoding the isolated CH1 and SH2 domains of RAI, RAI CH1 and RAI SH2. We reasoned that the overexpression of these vectors should be able to displace the interaction between RAI and GAB1 by competition with RAI for GAB1 binding. To address this issue, PC RET/PTC1-RAI cells were transiently transfected with RAI CH1 or RAI SH2. As shown in Figure 3b, RAI CH1 and RAI SH2 were able to disrupt the interaction between wild-type RAI and GAB1. As a consequence of this, p85 recruitment by RET/PTC1, and the levels of Akt

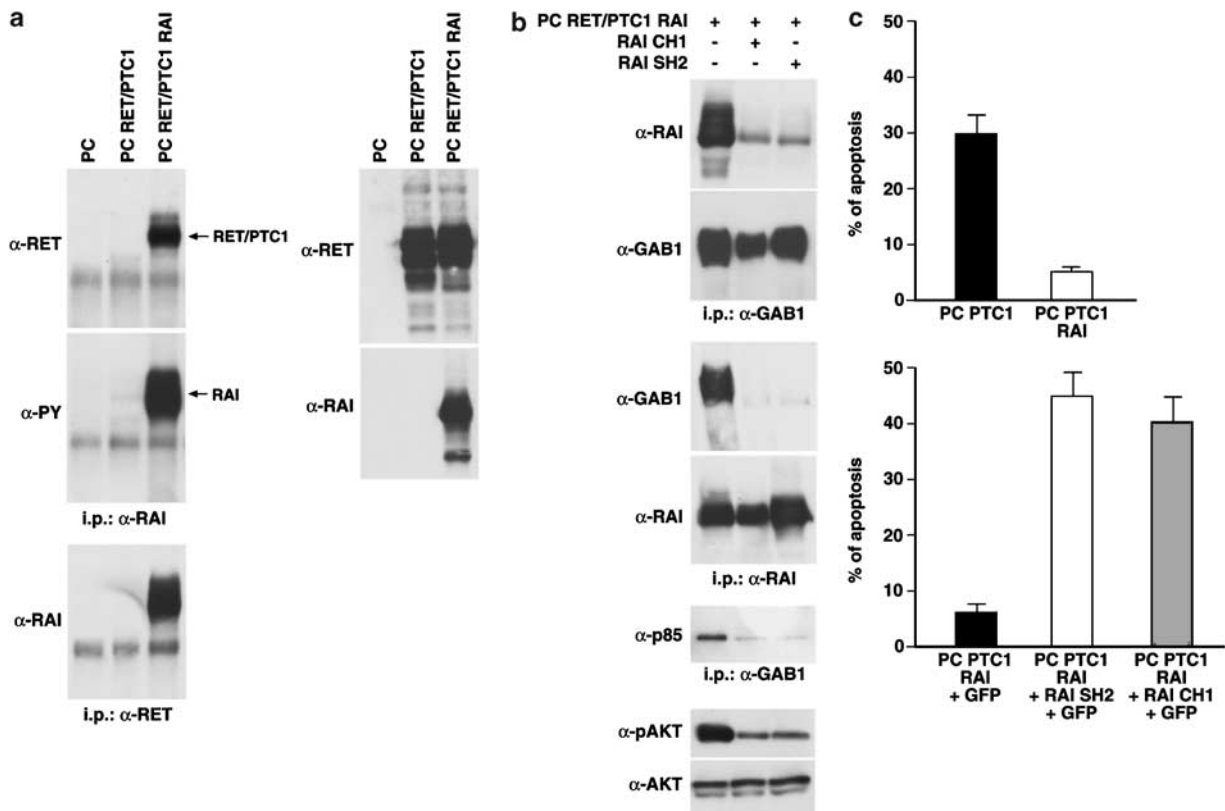


Figure 3 RAI exogenous expression promotes cell survival in PC RET/PTC1 cells. (a) PC RET/PTC1 cells were infected with a retroviral vector expressing RAI to generate the PC RET/PTC1 RAI cells. Cell lysates were immunoprecipitated with anti-RAI or anti-RET antibodies, and immunoblotted with anti-PY, anti-RAI, and anti-RET antibodies. Total cell lysates of the corresponding transfections were immunoblotted with anti-RAI and anti-RET antibodies. (b) PC RET/PTC1 RAI cells were transfected with cDNAs encoding either the isolated RAI-CH1 or RAI-SH2 domains. Cell lysates were immunoprecipitated with anti-RAI or with anti-GAB1 antibodies, and immunoblotted with the reciprocal antibodies: the interaction RAI-GAB1 strongly decreased. Furthermore, GAB1 recruitment of p85 and Akt phosphorylation decreases. Total cell lysates of the corresponding transfections were immunoblotted with anti-Akt antibodies. (c) The TUNEL reaction was performed on PC RET/PTC1 and PC RET/PTC1-RAI cells in complete serum in the presence of 0.9 mM DEM. When indicated, cells were transfected with either GFP alone or GFP and RAI-CH1 or GFP and RAI-SH2. GFP-positive cells were observed under an epifluorescent microscope to detect TUNEL-positive cells (TMR-dUTP, red) and total cells on the glass slide (Hoechst, blue stain). Bars are the mean \pm s.d. of three assays. Apoptotic cells were calculated by counting at least 400 GFP-positive cells in five randomly selected microscopic fields

activation decreased (Figure 3b). To verify whether the disruption of RAI-GAB1 interaction resulted in a decreased pro-survival effect in RET/PTC1-RAI expressing cells, we transiently transfected these cells with RAI CH1 or RAI SH2 together with a GFP expressing vector. Transfected cells were treated with DEM, and the rate of apoptotic death was evaluated in GFP-positive cells by TUNEL assay. As shown in Figure 3c, the expression of either RAI CH1 or RAI SH2 inhibited the survival effect exerted by RAI in PC RET/PTC1 cells.

RAI is expressed in human thyroid carcinoma cell lines and in primary PTC

To investigate whether RAI is involved in RET-mediated signalling in thyroid tumors in which RET is involved, we screened a series of human cell lines derived from either PTCs or MTCs for RET and RAI expression by Western blot. As a positive control, the MN1, a mouse motoneuron cell line expressing both RET and RAI, was used. As shown in Figure 4a, several PTC and one MTC cell line, coexpressed RAI and the RET oncogenic proteins. In these cells, both the p64 and

the p52 isoforms of RAI were detected. A summary of RET and RAI expression status in these cell lines is showed in the table in Figure 4a. Furthermore, by comparing RAI expression in the normal human primary culture (P5) with its expression in TPC cell lines, we verified that RAI is overexpressed in PTC cells. To extend this observation to human tumors we also tested, by Western blot and quantitative PCR, RAI expression in a set of primary tumors from PTC patients and a pool of normal thyroid samples. As shown in Figure 4b, some PTCs samples scored positive for RAI expression. Normal thyroid tissue displayed a lower, but detectable reactivity. To further confirm that RAI is indeed expressed in human thyroid tumors, we extracted total RNAs from a different set of human PTCs and from a pool of 4 normal thyroid tissues, and analysed them by Q-PCR. As shown in Figure 4c, RAI mRNA expression was strongly increased in tumors *versus* normal thyroids.

To determine whether RAI is involved in RET signalling in human tumors, we analysed, in FB2 and TT cells (derived, respectively, from a papillary and a MTC), anti-RET immunoprecipitates with anti-RAI antibodies, and showed binding of RAI to endogenous

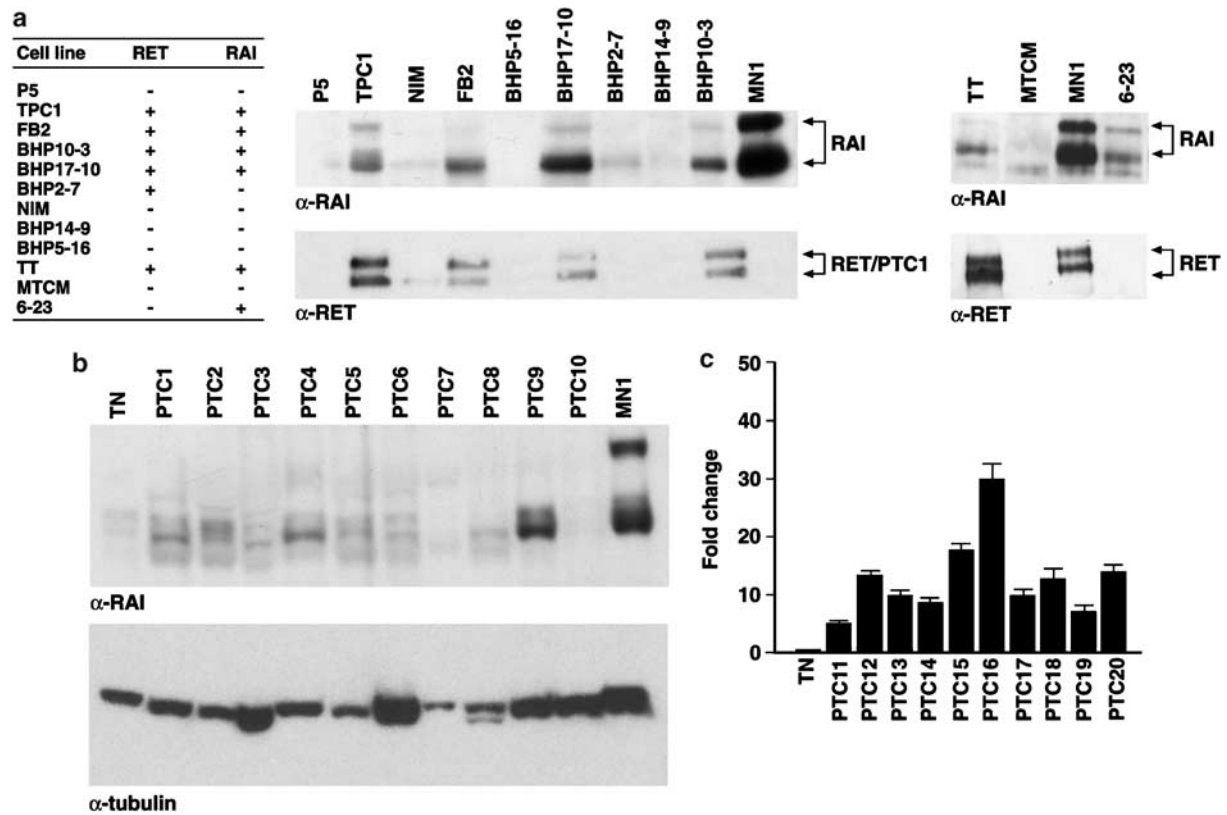


Figure 4 RAI expression in human thyroid cancer cell lines and human PTCs. (a) The expression levels of RAI proteins were analysed in human PTC and MTC cell lines and summarized in the table. Equal amounts of proteins were immunoblotted and stained with anti-RAI mouse monoclonal antibody. As a control for equal loading, filters were stained with the anti-alpha tubulin monoclonal antibody. (b) Human PTCs express high levels of RAI proteins. Tissues from human PTC samples were snap-frozen and immediately homogenized by using the Mixer Mill apparatus (Qiagen) in lysis buffer. Equal amounts of proteins were immunoblotted and stained with anti RAI polyclonal antibodies. As a control for equal loading, the anti-alpha tubulin monoclonal antibody was used. (c) Human PTCs express high levels of RAI mRNA. After RNA extraction, quantitative PCR was used to calculate RAI mRNA fold induction in the indicated tumor samples and in a pool of normal thyroid tissues; results are the average of three independent amplifications \pm s.d.

RET/PTC1 and RET/MEN2A (Figure 5a). Furthermore, by probing anti-RAI immunoprecipitates with anti-phosphotyrosine antibodies, we observed tyrosine phosphorylation of RAI. By using the anti-GAB1 antibodies we detected a 115 kDa protein in RAI immunoprecipitates (Figure 5b). Furthermore, when GAB1 was immunoprecipitated from FB2 and TT cells, anti-phosphotyrosine antibodies recognized a 52 kDa protein, which was identified by the anti-RAI antibody (Figure 5c). These data confirm that RAI and RET/PTC interact also when expressed at physiological levels and support the concept that RAI is indeed involved in RET/PTC signalling in human PTCs. To further support the critical role of Gab1 in p85 recruitment and Akt activation by RAI, we depleted FB2 cells of endogenous Gab1 through small interference RNA. As shown in Figure 5d, transient transfection of FB2 cell with human Gab1 small silencing RNA (siRNA) significantly reduced Gab1 levels at 48 h, without affecting RAI and p85 levels. Gab1 knockdown resulted in a reduction of the p85 quantity coprecipitated with RAI, as shown by coimmunoprecipitation experiments. Furthermore, Gab1 knockdown caused the consequent inactivation of Akt, as shown by the staining of the same filters with Akt phospho-specific antibodies (Figure 5d).

Inactivation of endogenous RAI expression reduces survival of human papillary thyroid cells expressing RET/PTC1

To evaluate the effect of RAI inhibition in human thyroid papillary cancer, we used RNA interference on FB2 cells to deplete endogenous RAI. As shown in Figure 6a, an siRNA duplex oligonucleotide was able to sharply reduce RAI expression, whereas a scrambled oligo did not. On the other hand, RAI siRNA did not inhibit α -tubulin levels. RAI depletion suppressed constitutive Akt activation in FB2 cells (Figure 6a) while it did not affect endogenous Akt levels (not shown). We performed a TUNEL assay on parental and RAI-depleted FB2 cells. As shown in Figure 6b, RAI depletion induced a significant increase in the number of apoptotic cells after 48 and 72 h. These data suggest that RAI provides a survival signal to this cell line.

Discussion

In this study, we have investigated the role played by RAI in oncogenic RET signalling. We focused on identifying the protein complexes involved in RET-mediated PI3-K/Akt activation through RAI. It has

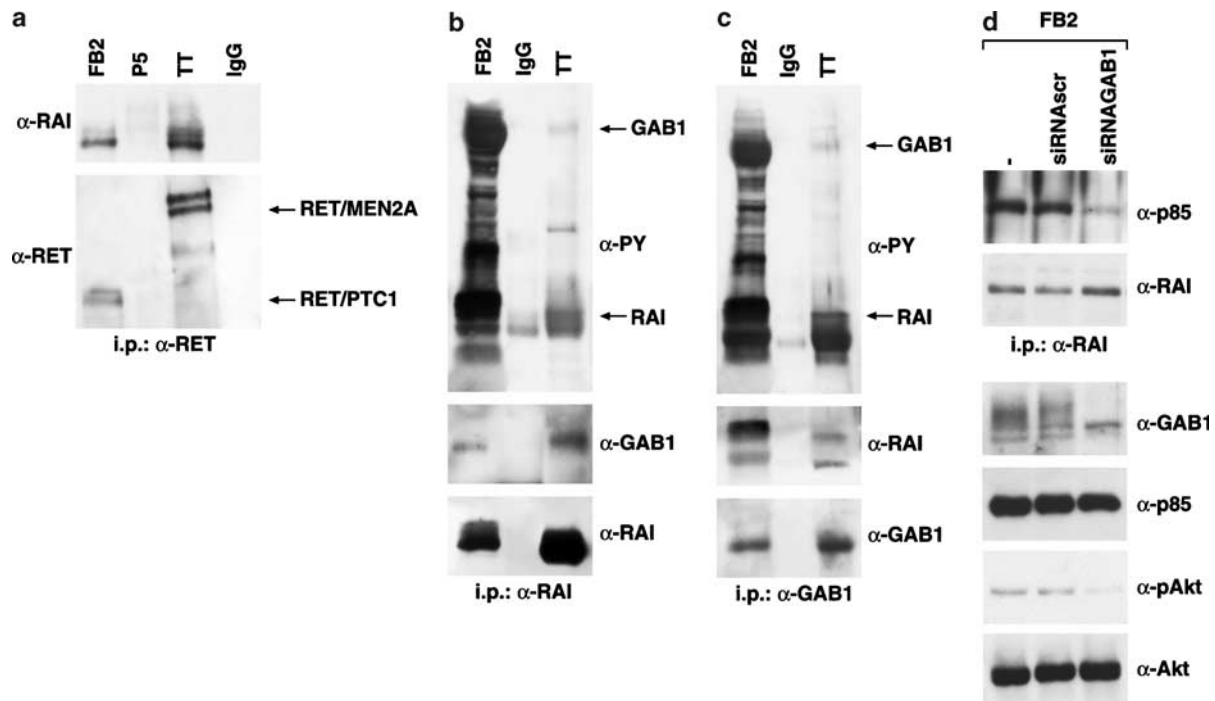


Figure 5 Molecular complexes containing RET, RAI and GAB1 in human thyroid cancer cell lines. (a) FB2 and TT cells, expressing endogenous RET and RAI, and P5 primary thyroid cells were serum-deprived for 12 h. Protein lysates were immunoprecipitated with anti-RET antibodies, followed by SDS-PAGE and immunoblotting with the anti-RAI and anti-RET antibodies. Arrows indicate the position of RAI and GAB1 proteins. (b) Anti-RAI immunoprecipitates from serum-deprived FB2 and TT cells were probed with anti-PY, anti-RAI and anti-GAB1 antibodies. (c) Anti-GAB1 immunoprecipitates from FB2 and TT cells were probed with anti-PY, anti-RAI and anti-GAB1 antibodies. (d) FB2 cells were transiently transfected with siRNA targeting Gab1. A scrambled oligo was used as control. Cells were harvested at 48 h, and endogenous Gab1 protein levels were evaluated by Western blot analysis. Anti-RAI immunoprecipitates from FB2 cells were probed with anti-p85 antibodies. Total protein lysates were probed with anti-phospho Akt antibodies. Anti-Akt and anti-p85 antibodies were used as a control for equal protein loading and to shown the specific effect of the siRNA

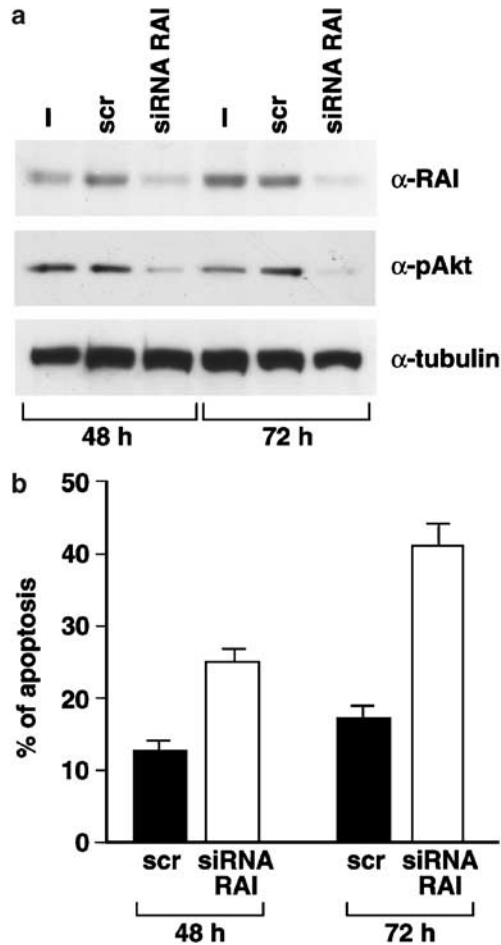


Figure 6 Effect of RNAi for RAI in FB2 Cells. (a) FB2 cells were transiently transfected with siRNA targeting RAI. A scrambled oligo was used as control. Decrease of endogenous RAI protein in FB2 cells at the indicated time points was detected by Western blot analysis. The knockdown of endogenous RAI resulted in the inhibition of Akt activation, as measured by Western blotting with anti-pAKT antibodies. Alpha-tubulin staining was used to show the specific effect of the siRNA. (b) Inhibition of endogenous RAI increases the percentage of apoptotic cells in FB2 cells. FB2 cells were transiently transfected with RAI siRNA or with a scrambled oligo, and fixed after 48 or 72 h. TUNEL positive cells were counted under an epifluorescent microscope. Bars are the mean \pm s.d. of three assays. Apoptotic cells were calculated by counting at least 400 cells in five randomly selected microscopic fields

been previously shown that RET can indirectly recruit p85 through an Shc-Grb2-GAB1/2 complex. When RET is activated, Shc binds to phosphorylated tyrosine 1062. Grb2 is then recruited by binding a phosphotyrosine in the CH1 of Shc with its SH2 domain. Grb2, in turn, constitutively interacts with GAB1/2 through its SH3 domain, which binds a non canonical polyproline motif in GAB1/2. GAB1/2, in turn, binds the SH2 domain of p85 through several phosphotyrosine residues (Besset *et al.*, 2000; Lock *et al.*, 2000; Schaeper *et al.*, 2000; Lewitzky *et al.*, 2001). We previously showed that RAI is able to complex with p85 *in vivo*, both in the presence and in the absence of RET (Pelicci *et al.*, 2002). Here, we identify GAB1 as a key mediator of RET/RAI

signalling. This protein belongs to a group of docking proteins which includes GAB1/2, IRS1/2, FRS2, and p62 Dok, that function as substrates of tyrosine kinases (Gu and Neel, 2003). GAB1, in particular, has been identified as a specific substrate of the c-Met receptor. This protein contains a NH₂-terminal PH domain, a central non canonical phosphotyrosine-binding domain, the MBD, and a carboxyl-terminal domain which contains several tyrosines that serve as docking sites for downstream signalling components, such as p85, PLC- γ , Shc, Shp2 and Crk (Gu and Neel, 2003). Here we show that RAI and GAB1 associate constitutively. This association seems to be mediated by the CH1 domain of RAI, as shown by pull-down assays performed with the GST-CH1 RAI recombinant protein. Given the high degree of conservation between RAI and Shc, we hypothesized that RAI could recruit GAB1 through the adapter Grb2. By coimmunoprecipitation assays and use of RAI mutants we showed that Grb2 was not involved in RAI-GAB1 interaction. Indeed we could demonstrate, by Far Western overlay experiments, that RAI is involved in a direct interaction with GAB1. It is conceivable that overexpression of RAI leads to a stoichiometric recruitment of GAB1, and to the consequent activation of GAB1-mediated signalling pathways, such as PI3-K/Akt. How the recruitment of GAB1 by RAI can trigger GAB1 and activate downstream pathways remains to be solved. One possibility is that RAI binding could localize GAB1 in the proximity of a putative activator. Alternatively, this interaction could exert a conformational change in GAB1, with its consequent activation.

The interaction between RAI and GAB1 is potentiated by the presence of activated RET. Indeed, activated RET recruits RAI/GAB1 through its tyrosine 1062 and the PTB domain of RAI (Pelicci *et al.*, 2002). RAI/GAB1 interaction is further stabilized by tyrosine phosphorylation of both RAI and GAB1, which creates other interaction sites. The RAI SH2 domain possibly recognizes a phosphotyrosine residue in GAB1, and the GAB1 MBD region could bind one of the phosphotyrosines in RAI. Alternatively, GAB1 MBD could bind a novel phosphotyrosine residue in RET. Whatever the case, once GAB1 is phosphorylated, an increased recruitment of p85 on activated RET is observed parallel to an enhanced activation of Akt, and potentiation of cell survival. The relevance of RAI interaction with GAB1 is supported by the experiments with the isolated RAI-CH1 and SH2 domains and by the knockdown of endogenous Gab1, which inhibit downstream signalling events and biological activity. Ectopic expression of RAI in RET/PTC1 expressing rat thyroid cells potentiates the ability of these cells to survive in stress conditions, while depletion of endogenous RAI in FB2 PTC cells increases the rate of spontaneous apoptosis. These data, taken together, suggest a role for this protein in human thyroid tumorigenesis. This is further supported by the observation that RAI and oncogenic isoforms of RET (RET/PTC1 or RET/MEN2A) are coexpressed in a series of cell lines derived from thyroid malignancies in which

RET is involved, PTCs and MTCs. It is interesting to note that RAI expression has been reported to be restricted to the nervous system in post-mitotic neurons (Ganju *et al.*, 1998; Nakamura *et al.*, 1998; Tanabe *et al.*, 1998; Conti *et al.*, 2001). Despite this, we found expression of RAI in human cell lines derived from human thyroid tumors. While expression of RAI in MTCs is not surprising, since these tumors derive from cells of neural origin, its expression in PTCs, derived from thyroid epithelial cells, is unexpected. It is possible that in these tumors RAI expression is reactivated and that this event is positively selected since it increases the survival of cancer cells. In support of this hypothesis, preliminary data obtained in our laboratory show that RAI expression is also detected in surgical samples of human PTCs by real-time PCR and Western blot. RET/PTC rearrangements are considered tumor initiating events (Viglietto *et al.*, 1995). The early events that follow RET/PTC activation do not lead to cell growth, possibly due to concomitant stimulation of DNA synthesis and apoptosis (Castellone *et al.*, 2003; Wang *et al.*, 2003). RAI overexpression could be an event that PTC cells select to overcome RET/PTC induced apoptosis, thus promoting cancer progression. This is not the only example of RAI involvement in human tumors. Expression and tyrosine phosphorylation of RAI has been found in a large set of neuroblastoma cell lines. In these cells the ALK kinase is overexpressed due to gene amplification, and as a consequence of this, constitutively activated. Activation of ALK was responsible for RAI hyperphosphorylation in these cells (Miyake *et al.*, 2002). Thus, the role of RAI in human tumors is just starting to be elucidated.

Materials and methods

Cell lines and plasmids

293 cells were maintained in Dulbecco's Modified Eagle's medium (DMEM, Invitrogen Groningen, The Netherlands) supplemented with 10% foetal calf serum. Transient transfections were effectuated with FUGENE reagent, as suggested by the manufacturer (Roche Molecular Diagnostics, Basel, Switzerland). P5 thyroid normal primary culture has been previously described (Curcio *et al.*, 1994).

Human papillary thyroid cancer cell lines TPC-1, FB2, NIM, BHP10-3, BHP17-10, BHP14-9, BC-PAP, BHP2-7, BHP5-16, have been described previously (Cerutti *et al.*, 1996; Ohta *et al.*, 2001; Basolo *et al.*, 2002), and were maintained in DMEM supplemented with 10% foetal bovine serum, 1% penicillin-streptomycin, and 1% glutamine. Medullary thyroid cancer cell lines TT, MZ-CRC-1 (human), 6-23 (rat), MTC-M (mouse) have also been previously described (Cooley *et al.*, 1995).

PC Cl 3 is a differentiated thyroid epithelial cell line derived from 18-month-old Fischer rats. They were maintained in Coon's modified F12 medium supplemented with 5% calf serum and six hormones (6H) (thyrotropin, i.e., TSH, insulin, transferrin, somatostatin, hydrocortisone and glycyl-histidyllysine) (Invitrogen, Groningen, The Netherlands) as described (Castellone *et al.*, 2003). PC RET/PTC1 cells have been previously described (Santoro *et al.*, 1993). To obtain the PC

RET/PTC1-RAI cells, the PC RET/PTC1 cells were infected with a PINCO-RAI virus, as described (Pelicci *et al.*, 2002). The efficiency of infection, measured as GFP positivity, was evaluated by FACS scanning.

For transient transfections of PC Cl 3 cells, calcium phosphate precipitates were added to the cells and removed after 1 h. Cells were then subjected to glycerol shock and kept in medium containing 5% calf serum and 6H.

Human RET/MEN2A and RET/PTC1 (subcloned into pCDNA 3, Invitrogen) have been previously described (Carlomagno *et al.*, 2001). RAI and RAI 3F, in which tyrosines 221, 222, 304 were replaced by phenylalanine, expression vectors have been previously described (Pelicci *et al.*, 2002). To generate RAI 6F, point mutations in Y259, 260 and 286 were introduced into RAI 3F plasmid by using the Quick-change site-directed mutagenesis kit (Stratagene), and verified by sequencing. Plasmids encoding the isolated PTB, CH1 and SH2 domains were obtained by PCR and subcloning into pCDNA 3 vector (Invitrogen). The plasmid encoding GAB1 was a kind gift of S Giordano and P Gual (Institute for Cancer Research and Treatment, University of Torino School of Medicine, Candiolo, Italy).

RNA extraction and real-time PCR

Retrospectively collected archival frozen thyroid tissue samples from patients affected by PTC and normal thyroid tissue samples were retrieved from the files of the Pathology Department of the University of Pisa upon informed consent. Total RNA from the indicated samples was prepared using the RNeasy Midi Kit (Qiagen, Crawley, West Sussex, UK) and subjected to on-column Dnase digestion with the Rnase-free Dnase set (Qiagen, Crawley, West Sussex, UK) following the manufacturer's instructions. The quality of RNA from each sample was verified by electrophoresis through 1% agarose gel and visualization with ethidium bromide.

Random-primed first-strand cDNA was synthesized in a 50 μ l reaction volume starting from 2.5 μ g RNA by using the GeneAmp RNA PCR Core Kit (Applied Biosystems, Warrington, UK). PCR amplification was performed using the GeneAmp RNA PCR Core Kit system starting from 2 μ l of RT product in a reaction volume of 25 μ l, according to the manufacturer's instructions. Primers were designed by using a software available at http://www-genome.wi.mit.edu/cgi-bin/primer/primer3_www.cgi, and synthesized by the MWG Biotech (Ebersberg, Germany). Primer sequences were as follows:

RAI F:	5'-AGTTCTGCGCTCAATGAGGT-3'
RAI R:	5'-TTGCTCTTTCCCAAGATGCT-3'
β -actin F:	5'-TGCGTGACATTAAGAAG-3'
β -actin R:	5'-GCTCGTAGCTCTTCTCCA-3'

To exclude DNA contamination, each PCR reaction was also performed on untranscribed RNA. Levels of β -actin transcripts served as a control for equal RNA loading. Quantitative (real-time) reverse transcription polymerase chain reactions (qRT-PCR) were performed by using the SYBR Green PCR Master mix (Applied Biosystems) in the iCycler apparatus (Bio-Rad, Munich, Germany). Amplification reactions (25 μ l final reaction volume) contained 200 nM of each primer, 3 mM MgCl₂, 300 μ M dNTPs, 1 \times SYBR Green PCR buffer, 0.1 U/ μ l AmpliTaq Gold DNA polymerase, 0.01 U/ μ l Amp Erase, RNase-free water, and 2 μ l cDNA samples. Thermal cycling conditions were optimized for each primer pair and are available upon request. To verify the absence of nonspecific products, melting curves were performed (80 cycles

starting from 55°C for 10 s with increments of 0.5°C). In all cases, the melting curve confirmed that a single product was generated. Amplification was monitored by measuring the increase in fluorescence caused by the SYBR-Green binding to double-stranded DNA. Fluorescent threshold values were measured in triplicate and fold changes were calculated by the formula: $2^{-(\text{sample 1 } \Delta\text{Ct} - \text{sample 2 } \Delta\text{Ct})}$, where ΔCt is the difference between the amplification fluorescent thresholds of the mRNA of interest and the β -actin mRNA.

Protein studies

Immunoblotting experiments were performed according to the standard procedures. Briefly, cells were harvested in lysis buffer (50 mM HEPES, pH 7.5, 150 mM NaCl, 10% glycerol, 1% Triton X-100, 1 mM EGTA, 1.5 mM MgCl₂, 10 mM NaF, 10 mM sodium pyrophosphate, 1 mM Na₃VO₄, 10 μ g of aprotinin/ml, 10 μ g of leupeptin/ml) and clarified by centrifugation at 10 000 *g*. Protein concentration was estimated with a modified Bradford assay (Bio-Rad, Munich, Germany). RET/PTC3 immunoprecipitation was performed with an anti-RET antibody, as previously described (Santoro *et al.*, 1994). RAI immunoprecipitation was performed with an anti-RAI rabbit polyclonal antibodies (Pelicci *et al.*, 2002). Total lysates and immunoprecipitates were separated by SDS-PAGE and then transferred onto nitrocellulose filters (Schleicher & Schuell). Filters were then probed with the indicated antibodies. Antiphosphotyrosine (4G10), anti-p85 and anti-GAB1 antibodies were from Upstate Biotechnology Inc., Lake Placid, NY, USA. Anti-phospho Akt and anti-Akt antibodies were from New England Biolabs, Beverly, MA, USA. Secondary anti-mouse and anti-rabbit antibodies coupled to horseradish peroxidase were from Bio-Rad Inc. Proteins were revealed by an enhanced chemiluminescence detection kit (ECL, Amersham, Bucks, England).

Binding assays and Far Western blotting

Expression vectors for GST-CH1 RAI, GST-SH2 RAI and GST-PTB RAI were generated by cloning the respective domains of RAI, obtained by PCR amplification of the fragments, in the vector pGEX (Pelicci *et al.*, 2002). GST-GAB1 and GST-MBD were obtained from S Giordano (Institute for Cancer Research and Treatment, University of Torino School of Medicine, Candiolo, Italy). Recombinant proteins were produced in *Escherichia coli* and purified on glutathione-conjugated sepharose (Amersham). For pull-down assays, 5 μ g of the indicated recombinant protein bound to sepharose were incubated with cell lysates 2 h at 4°C. After washing the beads, proteins were separated by SDS-PAGE and probed with the indicated antibodies.

For Far Western blotting, total lysates or immunoprecipitates, after SDS-PAGE and blotting on nitrocellulose filters, were first blocked for 2 h in the presence of 10 mM glutathione, and then incubated overnight with purified GST recombinant proteins (1 μ g/ml), extensively washed and then developed with anti-GAB1 antibodies.

References

Basolo F, Giannini R, Toniolo A, Casalone R, Nikiforova M, Pacini F, Elisei R, Miccoli P, Berti P, Faviana P, Fiore L, Monaco C, Pierantoni GM, Fedele M, Nikiforov YE, Santoro M and Fusco A. (2002). *Int. J. Cancer*, **97**, 608–614.
Besset V, Scott RP and Ibanez CF. (2000). *J. Biol. Chem.*, **275**, 39159–39166.

TUNEL assay

For the TUNEL, an equal number (5×10^3) of cells from the different lines was seeded onto single well Costar L-polylysine-treated glass slides. After 24 h treatment with 0.9 mM DEM, cells were fixed in 4% (w/v) paraformaldehyde and, then, they were permeabilized by the addition of 0.1% Triton X-100/0.1% sodium citrate. Slides were rinsed twice with PBS, air-dried and subjected to the TUNEL reaction (Boehringer, Mannheim). All coverslips were counterstained in PBS containing Hoechst 33258 (final concentration, 1 μ g/ml; Sigma Chemical Co.), rinsed in water and mounted in Moviol on glass slides. The fluorescent signal was visualized with an epifluorescent microscope (Axiovert 2, Zeiss) (equipped with a $\times 100$ objective) interfaced with the image analyser software KS300 (Zeiss). For the experiments of survival inhibition by the isolated RAI domains, PC RET/PTC1 RAI cells were transiently transfected with vectors encoding RAI-CH1 or RAI-SH2 together with a GFP expressing vector, or with GFP alone. After 24 h treatment with 0.9 mM DEM, cells were then subjected to TUNEL reaction, as described. At least 100 GFP-positive cells were counted in five different microscopic fields. For the experiments of survival inhibition in RAI-depleted FB2 cells, FB2 cells were transfected with the siRNA targeting RAI or with the scrambled oligo. At 48 and 72 h post-transfection, cells were fixed for TUNEL reaction.

RNA silencing

Duplex oligonucleotides (Tuschl *et al.*, 1999; Elbashir *et al.*, 2001), designed with an siRNA selection program available online at <http://jura.wi.mit.edu/siRNAext/>, were chemically synthesized by PROLIGO, Boulder, CO, USA. Sense strand for siRNA targeting RAI was the following:

RAIs: 5'-GUA CUU GGG GUG CAU UGA AG TT-3'

The scrambled oligo was

5'-AGG AUA GCG UGG AUU UCG GU TT-3'

The sequences of specific siRNA against human Gab1 were as described (Jin *et al.*, 2005). For siRNA transfection, FB2 cells were grown under standard conditions. The day before transfection, cells were plated in six-well dishes at 30–40% confluency. Transfection was performed using 5 μ g of duplex RNA and 6 μ l of Oligofectamine reagent (Invitrogen), as previously described (Hingorani *et al.*, 2003). Cells were harvested at 48 and 72 h post-transfection.

Acknowledgements

We thank Francesco Curcio for P5 cells, JM Hershman for BHP cells, and S Giordano and P Gual for GAB1 plasmids. We are also grateful to Fulvio Basolo, who provided us the human tumor samples. This work was supported by the Associazione Italiana per la Ricerca sul Cancro (AIRC), by the Ministero Italiano per l'Università, Istruzione e Ricerca Scientifica (MIUR), by the BIOGEM s.c.a.r.l. (Biologia e Genetica Molecolare nel Mezzogiorno d'Italia) and by the Centro Regionale di Competenza GEAR (Genomic for Applied Research). VG was a fellow of the Centro Regionale di Competenza GEAR.

Carlomagno F, Vitagliano D, Guida T, Napolitano M, Vecchio G, Fusco A, Gazit A, Levitzki A and Santoro M. (2001). *Cancer Res.*, **62**, 1077–1082.
Castellone MD, Cirafici AM, De Vita G, De Falco V, Malorni L, Tallini G, Fagin JA, Fusco A, Melillo RM and Santoro M. (2003). *Oncogene*, **22**, 246–255.

- Cattaneo E and Pelicci PG. (1998). *Trends Neurosci.*, **21**, 476–481.
- Celetti A, Cerrato A, Merolla F, Vitagliano D, Vecchio G and Grieco M. (2004). *Oncogene*, **23**, 109–121.
- Cerutti J, Trapasso F, Battaglia C, Zhang L, Martelli ML, Berlingieri MT, Fagin J, Santoro M and Fusco A. (1996). *Clin. Cancer Res.*, **2**, 119–126.
- Conti L, Sipione S, Magrassi L, Bonfanti L, Rigamonti D, Pettirossi V, Peschanski M, Haddad B, Pelicci P, Milanesi G, Pelicci G and Cattaneo E. (2001). *Nat. Neurosci.*, **4**, 579–586.
- Cooley LD, Elder FF, Knuth A and Gagel RF. (1995). *Cancer Genet Cytogenet.*, **80**, 138–149.
- Curcio F, Ambesi-Impombato FS, Perrella G and Coon HG. (1994). *Proc. Natl. Acad. Sci. USA*, **91**, 9004–9008.
- Elbashir SM, Harborth J, Lendeckel W, Yalcin A, Weber K and Tuschl T. (2001). *Nature*, **411**, 494–498.
- Ganju P, O'Bryan JP, Der C, Winter J and James IF. (1998). *Eur. J. Neurosci.*, **10**, 1995–2008.
- Gu H and Neel BG. (2003). *Trends Cell Biol.*, **13**, 122–130.
- Hayashi H, Ichihara M, Iwashita T, Murakami H, Shimono Y, Kawai K, Kurokawa K, Murakumo Y, Imai T, Funahashi H, Nakao A and Takahashi M. (2000). *Oncogene*, **19**, 4469–4475.
- Hingorani SR, Jacobetz MA, Robertson GP, Herlyn M and Tuveson DA. (2003). *Cancer Res.*, **63**, 5198–5202.
- Jin ZG, Wong C, Wu J and Berk BC. (2005). *J. Biol. Chem.*, **280**, 12305–12309.
- Lewitzky M, Kardinal C, Gehring NH, Schmidt EK, Konkol B, Eulitz M, Birchmeier W, Schaeper U and Feller SM. (2001). *Oncogene*, **20**, 1052–1062.
- Liu HY and Meakin SO. (2002). *J. Biol. Chem.*, **277**, 26046–26056.
- Lock LS, Royal I, Naujokas MA and Park M. (2000). *J. Biol. Chem.*, **275**, 31536–31545.
- Luzi L, Confalonieri S, Di Fiore PP and Pelicci PG. (2000). *Curr. Opin. Genet. Dev.*, **10**, 668–674.
- Maeda K, Murakami H, Yoshida R, Ichihara M, Abe A, Hirai M, Murohara T and Takahashi M. (2004). *Biochem. Biophys. Res. Commun.*, **323**, 345–354.
- Miyake I, Hakomori Y, Shinohara A, Gamou T, Saito M, Iwamatsu A and Sakai R. (2002). *Oncogene*, **21**, 5823–5834.
- Nakamura T, Komiya M, Gotoh N, Koizumi S, Shibuya M and Mori N. (2002). *Oncogene*, **21**, 22–31.
- Nakamura T, Muraoka S, Sanokawa R and Mori N. (1998). *J. Biol. Chem.*, **273**, 6960–6967.
- Nakazawa T, Nakano I, Sato M, Nakamura T, Tamai M and Mori N. (2002). *J. Neurosci. Res.*, **68**, 668–680.
- Nakamura T, Sanokawa R, Sasaki Y, Ayusawa D, Oishi M and Mori N. (1996). *Oncogene*, **13**, 1111–1121.
- Nikiforov YE. (2002). *Endocr. Pathol.*, **13**, 3–16.
- O'Bryan JP, Lambert QT and Der CJ. (1998). *J. Biol. Chem.*, **273**, 20431–20437.
- O'Bryan JP, Songyang Z, Cantley L, Der CJ and Pawson T. (1996). *Proc. Natl. Acad. Sci. USA*, **93**, 2729–2734.
- Ohta K, Endo T, Haraguchi K, Hershman JM and Onaya T. (2001). *J. Clin. Endocrinol. Metab.*, **86**, 2170–2177.
- Pelicci G, Dente L, De Giuseppe A, Verducci-Galletti B, Giuli S, Mele S, Vetriani C, Giorgio M, Pandolfi PP, Cesareni G and Pelicci PG. (1996). *Oncogene*, **13**, 633–641.
- Pelicci G, Troglio F, Bodini A, Melillo RM, Pettirossi V, Coda L, De Giuseppe A, Santoro M and Pelicci PG. (2002). *Mol. Cell. Biol.*, **22**, 7351–7363.
- Pierotti MA. (2001). *Cancer Lett.*, **166**, 1–7.
- Ravichandran KS. (2001). *Oncogene*, **20**, 6322–6330.
- Sakai R, Henderson JT, O'Bryan JP, Elia AJ, Saxton TM and Pawson T. (2000). *Neuron*, **28**, 819–833.
- Santoro M, Carlomagno F, Melillo RM and Fusco A. (2004). *Cell Mol. Life Sci.*, **61**, 2954–2964.
- Santoro M, Melillo RM, Grieco M, Berlingieri MT, Vecchio G and Fusco A. (1993). *Cell Growth Differ.*, **4**, 77–84.
- Santoro M, Wong WT, Aroca P, Santos E, Matoskova B, Grieco M, Fusco A and di Fiore PP. (1994). *Mol. Cell. Biol.*, **14**, 663–675.
- Schaeper U, Gehring NH, Fuchs KP, Sachs M, Kempkes B and Birchmeier W. (2000). *J. Cell Biol.*, **149**, 1419–1432.
- Segouffin-Cariou C and Billaud M. (2000). *J. Biol. Chem.*, **275**, 3568–3576.
- Tanabe K, Kiryu-Seo S, Nakamura T, Mori N, Tsujino H, Ochi T and Kiyama H. (1998). *Brain Res. Mol. Brain Res.*, **53**, 291–296.
- Tuschl T, Zamore PD, Lehmann R, Bartel DP and Sharp PA. (1999). *Genes Dev.*, **13**, 3191–3197.
- Viglietto G, Chiappetta G, Martinez-Tello FJ, Fukunaga FH, Tallini G, Rigopoulou D, Visconti R, Mastro A, Santoro M and Fusco A. (1995). *Oncogene*, **11**, 1207–1210.
- Wang J, Knauf JA, Basu S, Puxeddu E, Kuroda H, Santoro M, Fusco A and Fagin JA. (2003). *Mol. Endocrinol.*, **17**, 1425–1436.



The RET/PTC-RAS-BRAF linear signaling cascade mediates the motile and mitogenic phenotype of thyroid cancer cells

Rosa Marina Melillo,¹ Maria Domenica Castellone,¹ Valentina Guarino,¹ Valentina De Falco,¹ Anna Maria Cirafici,¹ Giuliana Salvatore,¹ Fiorina Caiazzo,¹ Fulvio Basolo,² Riccardo Giannini,² Mogens Kruhoffer,³ Torben Orntoft,³ Alfredo Fusco,¹ and Massimo Santoro¹

¹Istituto di Endocrinologia ed Oncologia Sperimentale del CNR "G. Salvatore," Dipartimento di Biologia e Patologia Cellulare e Molecolare, University "Federico II," Naples, Italy. ²Dipartimento di Oncologia, Università di Pisa, Pisa, Italy. ³Molecular Diagnostic Laboratory, Department of Clinical Biochemistry, Aarhus University Hospital, Skejby, Aarhus, Denmark.

In papillary thyroid carcinomas (PTCs), rearrangements of the *RET* receptor (*RET/PTC*) and activating mutations in the *BRAF* or *RAS* oncogenes are mutually exclusive. Here we show that the 3 proteins function along a linear oncogenic signaling cascade in which *RET/PTC* induces *RAS*-dependent *BRAF* activation and *RAS*- and *BRAF*-dependent *ERK* activation. Adoptive activation of the *RET/PTC*-*RAS*-*BRAF* axis induced cell proliferation and Matrigel invasion of thyroid follicular cells. Gene expression profiling revealed that the 3 oncogenes activate a common transcriptional program in thyroid cells that includes upregulation of the *CXCL1* and *CXCL10* chemokines, which in turn stimulate proliferation and invasion. Thus, motile and mitogenic properties are intrinsic to transformed thyroid cells and are governed by an epistatic oncogenic signaling cascade.

Introduction

Papillary thyroid carcinoma (PTC) is the most prevalent endocrine malignancy in humans (1). Four genetic lesions, at the somatic level, are associated with PTC: chromosomal alterations that affect the *RET* or *TRKA* tyrosine kinase receptors and oncogenic activation of the *RAS* or *BRAF* genes. *RET* encodes the tyrosine kinase receptor of growth factors belonging to the glial-derived neurotrophic factor (GDNF) family (2). *RET* gene rearrangements occur in up to 30% of PTCs (3). They cause the recombination of the intracellular kinase-encoding domain of *RET* with heterologous genes, thereby generating *RET/PTC* chimeric oncogenes. *RET/PTC1* (the *H4-RET* fusion) and *RET/PTC3* (the *RET-fused gene-RET* [*RFG-RET*] fusion) are the most prevalent variants. *RET/PTC3* is frequently found in radiation-associated PTC (4). The finding that *RET/PTC*-transgenic mice develop PTC demonstrates that *RET/PTC* oncogenes can initiate thyroid carcinogenesis (5, 6). *RET/PTC* oncogenes are frequent in clinically silent small PTCs and are thus an early event of thyroid tumorigenesis (7). Similar rearrangements of *TRKA*, e.g., the high-affinity receptor for the nerve growth factor (NGF), can also be found, at a low frequency, in human PTC (8). Activating point mutations in *RAS* small GTPases occur in about 10% of PTCs, mainly in the follicular variant (9). Finally, point mutations in *BRAF* are the most common genetic lesions found in PTCs (up to 50% of cases) (10). *BRAF* belongs to the *RAF* family of serine/threonine kinases that includes *c-RAF* and *ARAF*. *RAF* proteins

are components of the *RAF*-*MAPK* kinase-*ERK* (*RAF*-*MEK*-*ERK*) pathway, which is a highly conserved signaling module in eukaryotes. They are activated through binding to *RAS* in its GTP-bound state. Once activated, *RAF* kinases can phosphorylate *MEK*, which in turn phosphorylates and activates *ERKs* (11). As occurs in melanomas (12), a V600E substitution (formerly designated V599E), in the activation segment accounts for more than 90% of *BRAF* mutations in PTC (10, 13–15). This mutation enhances *BRAF* activity by disrupting the autoinhibited state of the kinase (15).

Thanks to their intrinsic kinase activity, receptor tyrosine kinases (RTKs) activate many intracellular signaling pathways. Upon binding to ligand, RTKs dimerize and autophosphorylate various cytoplasmic tyrosines. The phosphorylated tyrosines thus become binding sites for intracellular molecules containing phosphotyrosine-binding motifs, thereby initiating a diverse array of signaling pathways (16). In *RET/PTC* rearrangements, fusion with protein partners possessing protein-protein interaction motifs provides *RET/PTC* kinases with dimerizing interfaces, which results in ligand-independent autophosphorylation. The *RET* intracellular domain contains at least 12 autophosphorylation sites, 11 of which are maintained in *RET/PTC* proteins (17). Tyrosine 905 (Y905) is a binding site for Grb7/10 adaptors (18), Y1015 for phospholipase C γ (19), and Y981 for *c-Src* (20). Tyrosine 1062 is the binding site for several proteins, including the *Shc* proteins, insulin receptor substrate-1/2 (*IRS*-1/2), *FGFR* substrate 2 (*FRS2*), downstream of kinase 1/4/5 (*DOK*1/4/5), and Enigma, which, in turn, lead to the activation of many signaling pathways (2, 21). Binding to *Shc* and *FRS2* mediates recruitment of *Grb2*-*SOS* complexes, which thus leads to GTP exchange on *RAS* and *RAS/ERK* stimulation (22).

In human PTC, *RET/PTC*, *RAS*, and *BRAF* genetic alterations are mutually exclusive, which suggests that mutations at more than 1 of these sites are unlikely to provide an additional biological advantage (10, 13, 14). This is what would be expected if the 3 proteins function in tandem along a common signaling cascade. To verify whether this is indeed the case, we examined the link

Nonstandard abbreviations used: EST, expressed sequence tag; GDNF, glial-derived neurotrophic factor; GRO- α , growth-related oncogene- α ; 6H, 6 hormones; IP-10, interferon- γ -inducible protein 10; MCP-1, monocyte chemoattractant protein-1; MEK, *MAPK* kinase; NGF, nerve growth factor; PTC, papillary thyroid carcinoma; PTX, *Bordetella pertussis* toxin; Q-RT-PCR, quantitative RT-PCR; RTK, receptor tyrosine kinase; siRNA, small interfering duplex RNA; SLR, signal log ratio; TG, thyroglobulin; TSH, thyrotropic hormone.

Conflict of interest: The authors have declared that no conflict of interest exists.

Citation for this article: *J. Clin. Invest.* 115:1068–1081 (2005). doi:10.1172/JCI200522758.

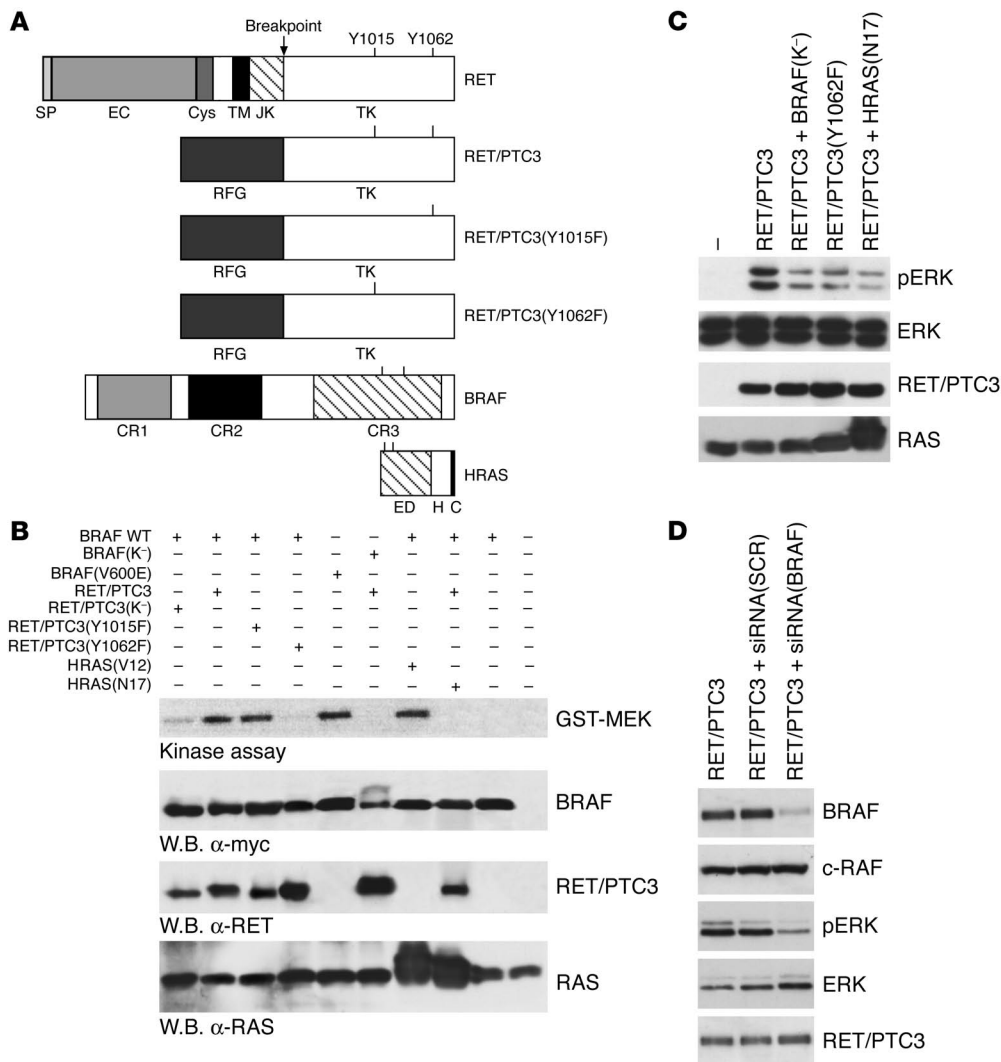


Figure 1 RET/PTC-mediated ERK activation is dependent on RAS and BRAF. **(A)** Schematic representation of the RET, HRAS, and BRAF constructs. The *RET/PTC* breakpoint and *RET* tyrosines 1015 and 1062 are indicated. Residues V600 and K483 are mutated to E and M, respectively, in the BRAF(V600E) and BRAF(K⁻) plasmids. Residues G12 and S17 are mutated to V and N in the HRAS(V12) and HRAS(N17) plasmids. C, CAAX tail; CR1–3, conserved BRAF regions 1–3; Cys, cysteine-rich; EC, extracellular domain; ED, HRAS effector domain; H, heterogeneous region; JX, juxtamembrane; SP, RET signal peptide; TK, tyrosine kinase; TM, transmembrane. **(B)** Protein lysates (500 μg) extracted from HEK293 cells transfected with the indicated plasmids underwent immunoprecipitation with anti-tag (myc) antibody. Kinase assay was performed with GST-MEK as a substrate. BRAF and RET/PTC3 were detected by Western blotting (W.B.) with anti-myc and anti-RET antibodies, respectively. RAS expression was detected with an anti-RAS monoclonal antibody that also recognizes the endogenous protein. **(C)** HEK293 cells transfected with the indicated plasmids were harvested, and protein extracts were subjected to immunoblotting with anti-phospho-p44/p42 ERK (pERK) antibodies. The blot was reprobbed with anti-p44/p42 antibodies for normalization. RET/PTC3 and RAS were detected by Western blotting with specific antibodies. These experiments are representative of at least 3 independent assays. **(D)** Transient BRAF suppression was achieved by RNA interference. Whole cell lysates were prepared 48 hours after transfection and analyzed for protein expression by Western blotting with the indicated antibodies. siRNA(SCR), scrambled siRNA.

overlapping sets of genes. The RET/PTC3-RAS-BRAF axis triggered upregulation of CXC chemokines and their receptors, which in turn stimulated the mitogenic and invasive capacity of thyroid cancer cells.

Results

A biochemical cascade linking RET/PTC to the activation of RAS, BRAF, and ERK. We previously showed that oncogenic RET/PTC proteins activate GTP loading on RAS (23). Here, we transiently transfected HEK293 cells with myc-tagged BRAF and with the constructs shown in Figure 1A. We examined BRAF activity in an immunocomplex kinase assay, with the oncogenic BRAF(V600E) and the kinase-dead BRAF(K⁻) mutants as positive and negative controls, respectively. As shown in Figure 1B, BRAF activation was induced by the expression of the RET/PTC3 and HRAS(V12) oncogenes. Activation of BRAF depended on RET/PTC3 kinase activity and on the integrity of tyrosine 1062. Indeed, neither the kinase-dead RET/PTC3(K⁻) mutant nor a RET/PTC3 mutant carrying a tyrosine to phenylalanine (Y → F) mutation at Y1062 activated BRAF. In contrast, the Y → F mutation at tyrosine 1015 had virtually no effect on BRAF activation. By Western blot analysis with phospho-specific anti-RET antibodies, we demonstrated that the tyrosine 1062 substitution does not affect RET/PTC3 autophosphorylation levels overall or Y1015 and Y905 phosphorylation (Supplemental Figure 1; supplemental material available online with this article; doi:10.1172/

JCI200522758DS1). Expression of the dominant-interfering HRAS(N17) mutant blocked RET/PTC3-mediated BRAF activation, which indicates that in this context, BRAF activation requires RAS (Figure 1B). We explored whether the RET/PTC3(Y1062)-RAS-BRAF cascade resulted in ERK1/2 stimulation. RET/PTC3

JCI200522758DS1). Expression of the dominant-interfering HRAS(N17) mutant blocked RET/PTC3-mediated BRAF activation, which indicates that in this context, BRAF activation requires RAS (Figure 1B). We explored whether the RET/PTC3(Y1062)-RAS-BRAF cascade resulted in ERK1/2 stimulation. RET/PTC3

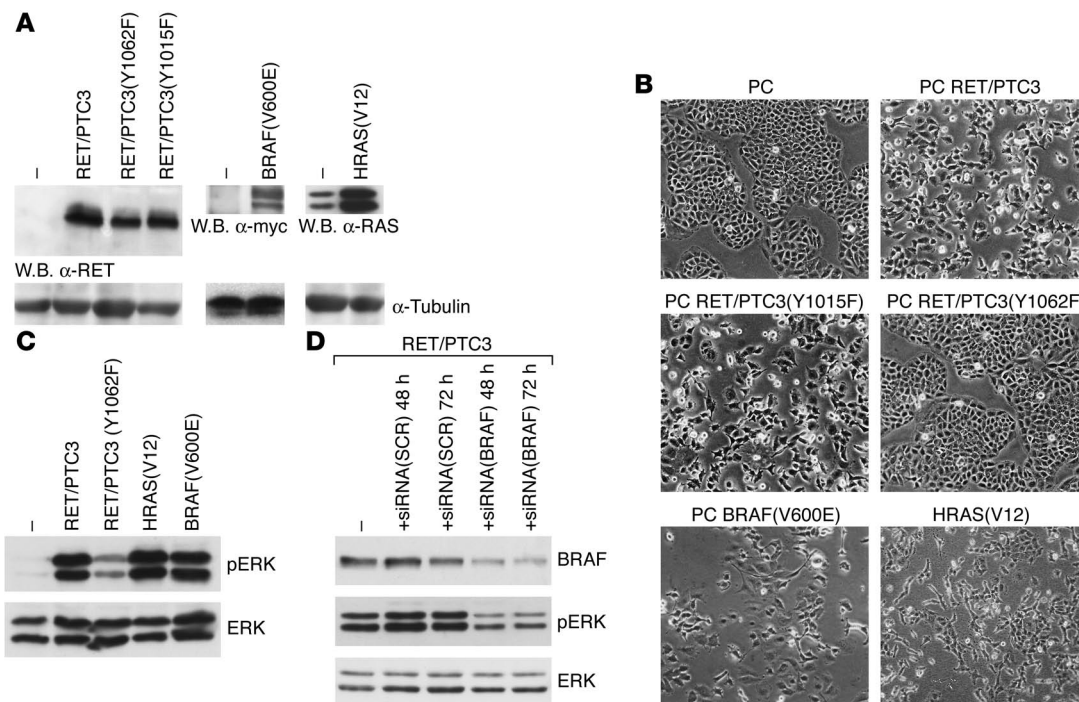


Figure 2

Generation of thyroid cell cultures. **(A)** Protein lysates (50 μ g) extracted from the indicated cell lines underwent Western blotting with anti-RET, -tag (myc), or -RAS antibodies. Equal protein loading was ascertained by anti-tubulin immunoblot. **(B)** Mass populations of PC cells transfected with the indicated plasmids were photographed using a phase-contrast light microscope (magnification, $\times 150$). RET/PTC3-, RET/PTC3(Y1015F)-, BRAF(V600E)-, and HRAS(V12)-expressing cells displayed a transformed morphology, whereas RET/PTC3(Y1062F)-expressing cells were virtually indistinguishable from parental cells. **(C)** Protein extracts from the indicated cell lines were subjected to immunoblotting with anti-phospho-p44/42 ERK antibodies. The blot was reprobed with anti-p44/42 antibodies for normalization. **(D)** BRAF targeting by siRNA but not by scrambled siRNA induced BRAF downregulation and ERK inhibition, as shown by Western blotting with specific antibodies.

stimulated ERK activation, as revealed by immunoblot with a phospho-specific antibody (Figure 1C). This activation did not depend on Y1015 (data not shown); instead, it was dependent on the integrity of Y1062 and on the activity of RAS and BRAF, being obstructed by the expression of HRAS(N17) and BRAF(K-) dominant negative mutants (Figure 1C). The BRAF(K-) dominant negative mutant probably acts as a pan-RAF inhibitor in that it blocks the activity of the various RAF proteins. To specifically block BRAF, we used small interfering duplex RNA (siRNA) oligonucleotides that target endogenous BRAF. This duplex affected only BRAF and no other member of the RAF family (Figure 1D and data not shown). Silencing of BRAF in RET/PTC3-transfected HEK293 cells inhibited ERK activation. This effect was specific, since a control scrambled siRNA did not alter ERK activity (Figure 1D). Taken together, these findings demonstrate that phosphorylation of RET/PTC tyrosine 1062 triggers RAS-dependent stimulation of BRAF signaling.

Generation of the cellular model system. PC Cl 3 (referred to hereafter as PC) is a continuous line of follicular thyroid cells, derived from Fischer rats, that constitutes a model system with which to study differentiation and growth regulation in an epithelial thyroid cell setting. PC cells express the thyroid-specific gene thyroglobulin (TG) and the thyroid-specific transcription factors TTF-1 and PAX-8. They require a mixture of 6 hormones (6H), including thyrotropic hormone (TSH) for proliferation (24). RET/PTC1 expression causes hormone-independent proliferation of PC cells

(25–27); hence, the system lends itself to the study of RET/PTC-mediated effects. We generated marker-selected mass populations of several PC cell clones stably transfected with RET/PTC3, HRAS(V12), or BRAF(V600E). The corresponding proteins were correctly synthesized (Figure 2A); ERK activity was stimulated by each of the 3 oncoproteins (Figure 2C). The oncogene-transfected cell populations showed a similar, albeit not identical, morphologically transformed phenotype, i.e., spindle-shaped and refractile cells scattered on the surface of the culture dish (Figure 2B). RET/PTC3, HRAS(V12), and BRAF(V600E) oncogenes abolished the dependency of PC cell proliferation on the 6H (Figure 3A). Efficiency of colony formation was $35\% \pm 5\%$ in the case of HRAS(V12), perhaps due to the reported proapoptotic role of acute overexpression of the oncoproteins (23, 27). Oncogene-transfected cells maintained increased levels of G₁ cyclin D1 under conditions of 6H deprivation (Figure 3A, inset). Moreover, oncogene-transfected PC cells exerted an invasive phenotype through Matrigel (Figure 3B) and lost the differentiated phenotype (data not shown). In the case of RET/PTC3, all these features, as well as BRAF-ERK activation, depended on tyrosine 1062 but not on tyrosine 1015 (Figures 2 and 3). Since tyrosine 1062 is a multi-docking site in RET and is required to activate several signaling pathways, we used RNA interference to specifically downregulate BRAF in PC cells transfected with RET/PTC3 (PC RET/PTC3 cells). As shown in Figure 2D, transfection with BRAF siRNA, but not with the control scrambled siRNA, diminished BRAF protein levels. ERK

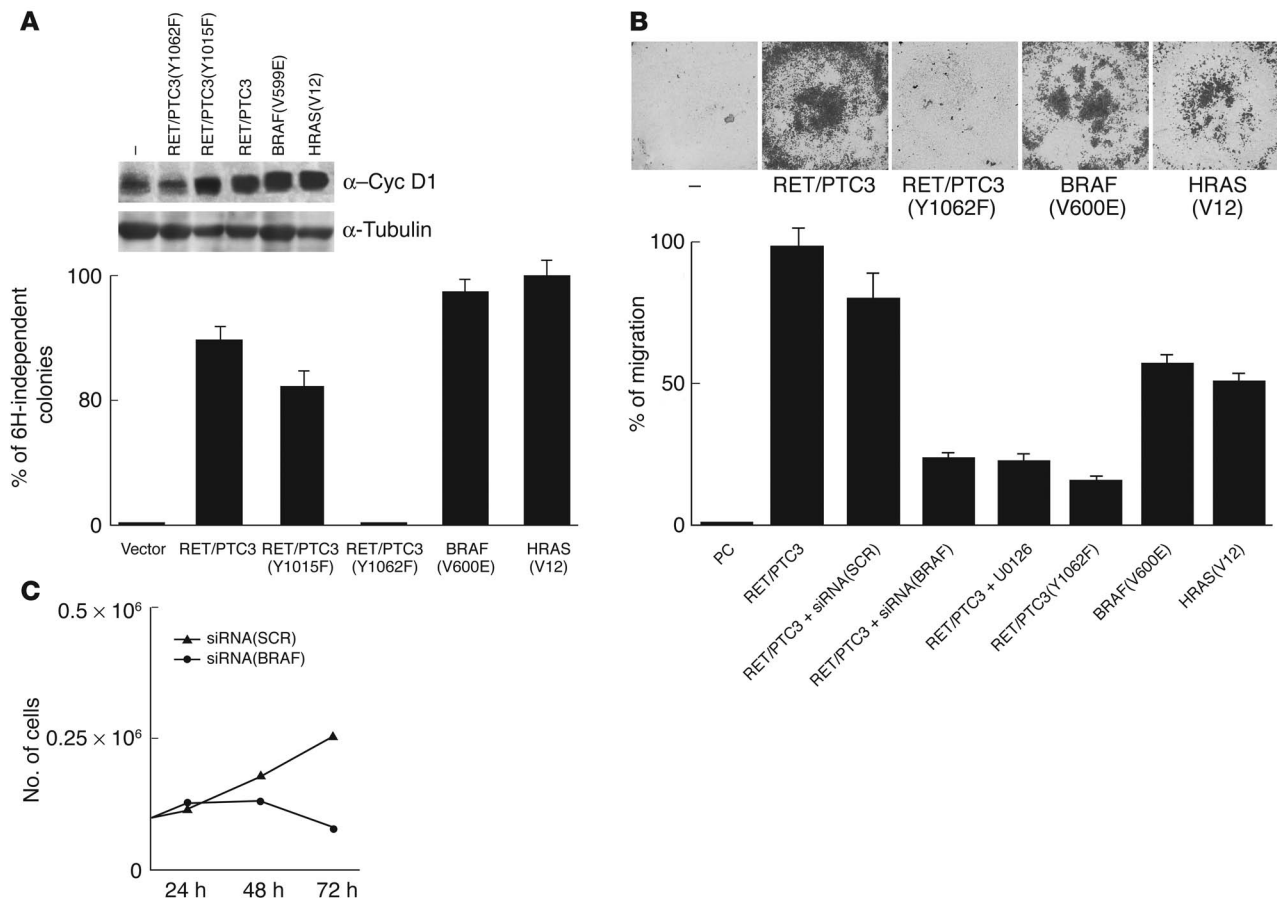


Figure 3

The transformed phenotype of RET/PTC3 thyroid cells requires the integrity of the Y1062-RAS-BRAF-ERK pathway. (A) PC cells were transfected with the indicated plasmids or the empty vector and either selected in neomycin-containing medium or left in the absence of 6H. Three weeks later, colonies were stained with crystal violet and counted. The ratio of neomycin-resistant clones to 6H-independent colonies was calculated. The results of 3 independent experiments performed in duplicate ± SD are reported [the number of 6H-independent colonies induced by HRAS(V12) was set at 100]. Inset: Protein lysates (50 µg) underwent Western blotting with the indicated antibodies. cyc D1, cyclin D1. (B) Matrigel invasion of parental and transformed PC cells. Where indicated, in PC RET/PTC3 cells, suppression of endogenous BRAF was obtained by transfection of RNA interference against BRAF, and ERK inhibition was achieved by U0126 treatment. Cells were seeded in the upper chamber of 8-µM-pore transwells and incubated for 24 hours. Thereafter, filters were fixed and stained. The upper surface was wiped clean and cells on the lower surface photographed (top) and then solubilized. Absorbance at 570 nm was measured with a microplate reader. Cell migration is expressed as percentage with respect to RET/PTC3 cells, whose migration was arbitrarily set at 100. Each column represents the average ± SD of 3 independent experiments (bottom). (C) Suppression of endogenous BRAF in PC RET/PTC3 cells was obtained by transfection of RNA interference against BRAF. Cells were counted at different time points, and the average results of 3 independent experiments are reported.

activity was downregulated by BRAF knockdown (Figure 2D). Importantly, the transient silencing of BRAF inhibited the invasive activity and growth of PC RET/PTC3 cells, whereas the negative control siRNA was ineffective (Figure 3, B and C). Downregulation of ERK activity achieved with U0126, a specific MEK inhibitor, also inhibited PC RET/PTC3 proliferation (data not shown) and Matrigel invasion (Figure 3B).

A gene expression signature of the RET/PTC3-RAS-BRAF axis in thyroid cells. We explored gene expression changes after PC cell transfection with RET/PTC3, HRAS(V12), or BRAF(V600E). We also used cells expressing RET/PTC3(Y1062F) and RET/PTC3(Y1015F) mutants. To study the expression profiles, we used oligonucleotide-based DNA microarrays (GeneChip; Affymetrix) containing oligonucleotide probe pairs corresponding to more than 16,000 known genes and expressed sequence tag (EST) clusters. RNA was extracted

from mass populations of cells (pool no. 3 for each oncogene), converted into fluorescently labeled complementary RNA (cRNA), and hybridized to arrays. Each chip was analyzed with Affymetrix Microarray Suite 5.0 Software to generate raw expression data. Fold change (signal log ratio [SLR]) was calculated by pairwise comparison of probe pairs from the experiment (cells expressing the different oncogenes) with baseline (untransfected parental cells). In order to sort the genes with changes in mRNA abundance in response to the different oncogenes, we defined a filter query that “passed” only data sets that were denoted “increased” or “decreased” by the software and that showed a fold change of 4 or more (SLR ≥ 2 for upregulated genes; SLR ≤ -2 for downregulated genes). The entire data set is available as Supplemental Table 1.

We first examined genes whose expression was expected to be modified by thyroid cell transformation. Consistent with the

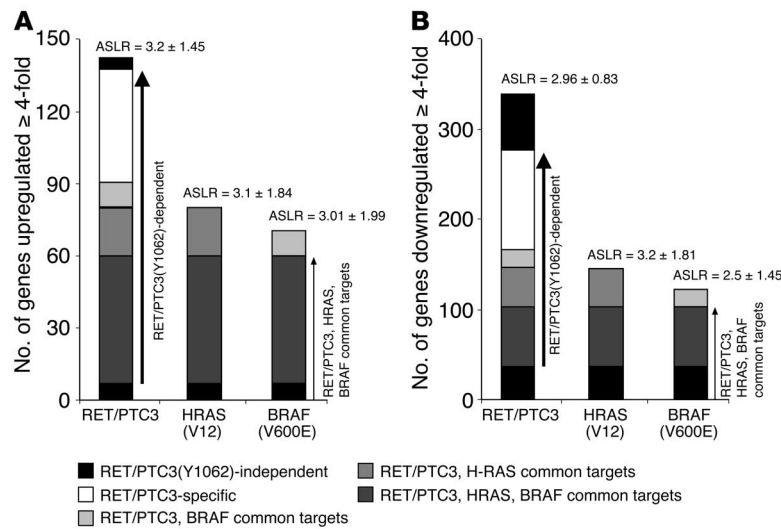


Figure 4

Graphic representation of the gene expression changes (fold change of at least 4) in RET/PTC3, BRAF(V600E), and HRAS(V12) cells versus baseline (PC): upregulated genes (A) and downregulated genes (B). The numbers of upregulated and downregulated genes are represented on the y axis. Thick arrows indicate the Y1062-dependent genes; thin arrows indicate the targets common to RET/PTC3, BRAF(V599E), and HRAS(V12). The different groups of genes are highlighted. Average SLRs (ASLR) are indicated.

above-described cell phenotype, microarray screening demonstrated upregulation of G₁ cyclins (D and E cyclins) and downregulation of thyroid differentiation markers (including TG, TTF-1, and PAX-8) (Supplemental Table 1). Then we examined the global expression profile. Some genes were regulated by only 1 or 2 oncoproteins. However, cross-comparison of the results revealed a group of sequences that were regulated in a similar fashion in RET/PTC3, HRAS(V12), and BRAF(V600E) cells (Figure 4 and Supplemental Figures 2 and 3). Whereas the former probably reflect the specific biological activity of each oncoprotein, the common targets represent a transcriptional signature of the expression of the 3 oncogenes in thyrocytes. Of the 786 oligonucleotide probe pairs whose expression was increased in RET/PTC3 cells (Supplemental Figure 2A), 146 showed an SLR of 2 or more (average SLR, 3.2; Figure 4A). Tyrosine 1062 played a pivotal role in these expression changes. In fact, upregulation of most sequences (131 of 146, 90%) required the integrity of Y1062; the remaining 15 sequences were still induced after the Y1062F mutation, albeit to a lesser extent (average SLR, 1.8) (Figure 4A). In contrast, upregulation of a few of them (less than 15%) depended on tyrosine 1015; most of them depended also on Y1062 (data not shown). Many of the sequences induced by RET/PTC3 were also induced by HRAS(V12) (80 of 146, 54%) and BRAF(V600E) (70 of 146, 48%) cells with a similar average SLR (Figure 4A). Overall, 60 (41%) of the oligonucleotide probe pairs induced in RET/PTC3 cells were induced in both HRAS(V12) and BRAF(V600E) cells, and as many as 87% (52 of 60) were Y1062 dependent (Figure 4A). These upregulated oligonucleotide probe pairs corresponded to the 32 genes and 19 ESTs listed in Table 1. Similarly, sorting of HRAS(V12)- and BRAF(V600E)-induced sequences showed that RET/PTC3 cells upregulated a large set of them in a Y1062-dependent fashion (Supplemental Figure 3). Of the 2,517 oligonucleotide probe pairs whose expression was decreased in RET/PTC3 cells (Supplemental Figure 2B), 338 were downregulated 4-fold or more (average SLR, -2.96). Again, a large fraction of these sequences was also downregulated in HRAS(V12) (148 of 338, 44%; average SLR, 3.2) and in BRAF(V600E) (121 of 338, 36%; average SLR, 2.5) cells (Figure 4B). Overall, 104 (31%) sequences were downregulated by all 3 oncogenes, with 66 of them (64%) being dependent on the integrity of Y1062 (Figure 4B). These downregulated oligonucleotide probe pairs corresponded to the 50 genes and 41 ESTs listed in Table 2.

Validation of the expression data in cultured cells and in human PTCs. We used quantitative RT-PCR (Q-RT-PCR) to evaluate the expression of 50 genes (31 of the 32 upregulated and 19 of the 50 downregulated genes listed in Tables 1 and 2). To verify that gene expression changes were not due to a clonal effect during selection, we analyzed gene expression levels in the mass population (pool no. 3) and in 2 individual clones (Cl1 and Cl2) for each cell line. We then statistically analyzed the expression changes induced by each oncogene. In most cases (37 of the 50 genes), RET/PTC3, HRAS(V12), and BRAF(V600E) activity altered the expression of a particular gene identified by the microarray method. The results of these experiments and the relative statistical analysis are reported in Table 3. In 5 cases (marked in bold in the table), Q-RT-PCR data were not statistically significant ($P > 0.05$); however, in these cases, expression changes showed a trend consistent with that in microarray data.

All the genes examined were affected by the Y1062F mutation, their expression changes being negligible in PC RET/PTC(Y1062F) cells (Tables 1 and 2 and data not shown). Moreover, using PC cells transfected by RET/PTC1, another RET/PTC variant, we also demonstrated that gene changes were not restricted to the isoform (RET/PTC3) used in the array screen (data not shown). To determine whether activation of the RAS-BRAF-ERK pathway was required for gene expression regulation induced by RET/PTC3, we used Q-RT-PCR to measure the expression levels of the 37 genes listed in Table 3 in RET/PTC3 cells in which the pathway was transiently obstructed, either by BRAF siRNA or by the MEK inhibitor U0126. As shown in Table 4, expression of 22 of the 37 genes was affected by both BRAF silencing and U0126 treatment. With the sole exception of the *Ca2* gene, which was obstructed by U0126 but not by BRAF silencing, there was complete concordance between the results obtained with siRNA and U0126 treatment (Table 4). Scrambled siRNA, used as a negative control, did not affect expression levels (Table 4). These findings support the notion that the BRAF-MEK cascade is essential for the gene expression signature of RET/PTC-transformed cells, but they do not necessarily prove that it is also sufficient. It might well be that additional pathways (perhaps triggered by the same Y1062) contribute to the establishment of the phenotype.

We selected 4 genes upregulated more than 4-fold and 3 genes (*Arpc1b*, *CD44*, *RUNX1*) upregulated less than 4-fold in the microarray screen. Using Q-RT-PCR, we compared the expression levels of these



Table 1
Genes upregulated 4-fold or more in RET/PTC3 cells^A

Gene	UniGene no.	RET/PTC3	Y1062F	HRAS	BRAF
Signaling/growth					
<i>Adm</i> ^B	Rn. 10232	3.6	NC	4.1	3.6
<i>Dusp6</i> ^B	Rn. 4313	3.3	D	2.5	3
<i>Itga1</i> ^B	Rn. 91044	2.9	NC	3.7	3.2
<i>Marks</i> ^C	Rn. 9560	2.4	NC	2.1	2.4
<i>Igf2r</i> ^C	Rn. 270	3	D	3.6	3.7
<i>Sgk</i> ^B	Rn. 4636	2	D	1.4	3.1
<i>PI4K2B</i> ^B	Rn. 21189	2.6	NC	2	0.8
Transcription					
<i>Fhl2</i> ^B	Rn. 3849	2.7	NC	3.5	2.8
<i>CITED2</i> ^B	Rn.31765	2.65	NC	2.45	2.65
<i>IRF7-like</i> ^C	Rn. 6246	2.1	D	2.3	2.7
Inflammation/immunity					
<i>Spp1</i> ^B	Rn. 8871	6.1	NC	7.3	2.3
<i>CCL2</i> ^B	Rn. 4772	7	NC	6.15	6.5
<i>CXCL1</i> ^B	Rn. 10907	5.3	NC	7.3	6.1
Proteolysis					
<i>Mmp13</i> ^B	Rn 10997	9.4	NC	8.9	9.6
<i>Mmp10</i> ^B	Rn. 9946	10	NC	8.6	10
<i>Mmp12</i> ^B	Rn. 33193	7.8	NC	5.1	6.7
<i>Mmp3</i> ^B	Rn. 32086	7.5	NC	5.2	6.9
<i>USP18-like</i> ^B	Rn. 4165	2.7	NC	4	2.7
Metabolism					
<i>GSTM2</i> ^C	Rn. 625	2.3	NC	0.7	3
<i>Th</i> ^B	Rn. 11082	2	NC	4.8	1.6
<i>Fdps</i> ^C	Rn. 2622	2.2	NC	1.9	0.4
<i>Ca2</i> ^B	Rn. 26083	4.9	NC	6.6	5.7
<i>Ddbj</i> ^C	Rn. 3285	2.3	1.5	1.3	1.3
<i>Ldlr</i> ^C	Rn. 10483	3	1	2.7	0.9
Structure/adhesion					
<i>Lgals3</i> ^B	Rn. 764	2.7	D	2.1	1.7
<i>Col1a1</i>	Rn. 2953	6.5	NC	1.4	4.9
<i>Tmsb4x</i> ^B	Rn. 2605	3.5	D	2.4	2.3
<i>Vim</i> ^C	Rn. 2710	2	D	0.5	0.6
<i>Lgals1</i> ^B	Rn. 57	2.5	NC	1.9	1.2
<i>Dysf2-like</i> ^B	Rn. 22869	2.9	2.9	3.5	2.3
Calcium binding					
<i>S100A4</i> ^B	Rn. 504	5	NC	3	3.6
<i>S100A6</i> ^B	Rn. 3233	2.9	D	3	3
EST					
AA849365	Rn. 22831	2.9	2.9	3.5	2.3
AA851210	Rn. 1392	2.4	NC	2.3	1.5
AA866419	Rn. 3099	2	NC	1.8	1.2
AA875032	Rn. 3212	2.1	D	1.2	0.7
AA900974		2	D	1.9	1.5
AA926129	Rn. 34404	2.6	D	1.1	1
AA944463	Rn. 7736	2.2	NC	3.9	3.9
AA945591	Rn. 1414	2.2	0.6	2.5	1.2
AA957167		3.2	NC	1.4	2.3
AA998535		2.6	1.8	2.6	1.4
AI010910	Rn. 17645	39	NC	2.5	2.2
AI013157	Rn. 98226	2.1	2.6	1.9	2.2
AI013888	Rn. 6715	2.6	0.9	2.5	2.2
AI029439	Rn. 18227	2.4	NC	2.3	2.3
AI029829	Rn. 18332	2.1	NC	2.3	1.6
AI044253	Rn. 15847	3.2	NC	3.3	3.6
AI059223	Rn. 19102	6.4	NC	2.7	7.2
AI059519	Rn. 19198	2.4	NC	2	0.8
AI059622	Rn. 105857	3.1	3.3	1.8	3.1

^AThe genes induced in RET/PTC3 cells 4-fold or more and also upregulated in HRAS and BRAF cells are listed. ^BTargets whose upregulation was confirmed by RT-PCR. ^CTargets whose upregulation was not confirmed. Targets not further studied by PCR are unmarked. NC, not changed; D, decreased; Rn., rattus norvegicus unigene cluster.

genes in a set of primary human PTC tissue specimens ($n = 13$) characterized for oncogene activation (*BRAF* or *RET/PTC*) (28) to those in 5 samples of normal thyroid tissue obtained from different donors. Successfully amplified samples are reported in Figure 5A. All 7 analyzed genes were found to be upregulated in most of the tumor samples, and for 5 of them, P was 0.05 or less. We then examined genes coding for the chemokines CXCL1/growth-related oncogene- α (CXCL1/GRO- α) and CXCL10/interferon- γ -inducible protein 10 (CXCL10/IP-10), using a larger set of tumor samples ($n = 18$) in this case. Both chemokine-encoding genes were significantly upregulated in PTC samples with respect to normal thyroid tissue (Figure 5B).

Autocrine loops that sustain mitogenesis and motility of thyroid cancer cells. Chemokines are small chemotactic cytokines that are subdivided into 2 main families (α or CXC and β or CC chemokines) on the basis of the relative position of cysteine residues (29). Chemokines bind to 7-transmembrane receptors present in the cell surface that are coupled to G α , class G proteins and are therefore inhibited by *Bordetella pertussis* toxin (PTX). Chemokine receptor activation leads to a cascade of cellular events: generation of diacylglycerol and inositol triphosphate, release of intracellular calcium, inhibition of adenylyl cyclase, and activation of several signaling proteins, including JAK/STATs, PKC, phospholipase C, PI3K, and small GTPases of the Ras and Rho families. This cascade results in activation of AKT and ERK and in cell polarization, adhesion, and migration (30, 31).

According to the microarray screen, CXCL1/GRO- α and CCL2/monocyte chemotactic protein-1 (CCL2/MCP-1) were upregulated more than 4-fold in transformed thyrocytes (Table 1). CXCL10/IP-10 was also upregulated, albeit to a lesser extent (Supplemental Table 1). CCL2 is known to be abundantly produced in human PTC (32). However, its receptor, CCR7, was not detectable in thyroid follicular cells (R.M. Melillo et al., unpublished observations). On the other hand, our Q-RT-PCR data demonstrated that CXCL1 and CXCL10 were upregulated in human PTCs (Figure 5B). According to the microarray data, CXCR2 (the CXCL1 receptor) and CXCR3 (the CXCL10 receptor) were expressed in parental and transformed PC cells (Supplemental Table 1).

First, an ELISA assay demonstrated that CXCL1 and CXCL10 were more abundantly secreted by human PTC cell lines spontaneously carrying the *RET/PTC1* rearrangement (TPC1, FB2, BHP2-7) or the *BRAF*(V600E) mutation (BCPAP, BHP5-16) than by P5, a primary culture of normal human thyroid follicular cells (Figure 6A). Moreover, the mRNA for CXCR2 and CXCR3 was upregulated in all the PTC cell lines compared with normal P5 cells (Figure 6B). Accordingly, both receptors were found to be expressed on the cell surface of the 5 PTC cell lines by flow cytometric analysis (Figure 6C and data not shown).

Treatment of TPC1 cells with BRAF siRNA caused a decrease in endogenous BRAF levels and a parallel reduction of ERK activity (Figure 6D). In parallel, BRAF siRNA, but not scrambled siRNA, remarkably attenuated CXCL1 and CXCL10 chemokine secretion (Figure 6E).

TPC1 cells were stimulated with recombinant CXCL1 or CXCL10; cells were harvested at different time points, and activation of ERK and AKT was analyzed with phospho-specific antibodies. Both chemokines stimulated potent ERK and AKT phosphorylation starting as early as 1 minute after treatment; ERK activation occurred earlier than AKT activation (Figure 7A). To measure DNA synthesis, we counted BrdU-positive cells upon a 1-hour BrdU pulse. The average results of 3 independent experiments are reported in



Table 2
Genes downregulated 4-fold or more in PC RET/PTC3 cells^A

Gene	UniGene no.	SLR				Gene	UniGene	SLR			
		RET/PTC3	Y1062F	HRAS	BRAF			RET/PTC3	Y1062F	HRAS	BRAF
Cell cycle						Inflammation/immunity					
<i>Gas 6^B</i>	Rn. 52228	3	3.3	3	3.3	<i>F10</i>	Rn. 21393	3	NC	3,8	3.1
Transcription						<i>TCRVaQ4a23</i>		2.4	1.3	2,9	2.7
<i>Nr4a1^C</i>	Rn. 10000	2.2	I	2.4	2.4	Proteolysis					
<i>Crem^B</i>	Rn. 10251	3.6	NC	1.6	1.2	<i>Kng</i>	Rn. 54394	3.3	3.85	5,55	4.6
<i>Hhex^B</i>	Rn. 12188	3.2	NC	5.3	2.7	Other					
<i>Nr4a3^C</i>	Rn. 62694	2	NC	3.2	2.3	<i>Dig-1</i>	Rn. 10656	2.3	0.9	1.5	2
<i>IRF8^B</i>	Rn. 3765	2.9	NC	5.1	3.4	<i>LOC 207125^C</i>	Rn. 10718	2.4	NC	2.5	1.5
Thyroid differentiation						<i>Tcp1</i>	Rn. 7102	3.2	2	2.6	2.2
<i>Titf1</i>	Rn. 34265	3.4	NC	3.3	1.1	EST					
<i>Tpo</i>	Rn. 91199	3.8	NC	3.8	4.5	AA875654		2.4	0.5	1.1	1.1
<i>Tshr</i>	Rn. 87913	2	NC	4	2.2	AA892287	Rn. 3658	2.4	NC	3.7	1.2
<i>Tg</i>	Rn. 10429	4.95	I	6.8	4.82	AA892779	Rn. 7319	2.5	1.1	2.3	0.7
<i>Dio1</i>	Rn. 87549	3.6	NC	2.5	3.15	AA893192	Rn. 3568	6.2	0.2	3.9	4.3
<i>Trg</i>	Rn. 10431	2.9	NC	2.6	1.2	AA899685	Rn. 3765	4.4	NC	3.3	3
<i>Slc5a5</i>	Rn. 10505	2.5	I	3.4	2.5	AA925302	Rn. 8149	2.4	0.6	3.7	2.6
Metabolism						AA945679	Rn. 22639	2.7	0.5	5.9	0.7
<i>Kcnk3</i>	Rn. 80679	2.9	2.5	3.8	3.3	AA946224	Rn. 8470	2	NC	2.2	0.9
<i>Decr1</i>	Rn. 2854	2	0.6	1.9	1	AA955287	Rn. 3271	2.2	NC	2.4	1.3
<i>Ephx1</i>	Rn. 3603	2.5	1.3	6.3	2.6	AA956626	Rn. 8943	2.7	NC	2	1.5
<i>Pygb</i>	Rn. 1518	2.5	NC	1.9	0.5	AA956720	Rn. 9069	5.4	I	6.3	1.3
<i>Ass</i>	Rn. 5078	2.8	0.8	2.5	1.6	AA957707	Rn. 9366	3.2	0.7	1.7	2.1
<i>Knkj16</i>	Rn. 1989	3.7	NC	3.9	3.3	AA957835	Rn. 104138	2.5	I	3.6	2.4
<i>Rdh10</i>	Rn. 19600	4.1	NC	0.9	0.8	AA963282	Rn. 11431	2.6	1.2	3.3	1.5
<i>Knk1</i>	Rn. 15693	2.2	NC	6.4	1.9	AA964069	Rn. 26652	2	NC	3.4	3.9
<i>Vdup1^B</i>	Rn. 2758	4.1	0.75	5.55	1.8	AA964863	Rn. 23239	5.6	I	7.4	6.5
<i>GCG^B</i>	Rn. 54383	5.8	2.2	6	5.6	AA965122	Rn. 12011	2.5	0.8	4.8	1.8
<i>ACY1^C</i>	Rn. 3679	3	NC	2.2	2.1	AA998543		2.8	1.9	4.3	1.7
Adhesion/structure						AA998660	Rn. 105756	3	0.6	4.4	1
<i>Spna2</i>	Rn. 5812	2.1	NC	1.7	0.8	AI008390	Rn. 13814	2.2	I	4.3	3
<i>Ibsp</i>	Rn. 9721	3.6	NC	1.6	3.7	AI009321	Rn. 22641	2.2	NC	1	2.2
<i>Sdc2</i>	Rn. 11127	2.2	NC	2.4	1.3	AI009822	Rn. 25030	2.6	0.3	7	2.4
<i>Acta1</i>	Rn. 39438	3.8	NC	1.9	2.2	AI010157	Rn. 17350	4.1	I	6	1.8
<i>WASL</i>	Rn. 104056	2.7	NC	1	2	AI013875	Rn. 12763	2.3	NC	2.9	1.1
Signaling						AI029070	Rn. 18139	3.5	NC	4.1	0.9
<i>Gira1^B</i>	Rn. 10109	3.4	NC	1.4	2.4	AI029492	Rn. 18238	3.7	0.6	3.8	3.6
<i>Pde4b</i>	Rn. 2485	3	NC	3.25	1.6	AI029741	Rn. 18312	4.4	2.3	3.2	2.2
<i>Pde4d</i>	Rn. 1004	2.4	NC	2.85	2.4	AI030145	Rn. 21563	2.3	2.3	1.9	3.2
<i>Pgf^B</i>	Rn. 6960	2.85	NC	4.25	2.95	AI030350	Rn. 21579	5.3	3.4	5.2	3.4
<i>Adra1b^B</i>	Rn. 10032	3.1	0.7	3.6	3.4	AI030351	Rn. 25503	5.1	2	3.5	4.1
<i>Pla2g4a^B</i>	Rn. 10162	2.5	NC	1.4	1.9	AI030569		3.1	1.2	2.5	1.7
<i>Itpr2</i>	Rn. 89152	2.3	I	4	1	AI043701		2.1	2.4	4.5	4.8
<i>Lrp2</i>	Rn. 26430	3.1	NC	3.4	0.6	AI043942	Rn. 17424	2.8	I	4.3	2.3
<i>Ppp1r1b</i>	Rn. 36206	3	I	2.9	2.9	AI045936	Rn. 20936	3.7	NC	2.2	4.7
<i>Pak3^B</i>	Rn. 10128	4	NC	1.2	2.9	AI058357	Rn. 18850	2.5	NC	9.5	2.1
<i>Rdc1^B</i>	Rn. 12959	4.4	0.3	6.4	2.8	AI058863	Rn. 21000	2.4	NC	2.6	3.9
<i>IRS-2^C</i>	Rn. 92308	3	0.5	3.5	1.3	AI059078	Rn. 19060	3.6	I	4.8	4.3
<i>Mig6^B</i>	Rn. 100336	3.5	1.2	1.7	4.1	AI070112	Rn. 19658	2.4	NC	3.3	1.1
<i>PELI1^B</i>	Rn. 22814	2	I	1.5	2.6	AI070185	Rn. 19684	3.2	NC	1.8	1.5
<i>PI4P5K-IB</i>	Rn. 22148	2	NC	1.9	1.9	AI639238	Rn. 8434	3.5	NC	0.6	0.8
						AI639473		4	I	4.9	3.1

^AThe genes downregulated in RET/PTC3 cells 4-fold or more and also downregulated in HRAS and BRAF cells are listed. ^BTargets whose downregulation was confirmed by RT-PCR. ^CTargets whose downregulation was not confirmed. Targets not further studied by PCR are unmarked. I, increased.



Table 3
Gene expression levels in transformed PC cells by Q-RT-PCR

Genes ^A	Cell type ^B											
	PTC3				BRAF				HRAS			
	C11	C12	Pool no. 3	P ^C	C11	C12	Pool no. 3	P ^C	C11	C12	Pool no. 3	P ^C
Upregulated												
<i>Adm</i>	10.6	10.6	13.3	<0.05	9	7.8	9.1	<0.05	1.6	2.2	2.8	<0.05
<i>Dups6</i>	78.6	51	39.9	<0.05	25	32.5	89.1	<0.05	>100	>100	>100	<0.05
<i>Itga1</i>	9.2	12.3	5.8	<0.05	16.4	13.7	24.3	<0.05	1.7	1.5	1.7	<0.05
<i>Sgk</i>	8	5	7.5	<0.05	9.4	9.2	9.2	<0.05	6.2	7.1	9.3	<0.05
<i>PI4K2B</i>	6.2	6.5	2.6	<0.05	11.2	12.1	23.7	<0.05	1.75	1.92	2.92	<0.05
<i>Fhl2</i>	10.3	9.6	6.2	<0.05	9.5	10.5	10.6	<0.05	7.6	7.9	13.3	<0.05
<i>CITED2</i>	2.5	9.2	1.4	<0.05	26.7	13.3	10.8	<0.05	2.6	2.9	1.7	<0.05
<i>Spp1</i>	20	15.5	37	<0.05	3.5	11.9	5	<0.05	30	>100	45	<0.05
<i>CCL2</i>	97	57	50	<0.05	37.8	>100	>100	<0.05	27.3	12.1	6.9	<0.05
<i>CXCL1</i>	42	35.9	14.5	<0.05	>100	67	80.6	<0.05	19.7	17.1	14.6	<0.05
<i>Mmp13</i>	>100	>100	32.7	<0.05	8.5	6.2	10	<0.05	27.9	48.5	35.9	<0.05
<i>Mmp10</i>	>100	>100	>100	<0.05	>100	>100	>100	<0.05	48.5	59.7	44.2	<0.05
<i>Mmp12</i>	>100	>100	48.5	<0.05	15.1	8.6	10	<0.05	1.8	1.9	2.1	<0.05
<i>Mmp3</i>	>100	>100	46.3	<0.05	1.6	1	10	>0.05	12.4	18.8	9.8	<0.05
<i>USP18-like</i>	31.4	28	18.2	<0.05	7.6	18	12.7	<0.05	3.6	4.2	4.8	<0.05
<i>Th</i>	20.6	45.3	21.6	<0.05	11.1	18.4	8.7	<0.05	19	21.6	18.6	<0.05
<i>Ca2</i>	17.6	9.9	23.3	<0.05	4	1.9	3	>0.05	1.3	1.5	1.9	<0.05
<i>Lgals3</i>	19.2	19.7	9.8	<0.05	12.1	3.7	9.8	<0.05	5.3	4.2	3	<0.05
<i>Lgals1</i>	4.4	4.9	6.5	<0.05	2.7	1.5	1.9	<0.05	1.6	4	1.5	<0.05
<i>Tmsb4x</i>	7.5	7.6	13.4	<0.05	1.7	2	2.6	<0.05	4.9	10.8	6.4	<0.05
<i>Dysf2-like</i>	13.3	8.6	19.7	<0.05	4.2	3	2	<0.05	56.8	69.7	54.4	<0.05
<i>S100A4</i>	12.5	9	33.5	<0.05	2.5	1.2	3.8	>0.05	3.1	6.2	10.4	<0.05
<i>S100A6</i>	13.5	3.5	18.9	<0.05	12	3.8	3	<0.05	6.2	8	10.3	<0.05
Downregulated												
<i>Gas6</i>	0.04	0.02	0.01	<0.05	0.005	0.08	0.02	<0.05	0.01	0.01	0.02	<0.05
<i>Crem</i>	0.1	0.14	0.06	<0.05	0.2	0.2	0.2	<0.05	0.04	0.08	0.05	<0.05
<i>Hhex</i>	0.1	0.07	0.12	<0.05	0.1	0.04	0.07	<0.05	0.02	0.03	0.1	<0.05
<i>IRF8</i>	0.003	0.004	0.003	<0.05	0.008	0.01	0.008	<0.05	0.004	0.004	0.009	<0.05
<i>Vdup1</i>	0.35	0.07	0.1	<0.05	0.06	0.03	0.02	<0.05	0.02	0.02	0.01	<0.05
<i>GCG</i>	<0.001	<0.001	0.001	<0.05	<0.001	<0.001	<0.001	<0.05	<0.001	<0.001	<0.001	<0.05
<i>Gira1</i>	0.2	0.4	0.3	<0.05	0.5	0.5	0.5	<0.05	0.3	0.4	0.2	<0.05
<i>Pgf</i>	0.06	0.1	0.04	<0.05	0.1	0.02	0.08	<0.05	0.006	0.005	0.006	<0.05
<i>Adra1b</i>	0.028	0.013	0.01	<0.05	0.03	0.02	0.01	<0.05	0.05	0.05	0.01	<0.05
<i>Pla2g4A</i>	0.05	0.11	0.02	<0.05	0.2	0.1	0.1	<0.05	0.007	0.01	0.007	<0.05
<i>Pak3</i>	0.17	0.7	0.07	>0.05	0.4	0.5	0.6	<0.05	0.008	0.01	0.008	<0.05
<i>Rdc1</i>	0.02	0.01	0.02	<0.05	0.16	0.07	0.01	<0.05	0.023	0.04	0.03	<0.05
<i>Mig-6</i>	0.2	0.3	0.3	<0.05	0.7	0.7	1.4	>0.05	0.1	0.2	0.2	<0.05
<i>PELI1</i>	0.18	0.44	0.13	<0.05	0.16	0.1	0.3	<0.05	<0.001	<0.001	0.3	<0.05

^AGenes are classified as up- or downregulated based on their behavior in RET/PTC3-transformed with respect to parental PC cells. ^BGene expression levels are expressed as fold change with respect to parental PC cells. PCRs were performed in triplicate; SD was always <15%. ^CSignificance was determined by the Mann-Whitney *U* test. *P* < 0.05 was considered statistically significant. Samples in which *P* values were not statistically significant are indicated in bold.

Figure 7B. Treatment with recombinant CXCL1 and CXCL10 stimulated (about 2- to 3-fold) DNA synthesis of TPC1 cells. In contrast, treatment with selective receptor antagonists or blocking antibodies, but not with nonspecific IgG, impaired basal DNA synthesis (about 2-fold). Finally, we asked whether chemokines stimulated cell invasiveness through Matrigel. Representative micrographs are shown in Figure 7C (left) together with the average results of 3 independent assays (right). TPC1 cells had basal levels of invasiveness; exogenous CXCL1 or CXCL10 further induced a strong migratory response. Basal TPC1 migration through Matrigel was inhibited by treatment with PTX, with CXCR2- or CXCR3-blocking antibodies,

and with CXCL1- or CXCL10-blocking antibodies but not with nonspecific IgG. Cell motility was also blocked by selective CXCR2 (SB225002) and CXCR3 (TAK-779) antagonists (33, 34). Finally, treatment of TPC1 cells with BRAF siRNA and U0126 inhibited basal migration in Matrigel. This effect was not observed when a scrambled control was used (Figure 7D).

Discussion

A RET/PTC-RAS-BRAF pathway drives thyroid cancer initiation. Here we show that the oncogenic proteins involved in the initiation of PTC work along the same signaling cascade. This pathway starts at the



Table 4
BRAF/MEK dependence of gene expression levels in PC RET/PTC3 cells

Gene ^A	UO126	Treatment ^B siRNA (SCR)	siRNA (BRAF)
Upregulated			
<i>Dusp6</i>	0.065	NC	0.43
<i>Sgk</i>	0.5	NC	0.8
<i>Spp1</i>	0.14	NC	0.3
<i>CCL2</i>	0.3	NC	0.4
<i>CXCL1</i>	0.16	NC	0.4
<i>Mmp12</i>	0.5	NC	0.5
<i>Mmp3</i>	0.19	NC	0.28
<i>Mmp13</i>	0.03	NC	0.3
<i>Ca2</i>	0.25	NC	NC
<i>Dysf2-like</i>	0.2	NC	0.7
<i>S100A6</i>	0.4	NC	0.25
Downregulated			
<i>Gas6</i>	20	NC	3
<i>Crem</i>	200	NC	5
<i>Vdup1</i>	2	NC	2
<i>GCG</i>	4	NC	15
<i>Glra1</i>	2	NC	7
<i>Pgf</i>	2.3	NC	2.5
<i>Adra1b</i>	2	NC	4.6
<i>Pla2g4a</i>	4	NC	2.5
<i>Pak3</i>	2.4	NC	7.1
<i>Rdc1</i>	2.5	NC	2
<i>PELI1</i>	2	NC	2

^AGenes are classified as up- or downregulated based on their behavior in RET/PTC3-transformed with respect to parental PC cells.

^BGene expression levels are expressed as fold change with respect to RET/PTC3 cells. NC, expression level not changed with respect to untreated RET/PTC3 cells.

level of RET tyrosine 1062 and sequentially triggers RAS, BRAF, and ERK stimulation. These conclusions are supported by a body of experimental evidence. First, the transient block of RAS or BRAF activity in HEK293 cells, either by dominant negative mutants or by RNA interference, inhibited RET/PTC-mediated ERK activation. Second, in a thyroid cell setting, RET/PTC3-induced ERK activity

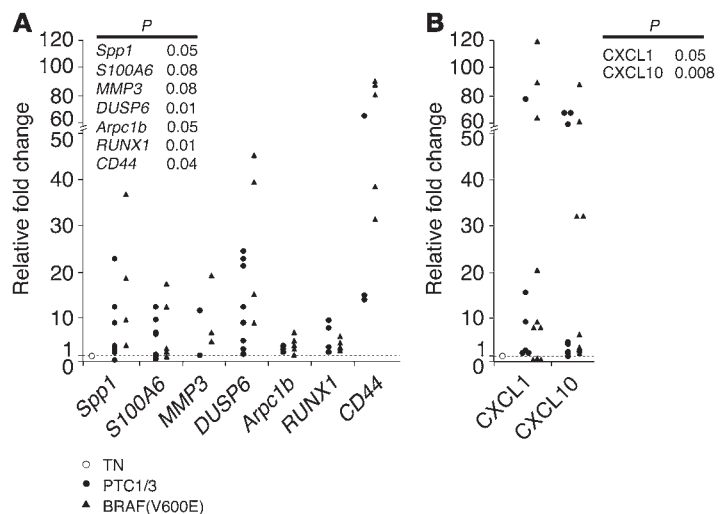
depended on BRAF. Finally, the biological effects mediated by RET/PTC3, i.e., cell proliferation and Matrigel invasion, depended on the integrity of the RET/PTC3-RAS-BRAF pathway.

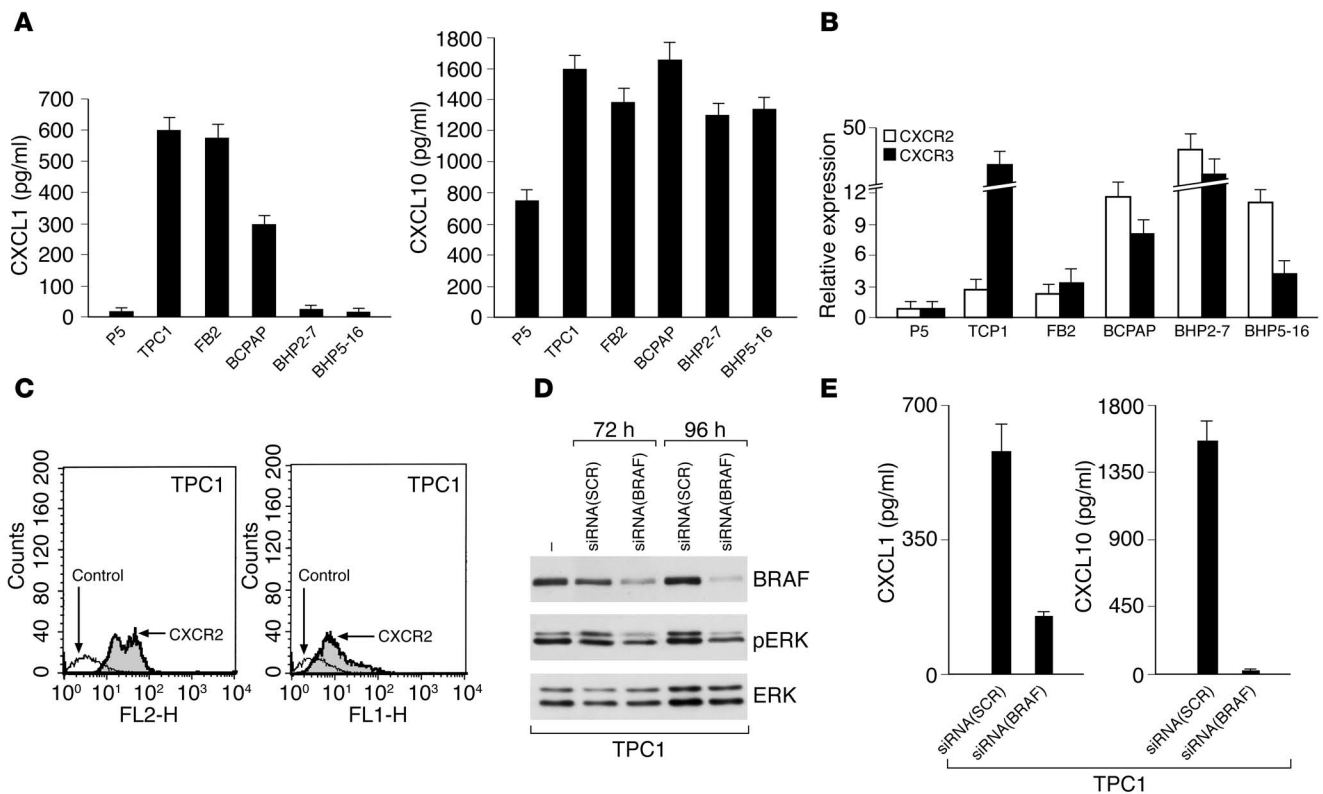
According to such a model, in PC thyroid cells, the 3 activated oncoproteins stimulated largely overlapping gene expression signatures. Most of the common targets were under the control of RET/PTC(Y1062), and the use of BRAF siRNA and chemical blockade of MEK demonstrated that 22 of the 37 genes tested were under the control of the RET/PTC3-RAS-BRAF-ERK cascade. Consistently, some genes had been previously shown to be regulated via the MAPK cascade. One example is DUSP6, a dual-specificity protein phosphatase, which binds to and inactivates ERK1/2 (35). It is likely that the gene expression signature shared by cells transformed by RET/PTC, RAS, or BRAF characterizes a vast number of PTCs. Accordingly, our analysis of a small sample set of primary tumors showed that this gene expression signature may be exploited as a clinical diagnostic test. A larger number of samples will be required to refine the test and to determine whether it is sufficiently robust for clinical implementation.

One corollary of these observations is that therapeutic approaches can be tailored to target the proteins that act downstream from this cascade. Although selective RET kinase inhibitors (36) are effective only in tumors featuring *RET* rearrangements, and not in those carrying activating mutations in genes functioning downstream from the cascade, chemical blockade of BRAF (37) might be beneficial in carcinomas characterized by oncogenic activation of 1 of the 3 proteins. Moreover, our findings imply that other proteins coupled, at different levels, to the RET/PTC-RAS-BRAF cascade could be involved in PTC samples negative for mutations in the 3 oncoproteins. For instance, it is likely that oncogenic versions of the TRKA receptor, which occur in a small fraction of PTCs (8), substitute RET/PTC upstream from the cascade. It is also conceivable that proteins that modulate the transmission of signals among RET, RAS, BRAF, and ERK can modify the phenotype of thyroid tumors carrying mutations at different levels of the cascade.

Differences in RET/PTC-, RAS-, and BRAF-driven transcriptional profiles. The analysis of transcriptional profiles indicated that the 3 oncoproteins are not completely equivalent. Indeed, in addition to targets common to *RET/PTC3*, *HRAS*, and *BRAF*, there were relatively large sets of genes specifically modulated by only 1 or 2 of the 3 oncogenes. Overall, the similarity between transcriptional

Figure 5
Expression levels of selected genes (A) and chemokines (B) in human PTC samples versus 5 normal thyroid tissues as determined by Q-RT-PCR. The PTC samples were characterized for the presence of either a *RET/PTC* rearrangement or a *BRAF*(V600E) mutation. For each target (indicated on the x axis), the expression levels values of tumors (y axis) were calculated relative to the average expression level in normal tissues (TN). All the experiments were performed in triplicate; SDs were smaller than 25% in all cases (data not shown). *P* values were calculated by the Mann-Whitney *U* test.



**Figure 6**

Chemokines and chemokine receptors are expressed in human PTC-derived cell lines. **(A)** CXCL1 and CXCL10 secretion in human PTC cells was evaluated by ELISA. Experiments were performed in triplicate, and the average value of the results \pm SD was plotted. Normal thyroid cells (P5) were used as a negative control. **(B)** Expression levels of CXCR2 and CXCR3 in PTC cell lines were evaluated by Q-RT-PCR. Expression values were calculated relative to the expression level in normal P5 cells. Experiments were performed in triplicate, and the average value of the results \pm SD was plotted. **(C)** Flow cytometric analysis of surface expression of CXCR2 and CXCR3 in TPC1 cells. **(D)** TPC1 cells were transfected by BRAF or scrambled siRNA and harvested 72 or 96 hours later. Protein lysates were subjected to immunoblotting with anti-BRAF and anti-phospho-p44/p42 ERK antibodies. **(E)** BRAF siRNA interference in TPC1 cells affected chemokine production as determined by ELISA.

profiles of HRAS(V12) and BRAF(V600E) thyroid cells was greater than that between RET/PTC3 and HRAS or RET/PTC3 and BRAF cells. For instance, HRAS and BRAF cells (but not RET/PTC cells) were characterized by overexpression of genes such as *IL-6*, *CXCR1*, *PDGF- α* , *SPARC*, *MCM6*, *RAF1*, and *Akt* and by downregulation of PLC- β 1. This was not unexpected; although the 3 oncoproteins work together along a single cascade, they are biochemically different and therefore able to trigger specific signals in addition to the common ones. Molecular genetics evidence nicely supports this concept. For instance, *BRAF* mutations are frequently associated with aggressive thyroid carcinomas, such as poorly differentiated and anaplastic carcinomas, that rarely, if ever, harbor *RET/PTC* rearrangements (28). On the other hand, *RAS* point mutations are rare in classic PTCs and, instead, characterize PTCs of the follicular variant that are rarely affected by mutations in *BRAF* or *RET* (9). Detailed analysis of the gene expression signatures in a large set of samples may help to identify molecular profiles that characterize each oncoprotein.

Function of the genes modulated by RET/PTC3, HRAS(V12) and BRAF(V600E). Many of the commonly modulated genes were involved in hallmarks of neoplastic transformation, e.g., altered cell morphology, uncontrolled growth, loss of differentiation, and apoptosis. Induced genes included MMPs (MMP3, -10, -12, -13) (38). Another category of genes that was greatly overexpressed

in transformed PC cells were those encoding adhesion/structure-associated proteins, such as collagen 1 (Col1 α 1), thymosin β 4, and galectin-3, previously reported to be overexpressed in thyroid carcinomas (39–42). The dual-specificity phosphatase (DUSP6) was also previously identified as a gene upregulated in human PTC samples (41). Finally, upregulated genes included those coding for S100A4 (p9KA) and S100A6 (calcylin); their elevated levels have been associated with cancer and metastasis (43). Consistent with the loss of the differentiated phenotype of transformed cells, genes coding for differentiation markers were downregulated. Interestingly, the gene *Hbex*, which encodes for a proline-rich homeodomain transcription factor and is regulated by thyroid-specific transcription factors, such as TTF-1 and PAX8 (44), was also downregulated. Another downregulated gene was mitogen-inducible gene-6 (Mig6). This protein is a negative-feedback regulator of the epidermal growth factor receptor and a potential tumor suppressor (45).

Chemokine autocrine loops in transformed thyroid cells. PTC is associated with a striking chronic inflammatory reaction in about 30% of cases (1, 32). Our data provide a molecular explanation for this phenomenon by showing that the RET/PTC-RAS-BRAF signaling cascade that drives PTC initiation stimulates the overexpression of several chemokines. In turn, chemokines secreted by tumor cells

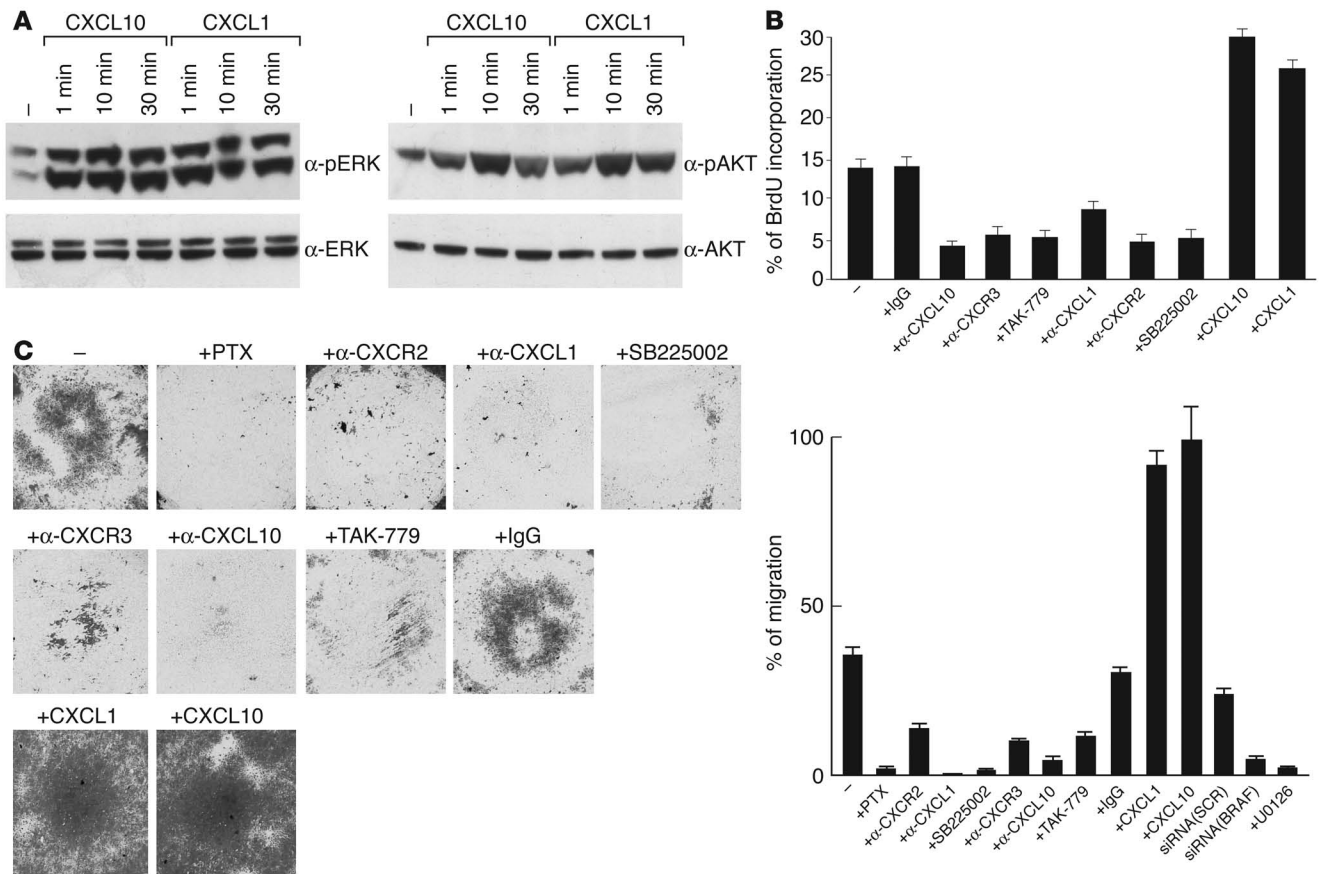


Figure 7 Functional activities of CXCL1 and CXCL10 in human PTC cell lines. (A) Stimulation with CXCL1 and CXCL10 (100 ng/ml) induced time-dependent ERK and AKT activation in TPC1 cells. Cell lysates were harvested at the indicated time points; Western blots were probed with the indicated antibodies. (B) BrdU incorporation was measured to evaluate S-phase entry upon treatment with CXCL1 or CXCL10 or the indicated inhibitors. The average of the results of 3 independent experiments ± SD is indicated. (C) TPC1 cells were allowed to migrate for 24 hours toward serum-free medium or, where indicated, a gradient of CXCL1 or CXCL10. Where indicated, cells were preincubated with blocking antibodies, control antibodies, chemical inhibitors, or PTX. Cells were treated with either BRAF siRNA or U0126. Representative micrographs (left) and absorbance at 570 nm (average ± SD of 3 experiments; right) are shown.

can recruit leukocytes (macrophages, dendritic cells, T cells, and natural killer cells) to tumor sites (30, 31). An interesting aspect of the relationship between inflammation and cancer is that several tumors use molecules of the innate immune system not only to recruit leukocytes, but also for growth, survival, and metastasis. It can be envisaged that a mixture of chemokines is produced in the tumor microenvironment and act in an autocrine/paracrine fashion between neighboring homotypic cells (46, 47). Expression of CXCR2 and CXCR3, the receptors for CXCL1 and CXCL10, respectively, was detected in transformed thyroid cells. Therefore, 2 autocrine/paracrine loops may mediate biological activities in PTCs that are relevant for the establishment of the neoplastic phenotype, e.g., autonomous proliferation and motility.

In conclusion, we propose that PTCs are initiated by a set of transforming events that target proteins that act along a linear signaling cascade. Activation of this signaling cascade results in upregulation of chemokines and their receptors that are relevant for sustained proliferation and cell motility of tumor cells. We suggest that these genes may act cooperatively to commit transformed thyroid cells to a malignant invasive phenotype.

Methods

Plasmids. All the molecular constructs used in this study were cloned in pCDNA3(Myc-His) (Invitrogen Corp.). The RET/PTC constructs encode the short spliced form of RET (RET9) and are described elsewhere (22). For simplicity, we numbered the residues of RET/PTC proteins according to the corresponding residues in unrearranged RET. RET/PTC1 and RET/PTC3 constructs encode the H4-RET and RFG-RET chimeric oncogenes, respectively. RET/PTC3(K⁻) is a kinase-dead mutant, carrying the substitution of the catalytic lysine (residue 758 in full-length RET) with a methionine. RET/PTC3(Y1062F) and RET/PTC3(Y1015F) carry substitutions of the indicated tyrosines with phenylalanine residues. BRAF and the kinase-dead BRAF(K⁻) were kindly donated by C.J. Marshall (Institute of Cancer Research, London, United Kingdom) (12). BRAF(V600E) was obtained by site-directed mutagenesis using the QuickChange mutagenesis kit (Stratagene). The mutation was confirmed by DNA sequencing. HRAS(V12) and HRAS(N17) plasmids are described elsewhere (23).

Cell cultures and transfections. PC Cl 3 (PC) is a differentiated thyroid follicular cell line derived from 18-month-old Fischer rats. PC cells were cultured in Coon's modified Ham F12 medium supplemented with 5% calf serum and a mixture of 6H, including thyrotropin (10 mU/ml), hydro-



cortisone (10 nM), insulin (10 µg/ml), apo-transferrin (5 µg/ml), somatostatin (10 ng/ml), and glycyl-histidyl-lysine (10 ng/ml) (Sigma-Aldrich) (24). For stable transfections, 5×10^5 PC cells were plated 48 hours before transfection in 60-mm tissue culture dishes. The medium was changed to DMEM (Invitrogen Corp.) containing 5% calf serum and 6H. Three hours later, calcium phosphate DNA precipitates were incubated with the cells for 1 hour. DNA precipitates were removed, and cells were washed with serum-free DMEM and incubated with 15% glycerol in HEPES-buffered saline for 2 minutes. Finally, cells were washed with DMEM and incubated in Coon's modified F12 medium supplemented with 5% calf serum and 6H. Two days later, G418 (neomycin) was added at a concentration of 400 µg/ml. Mass populations (pool no. 3) of several PC cell clones were pooled and expanded; 2 independent cell clones (C11 and C12) for each transfection were also isolated. For the colony formation assay, 2 dishes of PC were transfected with each plasmid. Two days later, G418 was added to 1 dish, whereas the other dish was kept in medium containing 5% calf serum without 6H. After 15 days, cells colonies were fixed in 11% glutaraldehyde in PBS, rinsed in distilled water, stained with 0.1% crystal violet in 20% methanol for 15 minutes, and counted. The percentage of hormone-independent colonies with respect to the total number of G418-resistant colonies was calculated as the average of 3 independent determinations \pm SD. HEK293 cells were from American Type Culture Collection and were grown in DMEM supplemented with 10% fetal calf serum. Transient transfections were carried out with 5 µg of total DNA in the Lipofectamine reagent according to the manufacturer's instructions (Invitrogen Corp.). TPC1, FB2, BCPAP, BHP2-7, and BHP5-16 human PTC cell lines were grown in DMEM supplemented with 10% fetal calf serum. The P5 primary culture of normal human thyroid follicular cells was kindly donated by F. Curcio (University of Udine, Udine, Italy) and was grown as previously described (48).

RNA silencing. siRNAs targeting human BRAF are described elsewhere (49). Duplex oligonucleotides targeting rat BRAF were designed with a siRNA selection program (50) and were chemically synthesized by PROLIGO. Sense strands for siRNA targeting were: rat BRAF, 5'-AAAGCCACAGCUGGCUAUUGUUA-3'; human BRAF, 5'-AGAAUUGGAUCUGGAUCAUdTdT-3'; and scrambled, 5'-rArCrCrGrUUU-CrArCrCrCrgrgTT-3'. For siRNA transfection, PC RET/PTC3 and TPC1 cells were grown under standard conditions. The day before transfection, cells were plated in 6-well dishes at 50–60% confluency. Transfection was performed using 5–15 µg of duplex RNA and 6 µl of Oligofectamine reagent (Invitrogen Corp.), as previously described (49). Cells were harvested at different time points after transfection and analyzed.

Tissue samples. Archival frozen thyroid tissue samples from 18 patients affected by PTCs were retrieved from the files of the Pathology Department of the University of Pisa upon informed consent. Special care was taken to select cases whose corresponding histological samples were available for matched analysis. Sections (4 µm thick) of paraffin-embedded samples were stained with H&E for histological examination to ensure that the samples fulfilled the diagnostic criteria required for the identification of PTCs (enlarged nuclei with fine, dusty chromatin, nuclear grooves, single or multiple micro-/macronucleoli, and intranuclear inclusions). Normal thyroid tissue samples were also retrieved from the files of the Pathology Department of the University of Pisa upon informed consent. All experiments were approved by the "Comitato etico per la sperimentazione clinica del farmaco" of the Azienda Ospedaliera – Universitaria Pisana (Pisa, Italy).

RNA extraction and RT-PCR. Total RNA was isolated using the RNeasy Kit (QIAGEN) and subjected to on-column DNase digestion with the RNase-free DNase set (QIAGEN) according to the manufacturer's instructions. Where indicated, cells were transfected with BRAF siRNA or treated with U0126 (20 µM) and harvested 72 hours after treatment. The quality of RNA was verified by electrophoresis through 1% agarose gel and visualized with

ethidium bromide. We synthesized random-primed first-strand cDNA in a 50-µl reaction volume starting from 2 µg RNA using the GeneAmp RNA PCR Core Kit (Applied Biosystems). Primers were designed using Primer3 software (http://frodo.wi.mit.edu/cgi-bin/primer3/primer3_www.cgi) and synthesized by MWG Biotech. Primer sequences are available in Supplemental Tables 2 and 3. To exclude DNA contamination, each PCR reaction was also performed on untranscribed RNA. We performed Q-RT-PCRs using the SYBR Green PCR Master Mix (Applied Biosystems) in the iCycler apparatus (Bio-Rad). Amplification reactions (25 µl final reaction volume) contained 200 nM of each primer, 3 mM MgCl₂, 300 µM deoxyribonucleoside triphosphates (dNTPs), 1× SYBR Green PCR buffer (Applied Biosystems), 0.1 U/µl AmpliTaq Gold DNA Polymerase (Applied Biosystems), 0.01 U/µl Amp Erase (Applied Biosystems), RNase-free water, and 2 µl cDNA samples. Thermal cycling conditions were optimized for each primer pair using standard conditions and varying annealing temperatures as suggested by Primer3. To verify the absence of nonspecific products, we performed 80 cycles of melting (55 °C for 10 seconds). In all cases, the melting curve confirmed that a single product was generated. Amplification was monitored by measuring the increase in fluorescence caused by the binding of SYBR Green to double-stranded DNA. Fluorescent threshold values were measured in triplicate, and fold changes were calculated by the formula $2^{-(\text{sample 1 } \Delta C_t - \text{sample 2 } \Delta C_t)}$, where ΔC_t is the difference between the amplification fluorescence thresholds of the mRNA of interest and the β -actin mRNA. We performed Q-RT-PCR for CXCL1 and CXCL10 using the predeveloped TaqMan assay reagent kit (Assay on Demand; Applied Biosystems).

Oligonucleotide DNA microarray. The detailed protocol for the microarray hybridizations, sample preparation, and the Rat Genome U34 Set are available from Affymetrix. Briefly, 10 µg purified total RNA was transcribed into a first cDNA using Superscript RT (Invitrogen Corp.), in the presence of T7-oligo(dT)₂₄ primer, dNTPs, and T7 RNA polymerase promoter (Invitrogen Corp.). The double-stranded cDNA was cleaned, and an in vitro transcription reaction was then performed to generate biotinylated cRNA, which, after fragmentation, was used in a hybridization assay on RG-U34A and RG-U34B GeneChip microarrays. The A array contains probes representing full-length or annotated genes as well as EST clusters. The B array contains only EST clusters. Before hybridization, we estimated the efficiency of cDNA synthesis by calculating, in a test chip, the ratios for 5' and middle intensities relative to 3' for the control genes *actin* and *GAPDH*. Biotinylated RNA used as a target in the microarray hybridization was stained with a streptavidin-phycoerythrin conjugation including an amplification step with a secondary antibody and scanned in a confocal laser-scanning microscope (GeneArray Scanner G2500A; Hewlett Packard). Normalization was performed by global scaling, with the arrays scaled to an average intensity of 150. We performed analysis of differential expression using Microarray Suite software 5.0 (Affymetrix). The final results were imported into Microsoft Excel (version 11.1; Microsoft).

Protein studies. Protein extractions and immunoblotting experiments were performed according to standard procedures. Briefly, cells were harvested in lysis buffer (50 mM HEPES, pH 7.5, 150 mM NaCl, 10% glycerol, 1% Triton X-100, 1 mM EGTA, 1.5 mM MgCl₂, 10 mM NaF, 10 mM sodium pyrophosphate, 1 mM Na₃VO₄, 10 µg aprotinin/ml, 10 µg leupeptin/ml) and clarified by centrifugation at 10,000 g. Protein concentration was estimated with a modified Bradford assay (Bio-Rad Laboratories). Immune complexes were detected with the enhanced chemiluminescence kit (ECL; Amersham Biosciences). Signal intensity was analyzed with Phosphorimager (Typhoon 8600; Amersham Biosciences) interfaced with ImageQuant software (version 5.0; Amersham Biosciences). Anti-RET is an affinity-purified polyclonal antibody raised against the tyrosine kinase protein fragment of human RET. Anti-ERK (no. 9101) and anti-phospho-ERK (no. 9102) were from Cell Signaling Technology. Anti-myc antibody and antibodies



against cyclin D1, BRAF, and c-RAF were from Santa Cruz Biotechnology Inc. Anti-RAS and anti-phosphotyrosine antibodies were from Upstate Biotechnology Inc. Anti-AKT and anti-phospho-AKT, specific for the active AKT phosphorylated at serine 473, were from Cell Signaling Technology. Monoclonal anti- α -tubulin was from Sigma-Aldrich. Secondary antibodies coupled to HRP were from Amersham Biosciences. For the BRAF kinase assay, cells were cultured for 12 hours in serum-deprived medium and harvested. BRAF kinase was immunoprecipitated with the anti-myc epitope antibody and resuspended in a kinase buffer containing 25 mM sodium pyrophosphate, 10 μ Ci [³²P]ATP, and 1 μ g recombinant glutathione-S-transferase-MEK (GST-MEK; Upstate Biotechnology Inc.). After 30 minutes incubation at 4°C, reactions were stopped by adding 2 \times Laemmli buffer. Proteins were then subjected to 12% SDS gel electrophoresis. The radioactive signal was analyzed with the Phosphorimager.

ELISA assay. Thyroid cells plated in 6-well dishes were allowed to grow to 70% confluency and then serum deprived for 24 hours. The culture medium was cleared by centrifugation at 800 g at 4°C to remove detached cells and debris. We measured CXCL1 and CXCL10 levels in culture supernatants using a quantitative immunoassay ELISA kit (QuantiKine ELISA kit; R&D Systems), following the manufacturer's instructions. For chemokine detection in TPC1 BRAF-depleted cells, supernatants were harvested 96 hours after siRNA transfection. Cells were serum starved for 4 hours before harvesting. Samples prepared in triplicate were analyzed at 490 nM with an ELISA reader (model 550 microplate reader; Bio-Rad Laboratories).

Flow cytometric analysis. Subconfluent TPC1 cells were detached from culture dishes with a solution of 0.5 mM EDTA and then washed 3 times in PBS buffer. After saturation with 1 μ g of human IgG/10⁵ cells, cells were incubated for 20 minutes on ice with fluorescein- or phycoerythrin-labeled antibodies specific for human CXCR2 or CXCR3 (R&D Systems) or isotype control antibody. After incubation, we removed unreacted antibody by washing cells twice in PBS buffer. Cells resuspended in PBS were analyzed on a FACSCalibur automated cell analysis system using CellQuest version 3.3 software (BD). Analyses were performed in triplicate. In each analysis, a total of 10⁴ events was calculated.

Matrigel invasion. In vitro invasiveness through Matrigel was assayed using transwell cell culture chambers according to previously described procedures (51). Briefly, confluent cell monolayers were harvested with trypsin/EDTA and centrifuged at 800 g for 10 minutes. The cell suspension (1 \times 10⁵ cells/well) was added to the upper chamber of a prehydrated polycarbonate membrane filter of 8- μ m pore size (Costar; Corning) coated with 35 μ g Matrigel (Collaborative Research Inc.). The lower chamber was filled with complete medium and, when required, purified CXCL1 or 10 (PeproTech), at a concentration of 100 ng/ml, was added to the lower chamber. When required, the cells were pretreated for 12 hours with U0126 (20 μ M) or for 20 minutes with CXCL1, CXCL10, CXCR2, and CXCR3 blocking antibodies (1 μ g/ml; R&D Systems), PTX (0.1 μ g/ml; Calbiochem), or the blocking compounds SB225002 (10 nM; Calbiochem) and TAK-779 (100 nM). The latter reagent was obtained from the NIH AIDS Research and Reference Reagent Program, Division of AIDS, National Institute of Allergy and

Infectious Diseases. Where indicated, PC RET/PTC3 and TPC1 cells were transfected with BRAF siRNA, harvested at 48 and 72 hours, respectively, and plated on Matrigel. Cells were then incubated at 37°C in a humidified incubator in 5% CO₂ and 95% air for 24 hours. Nonmigrating cells on the upper side of the filter and Matrigel were wiped off, and migrating cells on the reverse side of the filter were stained with 0.1% crystal violet in 20% methanol for 15 minutes and photographed. The stained cells were lysed in 10% acetic acid. Triplicate samples were analyzed at 570 nM with an ELISA reader (model 550 microplate reader). The results were expressed as percentage of migrating cells to PC RET/PTC3- or chemokine-stimulated TPC1 cells.

S-phase entry. S-phase entry was evaluated by BrdU incorporation and indirect immunofluorescence. Cells were grown on coverslips and serum deprived for 30 hours. When indicated, cells were treated with CXCL1 or CXCL10 (PeproTech), at a concentration of 500 ng/ml, for 30 hours. When required, the cells were treated for 24 hours with CXCL1, CXCL10, CXCR2, and CXCR3 blocking antibodies (1 μ g/ml; R&D Systems), PTX (0.1 μ g/ml; Calbiochem), or the blocking compounds SB225002 (10 nM; Calbiochem) and TAK-779 (100 nM). BrdU was added at a concentration of 10 μ M for the last 2 hours. Subsequently, cells were fixed in 3% paraformaldehyde and permeabilized with 0.2% Triton X-100. BrdU-positive cells were revealed with Texas red-conjugated secondary antibodies (Jackson ImmunoResearch Laboratories Inc.). Cell nuclei were identified by Hoechst staining. Fluorescence was visualized with a Zeiss 140 epifluorescence microscope (Carl Zeiss International).

Statistical analysis. Significance was determined by the Mann-Whitney U test using STATSOFT version 6.0 software. P values less than 0.05 were considered statistically significant.

Acknowledgments

We are grateful to C.J. Marshall for the BRAF expression plasmid; to F. Curcio for the P5 primary thyroid culture; to J.M. Hershman for the BHP2-7 and BHP5-16 cell lines; and to L. Vitiello and L. Racioppi for FACS analysis of thyroid cell cultures. We would like to thank J. Gilder for editing the text. This study was supported by the Associazione Italiana per la Ricerca sul Cancro (AIRC), the Progetto Strategico Oncologia of the CNR/Italiano Ministero per l'Istruzione, Università e Ricerca Scientifica (MIUR), Biotecnologia e Genetica Molecolare nel Mezzogiorno d'Italia (BioGeM) s.c.ar.l., the Italian Ministero della Salute, and the Centro Regionale di Competenza GEAR (Genomic for Applied Research). V. Guarino and M.D. Castellone were recipients of BioGeM s.c.ar.l. fellowships.

Received for publication July 19, 2004, and accepted in revised form January 25, 2005.

Address correspondence to: Massimo Santoro, Dipartimento di Biologia e Patologia Cellulare e Molecolare, via S. Pansini 5, 80131 Naples, Italy. Phone: 39-081-7463056; Fax: 39-081-7463037; E-mail: masantor@unina.it.

1. Rosai, J., Carcangiu, M.L., and DeLellis, R.A. 1992. *Atlas of tumor pathology: tumors of the thyroid gland*. 3rd series. Armed Forces Institute of Pathology. Washington, D.C., USA. 343 pp.
2. Manie, S., Santoro, M., Fusco, A., and Billaud, M. 2001. The RET receptor: function in development and dysfunction in congenital malformation. *Trends Genet.* **17**:580-589.
3. Santoro, M., et al. 1992. Ret oncogene activation in human thyroid neoplasms is restricted to the papillary cancer subtype. *J. Clin. Invest.* **89**:1517-1522.
4. Fagin, J.A. 2002. Perspective: lessons learned from molecular genetic studies of thyroid cancer--

- insights into pathogenesis and tumor-specific therapeutic targets. *Endocrinology.* **143**:2025-2028.
5. Santoro, M., et al. 1996. Development of thyroid papillary carcinomas secondary to tissue-specific expression of the RET/PTC1 oncogene in transgenic mice. *Oncogene.* **12**:1821-1826.
6. Buckwalter, T.L., et al. 2002. The roles of phosphotyrosines-294, -404, and -451 in RET/PTC1-induced thyroid tumor formation. *Oncogene.* **21**:8166-8172.
7. Fusco, A., et al. 2002. Assessment of RET/PTC oncogene activation and clonality in thyroid nodules with incomplete morphological evi-

- dence of papillary carcinoma: a search for the early precursors of papillary cancer. *Am. J. Pathol.* **160**:2157-2167.
8. Pierotti, M.A. 2001. Chromosomal rearrangements in thyroid carcinomas: a recombination or death dilemma. *Cancer Lett.* **166**:1-7.
9. Zhu, Z., Gandhi, M., Nikiforova, M.N., Fischer, A.H., and Nikiforov, Y.E. 2003. Molecular profile and clinical-pathologic features of the follicular variant of papillary thyroid carcinoma. An unusually high prevalence of ras mutations. *Am. J. Clin. Pathol.* **120**:71-77.
10. Kimura, E.T., et al. 2003. High prevalence of braf



- mutations in thyroid cancer: genetic evidence for constitutive activation of the RET/PTC-RAS-BRAF signaling pathway in papillary thyroid carcinoma. *Cancer Res.* **63**:1454–1457.
11. Malumbres, M., and Barbacid, M. 2003. RAS oncogenes: the first 30 years. *Nat. Rev. Cancer.* **3**:459–465.
 12. Davies, H., et al. 2002. Mutations of the BRAF gene in human cancer. *Nature.* **417**:949–954.
 13. Cohen, Y., et al. 2003. BRAF mutation in papillary thyroid carcinoma. *J. Natl. Cancer Inst.* **95**:625–627.
 14. Soares, P., et al. 2003. BRAF mutations and RET/PTC rearrangements are alternative events in the etiopathogenesis of PTC. *Oncogene.* **22**:4578–4580.
 15. Fagin, J.A. 2004. How thyroid tumors start and why it matters: kinase mutants as targets for solid cancer pharmacotherapy. *J. Endocrinol.* **183**:249–256.
 16. Schlessinger, J., and Lemmon, M.A. 2003. SH2 and PTB domains in tyrosine kinase signaling [review]. *Sci. STKE.* **191**:RE12.
 17. Kawamoto, Y., et al. 2004. Identification of RET autophosphorylation sites by mass spectrometry. *J. Biol. Chem.* **279**:14213–14224.
 18. Pandey, A., et al. 1996. Direct association between the Ret receptor tyrosine kinase and the Src homology 2-containing adapter protein Grb7. *J. Biol. Chem.* **271**:10607–10610.
 19. Borrello, M.G., et al. 1996. The full oncogenic activity of Ret/ptc2 depends on tyrosine 539, a docking site for phospholipase Cgamma. *Mol. Cell. Biol.* **16**:2151–2163.
 20. Encinas, M., Crowder, R.J., Milbrandt, J., and Johnson, E.M., Jr. 2004. Tyrosine 981, a novel Ret autophosphorylation site, binds c-Src to mediate neuronal survival. *J. Biol. Chem.* **279**:18262–18269.
 21. Ichihara, M., Murakumo, Y., and Takahashi, M. 2004. RET and neuroendocrine tumors. *Cancer Lett.* **204**:197–211.
 22. Melillo, R.M., et al. 2001. Docking protein FRS2 links the protein tyrosine kinase RET and its oncogenic forms with the mitogen-activated protein kinase signaling cascade. *Mol. Cell. Biol.* **21**:4177–4187.
 23. Castellone, M.D., et al. 2003. Ras-mediated apoptosis of PC CL 3 rat thyroid cells induced by RET/PTC oncogenes. *Oncogene.* **22**:246–255.
 24. Fusco, A., et al. 1987. One- and two-step transformations of rat thyroid epithelial cells by retroviral oncogenes. *Mol. Cell. Biol.* **9**:3365–3370.
 25. Santoro, M., et al. 1993. The TRK and RET tyrosine kinase oncogenes cooperate with ras in the neoplastic transformation of a rat thyroid epithelial cell line. *Cell Growth Differ.* **4**:77–84.
 26. Knauf, J.A., Kuroda, H., Basu, S., and Fagin, J.A. 2003. RET/PTC-induced dedifferentiation of thyroid cells is mediated through Y1062 signaling through SHC-RAS-MAP kinase. *Oncogene.* **22**:4406–4412.
 27. Shirokawa, J.M., et al. 2000. Conditional apoptosis induced by oncogenic ras in thyroid cells. *Mol. Endocrinol.* **14**:1725–1738.
 28. Nikiforova, M.N., et al. 2003. BRAF mutations in thyroid tumors are restricted to papillary carcinomas and anaplastic or poorly differentiated carcinomas arising from papillary carcinomas. *J. Clin. Endocrinol. Metab.* **88**:5399–5404.
 29. Dhawan, P., and Richmond, A. 2002. Role of CXCL1 in tumorigenesis of melanoma. *J. Leukoc. Biol.* **72**:9–18.
 30. Luster, A.D. 1998. Chemokines--chemotactic cytokines that mediate inflammation. *N. Engl. J. Med.* **338**:436–445.
 31. Mellado, M., Rodriguez-Frade, J.M., Manes, S., and Martinez-A, C. 2001. Chemokine signaling and functional responses: the role of receptor dimerization and TK pathway activation. *Annu. Rev. Immunol.* **19**:397–421.
 32. Scarpino, S., et al. 2000. Papillary carcinoma of the thyroid: hepatocyte growth factor (HGF) stimulates tumor cells to release chemokines active in recruiting dendritic cells. *Am. J. Pathol.* **156**:831–837.
 33. White, J.R., et al. 1998. Identification of a potent, selective non-peptide CXCR2 antagonist that inhibits interleukin-8-induced neutrophil migration. *J. Biol. Chem.* **273**:10095–10098.
 34. Gao, P., et al. 2003. The unique target specificity of a nonpeptide chemokine receptor antagonist: selective blockade of two Th1 chemokine receptors CCR5 and CXCR3. *J. Leukoc. Biol.* **73**:273–280.
 35. Eblaghie, M.C., et al. 2003. Negative feedback regulation of FGF signaling levels by Pyst1/MKP3 in chick embryos. *Curr. Biol.* **13**:1009–1018.
 36. Carlomagno, F., et al. 2002. ZD6474, an orally available inhibitor of KDR tyrosine kinase activity, efficiently blocks oncogenic RET kinases. *Cancer Res.* **62**:7284–7290.
 37. Lyons, J.F., Wilhelm, S., Hibner, B., and Bollag, G. 2001. Discovery of a novel Raf kinase inhibitor. *Endocr. Relat. Cancer.* **8**:219–225.
 38. Liotta, L.A., and Kohn, E.C. 2001. The microenvironment of the tumour-host interface. *Nature.* **411**:375–379.
 39. Dahlman, T., et al. 2002. Collagen type I expression in experimental anaplastic thyroid carcinoma: regulation and relevance for tumorigenicity. *Int. J. Cancer.* **98**:186–192.
 40. Califano, D., et al. 1998. Thymosin beta-10 gene overexpression correlated with the highly malignant neoplastic phenotype of transformed thyroid cells in vivo and in vitro. *Cancer Res.* **58**:823–828.
 41. Huang, Y., et al. 2001. Gene expression in papillary thyroid carcinoma reveals highly consistent profiles. *Proc. Natl. Acad. Sci. U. S. A.* **98**:15044–15049.
 42. Bartolozzi, A., et al. 2001. Application of an immunodiagnostic method for improving preoperative diagnosis of nodular thyroid lesions. *Lancet.* **357**:1644–1650.
 43. El-Rifai, W., et al. 2002. Gastric cancers overexpress S100A calcium-binding proteins. *Cancer Res.* **62**:6823–6826.
 44. Elsalini, O.A., von Gartzten, J., Cramer, M., and Rohr, K.B. 2003. Zebrafish hhex, nk2.1a, and pax2.1 regulate thyroid growth and differentiation downstream of Nodal-dependent transcription factors. *Dev. Biol.* **263**:67–80.
 45. Hackel, P.O., Gishizky, M., and Ullrich, A. 2001. Mig-6 is a negative regulator of the epidermal growth factor receptor signal. *Biol. Chem.* **382**:1649–1662.
 46. Balkwill, F., and Mantovani, A. 2001. Inflammation and cancer: back to Virchow? *Lancet.* **357**:539–545.
 47. Coussens, L.M., and Werb, Z. 2002. Inflammation and cancer. *Nature.* **420**:860–867.
 48. Curcio, F., Ambesi-Impiombato, F.S., Perrella, G., and Coon, H.G. 1994. Long-term culture and functional characterization of follicular cells from adult normal human thyroids. *Proc. Natl. Acad. Sci. U. S. A.* **91**:9004–9008.
 49. Hingorani, S.R., Jacobetz, M.A., Robertson, G.P., Herlyn, M., and Tuveson, D.A. 2003. Suppression of BRAF(V599E) in human melanoma abrogates transformation. *Cancer Res.* **63**:5198–5202.
 50. Yuan, B., Latek, R., Hossbach, M., Tuschl, T., and Liew, F. 2004. siRNA Selection Server: an automated siRNA oligonucleotide prediction server. *Nucleic Acids. Res.* **32**:W130–W134.
 51. Castellone, M.D., et al. 2004. Autocrine stimulation by osteopontin plays a pivotal role in the expression of the mitogenic and invasive phenotype of RET/PTC-transformed thyroid cells. *Oncogene.* **23**:2188–2196.

Functional expression of the CXCR4 chemokine receptor is induced by RET/PTC oncogenes and is a common event in human papillary thyroid carcinomas

Maria D Castellone¹, Valentina Guarino¹, Valentina De Falco¹, Francesca Carlomagno¹, Fulvio Basolo², Pinuccia Faviana², Mogens Kruhoffer³, Torben Orntoft³, John P Russell⁴, Jay L Rothstein⁴, Alfredo Fusco¹, Massimo Santoro¹ and Rosa Marina Melillo^{*1}

¹Istituto di Endocrinologia ed Oncologia Sperimentale del CNR 'G Salvatore', clo Dipartimento di Biologia e Patologia Cellulare e Molecolare, 80131 Naples, Italy; ²Dipartimento di oncologia, Pisa, Italy; ³Molecular Diagnostic Laboratory, Department of Clinical Biochemistry, Aarhus University Hospital, Skejby, Aarhus, Denmark; ⁴Departments of Microbiology/Immunology and Otolaryngology-Head and neck surgery, Kimmel Cancer Institute, Thomas Jefferson University, Philadelphia, PA 19107, USA

To identify genes involved in the transformation of thyroid follicular cells, we explored, using DNA oligonucleotide microarrays, the transcriptional response of PC Cl3 rat thyroid epithelial cells to the ectopic expression of the RET/PTC oncogenes. We found that RET/PTC was able to induce the expression of CXCR4, the receptor for the chemokine CXCL12/SDF-1 α/β . We observed that CXCR4 expression correlated with the transforming ability of the oncoprotein and depended on the integrity of the RET/PTC–RAS/ERK signaling pathway. We found that CXCR4 was expressed in RET/PTC-positive human thyroid cancer cell lines, but not in normal thyroid cells. Furthermore, we found CXCR4 expression in human thyroid carcinomas, but not in normal thyroid samples by immunohistochemistry. Since CXCR4 has been recently implicated in tumor proliferation, motility and invasiveness, we asked whether treatment with SDF-1 α was able to induce a biological response in thyroid cells. We observed that SDF-1 α induced S-phase entry and survival of thyroid cells. Invasion through a reconstituted extracellular matrix was also supported by SDF-1 α and inhibited by a blocking antibody to CXCR4. Taken together, these results suggest that human thyroid cancers bearing RET/PTC rearrangements may use the CXCR4/SDF-1 α receptor–ligand pathway to proliferate, survive and migrate.

Oncogene (2004) 23, 5958–5967. doi:10.1038/sj.onc.1207790
Published online 7 June 2004

Keywords: thyroid tumor; RET/PTC oncogenes; chemokine receptor

Introduction

Thyroid tumors include a broad variety of lesions with different biological and clinical behavior: benign adenomas and well-differentiated (papillary and follicular), poorly differentiated and undifferentiated (anaplastic) carcinomas (Kroll *et al.*, 2002). Papillary thyroid carcinomas (PTCs) are the most frequent thyroid tumors. Somatic rearrangements of the RET proto-oncogene are frequent genetic events in PTCs, ranging from 25 to 40%. Their prevalence is much higher in the PTCs that occurred in children after the nuclear fallout in the Chernobyl area (Nikiforov, 2002). RET/PTC genes derive from chromosomal rearrangements that juxtapose the TK domain of RET to heterologous genes. RET/PTC1 (H4-RET) and RET/PTC3 (RFG-RET) are the most prevalent variants (Nikiforov, 2002). When RET/PTC1 or RET/PTC3 are targeted to the thyroid in transgenic mice, animals develop thyroid tumors resembling human thyroid papillary carcinoma (Jiang *et al.*, 1996; Santoro *et al.*, 1996; Powell *et al.*, 1998; Buckwalter *et al.*, 2002). Consistent with their role in thyroid carcinogenesis, RET/PTC oncogenes, when ectopically expressed in PC Cl3 rat thyroid epithelial cells, induce morphological transformation, TSH-independent growth and the loss of the differentiated phenotype (Santoro *et al.*, 1993). Other frequent genetic events in PTCs are activating point mutations of the BRAF serine-threonine kinase (Kimura *et al.*, 2003). Activating point mutations of RAS are also seen in a small percentage of human PTCs (Namba *et al.*, 1990). Interestingly, RET, RAS and BRAF signal on the same pathway in thyroid cells and their mutations are mutually exclusive in human PTC samples (Kimura *et al.*, 2003).

To identify genes involved in RET/PTC-mediated transforming activity, we explored, using DNA oligonucleotide microarray, the transcriptional response of PC Cl3 cells to RET/PTC oncogenes. We identified CXCR4, the receptor for the chemokine SDF-1 α , as one of the genes whose expression was upregulated in RET/

*Correspondence: RM Melillo; E-mail: rosmelil@unina.it
Received 18 February 2004; revised 31 March 2004; accepted 31 March 2004; published online 7 June 2004

PTC-expressing cells and correlated with the transforming ability of RET/PTC. We show that CXCR4 expression depended on tyrosine 1062 of RET, which mediates the activation of the RAS/ERK pathway (Melillo *et al.*, 2001). Consistent with this, we observed upregulation of CXCR4 also in rat thyroid cell lines transformed by the RAS and the BRAF oncogenes. Human thyroid cancer cell lines derived from either RET/PTC- or BRAF-positive tumors also feature high levels of CXCR4, if compared with primary thyroid cells. Here, we provide evidences that proliferation, survival and migration of thyroid cancer cell lines can be sustained by the CXCR4–SDF-1 α receptor–ligand pair. In conclusion, we suggest that overexpression of CXCR4 is a common event in thyroid tumorigenesis and that this receptor can mediate, upon ligand addition, paracrine signals that promote malignant progression.

Results

RET/PTC oncogenes upregulate the expression of the CXCR4 chemokine receptor

To better understand the molecular mechanisms used by RET/PTC oncogenes to transform thyroid cells, we exploited the rat thyroid epithelial cell line PC Cl3, widely used as a model system for thyroid transformation. In our previous work, we generated and characterized PC Cl3 cell lines expressing the RET/PTC1 oncogene, PC-PTC1 (Santoro *et al.*, 1993). These cells display a transformed phenotype with altered morphology, loss of differentiation and hormone-independent growth. We performed gene expression profiling of parental and PC-PTC1 cell lines using the rat Affymetrix GeneChip U34 set. Among several genes that were induced upon RET/PTC expression (RM Melillo *et al.*, unpublished data), CXCR4, the receptor for the chemokine CXCL12/SDF-1 α/β , showed approximately a threefold increase. RT–PCR experiment on PC-PTC1 and PC-PTC3 cells validated these results; densitometric scanning revealed an induction of approximately fourfold in transformed *versus* parental cells (Figure 1a). Western blotting with anti-CXCR4 polyclonal antibodies confirmed the overexpression of CXCR4 in rat transformed thyroid cells (Figure 1b). To further characterize CXCR4 gene regulation by RET/PTC, we performed RT–PCR experiments on RET/PTC3 mutants, carrying mutations in residues corresponding to Y1015 and Y1062 of wild-type RET. RET/PTC3 Y1015F and RET/PTC3 Y1062F display, respectively, moderately and severely reduced biological activity (Melillo *et al.*, 2001; Knauf *et al.*, 2003). Here we show that CXCR4 mRNA expression depends on the integrity of Y1062, but not Y1015. Y1062 drives the activation of the RAS/ERKs and it is essential for the transforming ability of RET/PTC oncogenes in thyroid cells (Melillo *et al.*, 2001, Melillo *et al.*, in preparation). To verify whether CXCR4 expression depends on RAS–BRAF activation, we examined CXCR4 RNA levels in the PC-

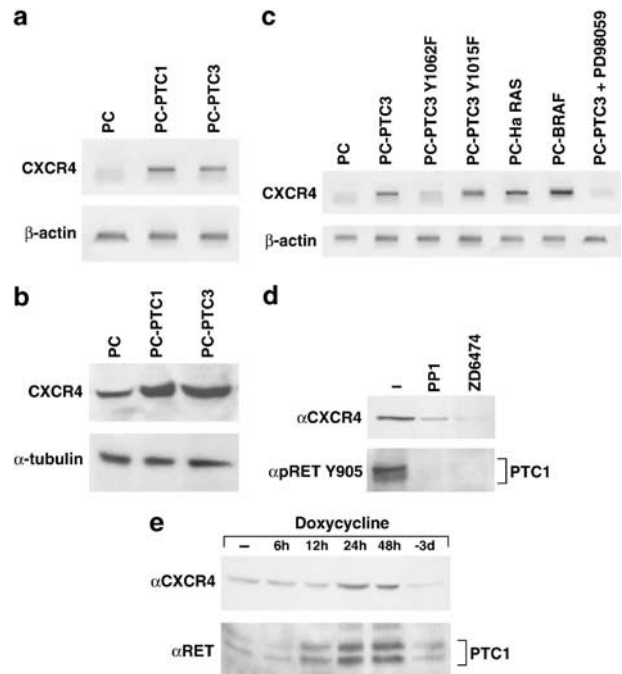


Figure 1 CXCR4 upregulation in PC-PTC rat thyroid cells. (a) The indicated cell lines were harvested and RNAs were isolated and analysed for CXCR4 expression by RT–PCR. PC-PTC cells display an increased CXCR4 mRNA expression in comparison to parental cells. The expression levels of CXCR4 mRNA were normalized to β -actin mRNA levels for each experimental point. (b) The overexpression of CXCR4 in transformed cells was also confirmed by Western blot analysis. Cell lines were harvested and proteins were extracted as indicated in Materials and methods, and analysed by Western blot with the anti-CXCR4 antibody (Santa Cruz). (c) CXCR4 expression depends on the RAS–MAPKs signaling, as shown by the RT–PCR analysis on PC Cl3 cell lines expressing RET/PTC3 mutants. A mutation in residue Y1062 or treatment with the compound PD98059 abolished CXCR4 expression. Consistent with this, PC-Ha RAS and PC-BRAF, carrying the corresponding activated oncogenes, overexpress CXCR4. (d) PC-PTC1 cells were treated with two RET TK inhibitors, PP1 (5 μ M) and ZD6474 (5 μ M), for 72 h. Protein lysates were analysed by immunoblot with anti-CXCR4 antibodies. To confirm the inhibition of RET/PTC1 kinase activity, an immunoblot with anti-phospho-Ret Y905-specific antibodies was also performed. (e) PC cells expressing an inducible RET/PTC1 protein were treated with doxycycline. Cells were then harvested at the indicated time points and after doxycycline washout. Protein lysates were analysed by immunoblot with anti-CXCR4 antibodies. To confirm the induction of PTC1, an immunoblot with anti-ret-specific antibodies was also performed

Ha RAS (Fusco *et al.*, 1987) and PC-BRAF cell lines, which express, respectively, the oncogenes Ha-RAS V12 and BRAF V599E. Furthermore, we treated RET-PTC3 cells for 12 h with the ERK inhibitor PD98059. We found CXCR4 upregulation in PC-Ha RAS and PC-BRAF cells. CXCR4 was instead downregulated in PC-PTC3 cells treated with PD98059 (Figure 1c). These results suggest that CXCR4 can be upregulated by RET/PTC, RAS and BRAF. They also suggest that PTC-dependent CXCR4 upregulation requires the activation of ERKs.

To show that CXCR4 expression depended on RET/PTC kinase activity, cells were treated with two pharmacological inhibitors of RET: a pyrazolo-pyrimi-

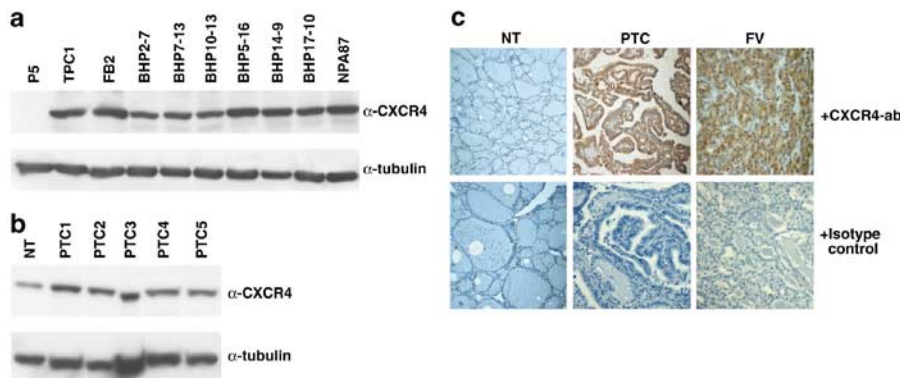


Figure 2 CXCR4 upregulation in human thyroid papillary cancer. (a) CXCR4 upregulation in cell lines derived from RET/PTC-positive human PTCs was evaluated by immunoblot with a polyclonal anti-CXCR4 antibody (Abcam). The expression levels of CXCR4 protein were analysed in the P5 human primary thyroid cells, and in the indicated cell lines, derived from human PTCs. TPC1, FB2 BHP2-7, BHP7-13 and BHP10-13 bear an endogenous RET/PTC1 rearrangement; BHP5-16, BHP14-9, BHP17-10 and NPA87 carry the typical V599E mutation in the BRAF gene. (b) The expression levels of CXCR4 protein were analysed in human PTC samples. Tissues were snap-frozen and immediately homogenized by using the Mixer Mill apparatus (Qiagen) in lysis buffer. Equal amounts of proteins were immunoblotted and stained with anti-CXCR4 polyclonal antibodies (Abcam). As a control for equal loading, the anti-alpha tubulin monoclonal antibody was used. (c) Immunohistochemical staining for CXCR4 of formalin-fixed, paraffin-embedded thyroid carcinoma; Harris hematoxylin counterstaining. Tissue samples from normal thyroid (NT) or PTCs either classic or follicular variant (PTC and FV) were incubated with a mouse monoclonal anti-CXCR4 antibody (R&D). PTC shows a strong immunoreactivity for CXCR4. Strong immunoreactivity is also present in the case of follicular variant of PTC (FV). Normal thyroid tissue is negative (NT). Representative pictures of normal and pathological positive samples are shown. Isotype control is represented in the lower panel

dine, PP1, and an anilino-quinazoline, ZD6474. We reported that these compounds are able to inhibit RET/PTC enzymatic activity (Carlomagno *et al.*, 2002a, b). As shown in Figure 1d, CXCR4 protein levels decreased following treatment with the two inhibitors. The inhibition of RET/PTC kinase activity was monitored with a RET antibody that recognizes the tyrosine residue 905 when phosphorylated.

To further support the hypothesis that CXCR4 expression is directly dependent on RET/PTC, and not a late event that cells select during neoplastic transformation, we used a PC Cl3 cell line in which the expression of RET/PTC1 is under the control of a Tet-on promoter (Wang *et al.*, 2003), and can be induced by treatment of cell with doxycycline, a tetracycline analog. As shown in Figure 1e, CXCR4 protein upregulation followed RET/PTC1 expression, and peaked between 24 and 48 h, when RET/PTC1 levels reached a plateau. CXCR4 upregulation was abrogated upon doxycycline washout.

CXCR4 is expressed in human thyroid carcinoma cells and in primary papillary thyroid carcinomas

We then asked whether CXCR4 upregulation was also a feature of human thyroid cancer cells. To this aim, we determined the expression of CXCR4 in a series of cell lines, derived from human PTCs (Cerutti *et al.*, 1996; Ohta *et al.*, 2001; Basolo *et al.*, 2002) compared to a primary thyroid cell culture P5 (Curcio *et al.*, 1994). These cell lines are characterized by either a RET/PTC1 rearrangement (TPC-1, FB2, BHP2-7, BHP7-13, BHP10-13) or a BRAF V599E mutation (NPA87, BHP5-16, BHP14-9, BHP17-10) (Kimura *et al.*, 2003; Nikiforova *et al.*, 2003; Xu *et al.*, 2003). According to the concept of a common signaling pathway that

involves RET/PTC and BRAF, all the cancer cell lines tested, but not the normal thyrocytes, express CXCR4 (Figure 2a). CXCL12/SDF-1 α and β are the only physiological ligand so far known for the CXCR4 receptor. They are encoded by a single gene, and derive from an alternative splicing. The two encoded proteins are identical, except for the last four amino acids of SDF-1 β , which are absent in SDF-1 α . We failed to detect the chemokines in cell culture medium by using an ELISA assay, and we found a very weak expression of the chemokines in both normal and cancer-derived thyroid cells by RT-PCR (not shown). We also tested, by Western blot, CXCR4 expression in a set of primary tumors from PTC patients and a normal thyroid sample. As shown in Figure 2b, PTC samples scored positive for CXCR4 expression. Normal thyroid tissue displayed a lower, but detectable reactivity. This reactivity could be due to follicular thyroid cells, stromal cells or infiltrating lymphocytes. To answer this question and to confirm CXCR4 expression, we tested receptor expression in a set of primary tumors ($N=19$) from PTC patients by immunohistochemistry. In most of the samples, we detected immunoreactivity against CXCR4 in epithelial cancer cells (17/19). This reactivity was specific, since it could be displaced with the corresponding immunizing peptide (not shown), and it could not be detected with an isotype control antibody. Tissue samples from normal thyroid scored negative for CXCR4 expression. A representative example of these experiments is shown in Figure 2c.

CXCR4 activates downstream signaling pathways in thyroid cancer cells

To evaluate whether CXCR4 receptor expressed on thyroid cells is functional, we stimulated rat and human

cancer cells with recombinant SDF-1 α . In Figure 3a and b, the results obtained from PC-PTC1 (Santoro *et al.* 1993) and FB2 (Basolo *et al.*, 2002) cell lines are shown; similar results were also obtained when PC-PTC3 and TPC1 were used (not shown). Cells were harvested at different time points. Since it has been described that SDF-1 α activates the ERK and PI3K/Akt pathways (Zhou *et al.*, 2002), cell lysates were subjected to Western blot analysis and probed, respectively, with

anti-phospho-MAPK and anti-phospho-Akt antibodies. As shown in Figure 3a and b, activation of both p44/42 MAPK and Akt readily occurred in stimulated cells. MAPK activation occurred at 1 min of stimulation and was biphasic in PC-PTC1 and in human FB2 cells (Figure 3a and b). In contrast, the highest activation of Akt was observed at 30 min in both the cell lines (Figure 3a and b). These observations demonstrate that CXCR4 can function in both rat and human thyroid cells as a signaling receptor.

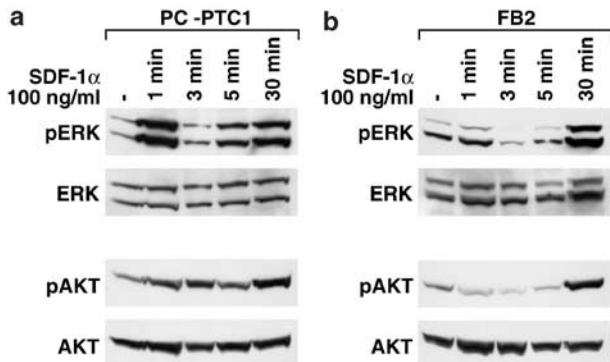


Figure 3 Effects of SDF-1 α in cells overexpressing CXCR4. PC RET/PTC1 (a) and FB2 (b) cells were cultured in complete medium, as indicated in Materials and methods, starved for 12 h with the respective serum-free media and then stimulated with 100 ng/ml SDF-1 α . Cell lysates were prepared and analysed by Western blot with the anti-phospho-MAPK and the anti-phospho-Akt antibodies. To confirm equal loading of the lysates, blots were also probed with total MAPK and total Akt antibodies

SDF-1 α induces S-phase entry and survival of transformed thyroid cells

Since CXCR4 is expressed and functional in thyroid cells, its triggering could contribute to the phenotype of cancer cells. We first asked whether SDF-1 α treatment increased the proliferation rate of parental PC and PC-PTC1 cells. To address this point, we measured BrdU incorporation as a readout of DNA synthesis after 24 h treatment with 100 ng/ml of SDF-1 α . Figure 4a shows that treatment with SDF-1 α caused an increase in BrdU incorporation rate in PC-PTC1 but not in parental cells. The average results of three independent experiments are reported. To evaluate whether the addition of SDF-1 α was able to inhibit apoptosis, we measured inter-nucleosomal DNA fragmentation by the TUNEL assay. Cells were subjected to serum starvation or treated with 2 ng/ml vincristine, two potent apoptotic stimuli (Figure 4b): both treatments induced apoptosis. The effect of both serum deprivation and vincristine treat-

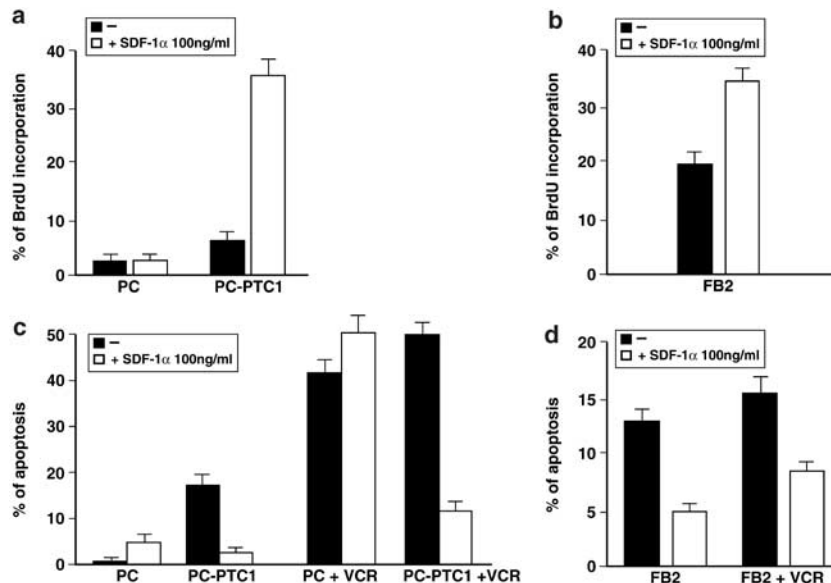


Figure 4 Effects of SDF-1 α on thyroid cell proliferation and survival. (a) S-phase entry was evaluated by BrdU incorporation and indirect immunofluorescence. PC and PC-PTC1 cells were grown on coverslips, serum deprived and treated with SDF-1 α (100 ng/ml) for 48 h. Cells were observed under an epifluorescent microscope to detect BrdU-positive cells. S-phase cells were calculated by counting at least 400 cells in five randomly selected microscopic fields. Results are from three independent experiments. (b) The TUNEL reaction was performed on PC and PC-PTC1 upon 24 h serum deprivation or in complete serum with vincristine, as indicated, in the presence or in the absence of 100 ng/ml SDF-1 α . Cells were observed under an epifluorescent microscope to detect TUNEL-positive cells (TMR-dUTP, red) and total cells on the glass slide (Hoechst, blue stain). Bars are the mean \pm s.d. of three assays. Apoptotic cells were calculated by counting at least 400 cells in five randomly selected microscopic fields. (c, d) S-phase entry and survival were analysed in human FB2 cells. SDF-1 α increased proliferation and survival also in these cells

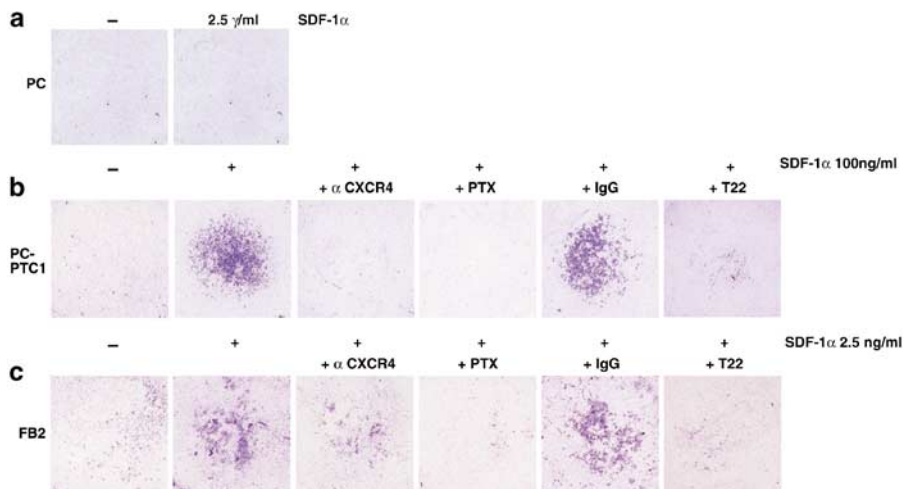


Figure 5 Effects of SDF-1 α on thyroid cell matrigel invasion. (a) PC cells were grown in complete medium to 70% confluence, and then 1×10^5 cells were incubated in the upper chamber. Extracellular matrix was placed into the top chamber of Transwells. The lower chamber was treated with the indicated concentration of SDF-1 α . Cells were incubated for 24 h. Migration was evaluated by the intensity of the spot. A representative experiment is shown. (b, c). PC-PTC1 and FB2 cells were seeded in the upper chamber and allowed to migrate toward the indicated concentrations of SDF-1 α in the absence or in the presence of CXCR4-blocking antibodies, T22-blocking peptide or PTX. Migration was evaluated by the intensity of the spot. A representative experiment is shown

ment is stronger in PC-PTC1 than in parental cells, due to the ability of RET/PTC oncogenes to induce apoptosis, as previously shown (Castellone *et al.*, 2003). SDF-1 α displayed a strong protective effect in PC-PTC1, but not in parental cells. Apoptosis was measured in five randomly selected microscopic fields; the average results of three experiments are reported in the figure.

To show that SDF-1 α induced the same effects also in human cells, we treated FB2 cells with the chemokine and evaluated both proliferative and antiapoptotic effects. As shown in Figure 4c and d, SDF-1 α was able to increase BrdU incorporation and inhibit apoptosis also in these cells.

SDF-1 α triggers chemotaxis and enhances the invasive behavior of cancer thyroid cell lines

CXCR4 has been recently shown to be involved in migration and extracellular matrix invasion of different cancer cells (Muller *et al.*, 2001; Murphy *et al.*, 2001). To verify whether thyroid cancer cells also use CXCR4 to migrate in response to SDF-1 α , PC, PC-PTC1 and FB2 cells were seeded into the top chamber of transwells, and their ability to invade a reconstituted extracellular matrix (matrigel) was evaluated. Parental PC cells were not responsive to SDF-1 α even when exposed to a high concentration of the chemokine (Figure 5a). A concentration of 100 ng/ml was able to support the invasive ability of PC-PTC1 cells. Even a very low concentration of the factor (2.5 ng/ml) was sufficient to induce matrix invasion of the human FB2 cells (Figure 5c). The activity of CXCR4 can be inhibited by pertussis toxin, which inactivates the regulatory proteins Gi and Go, by CXCR4-blocking antibodies, or by blocking peptides. One of these peptides, T22, has been shown to inhibit chemotaxis induced by SDF-1 α in human cells (Mur-

akami *et al.*, 2002). We found that the ability to invade matrigel of both rat and human cells was inhibited by each one of these compounds (Figure 5).

The induction of branching morphogenesis in type I collagen gels efficiently reflects invasive and motile properties of malignant cells, also defined as 'invasive growth' (Comoglio and Trusolino, 2002). Untransformed cells form small and regular nests in collagen gel and they do not proliferate, whereas malignant cells proliferate and form branched colonies with protruding cells, which invade the surrounding matrix (Medico *et al.*, 1996). We tested the ability of PC, PC-PTC1 cells and human FB2 cell lines to grow in type I collagen gels and the effects of SDF-1 α . In cancer, but not in parental cells, SDF-1 α supported the formation of irregularly shaped colonies with protruding cells. This phenomenon was inhibited by the addition of a blocking antibody to CXCR4. In the absence of SDF-1 α , most cells remained single, with very few cells showing proliferation and scattering (Figure 6).

Discussion

In this report, we show that CXCR4 expression is induced in rat thyroid cell lines that ectopically express the RET/PTC oncoproteins. This result was verified by RT-PCR and Western blot experiments. Using a tetracycline-inducible RET/PTC1, we could confirm that the expression of CXCR4 in thyroid cells depends on the expression of the oncoprotein. We also show that CXCR4 induction depends on a specific tyrosine residue, tyrosine 1062, that is critical in mediating downstream signaling (Asai *et al.*, 1996; De Vita *et al.*, 2000; Grimm *et al.*, 2001; Melillo *et al.*, 2001; Murakami *et al.*, 2002; Pelicci *et al.*, 2002). In particular, we

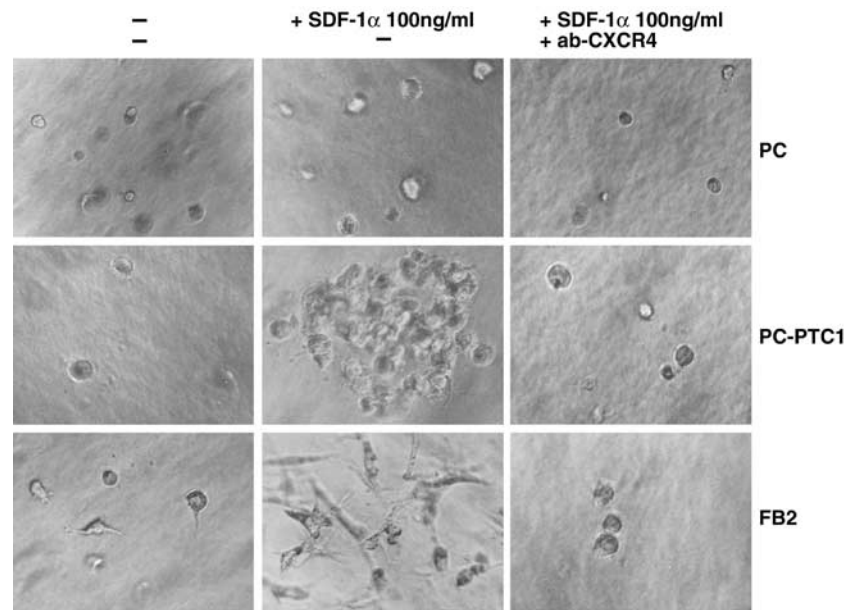


Figure 6 Effects of SDF-1 α in thyroid cell spreading in collagen gel. The indicated cell lines were suspended at a concentration of 10^5 cells in collagen gels and allowed to gel for about 15 min at 37°C before adding 200 μ l of complete medium. Recombinant SDF-1 α (Peprotech) was added to the medium to a concentration of 100 ng/ml. Micrographs of representative fields were taken. A representative experiment is shown

demonstrate that the RAS/ERK pathway, which depends on the integrity of tyrosine 1062, is required for CXCR4 mRNA induction in thyroid cells. RET/PTC oncogenes are able to activate the BRAF isoform of the RAF family of serine-threonine kinases and this activity also requires the integrity of Y1062 (RM Melillo *et al.*, unpublished). It is interesting to note that PC C13 thyroid cells preferentially express the BRAF isoform (RM Melillo *et al.*, unpublished), and BRAF-activating mutations are found in a high percentage of human PTCs (Kimura *et al.*, 2003). Given the foregoing, it is tempting to speculate that CXCR4 expression could depend on the integrity of a RET-PTC/RAS/BRAF/ERK pathway, and that oncogenic activation of each of these proteins can drive CXCR4 overexpression. Tyrosine 1062 is also implicated in the activation of other pathways. Indeed, oncogenic RET is able to induce NF-kappaB activity, and this activity depends on tyrosine 1062 and PI3-K signaling (Hayashi *et al.*, 2000; Ludwig *et al.*, 2001; Russell *et al.*, 2003). It has been previously shown that CXCR4 expression is regulated by NF-kappaB in mammary cell carcinomas (Helbig *et al.*, 2003). It is possible that RET/PTC oncoproteins can also induce CXCR4 by activating the NF-kappaB pathway. More recently, it has been shown that the hypoxia-inducible factor (HIF) is capable of positively regulating the expression of CXCR4 (Bernards, 2003; Schioppa *et al.*, 2003; Staller *et al.*, 2003). Upregulation of HIF protein levels in human tumors is a common event, which can be induced by hypoxia and leads to the block of degradation of the HIF1 subunit via the proteasome pathway. Alternatively, growth factor receptor activation, either by ligand triggering or by oncogenic mutations, can upregulate the levels of HIF1

by increasing its synthesis (Bernards, 2003). It will be interesting to test whether HIF is involved in RET/PTC-mediated CXCR4 induction.

SDF-1 α/β are ubiquitous chemokines and are the only known ligands for CXCR4. Chemokines are chemoattractant cytokines that play a major role in the recruitment of leukocytes to sites of inflammation. Chemokines are also secreted in the tumor microenvironment by infiltrating inflammatory cells and by tumor cells (Balkwill and Mantovani, 2001; Coussens and Werb, 2002). These small molecules have been classified into four groups, based on the position of their conserved cysteine residues: CXC, CC, C and CX3C. Most tumors produce CXC and CC chemokines, which interact with seven-transmembrane G-protein-linked receptors, CXCR and CCR, respectively. These receptors mediate several biological activities, such as chemotaxis, cytoskeletal rearrangements and adhesion to specific cells. Binding of chemokines to their receptors triggers a cascade of events including receptor dimerization and tyrosine phosphorylation, recruitment of the heterotrimeric G proteins of the G α i family, activation of the JAK/STAT, PI3-kinase and MAP kinase pathways, and the activation of the Rho family of small G proteins (Rossi and Zlotnik, 2000). Here we show that in PC-PTC1 cells, SDF-1 α stimulation induced MAPK and AKT activation. Consistently, SDF-1 α treatment increased the percentage of cells in the S phase, exerted a significant antiapoptotic effect and induced cell motility and invasive capacity. These results imply that SDF-1 α in these cells contributes not only to cell growth but also to survival and migration. Stimulation of CXCR4 in PC parental cells is able to stimulate ERK and Akt activation (data not shown), but could not elicit

biological events such as cell growth, survival and motility. This is likely due to the lower levels of CXCR4 in PC cells. However, preliminary observations suggest that stimulation of the receptor, even when ectopically overexpressed in PC cells, induces increased adhesion, but does not confer to these cells the ability to migrate and proliferate (MD Castellone and V Guarino, unpublished data), suggesting that other signals are required. We suggest that in PC-PTC cells, RET/PTC and CXCR4 cooperate to trigger biological effects. A similar cooperation has also been observed in small cell lung cancer (SCLC) cells, in which the c-kit tyrosine kinase receptor and CXCR4 are commonly coexpressed (Kijima *et al.*, 2002). An alternative explanation to the different activity of the receptor in PC and PC-PTC cells might be a difference in CXCR4 desensitization, possibly due to inhibition of G-protein-coupled receptor kinases (GRKs) (Lorenz *et al.*, 2003) or interference with the β -arrestins activity (Kohout *et al.*, 2001) in RET/PTC-transformed cells.

We found that CXCR4 is expressed and functional in human cell lines derived from papillary thyroid cancers, but not in normal cells. The presence of this receptor has also been confirmed in a set of human PTCs by immunohistochemistry. The expression of CXCR4 in human PTCs is of peculiar interest for several reasons. First, its activity on thyroid tumor cells could contribute to the biological features of the tumor, that is, the ability to grow autonomously, to survive and to invade and metastasize. In a recent report, SDF-1 α expression was detected in stromal thyroid fibroblasts, while very low levels were found in thyrocytes and leukocytes (Aust *et al.*, 2001), suggesting that fibroblasts might be the main source of chemokines. Second, these tumors preferentially metastasize via the lymphatic stream to latero-cervical lymphonodes. It is possible that the preferential localization of PTC metastases depends on the repertoire of chemokine receptors that they express on the cell surface. Indeed, lymphonodes have been described as sites of high production of SDF-1 α (Muller *et al.*, 2001). The expression of RET/PTC itself could induce proinflammatory pathways in thyroid epithelial cells (Russell *et al.*, 2003). For instance, it has been shown that stimulation of CXCR4 in ovarian cancer leads to the production of other proinflammatory factors, such as TNF-alpha, which, in turn, can act as a growth factor for cancer cells or mediate other phenomena such as recruiting leukocytes to tumor site (Scotton *et al.*, 2002). In this view, CXCR4 expression can be considered as a factor that enhances the tumor inflammatory infiltrate.

Expression of chemokines and their receptors is not exclusive to thyroid cancer. Other tumors, such as breast, brain, ovarian, prostate, lung cancers, melanomas and lymphomas, express chemokine and chemokine receptors, implicating a general role for this class of molecules in tumor progression and metastasis (Oh *et al.*, 2001; ; Murakami *et al.*, 2002; Scotton *et al.*, 2002; Taichman *et al.*, 2002; Zhou *et al.*, 2002; Barbero *et al.*, 2003; Burger *et al.*, 2003; Kijima *et al.*, 2002; Zeelenberg *et al.*, 2003). Muller *et al.* (2001) showed that breast

cancer cells expressed CXCR4 and CCR7, and that the migration of these cells toward the sites of metastasis depended on local production of SDF-1 α . Indeed, small interfering RNAs and peptide antagonists have been used as breast cancer antimetastatic agents (Chen *et al.*, 2003; Tamamura *et al.*, 2003). The presence of CXCR4 on thyroid cancer deserves further investigation. Experiments to define the expression and the role of this receptor in other human thyroid malignancies, such as follicular, poorly differentiated and anaplastic tumors, and its potential use as a prognostic factor are under investigation. Finally, CXCR4 or its ligand can be potential targets for therapeutic intervention. Inhibitors of CXCR4 are already available. In particular, the bicyclam AMD3100, a specific antagonist for CXCR4, (Murakami *et al.*, 2002; De Clercq, 2003), is currently being tested in preclinical studies in human cancers (De Clercq, 2003). It would be interesting to test whether it is active in human thyroid cancers expressing CXCR4.

Materials and methods

Cell lines and plasmids

PC Cl3 is a differentiated thyroid epithelial cell line derived from 18-month-old Fischer rats. PC Cl3 were maintained in Coon's modified F12 medium supplemented with 5% calf serum and six hormones (6H) (thyrotropin, i.e. TSH, insulin, transferrin, somatostatin, hydrocortisone and glycyl-histidyl-lysine) (GIBCO-BRL, Paisley, PA, USA) as described (Castellone *et al.*, 2003). PC-PTC1, PC-PTC3, PC-PTC3 Y1015F and PC-PTC3 Y1062F cells have been described elsewhere (Castellone *et al.*, 2003). The residues Y1062 and Y1015 correspond to Y588 and Y541 in PTC3. PC Cl3 cells expressing a conditional PTC1 oncogene have been previously described (Wang *et al.*, 2003). To induce RET/PTC1 expression, cells were cultured in the presence of doxycycline (1 μ g/ml; Sigma Chemical Co.) for the indicated time points. PC-Ha RAS cells, carrying the mutant HaRAS V12 oncogene, have been previously described (Fusco *et al.*, 1987). PC-BRAF cells were obtained by transfection of the PC cells with the BRAF V599E mutant. The plasmid BRAF, which expresses a myc-tagged version of the protein, was a kind gift of C Marshall. To obtain the BRAF V599E mutant, site-directed mutagenesis was performed using the QuickChange mutagenesis kit (Stratagene, La Jolla, CA, USA). The mutation was confirmed by DNA sequencing. For transfections of PC Cl3 cells, calcium phosphate precipitates were added to the cells and removed after 1 h. Cells were then subjected to glycerol shock and kept in medium containing 5% calf serum and 6H, as described. After 2 days, G418 was added to a concentration of 400 μ g/ml. Cell clones and pools were further expanded, and proteins expression was detected by Western blot analysis with specific antibodies. They were maintained in Coon's modified F12 medium supplemented with 5% calf serum. Human primary cultures of thyroid cells (P5) were obtained from F Curcio and cultured as previously described (Curcio *et al.*, 1994). Human thyroid cancer cell lines TPC-1, FB2, NPA87, BHP2-7, BHP7-13, BHP10-13, BHP5-16, BHP14-9 and BHP17-10 have also been described previously (Cerutti *et al.*, 1996; Ohta *et al.*, 2001; Basolo *et al.*, 2002), and were maintained in DMEM supplemented with 10% fetal bovine serum, 1% penicillin-streptomycin and 1% glutamine. Treatment of cell cultures with RET TK inhibitors was performed as described by

Carlomagno *et al.* (2002a, b). PC-PTC3 cells were treated with 35 μ M of the ERK inhibitor PD98059 for 12 h (Calbiochem).

RNA extraction

Total RNA from the indicated cell cultures was prepared using the RNeasy Mini Kit (Qiagen, Crawley, West Sussex, UK) and subjected to on-column DNase digestion with the RNase-free DNase set (Qiagen, Crawley, West Sussex, UK) following the manufacturer's instructions. The quality of RNA from each sample was verified by electrophoresis through 1% agarose gel and visualization with ethidium bromide.

Semiquantitative RT-PCR

Transcript levels of the indicated genes were assayed by RT-PCR. A total of 2.5 μ g of total RNA was denatured, and cDNA was synthesized using the GeneAmp RNA PCR Core Kit system from Applied Biosystems following the manufacturer's instructions. Subsequent PCR amplification was performed using 2.5 μ l of RT product in a reaction volume of 25 μ l with primer pairs specific for the gene studied. To exclude DNA contamination, each PCR reaction was also performed on untranscribed RNAs. The levels of the house-keeping β -actin transcript were used as a control for equal RNA loading. Primers were designed according to the program Primer 3 (www-genome.wi.mit.edu/cgi-bin/primer/primer3_www.cgi), and synthesized by the MWG biotech.

For rat CXCR4 and β -actin, the primers were as follows:

CXCR4 F: 5'-AAGCTGTCACACTCCAAGGG-3'
CXCR4 R: 5'-TCCCCACGTAATACGGTAGC-3'
 β -Actin F: 5'-GTCAGGCAGCTCATAGCTCT-3'
 β -Actin R: 5'-TCGTGCGTGACATTAAGAG-3'

Each RT-PCR product was loaded on 2% agarose gel, stained with ethidium bromide (0.5 μ g/ml), and the corresponding image was saved by Typhoon 8600 laser scanning system (Amersham Pharmacia Biotech). The density and width of each band were quantified using IMAGEQUANT 5.0 (Molecular Dynamics).

TUNEL assay

For the terminal deoxynucleotidyl transferase-mediated deoxyuridine triphosphate nick end-labeling (TUNEL), an equal number (5×10^3) of cells from the different lines was seeded onto single-well Costar glass slides. After 48 h serum deprivation in the presence or in the absence of SDF-1 α (100 ng/ml, Peprotech) and vincristine (2 ng/ml, Sigma), cells were fixed in 4% (w/v) paraformaldehyde and then they were permeabilized by the addition of 0.1% Triton X-100/0.1% sodium citrate. Slides were rinsed twice with PBS, air-dried and subjected to the TUNEL reaction (Boehringer, Mannheim). All coverslips were counterstained in PBS containing Hoechst 33258 (final concentration, 1 μ g/ml; Sigma Chemical Co.), rinsed in water and mounted in Moviol on glass slides. The fluorescent signal was visualized with an epifluorescent microscope (Axiovert 2, Zeiss) (equipped with a $\times 100$ objective) interfaced with the image analyser software KS300 (Zeiss).

S-phase entry

S-phase entry was evaluated by BrdU incorporation and indirect immunofluorescence. Cells were grown on coverslips, serum deprived and treated with SDF-1 α (100 ng/ml) for 48 h. BrdU was added at a concentration of 10 μ M for the last 2 h. Subsequently, cells were fixed in 3% paraformaldehyde and

permeabilized with 0.2% Triton X-100. BrdU-positive cells were revealed with Texas-red-conjugated secondary antibodies (Jackson Immuno Research Laboratories Inc., Philadelphia, PA, PA). Cell nuclei were identified by Hoechst staining. Fluorescence was visualized with a Zeiss 140 epifluorescent microscope.

Protein studies

Immunoblotting experiments were performed according to standard procedures. Briefly, cells were harvested in lysis buffer (50 mM Hepes, pH 7.5, 150 mM NaCl, 10% glycerol, 1% Triton X-100, 1 mM EGTA, 1.5 mM MgCl₂, 10 mM NaF, 10 mM sodium pyrophosphate, 1 mM Na₃VO₄, 10 μ g of aprotinin/ml, 10 μ g of leupeptin/ml) and clarified by centrifugation at 10000 g. For protein extraction from human tissues, samples were snap-frozen and immediately homogenized in lysis buffer using the Mixer Mill apparatus (Qiagen). Protein concentration was estimated using a modified Bradford assay (Bio-Rad, Munich, Germany). Antigens were revealed by an enhanced chemiluminescence detection kit (ECL, Amersham, Bucks., England). Anti-CXCR4 antibodies were from Santa Cruz Biotechnology (Santa Cruz, CA, USA) and from Abcam Ltd (Cambridge, UK). Blocking anti-CXCR4 antibodies were from R&D and from Santa Cruz Biotechnology. Anti-phospho-p44/42 MAPK and anti-p44/42 MAPK, anti-phospho-Akt and anti-Akt antibodies were from New England Biolabs (Beverly, MA, USA). Anti-tubulin were from Sigma, and secondary anti-mouse and anti-rabbit antibodies coupled to horseradish peroxidase were from Bio-Rad Inc.

Chemoinvasion and morphogenic assays

Cell invasion was examined using a reconstituted extracellular matrix (Matrigel, Beckman Coulter Labware). Briefly, 40 μ l of the extracellular matrix was placed into the top chamber of Transwells. After 2 h incubation at 37°C, cells (1×10^5 cells/well) were seeded in the upper chamber in serum-free medium. Recombinant SDF-1 α (Peprotech), at the indicated concentrations, was added to lower chamber. For CXCR4 inhibition, cells were preincubated with the blocking antibody (1 μ g/ml, R&D for human cells and Santa Cruz Biotechnology for rat cells), pertussis toxin (0.1 μ g/ml, Calbiochem) or the blocking peptide T22 (1 μ M, Synpep corporation). The chamber was incubated for 24–30 h at 37°C in 5% CO₂ and filters were processed and analysed as described (Medico *et al.*, 1996). Invasion was quantified by the intensity of the spot. These experiments were performed in triplicate.

Morphogenic response of thyroid cells to SDF-1 α was evaluated by collagen gel cultures as described previously by Medico *et al.* (2001). Briefly, cells were harvested from cultures using trypsin-EDTA and suspended at a concentration of 10^5 cells/ml in collagen solution containing type I collagen (3 mg/ml; Collaborative Biomedical Products; Becton Dickinson Labware), $10 \times$ DMEM and 0.5 M Hepes pH 7.4. Aliquots (100 μ l) of the cell suspension were dispensed in microtiter 96-well plates and allowed to gel for about 15 min at 37°C before adding 200 μ l of complete medium. Recombinant SDF-1 α (Peprotech) was added to the medium to a concentration of 100 ng/ml. The medium was changed every 2 days. The morphogenic response was evaluated after 7 days in the presence of SDF-1 α or vehicle alone. These experiments were performed in triplicate.

Immunohistochemistry

Tissue samples were formalin fixed, paraffin embedded and stained with hematoxylin and eosin. For immunohistochem-

istry, paraffin sections (3–5 μm) were dewaxed in xylene, dehydrated through graded alcohols and blocked with 5% nonimmune mouse serum in PBS with 0.05% sodium azide for 5 min. Mouse monoclonal antibody against CXCR4 (clone 12G5; R&D) was added at 1:1000 dilution for 15 min. After incubation with biotinylated anti-mouse secondary antibody for 15 min followed by streptavidin–biotin complex for 15 min (Catalyzed Signal Amplification System; DAKO, Copenhagen, Denmark), sections were developed for 5 min with 0.05% 3,3'-diaminobenzidine tetrahydrochloride, 0.01% hydrogen peroxide in 0.05 M Tris-HCl buffer pH 7.6, counterstained with hematoxylin, dehydrated and mounted.

References

- Asai N, Murakami H, Iwashita T and Takahashi M. (1996). *J. Biol. Chem.*, **271**, 17644–17649.
- Aust G, Steinert M, Kiessling S, Kamprad M and Simchen C. (2001). *J. Clin. Endocrinol. Metab.*, **86**, 3368–3376.
- Bachelder RE, Wendt MA and Mercurio AM. (2002). *Cancer Res.*, **62**, 7203–7206.
- Balkwill F and Mantovani A. (2001). *Lancet*, **357**, 539–545.
- Barbero S, Bonavia R, Bajetto A, Porcile C, Pirani P, Ravetti JL, Zona GL, Spaziante R, Florio T and Schettini G. (2003). *Cancer Res.*, **63**, 1969–1974.
- Basolo F, Giannini R, Toniolo A, Casalone R, Nikiforova M, Pacini F, Elisei R, Miccoli P, Berti P, Faviana P, Fiore L, Monaco C, Pierantoni GM, Fedele M, Nikiforov YE, Santoro M and Fusco A. (2002). *Int. J. Cancer*, **97**, 608–614.
- Bernards R. (2003). *Nature*, **425**, 247–248.
- Buckwalter TL, Venkateswaran A, Lavender M, La Perle KM, Cho JY, Robinson ML and Jhiang SM. (2002). *Oncogene*, **21**, 8166–8172.
- Burger M, Glodek A, Hartmann T, Schmitt-Graff A, Silberstein LE, Fujii N, Kipps TJ and Burger JA. (2003). *Oncogene*, **22**, 8093–8101.
- Carlomagno F, Vitagliano D, Guida T, Ciardiello F, Tortora G, Vecchio G, Ryan AJ, Fusco A and Santoro M. (2002a). *Cancer Res.*, **62**, 7284–7290.
- Carlomagno F, Vitagliano D, Guida T, Napolitano M, Vecchio G, Fusco A, Gazit A, Levitzki A and Santoro M. (2002b). *Cancer Res.*, **62**, 1077–1082.
- Castellone MD, Cirafici AM, De Vita G, De Falco V, Malorni L, Tallini G, Fagin JA, Fusco A, Melillo RM and Santoro M. (2003). *Oncogene*, **22**, 246–255.
- Cerutti J, Trapasso F, Battaglia C, Zhang L, Martelli ML, Berlingieri MT, Fagin J, Santoro M and Fusco A. (1996). *Clin. Cancer Res.*, **2**, 119–126.
- Chen Y, Stamatoyannopoulos G and Song CZ. (2003). *Cancer Res.*, **63**, 4801–4804.
- Comoglio PM and Trusolino L. (2002). *J. Clin. Invest.*, **109**, 857–862.
- Coussens LM and Werb Z. (2002). *Nature*, **420**, 860–867.
- Curcio F, Ambesi-Impiombato FS, Perrella G and Coon HG. (1994). *Proc. Natl. Acad. Sci. USA*, **91**, 9004–9008.
- De Clercq E. (2003). *Nat. Rev. Drug Discov.*, **2**, 581–587.
- De Vita G, Melillo RM, Carlomagno F, Visconti R, Castellone MD, Bellacosa A, Billaud M, Fusco A, Tschlis PN and Santoro M. (2000). *Cancer Res.*, **60**, 3727–3731.
- Fusco A, Berlingieri MT, Di Fiore P P, Portella G, Grieco M and Vecchio G. (1987). *Mol. Cell. Biol.*, **9**, 3365–3370.
- Grimm J, Sachs M, Britsch S, Di Cesare S, Schwarz-Romond T, Alitalo K and Birchmeier W. (2001). *J. Cell Biol.*, **154**, 345–354.
- Hayashi H, Ichihara M, Iwashita T, Murakami H, Shimono Y, Kawai K, Kurokawa K, Murakumo Y, Imai T, Funahashi H, Nakao A and Takahashi M. (2000). *Oncogene*, **19**, 4469–4475.
- Helbig G, Christopherson II KW, Bhat-Nakshatri P, Kumar S, Kishimoto H, Miller KD, Broxmeyer HE and Nakshatri H. (2003). *J. Biol. Chem.*, **278**, 21631–21638.
- Jhiang SM, Sagartz JE, Tong Q, Parker-Thornburg J, Capen CC, Cho JY, Xing S and Ledent C. (1996). *Endocrinology*, **137**, 375–378.
- Kohout A, Lin FS, Perry SJ, Comer DA and Lefkowitz RJ. (2001). *Proc. Natl. Acad. Sci. USA*, **98**, 1601–1606.
- Kijima T, Maulik G, Ma PC, Tibaldi EV, Turner RE, Rollins B, Sattler M, Johnson BE and Salgia R. (2002). *Cancer Res.*, **62**, 6304–6311.
- Kimura ET, Nikiforova MN, Zho Z, Knauf JA, Nikiforova YE and Fagin JA. (2003). *Cancer Res.*, **63**, 1454–1457.
- Knauf JA, Kuroda H, Basu S and Fagin JA. (2003). *Oncogene*, **22**, 4406–4412.
- Kroll TG. (2002). *Am. J. Pathol.*, **160**, 1941–1944.
- Lorenz K, Ldise MJ and Quittour U. (2003). *Nature*, **426**, 574–579.
- Ludwig L, Kessler H, Wagner M, Hoang-Vu C, Dralle H, Adler G, Bohm BO and Schmid RM. (2001). *Cancer Res.*, **61**, 4526–4535.
- Medico E, Gentile A, Lo Celso C, Williams TA, Gambarotta G, Trusolino L and Comoglio PM. (2001). *Cancer Res.*, **61**, 5861–5868.
- Medico E, Mongiovi AM, Huff J, Jelinek MA, Follenzi A, Gaudino G, Parsons JT and Comoglio PM. (1996). *Mol. Biol. Cell*, **7**, 495–504.
- Melillo RM, Santoro M, Ong SH, Billaud M, Fusco A, Hadari YR, Schlessinger J and Lax I. (2001). *Mol. Cell. Biol.*, **12**, 4177–4187.
- Muller A, Homey B, Soto H, Ge N, Catron D, Buchanan ME, McClanahan T, Murphy E, Yuan W, Wagner SN, Barrera JL, Mohar A, Verastegui E and Zlotnik A. (2001). *Nature*, **410**, 50–56.
- Murakami H, Yamamura Y, Shimono Y, Kawai K, Kurokawa K and Takahashi M. (2002a). *J. Biol. Chem.*, **277**, 32781–32890.
- Murakami T, Maki W, Cardones AR, Fang H, Tun Kyi A, Nestle FO and Hwang ST. (2002b). *Cancer Res.*, **62**, 7328–7342.
- Murphy PM. (2001). *N. Engl. J. Med.*, **345**, 833–835.
- Namba H, Nakashima M, Hayashi T, Hayashidei N, Maida S, Rogounovitchi TI, Ohturu A, Saenko VA, Kaucmahw T and Yonarui S. (2003). *J. Clin. Endocrinol. Metab.*, **88**, 4393–4397.
- Nikiforov YE. (2002). *Endocr. Pathol.*, **13**, 3–16.

- Nikiforova MN, Kimura ET, Gandhi M, Biddinger PW, Knauf JA, Basolo F, Zhu Z, Giannini R, Salvatore G, Fusco A, Santoro M, Fagin JA and Nikiforov YE. (2003). *J. Clin. Endocrinol. Metab.*, **88**, 5399–5404.
- Oh JW, Drabik K, Kutsch O, Choi C, Tousson A and Benveniste EN. (2001). *J. Immunol.*, **166**, 2695–2704.
- Ohta K, Endo T, Haraguchi K, Hershman JM and Onaya T. (2001). *J. Clin. Endocrinol. Metab.*, **86**, 2170–2177.
- Pelicci G, Troglio F, Bodini A, Melillo RM, Pettirossi V, Coda L, De Giuseppe A, Santoro M and Pelicci PG. (2002). *Mol. Cell. Biol.*, **22**, 7351–7363.
- Powell Jr DJ, Russell J, Nibu K, Li G, Rhee E, Liao M, Goldstein M, Keane WM, Santoro M, Fusco A and Rothstein JL. (1998). *Cancer Res.*, **58**, 5523–5528.
- Rossi D and Zlotnik A. (2000). *Annu. Rev. Immunol.*, **18**, 217–242.
- Russell JP, Shinohara S, Melillo RM, Castellone MD, Santoro M and Rothstein JL. (2003). *Oncogene*, **22**, 4569–4577.
- Santoro M, Chiappetta G, Cerrato A, Salvatore D, Zhang L, Manzo G, Picone A, Portella G, Santelli G, Vecchio G and Fusco A. (1996). *Oncogene*, **12**, 1821–1826.
- Santoro M, Melillo RM, Grieco M, Berlingieri MT, Vecchio G and Fusco A. (1993). *Cell Growth Differ.*, **4**, 77–84.
- Schioppa T, Uranchimeg B, Saccani A, Biswas SK, Doni A, Rapisarda A, Bernasconi S, Saccani S, Nebuloni M, Vago L, Mantovani A, Melillo G and Sica A. (2003). *J. Exp. Med.*, **198**, 1391–1402.
- Scotton CJ, Wilson JL, Scott K, Stamp G, Wilbanks GD, Fricker S, Bridger G and Balkwill FR. (2002). *Cancer Res.*, **62**, 5930–5938.
- Staller P, Sulitkova J, Lisztwan J, Moch H, Oakeley EJ and Krek W. (2003). *Nature*, **425**, 307–311.
- Taichman RS, Cooper C, Keller ET, Pienta KJ, Taichman NS and McCauley LK. (2002). *Cancer Res.*, **62**, 1832–1837.
- Tamamura H, Hori A, Kanzaki N, Hiramatsu K, Mizumoto M, Nakashima H, Yamamoto N, Otaka A and Fujii N. (2003). *FEBS Lett.*, **550**, 79–83.
- Wang J, Knauf JA, Basu S, Puxeddu E, Kuroda H, Santoro M, Fusco A and Fagin JA. (2003). *Mol. Endocrinol.*, **17**, 1425–1436.
- Xu X, Quiros RM, Gattuso P, Ain KB and Prinz RA. (2003). *Cancer Res.*, **63**, 4561–4567.
- Zeelenberg IS, Ruuls-Van Stalle L and Roos E. (2003). *Cancer Res.*, **63**, 3833–3839.
- Zhou Y, Larsen PH, Hao C and Yong VW. (2002). *J. Biol. Chem.*, **277**, 49481–49487.

Autocrine stimulation by osteopontin plays a pivotal role in the expression of the mitogenic and invasive phenotype of RET/PTC-transformed thyroid cells

Maria Domenica Castellone¹, Angela Celetti¹, Valentina Guarino¹, Anna Maria Cirafici¹, Fulvio Basolo², Riccardo Giannini², Enzo Medico³, Mogens Kruhoffer⁴, Torben F Orntoft⁴, Francesco Curcio⁵, Alfredo Fusco¹, Rosa Marina Melillo¹ and Massimo Santoro^{*1}

¹Dipartimento di Biologia e Patologia Cellulare e Molecolare, University 'Federico II' clo Istituto di Endocrinologia ed Oncologia Sperimentale del CNR, Naples, Italy; ²Dipartimento di Oncologia, Pisa, Italy; ³Division of Molecular Oncology, Institute for Cancer Research and Treatment (IRCC), University of Turin, Candiolo (TO), Italy; ⁴Molecular Diagnostic Laboratory, Department of Clinical Biochemistry, Aarhus University Hospital, Skejby, Aarhus, Denmark; and ⁵Dipartimento di Patologia e Medicina Sperimentale e Clinica, University of Udine, Italy

Papillary thyroid carcinomas are characterized by rearrangements of the RET receptor tyrosine kinase generating RET/PTC oncogenes. Here we show that osteopontin (OPN), a secreted glycoprotein, is a major RET/PTC-induced transcriptional target in PC Cl 3 thyroid follicular cells. OPN upregulation depended on the integrity of the RET/PTC kinase and tyrosines Y1015 and Y1062, two major RET/PTC autophosphorylation sites. RET/PTC also induced a strong overexpression of CD44, a cell surface signalling receptor for OPN. Upregulation of CD44 was dependent on RET/PTC Y1062, as well. Constitutive OPN overexpression or treatment with exogenous recombinant OPN sharply increased proliferation, Matrigel invasion and spreading in collagen gels of RET/PTC-transformed PC Cl 3 cells. These effects were impaired by the treatment of PC Cl 3-RET/PTC cells with OPN- and CD44-blocking antibodies. Thus, RET/PTC signalling triggers an autocrine loop involving OPN and CD44 that sustains proliferation and invasion of transformed PC Cl 3 thyrocytes.

Oncogene (2004) 23, 2188–2196. doi:10.1038/sj.onc.1207322
Published online 23 February 2004

Keywords: kinase; carcinoma; motility; Ras; tyrosine; thyroid

Introduction

Papillary thyroid carcinoma (PTC) is the most prevalent malignancy of the thyroid gland. PTC hallmarks are chromosomal inversions or translocations that cause the recombination of the intracellular kinase-encoding

domain of the RET receptor with heterologous genes, generating the RET/PTC chimeric oncogenes. RET/PTC1, the H4-RET fusion, and RET/PTC3, the RFG-RET fusion, are the most prevalent variants (Fagin, 2002). RET/PTC-transgenic mice develop PTC, proving that RET/PTC oncogenes are able to initiate thyroid carcinogenesis (Santoro *et al.*, 1996; Buckwalter *et al.*, 2002).

Fusion with protein partners possessing protein–protein interaction motifs provides RET/PTC kinases with dimerizing interfaces. This results in constitutive dimerization and phosphorylation of the chimeric oncoproteins and constant upregulation of signal transduction. RET signalling mainly depends on three key tyrosine residues: tyrosine 905, in the activation loop, whose phosphorylation stabilizes the active conformation of the catalytic domain (Iwashita *et al.*, 1996), tyrosine 1015, a docking site for phospholipase C γ (Borrello *et al.*, 1996) and tyrosine 1062. This last residue is embedded in an NKLPY (single-letter amino-acid code) motif and mediates recruitment of various proteins to RET and RET/PTC (Hayashi *et al.*, 2000; Manie' *et al.*, 2001). Shc and FRS2 are recruited to pY1062 via their phosphotyrosine binding (PTB) domains (Melillo *et al.*, 2001; Mercalli *et al.*, 2001) and, by bridging RET/PTC to Grb2-Sos complexes, they play a key role in the activation of Ras small GTPases (Castellone *et al.*, 2003).

By using oligonucleotide microarrays, we have found that osteopontin (OPN) is one of the most heavily RET/PTC3-induced transcripts in PC Cl 3 thyroid follicular cells (Melillo RM, Castellone MD, Kruhoffer M, Orntoft TF Santoro M, unpublished). OPN, also known as secreted phosphoprotein 1 (*spp1*), is a highly acidic calcium-binding glycosylated phosphoprotein. OPN is also regarded as a cytokine (ETA-1, Early T-lymphocyte antigen or IL-28) regulating T helper cell-1 function (Ashkar *et al.*, 2000; Chabas *et al.*, 2001). CD44 is one of the cell surface receptors for OPN (Weber *et al.*, 1996). Furthermore, OPN contains an RGD (single-letter

*Correspondence: M Santoro, Dipartimento di Biologia e Patologia Cellulare e Molecolare, Facoltà di Medicina e Chirurgia, University 'Federico II' via S Pansini 5, 80131 Naples, Italy;
E-mail: masantor@unina.it

Received 27 June 2003; revised 29 October 2003; accepted 31 October 2003

amino-acid code) peptide that binds αv -containing integrins (Miyachi *et al.*, 1991). By binding to these receptors, OPN supports various functions including chemotaxis, cell attachment and cell migration. Recently, much interest has focused on the association of OPN with tumorigenesis and metastasis formation. OPN is expressed in many neoplastic tissues, such as colon, breast, prostate and lung carcinomas, being a circulating plasma marker for several neoplasms (for a review, see Weber, 2001).

Here, we show that signals elicited at the level of specific RET/PTC tyrosine residues stimulate an OPN-CD44 autocrine loop sustaining proliferation and invasiveness of transformed thyrocytes.

Results

RET/PTC induces OPN upregulation in PC Cl 3 cells

We used the oligonucleotide GeneChip[®] Rat Genome U34 Set (Affymetrix, SantaClara, CA, USA) to detect genes that are induced in thyroid cells upon RET/PTC-mediated transformation. Comparative analysis was performed by the GeneChip[®] software: 87 genes were upregulated < fivefold in RET/PTC3-transformed cells with respect to parental cells. One of the most strongly upregulated genes was OPN (9.4-folds) (Melillo RM, Castellone MD, Kruhoffer M, Orntoft TF Santoro M, unpublished).

We sought to confirm microarray data by quantitative RT-PCR (Q-PCR); we also asked whether OPN overexpression was specifically linked to the RET/PTC3 variant or it was a feature of different RET/PTC oncogenes (Figure 1a). Quantitation of the OPN mRNA by Q-PCR showed < 10-fold OPN induction in RET/PTC1- and RET/PTC3-expressing thyrocytes (Figure 1b). Thus, microarray screen underestimated OPN upregulation. To ascertain whether OPN upregulation was linked to RET/PTC expression and was not a late secondary effect of cell transformation, we analysed OPN mRNA expression by semiquantitative RT-PCR in PC Cl 3 cells expressing a doxycycline-inducible RET/PTC3. Actin mRNA detection was used for normalization. RET/PTC3 mRNA started to be detected at 12 h of doxycycline treatment and accumulated thereafter (Figure 1c). OPN transcripts were barely detectable in unstimulated cells. In stimulated cells, OPN upregulation followed that of RET/PTC3, starting after 24 h and peaking after 48 h of doxycycline treatment. Upon doxycycline washout, expression of both RET/PTC3 and OPN was no longer detectable (Figure 1c).

To confirm these findings, cells stably expressing RET/PTC1 or RET/PTC3 oncogenes were harvested, protein lysates were obtained and OPN protein levels were examined by Western blotting; housekeeping tubulin detection was applied to confirm equal gel loading. Accumulation of OPN protein was detected in RET/PTC1- and RET/PTC3-transformed cells (Figure 1d).

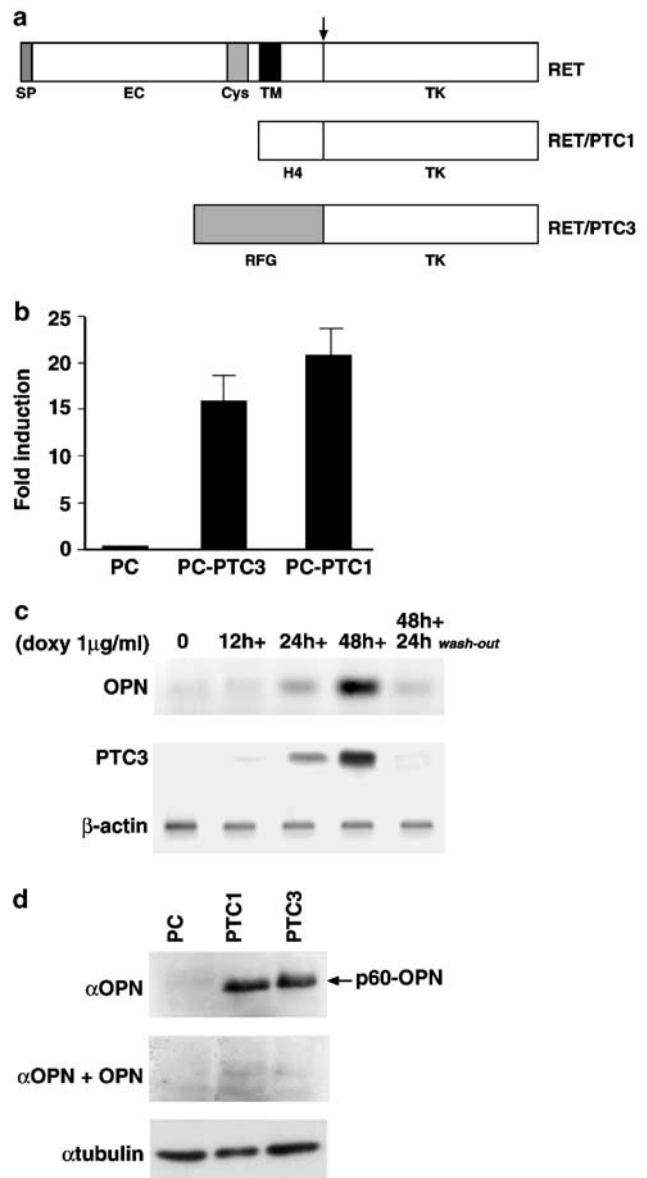


Figure 1 OPN overexpression in RET/PTC-transformed PC Cl 3 cells. **(a)** Schematic drawing of RET and RET/PTC proteins: SP: signal peptide, EC: extracellular domain, Cys: cysteine-rich domain, TM: transmembrane domain, TK: tyrosine kinase domain. **(b)** Q-PCR was used to calculate OPN mRNA fold induction in the indicated cell lines; results are the average of three independent amplifications \pm s.d.. **(c)** RT-PCR (25 cycles) was used to detect RET/PTC3 and OPN mRNA levels in PC Cl 3 cells expressing a tet-inducible RET/PTC3 construct upon treatment with doxycycline (1 μ g/ml) at the indicated time points or after 24 h of doxycycline washout. **(d)** Protein lysates (100 μ g) underwent Western blotting with anti-OPN antibody. Immunocomplexes were revealed by enhanced chemiluminescence. As a control of the specificity of the antibody, anti-OPN was preincubated with a fivefold molar excess of recombinant OPN. Anti- α -tubulin antibodies were used for normalization

OPN upregulation depends on tyrosines 1015 and 1062 of RET/PTC

OPN mRNA levels were measured by semiquantitative RT-PCR in mass populations of PC Cl 3 cells stably

expressing RET/PTC3, a kinase-dead mutant (K758M) or mutants harbouring substitutions of tyrosines 1015 or 1062 to phenylalanine (Figure 2a). Figure 2b shows that OPN stimulation was strongly dependent on the catalytic activity of RET/PTC3 and the integrity of tyrosine 1062. It was also dependent on tyrosine 1015, although the mutation of this last residue impaired OPN stimulation at a lower extent than mutation of Y1062 (Figure 2b). Accordingly, when RET/PTC3 kinase was turned-off by a 48h treatment with an RET/PTC3 kinase inhibitor (ZD6474, 1 μ M) (Carlomagno *et al.*, 2002), OPN mRNA was strongly downregulated (Figure 2b). One possible mediator of OPN upregulation was the Ras small GTPase. Indeed, oncogenic Ras stimulates OPN expression in various cell types (Guo *et al.*, 1995), and Y1062 is a crucial residue mediating Ras stimulation in PC Cl 3-RET/PTC cells (Castellone *et al.*, 2003). RNA was extracted from PC Cl 3 cells transformed by constitutively active v-Ha-Ras and used to assess OPN mRNA levels in comparison to parental cells. Similar to RET/PTC-expressing cells, PC-Ha-Ras cells featured high levels of OPN transcripts (Figure 2c).

Quantitation of the OPN mRNA by Q-PCR showed <threefold inhibition of OPN induction upon mutation of Y1015; mutation of Y1062 virtually abrogated OPN upregulation (Figure 2d). Furthermore, a 24 h treatment of RET/PTC3-expressing thyrocytes with 35 μ M PD98059 (a selective MEK1 inhibitor) sharply reduced OPN upregulation (Figure 2d). Thus, OPN upregulation by RET/PTC likely depends on the cooperation between Ras/MAPK stimulation by Y1062 and signals derived from Y1015.

PC-RET/PTC cells feature CD44 upregulation

OPN exerts biological effects by binding two types of cell surface receptors: CD44 and α v-containing integrins. We analysed PC-RET/PTC cells for CD44 and α v integrins expression by semiquantitative RT-PCR. The expression of α v integrins was detected at similar levels in normal and transformed cells (data not shown). Notably, CD44 resulted among the RET/PTC upregulated genes (fivefolds) in our microarray screening (Melillo RM, Castellone MD, Kruhoffer M, Orntoft TF Santoro M, unpublished). By amplifying exons 1–2 of CD44 mRNA, we found that CD44 mRNA was upregulated in PC Cl 3 cells transformed by RET/PTC1 or RET/PTC3 in comparison to parental cells, this upregulation being impaired, similarly to OPN, by a 24 h treatment with 35 μ M PD98059 (Figure 3a). Quantitation of RET/PTC-mediated CD44 mRNA stimulation was obtained by real-time PCR (Figure 3b). Finally, immunoblot experiments confirmed CD44 upregulation, showing a strong upregulation of a broad band of relative molecular mass of about 90 kDa likely containing multiple CD44 protein species (Figure 3c). Accumulation of CD44 protein in RET/PTC-expressing cells was even stronger than accumulation of CD44 mRNA, suggesting the contribution of post-transcriptional events.

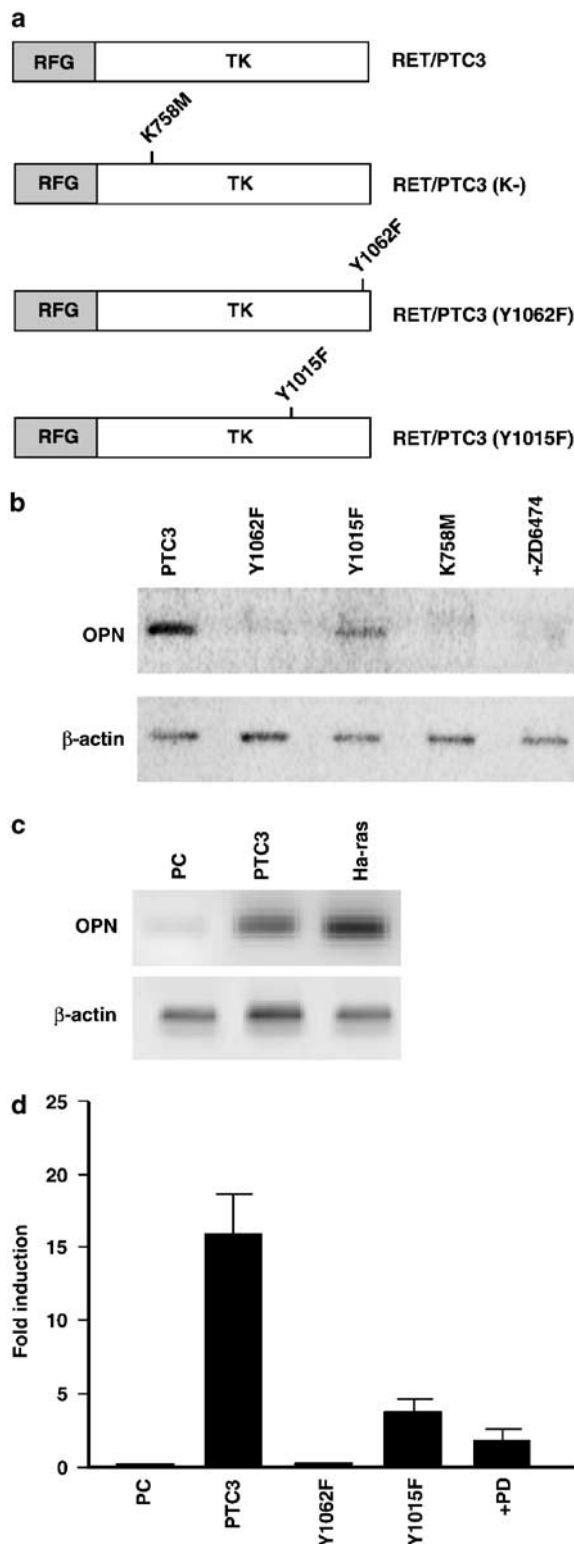


Figure 2 OPN upregulation depends on active RET/PTC signaling. (a) Schematic drawing of RET/PTC3 mutants used in this study. (b, c) RT-PCR (25 cycles) was performed to detect OPN mRNA levels in the indicated cell lines; β actin mRNA detection was used for normalization. ZD6474 (1 μ M, 48 h) was used to inhibit the RET/PTC3 kinase. This figure is representative of three independent experiments. (d) Q-PCR was used to calculate OPN mRNA fold induction in the indicated cell lines; results are the average of three independent amplifications \pm s.d.

CD44 transcripts are subject to alternative splicing. CD44 pre-mRNA is encoded by 20 exons. The constant 5'-terminal five exons encode the N-terminal extracellular portion of the CD44 protein, while the constant 3'-terminal five exons encode the transmembrane and the short cytosolic tail. Additional 10 exons (variant 'v1-v10' exons) are alternatively spliced and code for the extracellular membrane-proximal stem structure. Cancer cells often overexpress CD44 variants that include variable numbers of small 'v' exons. The presence of the v6 exon has been reported to be important for efficient OPN binding, while v3 is important for the binding of heparin-associated growth factors (Ponta *et al.*, 2003). Thus, by using different combinations of amplimers, we explored whether CD44 transcripts, accumulated in RET/PTC-transformed thyroid cells, contained variant exons. Figure 3d shows that CD44 mRNAs upregulated in PC-RET/PTC cells contained v3, v6 or both v3 and v6 exons. Overexpression of CD44 mRNAs was strongly dependent on Y1062, but not on Y1015. CD44 expression was induced by v-Ha-Ras, as well (Figure 3d).

OPN cooperates with RET/PTC to increase DNA synthesis of PC Cl 3 cells

We asked whether OPN upregulation played any role in the establishment of the neoplastic phenotype of RET/PTC-transformed PC Cl 3 cells. We either stimulated cells with recombinant purified OPN or transduced cells with a lentiviral vector for OPN fused to enhanced GFP

autofluorescent protein (OPN-GFP: OG) (Medico *et al.*, 2001) (Figure 4a). For lentiviral transduction, normal and RET/PTC3-transformed PC Cl 3 cells were subjected to three subsequent rounds of infection with high titre OG vector (multiplicity of infection <1). OG transduction was confirmed by flow cytometry: 49.21% of PC Cl 3 and 48.53% of PC-RET/PTC3 cells scored GFP-positive (not shown). Western blot with an anti-OPN antibody confirmed OG transduction: of note, OG migrated more slowly than endogenous OPN protein due to the GFP protein moiety (Figure 4a).

We asked whether OPN stimulated proliferation of RET/PTC-expressing cells. As a measure of DNA synthesis, we counted BrdU-positive cells upon a 1 h BrdU pulse. Average results of three independent experiments are reported in Figure 4b. OG gene transduction potently stimulated the rate of BrdU incorporation in RET/PTC3-transformed cells (about 10-fold increase). Treatment with recombinant OPN also stimulated DNA synthesis of transformed thyroid cells, albeit at a lower extent (about fivefold increase). Notably, in both cases, the response of parental cells to OPN was significantly smaller than that of RET/PTC3-transformed cells (Figure 4b). This could be due to the

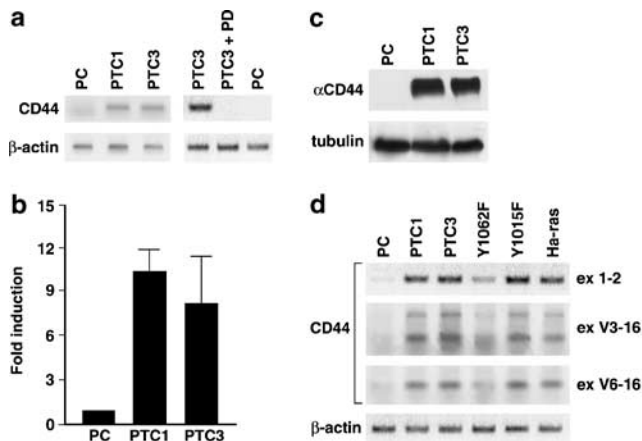


Figure 3 CD44 overexpression in RET/PTC-transformed PC Cl 3 cells. (a) RT-PCR (25 cycles) was performed to detect CD44 mRNA levels in the indicated cell lines; amplimers mapping on exons 1 and 2 (all CD44 mRNAs) were used. (b) Quantitative PCR was used to calculate CD44 mRNA fold induction in the indicated cell lines; results are the average of three independent amplifications \pm s.d. (c) Protein lysates (100 μ g) underwent Western blotting with anti-CD44 antibody. Anti- α -tubulin antibodies were used for normalization. (d) RT-PCR (25 cycles) was performed to detect CD44 mRNA levels in the indicated cell lines. Amplimers mapping on exons 1 and 2 (standard CD44 mRNA), exons v3 and 16, and v6 and 16 were used. The v3-16 primer pair amplified two products of 489- and 283 bp-containing exons v3-v6-16 and v3-16, respectively, as proved by subsequent Southern hybridization with exon-specific probes (not shown)

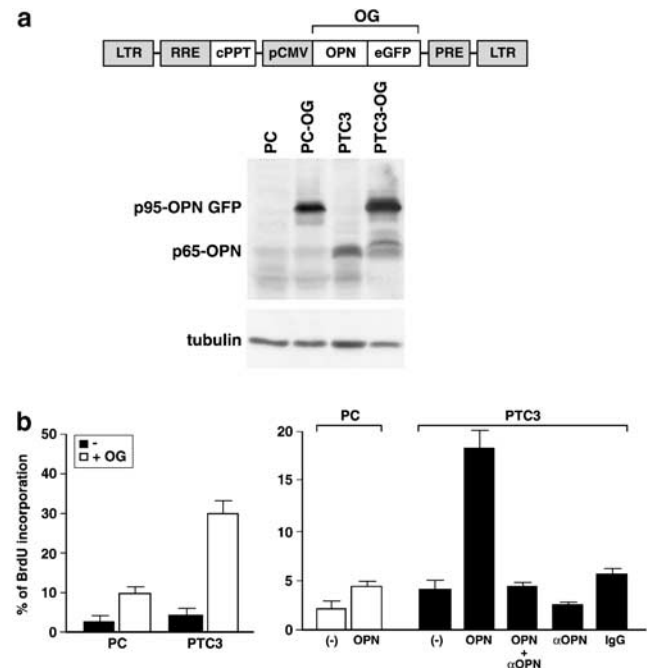


Figure 4 OPN stimulates DNA synthesis of RET/PTC-transformed PC Cl 3 cells. (a) Schematic drawing of the OG-expressing lentivirus. Protein lysates (50 μ g) underwent Western blotting with anti-OPN antibody to ascertain OG gene transduction. Anti- α -tubulin antibodies were used for normalization. (b) BrdU was added for 1 h and cells were fixed and processed for immunofluorescence: anti-BrdU, monitored by a FITC-conjugated anti-mouse antibody, was used to detect the fraction of cells in S-phase. The average results \pm s.d. of three independent experiments in which at least 60 cells were counted are reported. When indicated, cells were pretreated (15 min) with exogenous recombinant OPN (100 ng/ml), anti-OPN-blocking antibodies (5 μ g/ml) or unrelated IgG (5 μ g/ml). Where indicated, cells infected with the OG lentivirus were used

parallel upregulation of the CD44 receptor in transformed cells or to OPN cooperation with additional pathways triggered by RET/PTC. Treatment with anti-OPN-blocking antibodies (5 $\mu\text{g/ml}$), but not with non-specific IgG, impaired DNA synthesis of both PC-RET/PTC3 and OPN-stimulated PC-RET/PTC3 cells (Figure 4b). Thus, although in many cell systems OPN has been shown to produce effects other than cell mitogenesis (Zhang *et al.*, 2003), in RET/PTC-transformed thyrocytes (see also below) OPN exerts detectable stimulation of DNA synthesis.

OPN cooperates with RET/PTC to increase invasiveness of PC Cl 3 cells

We examined cell invasiveness through Matrigel in basal conditions, upon OG transduction and towards exogenous recombinant OPN in the lower chamber of transwells. Figure 5a shows that PC-RET/PTC3 cells had basal levels of invasiveness higher than parental cells. Treatment with exogenous OPN further induced migratory response of PC-RET/PTC3 cells but not of parental cells (Figure 5a). Importantly, PC-RET/PTC3 migration through Matrigel was inhibited by pretreatment with anti-OPN-blocking antibodies, but not by nonspecific IgG (Figure 5a). Also, anti-CD44-blocking antibodies (IM7) blocked cell migration, consistent with known effects exerted by CD44 either upon binding to OPN (Lin *et al.*, 2000; Weiss *et al.*, 2001) or when triggered otherwise. Finally, OG gene transduction strongly stimulated Matrigel invasion of RET/PTC3-transformed cells (Figure 5b), while it only slightly stimulated that of parental cells (not shown). These effects were inhibited by anti-CD44 antibodies, as well (Figure 5b).

Finally, we asked whether OPN increased the capacity of PC Cl 3 cells to spread in tridimensional type I collagen gels. When seeded in collagen, wild-type PC Cl 3 cells showed a round phenotype and no spreading ability (Figure 6). In contrast, a sizeable fraction of PC-RET/PTC3 cells dispersed in the collagen matrix during the first few hours of incubation (Figure 6). OG gene transduction significantly increased spreading ability of RET/PTC3 cells. According to known effects of CD44 in mediating cell spreading, these effects were reduced when cells were incubated with anti-CD44 antibodies (Figure 6). After 48 h, most RET/PTC cells lost the spreading phenotype and started to die, while OG-expressing cells continued to be alive and spreading (not shown).

OPN and CD44 overexpression in human thyroid papillary carcinoma cell lines

To confirm our findings in a different cell system, we used human thyroid carcinoma cells. TPC1 (Ishizaka *et al.*, 1990) and FB2 (Basolo *et al.*, 2002) are human cell lines established from thyroid papillary carcinomas spontaneously harbouring the RET/PTC1 oncogene. Both cancer cell lines expressed increased levels of OPN (Figure 7a) and CD44 (Figure 7b) with respect to P5, a

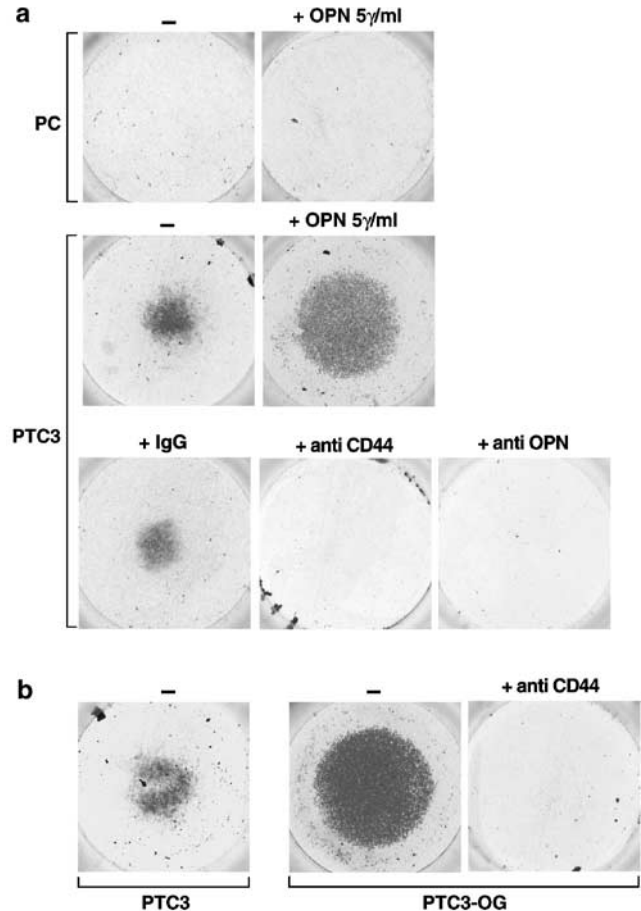


Figure 5 OPN stimulates Matrigel invasion of RET/PTC-transformed PC Cl 3 cells. Matrigel invasion of parental PC Cl 3 and RET/PTC3-transformed cells (a) or OG transduced cells (b) in response to normal culture medium or exogenous recombinant OPN in the lower chamber of 8 μM pore transwells. Where indicated, blocking anti-CD44 or -OPN antibodies were used. In this case, cells were pretreated for 15 min with the required antibody (10 $\mu\text{g/ml}$) and then seeded in transwells in which the lower chamber contained the antibody (20 $\mu\text{g/ml}$). Cells were seeded in the upper chamber and incubated for 24 h. Thereafter, filters were fixed and stained. The upper surface was wiped clean and cells on the lower surface were photographed. This figure is representative of three independent experiments

primary culture of normal human thyrocytes. We transduced TPC1 cells with the OG lentiviral vector: 70.62% of cells scored GFP-positive (not shown). OG gene transduction significantly stimulated the rate of BrdU incorporation in TPC1 cells (about fivefold increase). Treatment with recombinant OPN also stimulated DNA synthesis of TPC1 cells (about 2.5-fold increase). Treatment with anti-OPN-blocking antibodies (5 $\mu\text{g/ml}$), but not with nonspecific IgG (not shown), impaired DNA synthesis of TPC1 and OPN-treated TPC1 cells (Figure 7c).

We examined cell invasiveness through Matrigel in basal conditions and towards exogenous recombinant OPN. Figure 7d shows that treatment with exogenous OPN induced a strong migratory response of TPC1 cells. Migration through Matrigel was inhibited by

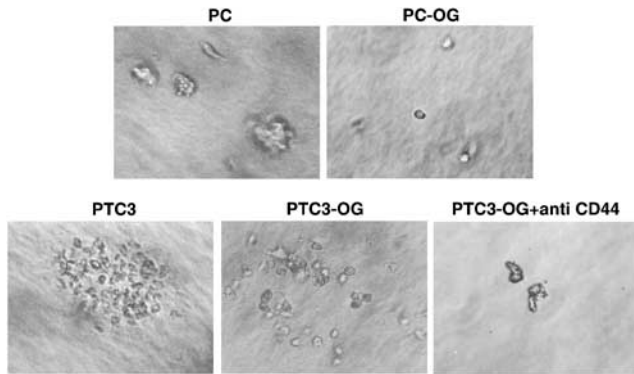


Figure 6 OPN stimulates spreading in collagen gels of RET/PTC-transformed PC Cl 3 cells. The indicated cell types were kept in collagen gels for 6 h, micrographs of representative fields were taken. This figure is representative of three independent experiments

pretreatment with anti-OPN-blocking antibodies, but not by nonspecific IgG (Figure 7d).

When seeded in tridimensional type I collagen gel, TPC1 cells showed a flat elongated phenotype and modest spreading ability (Figure 7e). OG gene transduction significantly increased proliferative and spreading ability of TPC1 cells, these effects being greatly reduced when cells were incubated with anti-CD44 antibodies (Figure 7e).

Materials and methods

Plasmids, recombinant proteins, antibodies and cell lines

All the constructs used in this study encode the short (RET-9) RET spliced form and were cloned in pCDNA3(Myc-His) (Invitrogen, Groningen, The Netherlands). For simplicity, we number the residues of RET/PTC proteins according to the corresponding residues in unrearranged RET. RET/PTC1 and RET/PTC3 constructs are described elsewhere (Melillo *et al.*, 2001). RET/PTC3(K-) is a kinase-dead mutant, carrying the substitution of the catalytic lysine (residue 758 in full-length RET) with a methionine. RET/PTC3(Y1062F) and RET/PTC3(Y1015F) carry substitutions of the indicated tyrosines with phenylalanine residues (Castellone *et al.*, 2003).

Parental and transformed PC Cl 3 cells were cultured in Coon's modified Ham F12 medium supplemented with 5% calf serum and a mixture of thyrotropin (10 mU/ml), hydrocortisone (10 nM), insulin (10 µg/ml), apo-transferrin (5 µg/ml), somatostatin (10 ng/ml) and glycyL-histidyl-L-lysine (10 ng/ml) (Sigma Chemical Co., St Louis, MO, USA) according to Fusco *et al.* (1987). PC Cl 3 transfected with RET/PTC1, RET/PTC3, Y1015F, Y1062F and K758M mutants have been described previously (Castellone *et al.*, 2003). PC Cl 3 transformed by v-Ha-Ras have been described (Fusco *et al.*, 1987). A PC Cl 3 cell line expressing RET/PTC3 in a doxycycline-dependent manner was obtained by sequential stable transfection with expression vectors for the tetracycline(tet)-dependent transactivating rtTA protein and for tet-inducible RET/PTC3 (Saavedra *et al.*, 2000). To induce RET/PTC3 expression, cells were treated for different times with 1 µg/ml doxycycline. TPC1 (Ishizaka *et al.*, 1990) and FB2 (Basolo *et al.*, 2002) cell lines derive from RET/PTC1-positive human PTC and were

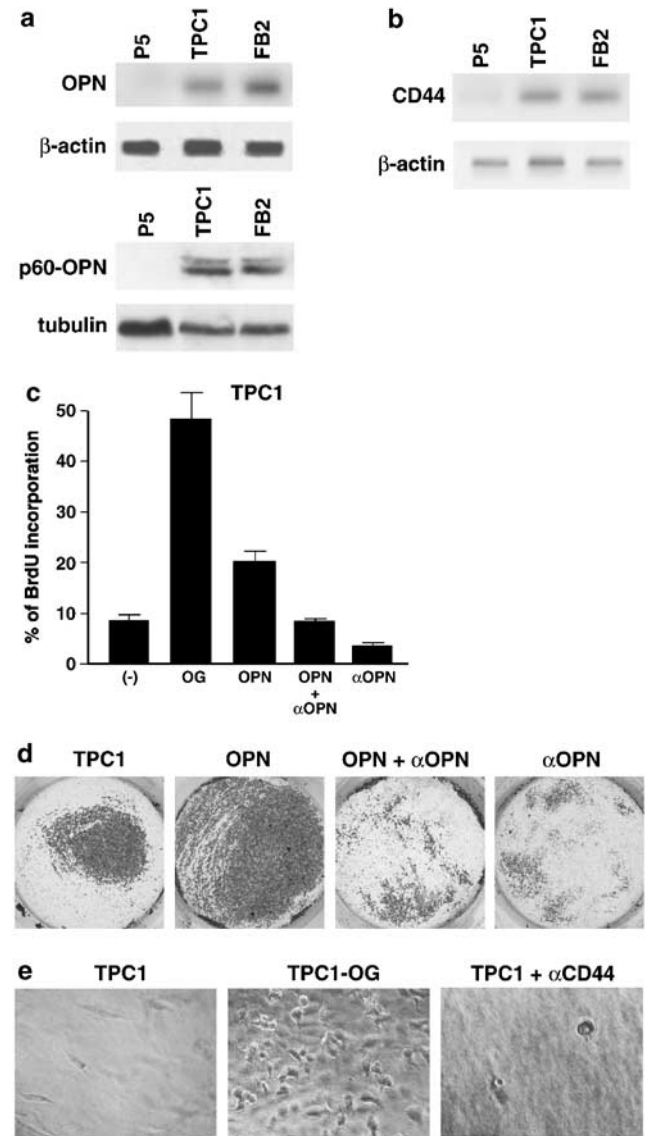


Figure 7 OPN and CD44 overexpression in human thyroid carcinoma cells. (a) RT-PCR (25 cycles) was performed to detect OPN mRNA levels in the indicated cell lines; β actin mRNA detection was used for normalization (top). Western blotting with anti-OPN antibody. Anti-α-tubulin was used for normalization (bottom). (b) RT-PCR (25 cycles) was performed to detect CD44 mRNA levels in the indicated cell lines; amplimers mapping on exons 1 and 2 were used. (c) BrdU was added for 1 hand cells were fixed and processed for immunofluorescence. When indicated, cells were pretreated (15 min) with anti-OPN-blocking antibodies (5 µg/ml) or unrelated IgG (5 µg/ml). Where indicated, cells infected with the OG lentivirus were used. The average results ±s.d. of three independent experiments are reported. (d) Matrigel invasion was assessed as described in Figure 5. This figure is representative of three independent experiments. (e) The indicated cell types were kept in collagen gels for 6 h and micrographs of representative fields were taken. Also, this figure is representative of three independent experiments

grown in Dulbecco's modified Eagle's medium (DMEM) supplemented with 10% FCS (Sigma Chemical Co.). The P5 primary culture of normal human thyroid follicular cells was a kind gift of F Curcio and was grown as described (Curcio *et al.*, 1994).

Recombinant mouse OPN protein and blocking goat anti-mouse OPN antibody (AF808) were from R&D Systems (Minneapolis, MN, USA). Blocking monoclonal antibody against CD44 (IM7 clone) was from BD Biosciences (San Jose, CA, USA). Anti-OPN goat polyclonal antibody (K-20) and rabbit polyclonal anti-CD44 (H-300) were from Santa Cruz Biotechnology (Santa Cruz, CA, USA). Monoclonal anti α -tubulin was from Sigma Chemical Co. Secondary antibodies were from Santa Cruz Biotechnology.

RNA extraction, PCR, real-time PCR

Total RNA was isolated by the RNeasy Kit (Qiagen, Crawley, West Sussex, UK) and subjected to on-column DNase digestion with the RNase-free DNase set (Qiagen) following the manufacturer's instructions. The quality of RNA was verified by electrophoresis through 1% agarose gel and visualization with ethidium bromide. Random-primed first-strand cDNA was synthesized in a 50 μ l reaction volume starting from 2 μ g RNA by using the Gene Amp RNA PCR Core Kit (Applied Biosystems, Warrington, UK). PCR amplification was performed using the GeneAmp RNA PCR Core Kit system following the manufacturer's instructions. To exclude DNA contamination, each PCR reaction was also performed on untranscribed RNA. Levels of β -actin transcripts were used as a control for equal RNA loading. RT-PCR products were loaded on 2% agarose gel, stained with ethidium bromide and the image saved by the Typhoon 8600 laser scanning system (Amersham Pharmacia Biotech, Bucks, England). The density and width of each band was quantified using the IMAGEQUANT 5.0 software.

Quantitative PCR reactions were performed by using the SYBR Green PCR Master mix (Applied Biosystems) in the iCycler apparatus (Bio-Rad, Munich, Germany). Amplification reactions (25 μ l final reaction volume) contained 200 nM of each primer, 3 mM MgCl₂, 300 μ M dNTPs, 1 \times SYBR-Green PCR buffer, 0.1 U/ μ l AmpliTaq Gold DNA Polymerase, 0.01 U/ μ l Amp Erase, RNase-free water and 2 μ l cDNA samples. Thermal cycling conditions consisted of an initial cycle of 2 min at 50°C, a cycle of 10 min at 95°C and 40 cycles of 15 s of denaturation (95°C) followed by 1 min of annealing/extension (60°C). To verify the absence of nonspecific products, 80 cycles of melting (55°C for 10 s) were performed. In all cases, the melting curve confirmed that a single product was generated. Real-time amplification was monitored by measuring the increase in fluorescence caused by the SYBR-Green binding to double-stranded DNA. Fluorescent threshold values were measured in triplicate and fold changes were calculated by the formula: $2^{-(\text{sample } 1 \Delta Ct - \text{sample } 2 \Delta Ct)}$, where ΔCt is the difference between the amplification fluorescent thresholds of the mRNA of interest and the β actin mRNA.

Primers were designed by using a software available at http://www-genome.wi.mit.edu/cgi-bin/primer/primer3_www.cgi and synthesized by the MWG biotech (Ebersberg, Germany). Primers sequences were as follows:

rat β actin forward: 5'-GTCAGGCAGCTCATAGCTCT-3'
rat β actin reverse: 5'-TCGTGCGTGACATTAAGAG-3'
human β actin forward: 5'-TGCGTGACATTAAGGA-GAAG-3'
human β actin reverse: 5'-GCTCGTAGCTCTTCTCCA-3'
ratOPN forward: 5'-GAGGAGAAGGCGCATTACAG-3'
ratOPN reverse: 5'-ACAGAATCCTCGCTCTCTGC-3'
humanOPN forward: 5'-AGGAGGAGGCAGAGCACA-3'
humanOPN reverse: 5'-CTGGTATGGCACAGGTGATG-3'
humanCD44 (exon1) forward: 5'-GCTTCAATAGCACC TTGCC-3'

humanCD44 (exon2) reverse: 5'-GTTGTTTGCTGCACA-GATGG-3'
ratCD44 (exon1) forward: 5'-CAGCTTGGGGACTACTTTGC-3'
ratCD44 (exon 2) reverse: 5'-CTGCATGTTTCAAACC CCTT-3'
ratCD44 (exon v3) forward: 5'-CTGGAAGCCAAATGAG GAAA-3'
ratCD44 (exon v6) forward: 5'-TGGTTTGAGAAT-GAATGGCA-3'
ratCD44 (exon 16) reverse: 5'-TTCGGATCCATGAGT-CACAG-3'
RET/PTC3 forward: 5'-AAGCAAACCTGCCAGTGG-3'
RET/PTC3 reverse: 5'-TGCTTCAGGACGTTGAAC-3'.

Protein extraction and Western blotting

Protein extractions and immunoblotting experiments were performed according to standard procedures. Briefly, cells were harvested in lysis buffer (50 mM HEPES, pH7.5, 150 mM NaCl, 10% glycerol, 1% Triton X-100, 1 mM EGTA, 1.5 mM MgCl₂, 10 mM NaF, 10 mM sodium pyrophosphate, 1 mM Na₂VO₄, 10 μ g of aprotinin/ml, 10 μ g of leupeptin/ml) and clarified by centrifugation at 10000 g. Protein concentration was estimated with a modified Bradford assay (Bio-Rad). Immune complexes were detected with the enhanced chemiluminescence kit (ECL, Amersham). Signal intensity was analysed at the Phosphorimager (Typhoon 8600, Amersham Pharmacia Biotech) interfaced with the ImageQuant software.

Lentiviral infection with the OPN-GFP fusion gene

The lentiviral transfer vector pLC-OG, standing for Lentiviral (vector)-CMV (promoter)-OPN-GFP (transgene), is described elsewhere (Medico *et al.*, 2001). The virus was produced by transient transfection of 293T cells with pLC-OG together with the VSV-G and pCMVR8.93 plasmids, as described. Viral p24 concentration was determined by HIV-1 p24 Core profile ELISA (NEN Life Science Products). Transduction experiments were performed by adding a 1:2 dilution of the virus-containing 293T supernatant onto cells in six-well plates (Costar) in the presence of polybrene (8 μ g/ml). Transduced cells were checked by flow cytometry and Western blot for expression of the recombinant protein.

BrdU incorporation

DNA synthesis was measured by the 5'-bromo-3'-deoxyuridine Labeling and Detection Kit from Boehringer Mannheim (Germany). Cells were seeded on glass coverslips, BrdU was added to the cell culture media at a final concentration of 100 μ g/ml. Cells were incubated for 1 h, permeabilized with Triton X-100 (0.2%) and fixed with paraformaldehyde (4%) prior to staining. Coverslips were incubated with anti-BrdU mouse monoclonal antibody and with an FITC-conjugated anti-mouse antibody. All coverslips were counterstained in PBS containing Hoechst 33258 (final concentration, 1 μ g/ml; Sigma Chemical Co.), rinsed in water and mounted in Moviol on glass slides. The fluorescent signal was visualized with an epifluorescent microscope (Axiovert 2, Zeiss) (equipped with a \times 100 lens) interfaced with the image analyzer software KS300 (Zeiss).

Matrigel invasion

In vitro invasiveness through Matrigel was assayed using Transwell cell culture chambers according to described procedures (Yue *et al.*, 1994). Briefly, confluent cell mono-

layers were harvested with trypsin/EDTA and centrifuged at 800 g for 10 min. The cell suspension (1×10^5 cells/well) was added to the upper chamber of a prehydrated polycarbonate membrane filter of 8 μ m pore size (Costar, Cambridge, MA, USA) coated with 35 μ g Matrigel (Collaborative Research Inc., Bedford, MA, USA). The lower chamber was filled with F12 complete medium and, when required, purified intact OPN. When required, the cells were pretreated with blocking antibodies for 20 min. Plates were incubated at 37°C in a humidified incubator in 5% CO₂ and 95% air for 24 h. Nonmigrating cells on the upper side of the filter and Matrigel were wiped off and migrating cells on the reverse side of the filter were stained with 0.1% crystal violet in 20% methanol for 15 min, counted and photographed.

Cell spreading in collagen gel

Cells were harvested from cultures using trypsin-EDTA and resuspended in gelling solution prepared as described (Medico *et al.*, 1996). Briefly, eight parts of type I collagen solution (2 mg/ml) (ICN Biomedicals, Eschwege, Germany) was mixed with one part of $10 \times$ DMEM and one part of HEPES 0.5 M (pH 7.4) and kept on ice to prevent premature gelation. Resuspended cells were seeded into 24-well plates (4×10^4 /well). After gelation, F12 medium containing 5% FCS and six hormones was added. Cell spreading was examined at regular time intervals for 4 days.

Discussion

RET/PTC rearrangements are prevalent in thyroid papillary carcinomas and experimental evidence indicate that they are able to initiate thyroid carcinogenesis. This notwithstanding, very little is known about the mechanisms by which RET/PTC oncogenes transform thyroid follicular cells. Model systems of thyroid follicular cells have been widely used to study growth regulation and neoplastic transformation (Kimura *et al.*, 2001). By using PC Cl 3 cells, here we identify OPN as a major transcriptional target of RET/PTC in thyroid cells. By using recombinant OPN protein, an OPN-expressing lentivirus and OPN-blocking antibodies, we show that OPN upregulation is implicated in mitogenic and motile phenotype of RET/PTC-transformed PC Cl 3 cells. These results were confirmed in human cell lines spontaneously harbouring the RET/PTC1 oncogene.

OPN binds cell surface α v-containing integrins and the hyaluronate receptor CD44. CD44, in turn, has been implicated in cell–cell and cell–matrix interactions and homing of tumour cell metastasis (Ponta *et al.*, 2003). CD44 is a signalling receptor able to induce activation of the phosphatidylinositol 3-kinase/Akt pathway (Kamikura *et al.*, 2000; Lin and Yang-Yen, 2001) and to associate to ezrin to control cell motility in a PKC-regulated manner (Legg *et al.*, 2002). We show that CD44 is upregulated in RET/PTC-transformed cells. It is possible that, in thyroid cells, OPN effects are mediated in part by α v-containing integrins and that CD44 upregulation affects the transformed phenotype *per se*

References

- Andreozzi F, Melillo RM, Carlomagno F, Oriente F, Miele C, Fiory F, Santopietro S, Castellone MD, Beguinot F, Santoro M and Formisano P. (2003). *Oncogene*, **22**, 2942–2949.
Asai N, Murakami H, Iwashita T and Takahashi M. (1996). *J. Biol. Chem.*, **271**, 17644–17649.

independently of OPN (for instance by lateral recruitment of other membrane proteins). However, some evidences suggest that CD44 is implicated in OPN signalling in RET/PTC-transformed PC Cl 3 cells. Indeed, the increased response to OPN of RET/PTC-transformed with respect to parental cells parallels CD44 overexpression. Furthermore, anti-CD44 antibodies (Lin *et al.*, 2000; Weiss *et al.*, 2001) reduced OPN effects in thyroid cells. Finally, PC-RET/PTC cells overexpress CD44 mRNAs containing the v6 exon, important for efficient OPN binding. Intriguingly, CD44 and its splicing variants are often found overexpressed in human thyroid tumors (Ermak *et al.*, 1995; Bartolazzi *et al.*, 2001). Whether RET/PTC solely induces CD44 overexpression or it also stimulates CD44 activity (for instance by the recently described PKC-mediated phosphorylation mechanism, Legg *et al.*, 2002) remains to be determined.

An intact kinase activity and phosphorylation of Y1062 are essential for efficient stimulation of OPN and CD44 by RET/PTC. OPN upregulation, in turn, depended also on Y1015. Of note, both Y1062 and Y1015 are required for RET/PTC-mediated cell transformation (Asai *et al.*, 1996; Borrello *et al.*, 1996) and they are constitutively phosphorylated in RET/PTC proteins in human thyroid cancer specimens (Salvatore *et al.*, 2000). Moreover, both tyrosines are required for thyroid tumors formation in RET/PTC1-transgenic mice (Buckwalter *et al.*, 2002). Tyrosine 1015 is the docking site for PLC γ , implicated in RET-mediated activation of protein kinase C α (PKC α) (Andreozzi *et al.*, 2003). Tyrosine 1062 is implicated in the activation of multiple signalling pathways (Hayashi *et al.*, 2000), including the Ras one (Melillo *et al.*, 2001). The OPN promoter contains multiple AP-1 and ETS-family proteins binding sites (Chang and Prince, 1993; Guo *et al.*, 1995). Indeed, it responds to PKC α triggering (Chang and Prince, 1993) and to oncogenic Ras, as well (Guo *et al.*, 1995 and this paper). We suggest that in PC Cl 3 cells, CD44 upregulation is determined by signals starting from Y1062 and leading to Ras/MAPK activation, while OPN upregulation is the result of the cooperation of multiple signalling pathways downstream RET/PTC, the Ras/MAPK pathway being one of them.

In conclusion, our data demonstrate that RET/PTC signalling triggers the formation of an autocrine loop involving OPN and CD44 that stimulates proliferation and motility of PC Cl 3 cells. These findings prompt further studies to ascertain whether OPN could be a useful PTC tumour marker and a promising therapeutic target.

Acknowledgements

We thank J Fagin for RET/PTC inducible cells and F Carlomagno for ZD6474 experiment. This study was supported by the Associazione Italiana per la Ricerca sul Cancro (AIRC), the EC grant FIGH-CT1999-CHIPS, the Progetto Strategico Oncologia of the CNR/MIUR, grants from the Ministero per l'Istruzione, Università e Ricerca Scientifica (MIUR) and the Ministero della Salute. VG was recipient of a fellowship of the BioGeM s.c.ar.l. (Biotecnologia e Genetica Molecolare nel Mezzogiorno d'Italia).

- Ashkar S, Weber GF, Panoutsakopoulou V, Sanchirico ME, Jansson M, Zawaideh S, Rittling SR, Denhardt DT, Glimcher MJ and Cantor H. (2000). *Science*, **287**, 860–864.
Bartolazzi A, Gasbarri A, Papotti M, Bussolati G, Lucante T, Khan A, Inohara H, Marandino F, Orlandi F, Nardi F,

- Vecchione A, Tecce R and Larsson O. (2001). *Lancet*, **357**, 1644–1650.
- Basolo F, Giannini R, Toniolo A, Casalone R, Nikiforova M, Pacini F, Elisei R, Miccoli P, Berti P, Faviana P, Fiore L, Monaco C, Pierantoni GM, Fedele M, Nikiforov YE, Santoro M and Fusco A. (2002). *Int. J. Cancer*, **97**, 608–614.
- Borrello MG, Alberti L, Arighi E, Bongarzone I, Battistini C, Bardelli A, Pasini B, Piutti C, Rizzetti MG, Mondellini P, Radice MT and Pierotti MA. (1996). *Mol. Cell. Biol.*, **16**, 2151–2163.
- Buckwalter TL, Venkateswaran A, Lavender M, La Perle KM, Cho JY, Robinson ML and Jhiang SM. (2002). *Oncogene*, **21**, 8166–8172.
- Carlomagno F, Vitagliano D, Guida T, Ciardiello F, Tortora G, Vecchio G, Ryan AJ, Fontanini G, Fusco A and Santoro M. (2002). *Cancer Res.*, **62**, 7284–7290.
- Castellone MD, Cirafici AM, De Vita G, De Falco V, Malorni L, Tallini G, Fagin JA, Fusco A, Melillo RM and Santoro M. (2003). *Oncogene*, **22**, 246–255.
- Chabas D, Baranzini SE, Mitchell D, Bernard CC, Rittling SR, Denhardt DT, Sobel RA, Lock C, Karpuz M, Pedotti R, Heller R, Oksenberg JR and Steinman L. (2001). *Science*, **294**, 1731–1735.
- Chang PL and Prince CW. (1993). *Cancer Res.*, **53**, 2217–2220.
- Curcio F, Ambesi-Impiombato FS, Perrella G and Coon HG. (1994). *Proc. Natl. Acad. Sci. USA*, **91**, 9004–9008.
- Ermak G, Gerasimov G, Troshina K, Jennings T, Robinson L, Ross JS and Figge J. (1995). *Cancer Res.*, **55**, 4594–4598.
- Fagin JA. (2002). *Endocrinology*, **143**, 2025–2028.
- Fusco A, Berlingieri MT, Di Fiore PP, Portella G, Grieco M and Vecchio G. (1987). *Mol. Cell. Biol.*, **7**, 3365–3370.
- Guo X, Zhang YP, Mitchell DA, Denhardt DT and Chambers AF. (1995). *Mol. Cell. Biol.*, **15**, 476–487.
- Hayashi H, Ichihara M, Iwashita T, Murakami H, Shimono Y, Kawai K, Kurokawa K, Murakumo Y, Imai T, Funahashi H, Nakao A and Takahashi M. (2000). *Oncogene*, **19**, 4469–4475.
- Ishizaka Y, Ushijima T, Sugimura T and Nagao M. (1990). *Biochem. Biophys. Res. Commun.*, **168**, 402–408.
- Iwashita T, Asai N, Murakami H, Matsuyama M and Takahashi M. (1996). *Oncogene*, **12**, 481–487.
- Kamikura DM, Khoury H, Maroun C, Naujokas MA and Park M. (2000). *Mol. Cell. Biol.*, **20**, 3482–3496.
- Kimura T, Van Keymeulen A, Golstein J, Fusco A, Dumont JE and Roger PP. (2001). *Endocr. Rev.*, **22**, 631–656.
- Legg JW, Lewis CA, Parsons M, Ng T and Isacke CM. (2002). *Nat. Cell Biol.*, **4**, 399–407.
- Lin YH, Huang CJ, Chao JR, Chen ST, Lee SF, Yen JJ and Yang-Yen HF. (2000). *Mol. Cell. Biol.*, **20**, 2734–2742.
- Lin YH and Yang-Yen HF. (2001). *J. Biol. Chem.*, **276**, 46024–46030.
- Manie S, Santoro M, Fusco A and Billaud M. (2001). *Trends Genet.*, **17**, 580–589.
- Medico E, Gentile A, Lo Celso C, Williams TA, Gambarotta G, Trusolino L and Comoglio PM. (2001). *Cancer Res.*, **61**, 5861–5868.
- Medico E, Mongiovi AM, Huff J, Jelinek MA, Follenzi A, Gaudino G, Parsons JT and Comoglio PM. (1996). *Mol. Cell. Biol.*, **7**, 495–504.
- Melillo RM, Santoro M, Ong SH, Billaud M, Fusco A, Hadari YR, Schlessinger J and Lax I. (2001). *Mol. Cell. Biol.*, **21**, 4177–4187.
- Mercalli E, Ghizzoni S, Arighi E, Alberti L, Sangregorio R, Radice MT, Gishizky ML, Pierotti MA and Borrello MG. (2001). *Oncogene*, **20**, 3475–3485.
- Miyachi A, Alvarez J, Greenfield EM, Teti A, Grano M, Colucci S, Zamboni-Zallone A, Ross FP, Teitelbaum SL and Cheresch D. (1991). *J. Biol. Chem.*, **266**, 20369–20374.
- Ponta H, Sherman L and Herrlich PA. (2003). *Nat. Rev. Mol. Cell Biol.*, **4**, 33–45.
- Saavedra HI, Knauf JA, Shirokawa JM, Wang J, Ouyang B, Elisei R, Stambrook PJ and Fagin JA. (2000). *Oncogene*, **19**, 3948–3954.
- Salvatore D, Barone MV, Salvatore G, Melillo RM, Chiappetta G, Mineo A, Fenzi G, Vecchio G, Fusco A and Santoro M. (2000). *J. Clin. Endocrinol. Metab.*, **85**, 3898–3907.
- Santoro M, Chiappetta G, Cerrato A, Salvatore D, Zhang L, Manzo G, Picone A, Portella G, Santelli G, Vecchio G and Fusco A. (1996). *Oncogene*, **12**, 1821–1826.
- Weber GF. (2001). *Biochim. Biophys. Acta*, **1552**, 61–85.
- Weber GF, Ashkar S, Glimcher MJ and Cantor H. (1996). *Science*, **271**, 509–512.
- Weiss JM, Renkl AC, Maier CS, Kimmig M, Liaw L, Ahrens T, Kon S, Maeda M, Hotta H, Uede T and Simon JC. (2001). *J. Exp. Med.*, **194**, 1219–1229.
- Yue TL, McKenna PJ, Ohlstein EH, Farach-Carson MC, Butler WT, Johanson K, McDevitt P, Feuerstein GZ and Stadel JM. (1994). *Exp. Cell Res.*, **214**, 459–464.
- Zhang G, He B and Weber GF. (2003). *Mol. Cell. Biol.*, **23**, 6507–6519.